

AD-A132 033 A STUDY OF NORMAL SHOCK-WAVE TURBULENT BOUNDARY-LAYER INTERACTIONS AT MAC..(U) ROYAL AIRCRAFT ESTABLISHMENT FARNBOROUGH (ENGLAND) W G SAWYER ET AL. OCT 82 UNCLASSIFIED RAF-TR-82099 DRIC-BR-88360 F/G 20/4

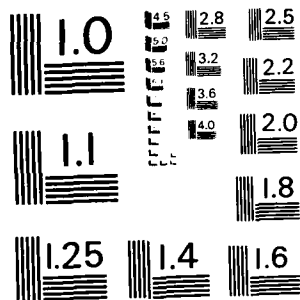
A STUDY OF NORMAL SHOCK-WAVE TURBULENT BOUNDARY-LAYER INTERACTIONS AT MAC..(U) ROYAL AIRCRAFT ESTABLISHMENT FARNBOROUGH (ENGLAND) W G SAWYER ET AL. OCT 82
RAE-TR-82099 DRIC-BR-88360 F/G 20/4

1/2

UNCLASSIFIED

F/G 20/4

NI



MICROCOPY RESOLUTION TEST CHART
NATIONAL BUREAU OF STANDARDS-1963-A

TR 82099

ADA 132033

UNLIMITED
PC (3-T) 11-7-83 JH

BR 88360

TR 82099

(4)



ROYAL AIRCRAFT ESTABLISHMENT

*

Technical Report 82099

October 1982

**A STUDY OF NORMAL SHOCK-WAVE
TURBULENT BOUNDARY-LAYER
INTERACTIONS AT MACH NUMBERS
OF 1.3, 1.4 AND 1.5**

by

W. G. Sawyer
Carol J. Long

*

DTIC
ELECTE
SEP 01 1983
S E

Procurement Executive, Ministry of Defence
Farnborough, Hants

DTIC FILE COPY

UNLIMITED

88 08 17 037

UDC 532.526.4 : 533.6.011.72

R O Y A L A I R C R A F T E S T A B L I S H M E N T

Technical Report 82099

Received for printing 27 October 1982

A STUDY OF NORMAL SHOCK-WAVE TURBULENT BOUNDARY-LAYER INTERACTIONS
AT MACH NUMBERS OF 1.3, 1.4 AND 1.5

by

W. G. Sawyer
Carol J. Long

SUMMARY

This Report presents the results of a study of seven flows involving the interaction between a normal shock wave and a two-dimensional turbulent boundary layer. The measurements were made at free-stream Mach numbers of 1.3, 1.4 and 1.5 and at Reynolds numbers based on an effective streamwise run of 10×10^6 to 30×10^6 . The results were obtained from comprehensive traverses with both pitot and static probes.

Standard boundary-layer integral parameters based on wall and measured static pressures are presented, together with velocity profiles and the Mach number distribution over the interaction region.

An investigation has been made of the 'law of the wall' and the 'law of the wake' under the influence of strong normal pressure gradients.

Departmental Reference: Aero 3532

Copyright
©
Controller HMSO London
1982

Accession For	
NTIS GRA&I	<input checked="" type="checkbox"/>
DTIC TAB	<input type="checkbox"/>
Unannounced	<input type="checkbox"/>
Justification	
By	
Distribution	
Availability	
Dist	
A	

LIST OF CONTENTS

	<u>Page</u>
1 INTRODUCTION	3
2 DESCRIPTION OF THE EXPERIMENT	4
2.1 Mechanical arrangement	4
2.2 Experimental measurements	6
2.2.1 Pitot measurements	6
2.2.2 Floor static pressure measurements	6
2.2.3 Reversed pitot measurements	6
2.2.4 Static probe measurements	6
2.2.5 Shock-wave position	7
3 REDUCTION OF DATA	7
3.1 Boundary-layer profiles	8
3.2 Integral parameters	9
3.2.1 Static pressure constant and equal to the measured wall pressure	10
3.2.2 Static pressure variation as measured	11
3.2.3 Equivalent inviscid static pressure together with measured static pressure	12
3.3 Skin friction	12
4 EXPERIMENTAL RESULTS	13
4.1 The general characteristics of the flow	13
4.1.1 Shock-wave patterns	13
4.1.2 Flow visualisation	13
4.1.3 Momentum balance	14
4.2 Edge Mach numbers and boundary layer parameters	16
4.3 Measured static pressures	17
4.4 Mach number distribution	17
4.5 Boundary-layer velocity profiles	18
4.5.1 General	18
4.5.2 Logarithmic velocity profiles	18
4.5.3 The law of the wall	19
4.5.4 Departures from equilibrium and the law of the wake	20
CONCLUSIONS	23
Appendix Static pressure probe corrections	25
Tables 1 to 3	30
List of symbols	94
References	96
Illustrations	Figures 1-33
Report documentation page	inside back cover

1 INTRODUCTION

A series of experiments¹⁻⁴ has been undertaken in the RAE Bedford 3ft x 3ft wind tunnel to investigate the interaction of a normal shock wave and a turbulent boundary layer at nominal upstream Mach numbers of 1.3, 1.4 and 1.5 over a Reynolds number range based on the undisturbed boundary-layer momentum thickness at the start of the interaction of 12×10^3 to 34×10^3 .

This Report deals with the measurements made at a series of stations upstream and downstream of the interaction using conventional pitot and static probes traversed normal to the flat wall.

The series of experiments was planned because of the lack of knowledge of the interaction between normal shock waves and turbulent boundary layers at high Reynolds numbers and the need to predict the development of the boundary layer through and beyond the interaction region as, for example, in the flow over supercritical aerofoils.

A number of investigations have been reported over the past two decades and broadly speaking three techniques have been used to produce the interaction.

The first and most commonly used technique (Fig 1a) in supersonic tunnels is to position a shock generator with downstream choking flap over a flat plate so that the steady normal shock wave formed by the shock generator interacts with a turbulent boundary layer grown from the leading edge of the flat plate. This is the technique adopted by Seddon⁵, Vidal, *et al*⁶ and Kooi⁷.

The second technique^{8,9} is used in transonic wind tunnels and involves mounting a two-dimensional bump on the wind tunnel wall so that the shock-wave boundary-layer interaction approximates to that on an aerofoil (Fig 1b). More recently, small supercritical aerofoils have been tested¹⁰ and in fact these two experiments have been combined by Burdges¹¹ who let the aerofoil into the tunnel floor and bled away the floor boundary layer under its leading edge.

Gadd¹² and more recently Mateer, Brosch and Veigas¹³ used a third technique which was to hold the normal shock wave steady in a supersonic tube by the adjustment of a conical choke downstream of the working section as in Fig 1c. The turbulent boundary layer under consideration was allowed to grow naturally along the tube wall.

For the present experiment the facility which was available was the RAE 3ft x 3ft transonic-supersonic wind tunnel. The arrangements of Fig 1a or 1b could have been employed, but it was argued that if the tunnel floor was used, then the measuring techniques would be simpler, a higher Reynolds number could be obtained, and the interference effects of the wall boundary layers should be less than in the technique of Fig 1a where the test boundary layer is of smaller thickness than the interfering wall boundary layers. The simple technique was therefore used of holding a shock wave across the test section, set up to run at supersonic speed, by means of an adjustable sonic throat which was situated far downstream of the test section. The technique is in fact similar to that of Fig 1c.

The 3ft x 3ft wind tunnel has a good Reynolds number capability (up to $12 \times 10^6/m$ for continuous running) is easily accessible for non-intrusive measurements and, above all, is easy to modify in the working section region having removable supersonic liners and downstream wooden fairings. A further advantage is that the pressure distribution in the working section is not only similar to that over a supercritical aerofoil but also the dimensions and Reynolds numbers approximate to full-scale conditions. A ninth scale (4 in x 4 in) model of the tunnel is also available and this proved invaluable for the development of the experiment.

The most time-consuming aspect of the development has been providing a suitable downstream sonic throat to control the shock-wave position and to keep it acceptably steady. However it was also necessary to design and manufacture a new raised false tunnel floor (to house submerged boundary-layer traverse mechanisms and to raise the boundary-layer interaction region into view above the bottom of the schlieren windows) which would match the three alternative half-nozzle blocks used to generate the required free-stream Mach numbers and which form the upper wall.

During the period of time taken to manufacture the new floor and the necessary associated equipment, two interim experiments were made, the first² using a conventional boundary-layer pitot rake and the second¹ using non-intrusive laser-Doppler measurements. The first experiment differed in another important aspect from the present one in that the pitot rake was attached to the tunnel floor in a single, fixed, position and the shock wave moved fore-and-aft of the rake.

For the present experiment the location of the shock wave was fixed for each condition tested and measurements were made with probes which could be traversed both normal to the tunnel floor and streamwise. Measurements of the static pressure distribution along the floor were also made.

2 DESCRIPTION OF THE EXPERIMENT

2.1 Mechanical arrangement

The general arrangement of the experiment is shown in Fig 2. The unmodified parts of the 3ft x 3ft wind tunnel are shown shaded.

In its standard form, the 3ft x 3ft wind tunnel has a working section with a fixed lower liner and interchangeable upper liners which are matched to the lower liner to give 0.1 incremental steps in Mach number between 1.3 and 2.0. One of the major modifications made to the tunnel was the provision of a new raised bottom liner together with a false floor (Fig 3). This false floor contained two pitot traverse mechanisms so that a region close to the floor centre line could be investigated from approximately 0.8 m ahead of the schlieren window centre line to 3 m downstream using a total horizontal traverse movement of little more than 2 m. Because of the interest in the free-stream Mach number range of 1.3 to 1.5, the new bottom liner was designed to match the $M = 1.4$ upper liner and the consequent slight mismatch with the $M = 1.3$ and $M = 1.5$ upper liners had to be accepted. Although raising the floor by 152 mm had the advantage of bringing the shock-wave interaction region into full view through the schlieren windows, it reduced the height of the working section so that the tunnel was no longer square in cross

section. There was however no particular disadvantage in this because the asymmetrical nozzle which generated the supersonic flow inevitably resulted in boundary layers which were not the same on all four walls.

The other major item of redesign as described in Ref 2 involved the careful fairing of the existing 'spoiler door' arrangement* in the diffuser section to give an adjustable second throat. By adjusting the throat, the normal shock wave could be placed in the desired location within the view through the tunnel windows. Any subsequent small progressive movement of the shock wave could then be corrected by adjusting the tunnel compressor speed. Initially there was a large random movement of the normal shock wave but this was reduced to about 20 mm by the careful fairing of the shape of the second throat. The mean position of the normal shock wave was checked both visually and by means of a differential pressure transducer connected between a wall static pressure hole under the shock wave and a reference tapping near the working section sonic throat.

The region between the working section and diffuser was faired to give smooth side-wall and roof contours. The geometry of the fairing was such as to give an expanding passage, the cross sectional area at the diffuser entry increasing to 1.067 times the area of the working section over a distance of 3660 mm. In the region of the interaction, the standard taper of 0.004 m/m was maintained on the top liner. This is normally combined with a similar taper on the lower liner to allow for boundary-layer growth on all four tunnel walls. However, for this experiment, the taper on the false floor was approximately 0.003 m/m.

The traverse mechanism together with a twin pitot probe is shown in Fig 4. Two identical traverse mechanisms were supported 1800 mm apart from a slide which was approximately 6 m long and sufficiently flexible to submerge, at its upstream end, below the liner surface approximately 1 m ahead of the schlieren window centre line, and at its downstream end to retract into a covered channel between the spoiler doors in the diffuser section. Any leaks around the slide were sealed by two pvc tubes which inflated when the slide was stationary as shown in Fig 3. A chain drive was used to move the slide in the streamwise direction. A total streamwise distance of 3800 mm could be covered using the tandem boundary layer traverses. The slide was positioned 100 mm to the port of the row of static pressure holes on the tunnel centre line and the probes were cranked so that vertical traverses could be made half way between the slide and the tunnel centre line. In this way it was hoped to reduce the various interferences, namely, of the probe on the wall static pressure holes, of the slight irregularity of the slide on the probe measurements, and of the probe stem on the probe measurements.

Repeatability of the probe position was ± 0.02 mm vertically and ± 3 mm horizontally.

Details of the static probes can be seen in Fig 5. The pitot probes were designed to be fairly short in order to avoid vibrations in the expected highly turbulent flow. The same overall dimensions were then retained for the twin static probes. With hindsight, the twin static probes might have been lengthened to diminish the interference

* Used in normal testing for controlling the tunnel shock wave during starting or stopping the tunnel.

caused by the supporting structure because the vertical positional accuracy is not quite as important for these probes as for the pitot probes. However this was not done and large corrections had to be applied to the static pressure measurements especially at transonic Mach numbers. These corrections are described in the Appendix.

All the probes were electrically insulated from their vertical traverse mechanisms so that a touch indicator could be used to set the pitot datum at the surface of the false floor. The streamwise datum was set by aligning the tip of a pitot probe or the holes in a static probe with a line marked on the surface of the false floor.

Pressure measurements were made with differential transducers (Druck) of range 69 kN/m^2 in two D-type scanivalves placed outside the tunnel shell. The transducers were calibrated against a Texas Instrument 0-203 kN/m^2 absolute quartz Bourdon-tube pressure-controller. Corrections were made to the primary slopes and zeros of these calibrations for each data point, by comparing the transducer outputs with reference pressures applied to the first and last pairs of scanivalve ports.

2.2 Experimental measurements

2.2.1 Pitot measurements

Measurements were made at three nominal Mach numbers, 1.3, 1.4 and 1.5 at Reynolds numbers of approximately $10 \times 10^6/\text{m}$ (the maximum continuous running value permitted for the experiment) and $3.5 \times 10^6/\text{m}$. An intermediate Reynolds number was also included for $M = 1.5$. Details of the test conditions are given in Table 1.

Traverses normal to the floor were made using the twin-pitot probe over a large number of stations from 0.7 m ahead of the normal shock wave to approximately 3 m downstream of the normal shock wave. In most cases, a vertical distance of 200 mm was covered. The forward pitot was removed while measurements were being made with the rear one, and a flush plug was used to fill the hole left in the slide.

2.2.2 Floor static pressure measurements

Measurements of the static pressure distribution on the floor were made with only the rear pitot in place, set at its furthest downstream position. These measurements were used to calculate the wall reference static pressure for each pitot or static pressure probe traverse.

2.2.3 Reversed pitot measurements

Measurements were also made with a single reversed pitot probe (rather similar in shape to static probe B (Fig 5) but reversed) for conditions of separated flow which occurred for $M = 1.5$. Separation was indicated by the forward-pointing pitot recording a lower pressure than the corresponding wall static pressure hole. The measurements were made with the tip of the reversed pitot in the same streamwise position as the normal pitot tube. Although the flow was probably disturbed by either probe, a simple correction was made to both sets of results as described under section 3.1.

2.2.4 Static probe measurements

Before the static pressure measurements in the boundary layer were begun, the static probes were calibrated in the centre of the slotted transonic working section of

the tunnel over a Mach number range of 0.4 to 1.2 and similar free-stream Reynolds numbers to those encountered in the main experiment. Each probe was held at the end of its stem furthest away from the probe tip by a specially manufactured sting. Static probe B was also calibrated while supported at the near end of its stem to check for support interference. This appeared to be negligible. The probe measurements were compared with wall static pressures obtained from a tunnel calibration referred to a 3° conical static head probe. This probe has been described in Ref 14 and within the limits of the required accuracy was assumed to have no static pressure errors.

The real problem which arose when using static probes in an environment which invoked the problems of transonic flow combined with pressure gradients, wall interference effects and the presence of boundary layers, lay in obtaining sufficient calibration data in a tunnel which could not be used between $M = 0.88$ and $M = 1.3$ while modified to take the false floor and traverse mechanisms.

However some information was forthcoming from twin static probe calibrations made through the floor boundary layer between $M = 0.66$ and 0.88 at similar Reynolds numbers to the main experiment. Additional information was obtained during the actual shock-wave boundary-layer interaction experiment from the static and pitot probe traverses ahead of the interaction, while further data were available from traverses 1 to 3 m downstream of the normal shock wave at $M = 1.3$. In all these cases it was assumed that there was no static pressure variation normal to the wall through each vertical boundary-layer traverse, and that the pressure was equal to the estimated wall value. Because the free-stream calibration showed no apparent Reynolds number effects, data at the highest Reynolds number from the experiment were used.

Time limitations meant that nearly all the boundary layer static traverses were made with the twin-static probe rather than the single probes and the static investigation was omitted for $M = 1.4$ at a Reynolds number of $3.5 \times 10^6/\text{m}$. Single static probes were in fact used only as a check on the validity of the results obtained from the twin probe. Traverses were made in rather different streamwise positions from those made with the pitot probes and each traverse contained about half the measurements made using the pitot.

2.2.5 Shock-wave position

A careful check was made of the shock-wave position using the output from the shock-position transducer and readings were only taken while the shock wave was within prescribed limits. Subsequently, during the analysis of the results, the average position of the normal part of the shock wave was ascertained from the large number of schlieren photographs taken for each set of tunnel conditions. This was necessary because there was an interval of a year between making the static pressure measurements and the pitot measurements. It was difficult to reset the shock wave in the same position, and so corrections had to be applied to make both sets of results compatible.

3 REDUCTION OF DATA

The data have been reduced as follows to produce the boundary layer profiles of Table 2 and the integral parameters of Table 3.

3.1 Boundary-layer profiles

These have been tabulated against y (the equivalent height of the pitot or static tube above the wall) where for pitot measurements

$$y = h + 0.15d \quad (1)$$

and for static measurements

$$y = h \quad (2)$$

where h = height of probe centre line above floor
and d = diameter of probe.

The profiles have been derived

- (a) assuming constant wall static pressure applied throughout each traverse,
- (b) using measured static pressures after correction (see Appendix).

Standard formulae were used to calculate Mach numbers, velocities and densities from the pitot and static results. Total temperature was assumed constant across the boundary layer except at the wall where a recovery factor of 0.89 was used. Wall static pressures were calculated for each traverse position by linear interpolation of the floor static measurements made with the front pitot removed and the rear pitot as far downstream as possible.

The flow was assumed reversed when the pitot pressure was lower than the wall static pressure. In such cases measurements were also made with the pitot tube reversed in direction. The Mach number was taken as the mean derived from the two sets of measurements. When the pitot tube was effectively facing downstream, it was assumed that the pressure recorded was that for a base with a pressure coefficient of -0.6. The wall static pressure was used for both sets of calculations in the reversed flow region.

Unit Reynolds numbers were calculated using the following formula based on Sutherland's law for viscosity

$$Re/m = \frac{M_\delta p_\delta}{T_\delta^2} (T_\delta + 110.4) \times 47.91 \times 10^3 \quad (3)$$

where subscript δ denotes conditions at the edge of the boundary layer

p is the static pressure in N/m^2

and T is the temperature in K.

A further parameter, namely p_i/p_{t0} has been presented where p_i is an estimated static pressure in the 'equivalent inviscid flow' (see Ref 15). The static pressure p_i is that in the equivalent inviscid flow which is defined as the flow external to the shear layers continued as an inviscid flow to the wall bounding the real flow with the growth of the viscous layer represented by transpiration at the boundary. p_i has been non-dimensionalised by dividing by the tunnel total pressure p_{t0} .

An estimate of p_i/p_{t0} has been attempted in the region ahead of the normal shock-wave. Here, the flow at the edge of the boundary layer is supersonic and influence lines of constant p/p_{t0} following Mach lines may be constructed back to the wall from the edge of the viscous region. An estimate of p_i/p_{t0} as a function of y for each traverse can then be made from the carpet of influence lines which are assumed straight and inclined at the Mach angle μ plus the flow inclination at $\delta_{0.999}$ (the distance from the wall where $U/U_\delta = 0.999$) viz

$$\mu + \tan^{-1}\left(\frac{V}{U}\right)_\delta$$

where

$$\left(\frac{V}{U}\right)_\delta = \frac{d\delta^*}{dx} - (\delta_{0.999} - \delta^*) \frac{d}{dx} \left(\ln(\rho_\delta U_\delta) \right) \quad (4)$$

and V is the vertical component of velocity
 U is the horizontal component of velocity
 δ^* is the displacement thickness
 ρ is the density.

It will be noted (see section 4.4) that there is a supersonic region at the edge of the boundary layer behind the normal shock wave for $M = 1.5$. However estimates of p_i/p_{t0} have not been included for this region because they become discontinuous in the region of the shock wave.

3.2 Integral parameters

Boundary-layer thickness parameters were obtained by trapezoidal integration. Velocity profiles were faired between the wall and the pitot position corresponding to 0.8 mm from the wall by applying East's prediction of the law of the wall¹⁶ in compressible boundary layers as a 20 point curve.

East's prediction is based on an incompressible law of the wall combined with a compressibility factor. For this experiment Cole's law of the wall¹⁷ has been used with the constants recommended at the Stanford conference¹⁸ namely

$$\frac{U}{U_\tau} = 5.62 \log \frac{yU_\tau}{\nu_\delta} + 5.0, \quad (5)$$

where U_τ is the friction velocity.

The form of East's prediction which is faired into Cole's law of the wall is

$$\frac{U}{U_\tau} = \frac{1}{F} \sin \left[F \left\{ 2K \ln \left(y^{*2} \frac{K}{D} + 1 \right) + D \left(1 - e^{-y^*/D} \right) \right\} \right], \quad (6)$$

where the compressibility factor

$$F = M_{\tau} \sqrt{\frac{\gamma(\gamma-1)}{2}} = \frac{U_{\tau}}{\sqrt{T_w}} \times 0.021033 ,$$

$$D = 8.73(1 + 45F^2) ,$$

$$y^* = y \frac{U_{\tau}}{v_w} ,$$

$$K = 0.41 ,$$

r being the recovery factor, and suffix w denoting wall values.

A value of U_{τ} was obtained at $y \approx 0.8$ mm using equation (6) and values of U/U_{τ} were then calculated for 20 equispaced values of y between 0 and 0.8 mm.

A linear variation was assumed between $y = 0$ and 0.8 mm for reversed flow.

The following definitions of the integral quantities have been used as first proposed by Myring¹⁹ and later incorporated in East's modified momentum integral equation¹⁵.

They are (where suffices i and w denote equivalent inviscid flow quantities and wall values respectively)

$$\bar{\delta} = \frac{1}{\rho_{iw} U_{iw}} \int_0^{\delta} (\rho_i U_i - \rho U) dy , \quad (7)$$

$$\bar{\theta} = \frac{1}{\rho_{iw} U_{iw}^2} \int_0^{\delta} \left\{ (\rho_i U_i^2 - \rho U^2) - U_{iw} (\rho_i U_i - \rho U) \right\} dy , \quad (8)$$

shape parameter $H = \frac{\bar{\delta}}{\bar{\theta}} , \quad (9)$

shape parameter $\tilde{H} = \frac{1}{\rho_{iw} U_{iw}} \int_0^{\delta} \rho (U_i - U) dy . \quad (10)$

The integral parameters were calculated for three different distributions of static pressure across the boundary layers as described in the following paragraphs.

3.2.1 Static pressure constant and equal to the measured wall pressure

Equations (7), (8), (9) and (10) reduce to the familiar standard integrals when static pressure is constant across the boundary layer giving

$$\text{displacement thickness} \quad \delta^* = \int_0^{\delta} \left(1 - \frac{\rho U}{\rho_{\delta} U_{\delta}} \right) dy, \quad (11)$$

$$\text{momentum thickness} \quad \theta = \int_0^{\delta} \frac{\rho U}{\rho_{\delta} U_{\delta}} \left(1 - \frac{U}{U_{\delta}} \right) dy, \quad (12)$$

$$\text{shape factor} \quad H = \frac{\delta^*}{\theta}, \quad (13)$$

$$\text{shape factor} \quad \bar{H} = \frac{1}{\theta} \int_0^{\delta} \frac{\rho}{\rho_{\delta}} \left(1 - \frac{U}{U_{\delta}} \right) dy. \quad (14)$$

$$\text{The energy thickness was also evaluated:} \quad \delta_E = \int_0^{\delta} \frac{\rho U}{\rho_{\delta} U_{\delta}} \left[1 - \left(\frac{U}{U_{\delta}} \right)^2 \right] dy. \quad (15)$$

3.2.2 Static pressure variation as measured

Equations (7), (8), (9) and (10) can be used in an 'intermediate form' as in Cook, McDonald and Firmin²⁰. In this form the boundary layer defect thicknesses are referred to a fictitious potential flow having the same static pressure distribution as that for the actual viscous flow and a total pressure equal to that at the edge of the boundary layer (p_{t1}).

Thus for example

$$M_p = \sqrt{5 \left[\left(\frac{p_{t1}}{p} \right)^{\frac{2}{\gamma}} - 1 \right]} \quad (16)$$

$$\text{where} \quad p_{t1} = p_{\delta} (1 + 0.2 M_{\delta}^2)^{3.5}. \quad (17)$$

The revised integral quantities are as follows:

$$\text{displacement thickness} \quad \delta^* = \frac{1}{\rho_w U_w} \int_0^{\delta} (\rho_p U_p - \rho U) dy, \quad (18)$$

$$\text{momentum thickness} \quad \theta = \frac{1}{\rho_w U_w^2} \int_0^{\delta} \left\{ (\rho_p U_p^2 - \rho U^2) - U_p (\rho_p U_p - \rho U) \right\} dy, \quad (19)$$

$$\text{shape factor} \quad H = \frac{\delta^*}{\delta} ,$$

$$\text{shape factor} \quad \bar{H} = \frac{1}{\theta} \frac{1}{\rho_w U_w} \int_0^{\delta} \rho_p (U_p - U) dy . \quad (20)$$

3.2.3 Equivalent inviscid static pressure together with measured static pressure

$\bar{\tau}$, $\bar{\theta}$, H and \bar{H} have already been defined by equations (7), (8), (9) and (10).

Equivalent inviscid static pressures were estimated as described in section 3.1 for traverse positions ahead of the normal shock. Equivalent inviscid Mach numbers were obtained from these pressures, and the total pressure calculated at the edge of the boundary layer (equation (17)) so that

$$M_i = \sqrt{5 \left[\left(\frac{P_{t_i}}{P_i} \right)^{\frac{2}{\gamma}} - 1 \right]} . \quad (21)$$

ρ_i and U_i were obtained from M_i using a temperature recovery factor of unity while the values of ρ and U were identical to those in section 3.2.2 (being calculated from the measured pitot and static pressures).

Linear interpolation was used to obtain ρ_i and U_i for the 20 points between the wall and $y \approx 0.8 \text{ mm}$.

3.3 Skin friction

Three estimates of skin friction are given.

The first estimate C_{f_p} has been deduced by considering the pitot tube when in contact with the wall to be a Preston tube and applying Patel's²¹ calibration as formulated by Head and Vasanta Ram²² and transformed for compressible flow by the method of Fenter and Stalmach²³.

The second and third estimates emerge directly from U_τ which was calculated by fitting East's law of the wall (equation (6)) to the pitot reading for $y \approx 0.8 \text{ mm}$. The second estimate was obtained assuming constant wall static pressure to apply across the boundary layer and the third was obtained using measured static pressures. Because at $y \approx 0.8 \text{ mm}$ wall static pressure applied for both cases, the differences are entirely due to the boundary layer edge conditions obtained from the different static pressures.

It will be noted that several values of C_f are missing from Table 3 and these omissions occur where reversed flow is indicated at $M = 1.5$.

4 EXPERIMENTAL RESULTS

4.1 The general characteristics of the flow

4.1.1 Shock-wave patterns

Fig 6a shows the vertical cross sections of the main interactions traced from schlieren photographs. Typical photographs have been reproduced in Fig 6b. For completeness, the calculated boundary layer thickness ($\delta_{0.995}$) and the start of the measured reversed flow regions at $M = 1.5$ have been added to the diagrams. The progression from the pattern at $M = 1.3$ of a single normal shock wave distorted by the influence of compression curves emanating from the thickening of the upstream boundary layer, to the established triple shock system with the shear layer emanating from the point of bifurcation at $M = 1.5$, is well illustrated. The increase in size of the shock system with reduction in Reynolds number can also be seen.

The main interaction region has been described in detail by East³ and the present results at high Reynolds numbers agree with his at $M = 1.3$ and 1.4 . However there is a discrepancy between the sets of results at $M = 1.5$. The shock bifurcation point for the present experiments is at 180 mm from the floor compared with a value, presumed to be erroneous, of 215 mm given by East.

4.1.2 Flow visualisation

After the completion of the traverse measurements the interaction region was examined by oil flow*.

Photographs of the surface oil flow were taken for all three Mach numbers at a Reynolds number of $10 \times 10^6/\text{m}$. These photographs, reproduced in Fig 7, were taken after shutting down the tunnel and removing the roof and therefore suffer from slight blurring. The viewpoint looks downstream. The photographs reveal mild three-dimensional effects for $M = 1.3$ and $M = 1.4$ but a much more complex pattern for $M = 1.5$ when the flow is separated. The photograph for $M = 1.5$ is shown in more detail in Fig 8 together with an attempted interpretation of the wall streamlines.

The nature of the flow in this case appears to be such that there is flow along the arch of a vortex connecting a position on the port side, denoted by B in Fig 8, to a position denoted by A on the starboard side. Thus in a sense A is an attachment node and B a separation node. It should be remarked that whilst the streamwise extent of this region is roughly 300 mm the probe measurements suggest its depth to be only 7 mm.

Near the tunnel centre line between the two vortex patterns, the flow is tolerably two-dimensional except in the immediate regions of the saddle points at the start and end of the separation region.

Presumably because of the non-uniform boundary-layer thickness on the tunnel side wall arising from the flow field associated with the asymmetrical nozzle, the separation line on the sidewall is swept and a single vortex node only of separation type is formed.

* The oil-flow mixture was an amalgam of the following in the ratio of 4 cc Vitrea F2, to 2 cc Limea 931, to 3 cc TiO_2 , to 2 drops of oleic acid.

The vortex arising from this node is presumed to create the strong convergence towards the tunnel centre line occurring in the corner regions downstream of the interaction. The lines D in Fig 8 have the appearance of separation lines but may in fact indicate only a locally strong convergence of the boundary layer.

4.1.3 Momentum balance

Momentum balance calculations have been made using a rearranged form of East's modified momentum integral equation¹⁵

$$\begin{aligned}
 \frac{d\bar{\theta}}{dX} + (H + 2 - M_{iw}^2) \frac{\bar{\theta}}{U_{iw}} \frac{dU_{iw}}{dX} - \frac{\tau_w}{\rho_{iw} U_{iw}^2} \\
 \quad \text{①} \qquad \qquad \qquad \text{②} \\
 = - \frac{1}{2\rho_{iw} U_{iw}^2} \frac{d}{dX} \left\{ \rho_{iw} U_{iw}^2 \left(\frac{d^2 \bar{\delta}}{dX^2} + \kappa \right) (\bar{\theta} + \bar{\delta})^2 \right\} + \kappa (\bar{\theta} + \bar{\delta}) \frac{d\bar{\delta}}{dX} \\
 \quad \text{③} \\
 + \frac{1}{\rho_{iw} U_{iw}^2} \frac{d}{dX} \left\{ K \rho_{iw} U_{iw}^2 \bar{\theta} \left(\frac{\bar{H} - 1}{\bar{H}} \right) \right\} + \frac{M_{iw}^2 \bar{\theta} V_{iw}}{U_{iw}^2} \frac{dV_{iw}}{dX} . \quad (22)
 \end{aligned}$$

The last term has been neglected in the analysis because it is small and in any case cannot be evaluated with any reliability. The remaining terms in the right hand side of the equation are:

- ① the normal pressure gradient effect arising from the wall and stream curvature;
- ② the approximation to the direct effect of wall curvature on the flow momentum;
- ③ the approximation to the normal stress terms.

The integral parameters, H , \bar{H} , $\bar{\theta}$ and $\bar{\delta}$ are defined in equations (7) to (10) while ρ_{iw} , U_{iw} and M_{iw} are respectively the equivalent inviscid values of density, horizontal component of velocity and Mach number at the wall.

The surface curvature κ is zero for this example leaving

$$\begin{aligned}
 \frac{d\bar{\theta}}{dX} + (H + 2 - M_{iw}^2) \frac{\bar{\theta}}{U_{iw}} \frac{dU_{iw}}{dX} - \frac{\tau_w}{\rho_{iw} U_{iw}^2} \\
 = - \frac{1}{2\rho_{iw} U_{iw}^2} \frac{d}{dX} \left\{ \rho_{iw} U_{iw}^2 \frac{d^2 \bar{\delta}}{dX^2} (\bar{\theta} + \bar{\delta})^2 \right\} + \frac{1}{\rho_{iw} U_{iw}^2} \frac{d}{dX} \left\{ K \rho_{iw} U_{iw}^2 \bar{\theta} \left(\frac{\bar{H} - 1}{\bar{H}} \right) \right\} . \quad (23)
 \end{aligned}$$

After multiplying throughout by $\rho_{iw} U_{iw}^2$ and rearranging, the equation becomes

$$\frac{d}{dX} (\rho_{iw} U_{iw}^2 \bar{\theta}) = \tau_w - H \rho_{iw} U_{iw} \bar{\theta} \frac{dU_{iw}}{dX} + \frac{d}{dX} (f \rho_{iw} U_{iw}^2 \bar{\theta}) , \quad (24)$$

where $f = f_1 - f_2$,

$f_1 = 0.072 \left(\frac{\bar{H} - 1}{\bar{H}} \right)$, and is the contribution due to the normal stress,

and $f_2 = \frac{1}{2} \frac{d^2 \bar{\delta}}{dX^2} \frac{1}{\bar{H}} (\bar{H} + \delta^2) = \frac{1}{2} \frac{d^2 \bar{\delta}}{dX^2} (1 + H) (\bar{\theta} + \bar{\delta})$ and is the contribution due to the stream curvature

If suffix 0 represents the conditions at the start of the interaction, then dividing through by $\rho_{iw0} U_{iw0}^2 \bar{\theta}_{iw0}$ and integrating, results in the form of the momentum integral equation used in the momentum balance calculations shown in Fig 9:

$$\left[\frac{\rho_{iw} U_{iw}^2 \bar{\theta}}{\rho_{iw0} U_{iw0}^2 \bar{\theta}_0} - 1 \right] = \int_{X_0}^X \frac{C_f}{2} \frac{\rho_e U_e^2}{\rho_{iw0} U_{iw0}^2 \bar{\theta}_0} dX - \frac{1}{2} \int_1^{\left(\frac{U_{iw}}{U_{iw0}} \right)^2} \frac{\rho_{iw} \bar{\delta}}{\rho_{iw0} \bar{\delta}_0} d \left(\frac{U_{iw}}{U_{iw0}} \right)^2 + \left(\frac{f \rho_{iw} U_{iw}^2 \bar{\theta}}{\rho_{iw0} U_{iw0}^2 \bar{\theta}_0} - f_0 \right) . \quad (25)$$

In Figs 9 and 11 $\left(\frac{\rho_{iw} U_{iw}^2 \bar{\theta}}{\rho_{iw0} U_{iw0}^2 \bar{\theta}_0} - 1 \right)$ is called the left hand side while the remainder

of the expression is called the right hand side. The numbered terms are identified later (in Fig 12) as the contributions due to

- ④ skin friction
- ⑤ pressure gradient.

Both sides of equation (25) were calculated using the alternative assumptions of section 3.2 which were (for traverses across the boundary layer):

- (a) static pressure constant and equal to the measured wall pressure;
- (b) static pressure as measured;
- (c) equivalent inviscid static pressure together with measured static pressure. The equivalent inviscid static pressure was calculated for traverses ahead of the shock wave only.

Fig 9 shows the comparison between the left hand side and the right hand side of equation (25) plotted against the streamwise position. The calculations were made using assumption (c). It will be seen that the momentum balance is good over the main interaction region and only becomes significantly in error at approximately 800 mm downstream of the normal shock wave. Downstream of this point, the left hand side actually reduces for Mach numbers ahead of the interaction of 1.4 and 1.5. This indicates a flow divergence and it is interesting to calculate its magnitude.

In terms of equation (22) Green *et al*²⁴ showed that a flow divergence could be accounted for by subtracting the local rate of divergence $\bar{\theta}(d\phi/dz)$ from the right hand side. This quantity represents the rate of the deviation relative to the nominal flow direction with respect to distance Z perpendicular to the flow but parallel to the surface.

In equation (25) this divergence takes the form

$$\int_{x_0}^x \frac{\rho_{iw} U_{iw}^2 \bar{\theta}}{\rho_{iw0} U_{iw0}^2 \bar{\theta}_0} \frac{d\phi}{dz} dx$$

and this can be added to the left hand side. It is therefore easy to make an estimate of $d\phi/dz$.

This estimate is shown in Fig 10a-c in degrees per metre. For points further downstream of the normal shock wave than 300 mm the figures show a flow divergence of $7^\circ/\text{m}$ at $M = 1.3$ rising to $15^\circ/\text{m}$ at $M = 1.5$ (equivalent to 7° and 15° over the tunnel width). The wild fluctuations within the main interaction region are of course due to the rapidly changing conditions and the close streamwise spacing of the traverse positions.

Assumptions (a), (b) and (c) were used to provide comparisons of both sides of the momentum integral equation as shown in Fig 11. There appears little to choose between the momentum balance using any of these assumptions. However it is possible to see some improvement using assumption (b) rather than (a). If the region ahead of the shock wave is examined there is again some improvement if calculation assumption (c) is used.

Fig 12 shows the individual contributions to the right hand side of equation (25).

4.2 Edge Mach numbers and boundary layer parameters

Fig 13a-c shows the development of the Mach number at the edge of the boundary layer, M_δ , the boundary-layer displacement thickness, δ^* , the shape factor H , defined by equation (13), the boundary layer thickness, $\delta_{0.995}$, the skin friction coefficient C_{f_p} (section 3.3), and the shape factor \bar{H} defined by equation (14), all plotted against the longitudinal distance X from the normal part of the shock wave. The results in Fig 13 were calculated assuming constant static pressure, p_w , across the boundary layer normal to the tunnel wall. Further graphs of M_δ , δ^* , H and \bar{H} (Fig 14a-c) show the effect of using measured static pressures to calculate these parameters. The longitudinal region covered by these figures is from 500 mm ahead to 500 mm downstream of the normal shock wave. Outside this region it was assumed that the static pressures were constant normal to the wall and equal to the static pressures used in the first set of calculations (see Fig 15a&b and the Appendix).

Overall there appears to be little effect of variation of Reynolds number on the shape factors and the normalised variation of δ^* and $\delta_{0.995}$. A separation bubble occurs under the interaction region at $M = 1.5$ and its extent is indicated by the zero values of C_{f_p} . The bubble size decreases slightly with increase in Reynolds number. The shape of the bubble can, however, be seen in the plots of Mach number distribution, Fig 16a-f, and will be described in section 4.4.

The results agree broadly with those obtained in Ref 2 where a fixed pitot rake was used on the standard tunnel floor. However discrepancies begin to creep in 1 m downstream of the normal shock wave where in Ref 2 the Mach number at the start of the interaction was affected by the proximity of the tunnel throat. The results from Ref 2 at $M = 1.5$ were much more sensitive to Reynolds number in the interaction region and this was probably due to pitot-rake interference. One other point should be noted (and it can be seen in nearly all the following figures) and that is that the rehabilitation process behind the normal shock wave has not been completed after 3 m. This distance is equivalent to at least 400 times the undisturbed displacement thickness ahead of the interaction. It can be seen in Fig 13a-c that the edge Mach numbers, shape factors and boundary layer thicknesses have not yet reached their asymptotic values at the furthest downstream traverse positions.

4.3 Measured static pressures

Static pressure distributions normal to the wall are plotted on scale diagrams of the main interaction region in Fig 15a&b as the difference from the corresponding wall static pressure non-dimensionalised by dividing by the undisturbed stagnation pressure. Zero values are located at the appropriate streamwise station.

As described in the Appendix, the static pressure results have usually been made to merge into the appropriate wall values at floor level, however wall static values have been assumed to apply throughout the separated region in the absence of reliable local values. Static pressures recorded very close to the shock wave may have been affected by its movement and so local pressure gradients may have been reduced.

The diagrams show the expected static pressure variation throughout the main interaction region. The static pressures are fairly constant across the inner part of the shear flow and then decrease outwards across the compression region ahead of the normal shock wave to free-stream values. Behind the main shock wave they increase from one fairly constant level near the wall to a second level behind the normal part of the shock wave.

4.4 Mach number distribution

Mach number contours are plotted in Fig 16a-f over the main interaction region and over the whole of the region investigated downstream of the normal shock wave (note the change of streamwise scale). Measured pitot and the corrected static pressures were used to calculate Mach numbers and the figures result from linear interpolations of Mach number profiles in the vertical direction and from horizontal plots of Mach numbers at constant distances from the wall, y .

The results are therefore dependent on the accuracy of the corrected static pressure measurements and the interpolation procedures which are affected most critically by the smearing effect of the slightly unsteady shock wave. However the results in the interaction region are broadly confirmed by the laser-Doppler anemometer measurements of East³ and the results of Kooi⁷ at $M = 1.4$. A particular feature is the development of the supersonic tongue beneath the downstream shock wave for $M = 1.5$.

If East's and the present results at a Reynolds number of $10 \times 10^6/\text{m}$ are compared in slightly more detail, the Mach number contours are in good agreement ahead of the normal shock wave if due allowance is made for the smearing effect of the unsteady shock wave (see above). Very similar supersonic tongues may be seen behind the shock wave and they continue downstream (in both experiments) for 100 mm near the edge of the boundary layer. East's results at $M = 1.5$ do not cover the full extent of the supersonic tongue but show that it is more extensive than at $M = 1.4$. In fact the present experiment confirms that it persists near the edge of the boundary layer for 400 mm downstream of the shock wave while at a Reynolds number of $3.5 \times 10^6/\text{m}$ it persists for 600 mm.

It is difficult to be specific about the shape of the supersonic tongue immediately downstream of the trailing shock wave, but the present results agree well with Kooi⁷ who also used pitot and static pressure measurements. The rear shock wave appears to terminate at the edge of the boundary layer so that supersonic flow appears to exist above the boundary layer behind a normal shock wave.

There is evidence to suggest that the thin shear layer formed downstream of the shock bifurcation point is still intact 3 m behind the normal shock wave, and even at $M = 1.3$ there is no sign that the inviscid flow has recovered sufficiently to provide a uniform Mach number contour across the tunnel.

The other point of interest is the separation region at $M = 1.5$. There appears to be a small decrease in the overall dimensions of the separation bubble with increase in Reynolds number. In fact the length of the separation bubble is reduced from 300 mm at $Re/\text{m} = 3.5 \times 10^6$ to 200 mm at $Re/\text{m} = 10 \times 10^6$ while the height is reduced slightly from just over 9 mm at the lowest Reynolds number to 7 mm at the highest Reynolds number. This result is in disagreement with Sawyer *et al.*² where a much greater reduction in bubble size was indicated although as stated in section 4.2 the conditions were somewhat different.

4.5 Boundary-layer velocity profiles

4.5.1 General

Boundary-layer profiles are shown in Fig 17a-f plotted on a scale diagram of the main interaction region together with an extended diagram on a compressed scale showing the whole region of measurement behind the normal shock wave.

The figures indicate the general characteristics of the boundary-layer development. They show the progression from the undisturbed state through the leading compression which influences the shape of the outer part of the boundary layer, through the subsequent separation or near-separation region, to the final recovery towards a zero-pressure-gradient form for the profiles. It can be seen even on the small scale diagrams that the profiles are still disturbed after a distance of nearly 3 m downstream of the normal shock wave, or approximately 400 times the undisturbed displacement thickness.

4.5.2 Logarithmic velocity profiles

Representative velocity profiles are plotted in the logarithmic form adopted by Winter and Gaudet²⁵ as (U/U_τ^i) against $\log(yU_\tau^i/\nu_\delta)$ where U_τ^i is the equivalent

incompressible friction velocity. Values of U_τ^i were derived from the skin friction coefficient C_{f_p} using the formula

$$U_\tau^i = U_\delta \left(\frac{C_{f_p}}{2} \right)^{\frac{1}{2}} (1 + 0.2M_\delta^2)^{\frac{1}{2}} . \quad (26)$$

C_{f_p} was obtained by treating the pitot tube when in contact with the wall as a Preston tube and using the calculation method described in section 3.3.

The results are plotted separately for three regions. Fig 18 shows the undisturbed velocity profiles just ahead of the interaction region. These profiles were used to define the undisturbed conditions of Table 1. The profiles far downstream of the interaction region are shown in Fig 19. Fig 20 shows typical profiles just downstream of the main interaction region.

4.5.3 The law of the wall

Figs 18 to 20 show typical 'law of the wall' fits for small values of y (the distance from the wall). The law of the wall is defined in the form adopted by Winter and Gaudet²⁵ as

$$\frac{U}{U_\tau^i} = \frac{1}{\kappa} \ln \left(\frac{yU_\tau^i}{\nu_\delta} \right) + \phi(0) , \quad (27)$$

which may be expressed as

$$\frac{U}{U_\tau^i} = A \log \left(\frac{yU_\tau^i}{\nu_\delta} \right) + B . \quad (28)$$

The results have been compared with Winter and Gaudet's incompressible law of the wall

$$\frac{U}{U_\tau^i} = 6.05 \log \left(\frac{yU_\tau^i}{\nu_\delta} \right) + 4.05 , \quad (29)$$

and with Coles' incompressible form (equation (5))

$$\frac{U}{U_\tau^i} = 5.62 \log \left(\frac{yU_\tau^i}{\nu_\delta} \right) + 5.0 .$$

Coles' incompressible law of the wall is usually applied to compressible flow by making use of the Van Driest²⁶ transformation. It was therefore necessary to confirm that the transformations of Van Driest and Winter and Gaudet gave similar results when applied to the compressible profiles of the present experiment. Two profiles were checked and are plotted using both transformations in Figs 18 and 19. The first profile had a free-stream Mach number of 1.54 and was in the undisturbed region ahead of the

interaction region, while the second profile had a free-stream Mach number of 0.83 and was from a pitot traverse made 2759 mm downstream of the normal shock wave. It can be seen that both transformations gave identical values of A and B although the wake components were very different at the free-stream Mach number of 1.54 (Fig 18). Because both transformations gave identical values of A and B Coles' incompressible law of the wall has been presented in the form adopted by Winter and Gaudet.

It would appear from Fig 18 that within the data scatter there is little to choose between the forms of the law of the wall due to Coles and due to Winter and Gaudet.

The average fit made to all the profiles ahead of the interaction region is

$$\frac{U}{U_{\tau}^i} = 6.16 \log \frac{yU_{\tau}^i}{\nu_{\delta}} + 3.6 \quad (30)$$

which is somewhat closer to the latter.

However behind the normal shock wave (Figs 19 and 20) the average fit becomes

$$\frac{U}{U_{\tau}^i} = 4.77 \log \frac{yU_{\tau}^i}{\nu_{\delta}} + 6.6 \quad (31)$$

which is quite different from equation (30).

Equations (30) and (31) were obtained by fitting the best straight lines (using the method of least squares) to the linear logarithmic regions close to the wall and averaging the results ahead of, and downstream of, the normal shock wave. Straight line fitting was not attempted when there were less than eight measured points in the linear region, or when the pitot traverse results contained reversed flow. The two traverse positions that were closest to the wall were omitted when fitting best straight lines.

Fig 21 shows the variation of A and B with streamwise position for each undisturbed free stream condition. It demonstrates most clearly the reduction in A accompanied by an increase in B for the boundary-layer traverse positions downstream of the normal shock wave. There does not seem to be any consistent variation of A and B with Reynolds number.

It would appear therefore that either large perturbations or normal pressure gradients affect the law of the wall, in a way which implies an increase in the eddy viscosity.

4.5.4 Departures from equilibrium and the law of the wake

An attempt has been made to demonstrate violent departures of the flow from equilibrium by extracting from the measurements the parameters used to describe the equilibrium locus in integral models of turbulent boundary layers. The analysis is further extended in terms of the character and magnitude of the wake component.

In order to deal with separated flows, East, Smith and Merryman²⁷ redefined the usual parameters

$$G = \frac{\bar{H} - 1}{\bar{H}} \sqrt{\frac{2}{C_f}}, \quad (32)$$

$$\Pi = - \frac{2\delta^*}{C_f U_\delta} \frac{dU_\delta}{dX} \quad (33)$$

as
$$E_f^i = \frac{1}{G^2}, \quad (34)$$

and
$$E_p^i = \frac{\Pi}{G^2}, \quad (35)$$

thus removing the difficulty created as the skin friction coefficient passes through zero and becomes negative. With an empirically derived allowance for compressibility, the parameters become

$$E_f = \frac{1 + 0.04M_\delta^2}{G^2} \quad (36)$$

$$E_p = \frac{\Pi}{G^2} (1 + 0.04M_\delta^2). \quad (37)$$

In Fig 22, the loci for the measured boundary layer developments are compared with the equilibrium locus

$$E_f = 0.024 - 0.8E_p \quad (38)$$

which is substantiated by experiment for attached flow and tentatively assumed in Ref 27 to remain valid in separated flow.

Points to the right and left of the equilibrium locus correspond respectively to stronger and weaker adverse pressure gradients than those appropriate to equilibrium flow. Negative values of E_p represent favourable pressure gradients, while negative values of E_f represent separation.

In Fig 22 the results for each set of test conditions have been plotted using symbols to represent the following regions

- A represents equilibrium conditions ahead of the main interaction;
- B represents the strongly adverse pressure gradient under the leading compression (which causes separation at $M = 1.5$);
- C represents the rapid recovery just downstream of the normal shock wave;
- D represents the remainder of the flow which might be expected to approach equilibrium conditions.

Points on the loci where there are changes from one region to the next are indicated by the numerals 1 to 3.

The loci show that region A is approximately in equilibrium but the rapid rise of E_p while E_f only falls slowly in region B indicates that the boundary layer lags in its response to the strong adverse pressure gradient under the leading compression. In region C, E_p recovers rapidly to the equilibrium locus but then overshoots before returning. E_f only starts to increase after E_p has overshoot the equilibrium locus and this again indicates a lag in the response of the boundary layer to a change in pressure gradient. The failure of the boundary layer to return to the equilibrium locus far downstream (in region D) may be interpreted as a further indication of the persistently disruptive effect of the shock-wave boundary-layer interactions on the velocity profiles already detected in the law of the wall as shown in Fig 21.

On the other hand the wake components of the profiles, remain fairly close to the standard shape as shown in Figs 23 and 24. In these figures the normalised wake components have been plotted in the following way. Fig 23a shows the undisturbed wake components in region A, and the results under the first compression through which it is possible to fit a law of the wall are shown in Fig 23b. Fig 24a-c has been produced by grouping similar normalised wakes into one diagram. In fact Fig 24a&b covers the rapid recovery region C together with the beginning of D, while Fig 24c covers the downstream part of region D.

According to Winter and Gaudet²⁵ the law of the wake for compressible boundary layers in zero pressure gradients is

$$\frac{\Delta U}{U_\tau^i} = 0.89 \left[1 + \sin \frac{\pi}{0.707} \left(\frac{y}{\delta_{0.999}} - 0.483 \right) \right] . \quad (39)$$

which after normalisation and allowance for the difference between $\delta_{0.999}$ and $\delta_{0.995}$ becomes

$$\left(\frac{\Delta U}{U_\tau^i} \right)_N = 0.5 \left[1 + \sin \frac{\pi}{0.818} \left(\frac{y}{\delta_{0.995}} - 0.529 \right) \right] , \quad (40)$$

where the normalised wake component $\left(\Delta U / U_\tau^i \right)_N$ has been obtained by dividing the wake component by the maximum value for each traverse. The shape of the normalised wake components has been plotted in Figs 23 and 24. On each figure a curve in the form of equation (40) is shown with the constants adjusted to fit the particular set of results.

The maximum values of the wake component for each traverse $\left(\Delta U / U_\tau^i \right)_{\max}$ are plotted in Fig 25 against E_f . In Fig 25a the results for regions A and B ahead of the normal shock wave are given while the results downstream of the normal shock wave (in regions C and D) are shown in Fig 25b. It will be seen in Fig 25a that apart from the boundary layer profiles that have been perturbed by the leading edge of the strong compression, the maximum values of the wake components are in good agreement with the locus obtained from the equilibrium family of boundary layers described by East, Sawyer and Nash²⁸. However, in Fig 25b for locations downstream of the disruptive effect of the strong pressure gradient (points in the regions C and D downstream of the normal shock wave) the results depart considerably from the equilibrium locus.

The different behaviour upstream and downstream of the shock wave is illustrated further in Fig 26 where calculated values of J and K are plotted against the equilibrium parameter E_f . The values of J and K were obtained by fitting sine waves of the form

$$\left(\frac{\Delta U}{U_i^i}\right)_N = 0.5 \left[1 + \sin \frac{\pi}{J} \left(\frac{y}{\delta_{0.995}} - K \right) \right], \quad (41)$$

to the wake components for each boundary layer profile.

It should be noted that because of the quantity of data recorded, the values of $\left(\Delta U/U_i^i\right)_{\max}$ were taken at that y -position of the pitot probe which gave a maximum value rather than estimating the true value by curve fitting. This in part accounts for the spread of values of J . No attempt was made to investigate the region B under the first compression.

However in the undisturbed equilibrium boundary layers of region A, the averaged values of J and K result in a normalised law of the wake

$$\left(\frac{\Delta U}{U_i^i}\right)_N = 0.5 \left[1 + \sin \frac{\pi}{0.819} \left(\frac{y}{\delta_{0.995}} - 0.494 \right) \right] \quad (42)$$

which is extremely close to Winter and Gaudet's law (equation (40)). The average value of $\left(\Delta U/U_i^i\right)_{\max}$ for region A is 2.23 which is rather higher than Winter and Gaudet's value of 1.78 (equation (39)).

In the region downstream of the shock wave (Fig 26b) the parameters J and K show an appreciable variation with E_f . Thus in this region the velocity profiles cannot be represented by a family having either a standard law of the wall (section 4.5.3) or a standard form of the law of the wake.

5 CONCLUSIONS

Seven flows have been studied involving the interaction of normal shock waves with nominally two-dimensional turbulent boundary layers over a range of Mach numbers of 1.3 to 1.5 and of Reynolds numbers based on an effective streamwise run of 10×10^6 to 30×10^6 . The data extend from 700 mm upstream to 3000 mm downstream of the normal shock-wave position. These distances are equivalent to respectively 90 and 400 times the undisturbed boundary layer displacement thickness.

Oil flow investigations on the floor under the main interaction region indicate a highly three-dimensional flow at $M = 1.5$, but the results and momentum balance calculations support the view that this three-dimensionality is confined to the separation region. This region is very shallow having a depth of less than 10 mm and streamwise extent of 300 mm while the flow in the region of the tunnel centre line is tolerably two-dimensional, except in the immediate regions of the saddle points at the start and end of the separation. Further downstream of the main interaction region, the momentum balance calculations indicate a slight flow divergence over the width of the tunnel of between 7° at $M = 1.3$ to 15° at $M = 1.5$.

14

In calculating the momentum balance, use has been made of corrected static pressure measurements and an attempt has been made to follow the recent ideas of matching the free-stream conditions with the viscous layer by defining an equivalent inviscid flow.

A method has been evolved for correcting the static pressure measurements made with the twin static pressure probe used in the experiment, and static pressure distributions normal to the wall within the main shock-wave boundary-layer interaction are presented. Combined with pitot measurements this enables the Mach number distribution to be obtained.

The results agree with the laser measurements of East³ which cover a more limited area. The present experiment has also produced more detail of the separated region. Good agreement is also noted with Kooi's⁷ results at $M = 1.4$.

All the measurements confirm that the flow has not stabilised after 3 m downstream of the normal shock wave (or 400 times the undisturbed displacement thickness). Here the main shear layer which is produced at the bifurcation point of the shock waves at $M = 1.4$ and 1.5 is intact and there are still velocity gradients across the tunnel in the inviscid flow. Also the boundary-layer profiles have not recovered to the equilibrium shapes.

The analysis in terms of the law of the wall and the law of the wake for the region ahead of the interaction agree fairly closely with Winter and Gaudet (equation (29)) and others (equation (5)). However the evidence downstream of the normal shock wave suggests that the law of the wall has been changed by the large perturbations or normal pressure gradients. However a single law of the wall may be used for the whole region behind the main disturbance.

A normalised version of Winter and Gaudet's law of the wake (equation (40)) provides a fair estimate for the shape of the normalised wake components ahead of the normal shock wave. The disruptive effects of the normal shock waves appear mainly as changes in amplitude of the normalised wake components, but the form of the wake component is also changed.

Apart from the boundary layers immediately affected by the leading edge of the first compression, the maximum values of the wake function ahead of the normal shock wave have a similar correlation with the equilibrium function E_f (equation (36)) as the equilibrium family of flows of East, Sawyer and Nash²⁸. Although the maximum values of the wake functions downstream of the normal shock wave also correlate with E_f , they correlate in a quite different way from that expected for equilibrium boundary layers.

Appendix

STATIC PRESSURE PROBE CORRECTIONS

A.1 Calibration measurements

As stated previously (section 2.2.4) the corrections to be applied to the static pressure probes were based on limited measurements made in the free stream at transonic speeds together with the results of the calibrations of the twin static pressure probe by traverses through the floor boundary layers at free-stream Mach numbers between 0.66 and 0.88. Additional information was derived during the actual experiment from the static and pitot traverses ahead of the interaction region at free-stream Mach numbers of 1.3, 1.4 and 1.5. Data was also used from the static and pitot traverses made through the boundary layer 1 to 3 m downstream of the normal shock wave at $M = 1.3$. It was assumed that for all these regions the static pressure for each traverse was constant and equal to the wall value, p_w .

The results of the free-stream calibrations are shown in Fig 27 where the differences between the measured and actual static pressures are presented as pressure coefficients based on local conditions plotted against Mach number. Also (shown dotted) are the calibrations after three stages of smoothing which were used to correct the static pressure readings made under the severe velocity gradients of the region investigated (section A.2.2). There was no apparent Reynolds number effect on the calibrations but time limitations precluded much use of the single static pressure probes. The correction method described, therefore applies only to the twin static pressure probe. No static measurements were made at $M = 1.4$ for a unit Reynolds number of $3.5 \times 10^6/m$.

A.2 The correction method applied to the twin static pressure probe

Fig 28a&b shows typical static pressure measurement errors incurred while making boundary layer traverses with the twin static pressure probe. The boundary layers had constant static pressures normal to the wall.

The errors have been presented as the differences between the measured and actual static pressures and are shown as pressure coefficients based on local conditions. They are plotted against the distance from the wall, y , non-dimensionalised by dividing by the boundary layer thickness $\delta_{0.995}$.

Fig 28a shows typical errors when the maximum Mach number is less than the critical value of 1.098 (the point at which the free-stream calibration errors are shown in Fig 27, to become negligible). The errors have a different character if the maximum Mach number for the traverse is above the critical value as shown in Fig 28b. It is therefore convenient to divide the errors to be corrected into two categories:

- (1) when the outer static pressure probe is at a Mach number of less than or equal to 1.098;
- (2) when the outer static pressure probe is at a Mach number greater than 1.098.

This is a not unreasonable assumption because the main source of error in the free-stream calibrations and the static traverse measurements made away from the influence of the wall, can be shown to be mostly due to the interconnecting stem between the inner and outer static pressure probes (see Fig 27 and Read, Pope and Cooksey²⁹, pp 102&103). Therefore the main correction to be applied to the inner static probe depends on some estimate of the mean Mach number over the connecting stem provided the static pressure probes are both at Mach numbers below the critical 1.098. If however, the outer static probe is at a Mach number above this critical value, then there is no interference associated with the interconnecting stem in the region of the outer static probe. In this case a suitable course of action is to use the local Mach number to estimate the correction due to the interconnecting stem on the pressure measured by the inner static probe.

It is now proposed to deal with the errors in more detail by considering the three regions A, B and C indicated in Fig 28 in conjunction with the Mach number of the outer static pressure probe.

A.2.1 Region A

The error in this region is treated as arising mainly from wall interference. There is however some compressibility effect. The errors are presented in law of the wall terms for correlation purposes (Figs 29 and 30). Fig 29 shows the accumulated errors resulting from the subsonic boundary-layer traverses, while Fig 30 shows the errors resulting from the undisturbed boundary-layer traverses ahead of the interaction region at free-stream Mach numbers of 1.3, 1.4 and 1.5. To calculate the corrections, the errors of region A may be added to those of region B. However because the errors of regions B and C are based on local conditions rather than the conditions at the edge of the boundary layer used for region A, the region A errors are multiplied by a factor $M(M_\delta)^2$ to bring them into line.

Thus the corrections needed for the static pressure measurements made in region A are given by

$$C_{PA} = \frac{P_m - P}{\frac{1}{2}\rho U^2} = C_f \left(\frac{M_\delta}{M} \right)^2 f_n \left(\frac{yU_\tau}{\nu_\delta}, M \right).$$

A.2.1.1 Outer static pressure probe at $M \leq 1.098$

The measurement errors shown in Fig 29 have been presented as

$$\left(\frac{P_m - P_w}{\frac{1}{2}\rho_\delta U_\delta^2} \right) \frac{1}{C_f}$$

and plotted against yU_τ/ν_δ . The corrections needed are actually fairly small (for the Mach numbers are low) and so a single correction has been used and this is represented by the continuous line in the figure. The correction is given by

$$\begin{aligned}
 C_{p_A} &= 15C_f \left(\frac{M_\infty}{M} \right)^2 && \text{when } \frac{yU_\infty}{v_\infty} < 644 \\
 C_{p_A} &= C_f \left(\frac{M_\infty}{M} \right)^2 \left[50.37 - 5.469 \ln \left(\frac{yU_\infty}{v_\infty} \right) \right] && \text{when } 644 \leq \frac{yU_\infty}{v_\infty} < 1000 \\
 C_{p_A} &= 0 && \text{when } \frac{yU_\infty}{v_\infty} \geq 1000 .
 \end{aligned}$$

A.2.1.2 Outer static pressure probe at $M > 1.098$

Fig 30 shows the pressure measurement errors plotted in similar terms to those used in section A.2.1.1. Here the results are strongly Mach-number dependent. The corrections have been applied on the assumption that the pressure measurement errors in Fig 30 have a linear relation with Mach number for constant yU_∞/v_∞ . The slopes and zero intercepts of this linear variation are then assumed to be entirely dependent upon yU_∞/v_∞ . The corrections which are shown by the continuous lines in Fig 30 are given by

$$C_{p_A} = FC_f \left(\frac{M_\infty}{M} \right)^2 \left[M - 0.2725 - 0.1153 \ln \left(\frac{yU_\infty}{v_\infty} \right) \right]$$

$$\begin{aligned}
 \text{where } F &= 19.33 \ln \left(\frac{yU_\infty}{v_\infty} \right) - 433.5 && \text{when } \frac{yU_\infty}{v_\infty} \leq 7660 \\
 F &= 692.7 \ln \left(\frac{yU_\infty}{v_\infty} \right) - 6456 && \text{when } 7660 < \frac{yU_\infty}{v_\infty} < 11200 \\
 F &= 0 && \text{when } \frac{yU_\infty}{v_\infty} \geq 11200 .
 \end{aligned}$$

This correction is based on rather limited evidence but the magnitude is small and the probable accuracy of the correction is within 1½% of the true static pressure.

A.2.2 Regions B and C

The errors in these regions are treated as arising from a combination of shear flow and compressibility effects. It would therefore be expected that there would be an error which would correlate with $y/\delta_{0.995}$ and a larger error due to the geometry of the twin static pressure probe, which would correlate with Mach number. As stated in section A.2 the greater part of the latter error is due to the stem interconnecting the inner and outer static pressure probes, and the necessary correction depends on an estimate of Mach number and a form of the free-stream calibration of the twin static probe.

In fact, the average Mach number of the inner and outer static probes is used to give the necessary correction to the static pressure measured by the inner probe, when the outer probe is below the critical Mach number of 1.098. In all other instances the local Mach number is used to obtain the correction needed to the measured static pressure.

This applies to both the inner and outer static probes. The local Mach number is always used for the outer static pressure probe because it is normally in a region where the Mach number gradient normal to the wall is small.

It was found that the free-stream calibration overcorrected the static pressure measurement errors, and so a compromise calibration was used (shown dotted in Fig 27a) which involved three stages of smoothing. It may be noted from Fig 16a-f that the critical Mach number is only encountered ahead of and in the immediate vicinity of the main interaction region. The location of the point for critical Mach number is close to the wall for stations upstream of the influence of the normal shock wave. The environment is therefore one of severe shear strains and velocity gradients and the smoothing exercise is probably justified as it only affects the free-stream calibration in the region of the critical Mach number.

The form of the corrections is given by

$$C_{p_B} = \text{fn}\left(M_I, M_U, \frac{y}{\delta_{0.995}}\right)$$

$$C_{p_C} = \text{fn}\left(M_U, \frac{y}{\delta_{0.995}}\right) .$$

A.2.2.1 Outer static pressure probe at $M \leq 1.098$

The corrections are calculated in terms of local density and velocity. The modified calibration curves (shown dotted in Fig 27) are used to obtain $(p_m - p/\frac{1}{2}\rho U^2)$ from $\text{fn}(M)$ and the modification to the free-stream calibration due to probe position is shown in Fig 31.

Thus the total correction is given by

$$C_{p_B} = \text{fn}\left(\frac{M_I + M_U}{2}\right) \times 0.94 \left[\sin \left\{ 0.665 \left(\frac{y}{\delta_{0.995}} - 0.15 \right) \right\} \right]^{\frac{1}{2}}$$

$$C_{p_C} = \text{fn}(M_U) \times 0.94 \left[\sin \left\{ 0.665 \left(\frac{y}{\delta_{0.995}} - 0.15 \right) \right\} \right]^{\frac{1}{2}}$$

$$C_{p_B} = 0 \quad \text{if } \frac{y}{\delta_{0.995}} < 0.15 .$$

A.2.2.2 Outer static pressure probe at $M > 1.098$

$$C_{p_B} = \text{fn}(M_I) \times 0.94 \left[\sin \left\{ 0.665 \left(\frac{y}{\delta_{0.995}} - 0.15 \right) \right\} \right]^{\frac{1}{2}}$$

$$C_{p_C} = \text{fn}(M_U) \cdot 0.94 \left[\sin \left\{ 0.665 \left(\frac{y}{0.495} - 0.15 \right) \right\} \right]^{\frac{1}{2}}$$

$$C_{p_B} = 0 \quad \text{if} \quad \frac{y}{0.495} < 0.15$$

A.2.3 Total corrections

$$\text{Inner tube} \quad C_{p_I} = C_{p_A} + C_{p_B} = \frac{p_m - p}{\frac{1}{2} \rho U^2}$$

$$\text{Outer tube} \quad C_{p_U} = C_{p_C} = \frac{p_m - p}{\frac{1}{2} \rho U^2}$$

A.3 Applying the corrections

The following describes how the static pressure corrections are calculated and applied:

- (1) Calculate the Mach number at each measuring station from interpolated pitot and wall pressure measurements. Calculate $y/0.995$, C_f and $y(U_\tau/\nu_\tau)$.
- (2) Calculate the static pressure corrections and subtract from the measured values.
- (3) Recalculate the new Mach number using the new static pressure and the interpolated pitot measurement.

Steps (2) and (3) are repeated until the difference between the new and old Mach number is less than 0.001. A suitable damping factor is needed to prevent oscillations in the calculation.

- (4) Record the corrected Mach number and static pressure.

Fig 32 shows the effect of the correction on static pressures measured ahead and downstream of the interaction region where the static pressures may be expected to be nearly uniform across the boundary layer thickness. It will be seen that the static pressure errors have been reduced to $1\frac{1}{2}\%$ of the true static pressure.

A.4 Transferring the corrected static pressures to the pitot traverse measurements

The final stage of the procedure is to interpolate in the distribution of static pressure to obtain values at the location of the pitot-pressure measurements.

The calculated static pressures for each static pressure traverse are smoothed and transferred to a carpet plot of static pressure against streamwise position as shown in Fig 33. The appropriate static pressures are then transferred from the carpet plot for each pitot traverse. A final stage of smoothing ensures that the final static pressure curves are asymptotic to the wall static pressure within a few millimetres of the tunnel floor.

The corrected static pressure results may be seen in Fig 15a&b.

Table 1

TEST CONDITIONS

M_0	$Re/m \times 10^{-6}$	$Re \delta^* \times 10^{-3}$	$Re \theta \times 10^{-3}$	$Re \lambda \times 10^{-6}$	Distance of throat ahead of window centreline (m)	Effective turbulent run ahead of window centreline (m)
1.270	3.66	29.1	14.1	11.2	2.78	3.25
1.272	10.21	68.2	33.8	31.2	2.78	3.23
1.373	3.67	30.0	13.6	10.9	2.84	3.17
1.386	10.03	68.2	31.6	29.5	2.84	3.14
1.522	3.51	28.1	11.8	9.5	2.86	2.97
1.531	6.47	46.1	20.2	17.3	2.87	2.95
1.538	9.96	68.7	29.2	27.9	2.87	3.02

[illegible]

[illegible]

Table 2 (continued)

N (NUMBER) = 13									
X=40 MM									
DEL=25.0 K DEL 995=40.9 MM									
RE/PA=3.0MM/6 (REQUIRED P) RE=1.18 (REQUIRED P)									
V (MM)	CONST P	U/E	N	U/E	REQUIRED P	P/PTO	P/PTO	REQUIRED P	P/PTO
0.0	0.000	0.000	0.000	0.000	0.000	0.000	0.000	0.000	0.000
0.5	0.546	0.581	0.546	0.581	0.546	0.581	0.546	0.581	0.546
1.0	1.092	1.162	1.092	1.162	1.092	1.162	1.092	1.162	1.092
1.5	1.638	1.748	1.638	1.748	1.638	1.748	1.638	1.748	1.638
2.0	2.184	2.334	2.184	2.334	2.184	2.334	2.184	2.334	2.184
2.5	2.730	2.920	2.730	2.920	2.730	2.920	2.730	2.920	2.730
3.0	3.276	3.506	3.276	3.506	3.276	3.506	3.276	3.506	3.276
3.5	3.822	4.092	3.822	4.092	3.822	4.092	3.822	4.092	3.822
4.0	4.368	4.678	4.368	4.678	4.368	4.678	4.368	4.678	4.368
4.5	4.914	5.264	4.914	5.264	4.914	5.264	4.914	5.264	4.914
5.0	5.460	5.850	5.460	5.850	5.460	5.850	5.460	5.850	5.460
5.5	6.006	6.436	6.006	6.436	6.006	6.436	6.006	6.436	6.006
6.0	6.552	7.022	6.552	7.022	6.552	7.022	6.552	7.022	6.552
6.5	7.098	7.608	7.098	7.608	7.098	7.608	7.098	7.608	7.098
7.0	7.644	8.194	7.644	8.194	7.644	8.194	7.644	8.194	7.644
7.5	8.190	8.780	8.190	8.780	8.190	8.780	8.190	8.780	8.190
8.0	8.736	9.366	8.736	9.366	8.736	9.366	8.736	9.366	8.736
8.5	9.282	9.952	9.282	9.952	9.282	9.952	9.282	9.952	9.282
9.0	9.828	10.538	9.828	10.538	9.828	10.538	9.828	10.538	9.828
9.5	10.374	11.124	10.374	11.124	10.374	11.124	10.374	11.124	10.374
10.0	10.920	11.710	10.920	11.710	10.920	11.710	10.920	11.710	10.920
10.5	11.466	12.296	11.466	12.296	11.466	12.296	11.466	12.296	11.466
11.0	12.012	12.882	12.012	12.882	12.012	12.882	12.012	12.882	12.012
11.5	12.558	13.468	12.558	13.468	12.558	13.468	12.558	13.468	12.558
12.0	13.104	14.054	13.104	14.054	13.104	14.054	13.104	14.054	13.104
12.5	13.650	14.640	13.650	14.640	13.650	14.640	13.650	14.640	13.650
13.0	14.196	15.226	14.196	15.226	14.196	15.226	14.196	15.226	14.196
13.5	14.742	15.812	14.742	15.812	14.742	15.812	14.742	15.812	14.742
14.0	15.288	16.398	15.288	16.398	15.288	16.398	15.288	16.398	15.288
14.5	15.834	16.984	15.834	16.984	15.834	16.984	15.834	16.984	15.834
15.0	16.380	17.570	16.380	17.570	16.380	17.570	16.380	17.570	16.380
15.5	16.926	18.156	16.926	18.156	16.926	18.156	16.926	18.156	16.926
16.0	17.472	18.742	17.472	18.742	17.472	18.742	17.472	18.742	17.472
16.5	18.018	19.328	18.018	19.328	18.018	19.328	18.018	19.328	18.018
17.0	18.564	19.914	18.564	19.914	18.564	19.914	18.564	19.914	18.564
17.5	19.110	20.500	19.110	20.500	19.110	20.500	19.110	20.500	19.110
18.0	19.656	21.086	19.656	21.086	19.656	21.086	19.656	21.086	19.656
18.5	20.202	21.672	20.202	21.672	20.202	21.672	20.202	21.672	20.202
19.0	20.748	22.258	20.748	22.258	20.748	22.258	20.748	22.258	20.748
19.5	21.294	22.844	21.294	22.844	21.294	22.844	21.294	22.844	21.294
20.0	21.840	23.430	21.840	23.430	21.840	23.430	21.840	23.430	21.840
20.5	22.386	24.016	22.386	24.016	22.386	24.016	22.386	24.016	22.386
21.0	22.932	24.602	22.932	24.602	22.932	24.602	22.932	24.602	22.932
21.5	23.478	25.188	23.478	25.188	23.478	25.188	23.478	25.188	23.478
22.0	24.024	25.774	24.024	25.774	24.024	25.774	24.024	25.774	24.024
22.5	24.570	26.360	24.570	26.360	24.570	26.360	24.570	26.360	24.570
23.0	25.116	26.946	25.116	26.946	25.116	26.946	25.116	26.946	25.116
23.5	25.662	27.532	25.662	27.532	25.662	27.532	25.662	27.532	25.662
24.0	26.208	28.118	26.208	28.118	26.208	28.118	26.208	28.118	26.208
24.5	26.754	28.704	26.754	28.704	26.754	28.704	26.754	28.704	26.754
25.0	27.300	29.290	27.300	29.290	27.300	29.290	27.300	29.290	27.300
25.5	27.846	29.876	27.846	29.876	27.846	29.876	27.846	29.876	27.846
26.0	28.392	30.462	28.392	30.462	28.392	30.462	28.392	30.462	28.392
26.5	28.938	31.048	28.938	31.048	28.938	31.048	28.938	31.048	28.938
27.0	29.484	31.634	29.484	31.634	29.484	31.634	29.484	31.634	29.484
27.5	30.030	32.220	30.030	32.220	30.030	32.220	30.030	32.220	30.030
28.0	30.576	32.806	30.576	32.806	30.576	32.806	30.576	32.806	30.576
28.5	31.122	33.392	31.122	33.392	31.122	33.392	31.122	33.392	31.122
29.0	31.668	33.978	31.668	33.978	31.668	33.978	31.668	33.978	31.668
29.5	32.214	34.564	32.214	34.564	32.214	34.564	32.214	34.564	32.214
30.0	32.760	35.150	32.760	35.150	32.760	35.150	32.760	35.150	32.760
30.5	33.306	35.736	33.306	35.736	33.306	35.736	33.306	35.736	33.306
31.0	33.852	36.322	33.852	36.322	33.852	36.322	33.852	36.322	33.852
31.5	34.398	36.908	34.398	36.908	34.398	36.908	34.398	36.908	34.398
32.0	34.944	37.494	34.944	37.494	34.944	37.494	34.944	37.494	34.944
32.5	35.490	38.080	35.490	38.080	35.490	38.080	35.490	38.080	35.490
33.0	36.036	38.666	36.036	38.666	36.036	38.666	36.036	38.666	36.036
33.5	36.582	39.252	36.582	39.252	36.582	39.252	36.582	39.252	36.582
34.0	37.128	39.838	37.128	39.838	37.128	39.838	37.128	39.838	37.128
34.5	37.674	40.424	37.674	40.424	37.674	40.424	37.674	40.424	37.674
35.0	38.220	41.010	38.220	41.010	38.220	41.010	38.220	41.010	38.220
35.5	38.766	41.596	38.766	41.596	38.766	41.596	38.766	41.596	38.766
36.0	39.312	42.182	39.312	42.182	39.312	42.182	39.312	42.182	39.312
36.5	39.858	42.768	39.858	42.768	39.858	42.768	39.858	42.768	39.858
37.0	40.404	43.354	40.404	43.354	40.404	43.354	40.404	43.354	40.404
37.5	40.950	43.940	40.950	43.940	40.950	43.940	40.950	43.940	40.950
38.0	41.496	44.526	41.496	44.526	41.496	44.526	41.496	44.526	41.496
38.5	42.042	45.112	42.042	45.112	42.042	45.112	42.042	45.112	42.042
39.0	42.588	45.698	42.588	45.698	42.588	45.698	42.588	45.698	42.588
39.5	43.134	46.284	43.134	46.284	43.134	46.284	43.134	46.284	43.134
40.0	43.680	46.870	43.680	46.870	43.680	46.870	43.680	46.870	43.680
40.5	44.226	47.456	44.226	47.456	44.226	47.456	44.226	47.456	44.226
41.0	44.772	48.042	44.772	48.042	44.772	48.042	44.772	48.042	44.772
41.5	45.318	48.628	45.318	48.628	45.318	48.628	45.318	48.628	45.318
42.0	45.864	49.214	45.864	49.214	45.864	49.214	45.864	49.214	45.864
42.5	46.410	49.800	46.410	49.800	46.410	49.800	46.410	49.800	46.410
43.0	46.956	50.386	46.956	50.386	46.956	50.386	46.956	50.386	46.956
43.5	47.502	50.972	47.502	50.972	47.502	50.972	47.502	50.972	47.502
44.0	48.048	51.558	48.048	51.558	48.048	51.558	48.048	51.558	48.048
44.5	48.594	52.144	48.594	52.144	48.594	52.144	48.594	52.144	48.594
45.0	49.140	52.730	49.140	52.730	49.140	52.730	49.140	52.730	49.140
45.5	49.686	53.316	49.686	53.316	49.686	53.316	49.686	53.316	49.686
46.0	50.232	53.902	50.232	53.902	50.232	53.902	50.232	53.902	50.232
46.5	50.778	54.488	50.778	54.488	50.778	54.488	50.778	54.488	50.778
47.0	51.324	55.074	51.324	55.074	51.324	55.074	51.324	55.074	51.324
47.5	51.870	55.660	51.870	55.660	51.870	55.660	51.870	55.660	51.870
48.0	52.416	56.246	52.416	56.246	52.416	56.246	52.416	56.246	52.416
48.5	52.962	56.832	52.962	56.832	52.962	56.832	52.962	56.832	52.962
49.0	53.508	57.418	53.508	57.418	53.508	57.418	53.508	57.418	53.508
49.5	54.054	58.004	54.054	58.004	54.054	58.004	54.054	58.004	54.054
50.0	54.600	58.590	54.600	58.590	54.600	58.590	54.600	58.590	54.600
50.5	55.146	59.176	55.146	59.176	55.146	59.176	55.146	59.176	55.146
51.0	55.692	59.762	55.692	59.762	55.692	59.762	55.692	59.762	55.692
51.5	56.238	60.348	56.238	60.348	56.238	60.348	56.238	60.348	56.238
52.0	56.784	60.934	56.784	60.934	56.784	60.934	56.784	60.934	56.784
52.5	57.330	61.520	57.330	61.520	57.330	61.520	57.330	61.520	

[illegible]

—

H. MOHRIE, 1973

AT 2789 MH
 RE: No. 5 S41076 (MEASURED P) 19-291.7 K DEL 995-115 0 MH
 RE: No. 889 (MEASURED P)

CONET PA		MEASURED P	
V (MH)	H	DATE	DATE
0.00	0.0000	0.0000	0.0000
0.05	0.422	0.5279	0.5279
0.10	0.442	0.540	0.540
0.15	0.4500	0.5500	0.5500
0.20	0.4672	0.5646	0.5646
0.25	0.4736	0.5777	0.5777
0.30	0.4895	0.5904	0.5904
0.35	0.5124	0.6178	0.6178
0.40	0.5275	0.6338	0.6338
0.45	0.5387	0.6466	0.6466
0.50	0.5546	0.6648	0.6648
0.55	0.5747	0.6871	0.6871
0.60	0.5945	0.7093	0.7093
0.65	0.6147	0.7315	0.7315
0.70	0.6274	0.7414	0.7414
0.75	0.6279	0.7463	0.7463
0.80	0.6405	0.7607	0.7607
0.85	0.6554	0.7756	0.7756
0.90	0.6622	0.7859	0.7859
0.95	0.6801	0.8011	0.8011
1.00	0.6953	0.8165	0.8165
1.05	0.7087	0.8340	0.8340
1.10	0.7225	0.8488	0.8488
1.15	0.7367	0.8624	0.8624
1.20	0.7512	0.8802	0.8802
1.25	0.7662	0.8949	0.8949
1.30	0.7813	0.9177	0.9177
1.35	0.8133	0.9335	0.9335
1.40	0.8547	0.9527	0.9527
1.45	0.8645	0.9645	0.9645
1.50	0.8676	0.9686	0.9686
1.55	0.8676	0.9686	0.9686
1.60	0.8676	0.9686	0.9686
1.65	0.8676	0.9686	0.9686
1.70	0.8676	0.9686	0.9686
1.75	0.8676	0.9686	0.9686
1.80	0.8676	0.9686	0.9686
1.85	0.8676	0.9686	0.9686
1.90	0.8676	0.9686	0.9686
1.95	0.8676	0.9686	0.9686

4. NUMBER OF : 1
 4-22-88 10-29-88 56 55-44-00
 56 56-1 56 56-00000000

$\mu(\text{HMMINTEL}) = 1.3$
 $\sigma = .47 \text{ MM}$
 $TB = 207.6 \text{ K}$
 $UCL\ 99\% = 42.5 \text{ MM}$

$\mu_{\text{new}} = 1.5$
 $\sigma = 0.9$ mm $\mu = 69.1$ k $\sigma = 1.3$ mm
 $\mu = 10.0 \times 10^6$ $\sigma = 8.8 \times 10^6$ $\mu = 6.1 \times 10^6$

```

P (MATH) = 1 )
# = 94 MATH
10-299 5 K DEL 995 = 30 7 MATH
DEL 7-18 16-18 MATH P1 MATH = 1 249 MATH P1

```

V (M)	U (V)	I (A)	P (W)	R (Ω)	G (S)	C (F)	L (H)	Q (V)	φ (°)	θ (°)	δ (°)	ε (°)	ζ (°)	η (°)	ξ (°)	χ (°)	ψ (°)	ω (°)	ν (°)	μ (°)	τ (°)	σ (°)	ρ (°)	q (°)	r (°)	s (°)	t (°)	u (°)	v (°)	w (°)	x (°)	y (°)	z (°)	aa (°)	ab (°)	ac (°)	ad (°)	ae (°)	af (°)	ag (°)	ah (°)	ai (°)	aj (°)	ak (°)	al (°)	am (°)	an (°)	ao (°)	ap (°)	aq (°)	ar (°)	as (°)	at (°)	au (°)	av (°)	aw (°)	ax (°)	ay (°)	az (°)	ba (°)	bb (°)	bc (°)	bd (°)	be (°)	bf (°)	bg (°)	bh (°)	bi (°)	bj (°)	bk (°)	bl (°)	bm (°)	bn (°)	bo (°)	bp (°)	bq (°)	br (°)	bs (°)	bt (°)	bu (°)	bv (°)	bw (°)	bx (°)	by (°)	bz (°)	ca (°)	cb (°)	cc (°)	cd (°)	ce (°)	cf (°)	cg (°)	ch (°)	ci (°)	cj (°)	ck (°)	cl (°)	cm (°)	cn (°)	co (°)	cp (°)	cq (°)	cr (°)	cs (°)	ct (°)	cu (°)	cv (°)	cw (°)	cx (°)	cy (°)	cz (°)	da (°)	db (°)	dc (°)	dd (°)	de (°)	df (°)	dg (°)	dh (°)	di (°)	dj (°)	dk (°)	dl (°)	dm (°)	dn (°)	do (°)	dp (°)	dq (°)	dr (°)	ds (°)	dt (°)	du (°)	dv (°)	dw (°)	dx (°)	dy (°)	dz (°)	ea (°)	eb (°)	ec (°)	ed (°)	ee (°)	ef (°)	eg (°)	eh (°)	ei (°)	ej (°)	ek (°)	el (°)	em (°)	en (°)	eo (°)	ep (°)	eq (°)	er (°)	es (°)	et (°)	eu (°)	ev (°)	ew (°)	ex (°)	ey (°)	ez (°)	fa (°)	fb (°)	fc (°)	fd (°)	fe (°)	ff (°)	fg (°)	fh (°)	fi (°)	fj (°)	fk (°)	fl (°)	fm (°)	fn (°)	fo (°)	fp (°)	fq (°)	fr (°)	fs (°)	ft (°)	fu (°)	fv (°)	fw (°)	fx (°)	fy (°)	fz (°)	ga (°)	gb (°)	gc (°)	gd (°)	ge (°)	gf (°)	gg (°)	gh (°)	gi (°)	gj (°)	gk (°)	gl (°)	gm (°)	gn (°)	go (°)	gp (°)	gq (°)	gr (°)	gs (°)	gt (°)	gu (°)	gv (°)	gw (°)	gx (°)	gy (°)	gz (°)	ha (°)	hb (°)	hc (°)	hd (°)	he (°)	hf (°)	hg (°)	hh (°)	hi (°)	hj (°)	hk (°)	hl (°)	hm (°)	hn (°)	ho (°)	hp (°)	hq (°)	hr (°)	hs (°)	ht (°)	hu (°)	hv (°)	hw (°)	hx (°)	hy (°)	hz (°)	ia (°)	ib (°)	ic (°)	id (°)	ie (°)	if (°)	ig (°)	ih (°)	ii (°)	ij (°)	ik (°)	il (°)	im (°)	in (°)	io (°)	ip (°)	iq (°)	ir (°)	is (°)	it (°)	iu (°)	iv (°)	iw (°)	ix (°)	iy (°)	iz (°)	ja (°)	jb (°)	jc (°)	jd (°)	je (°)	jf (°)	jg (°)	jh (°)	ji (°)	jj (°)	jk (°)	jl (°)	jm (°)	jn (°)	jo (°)	jp (°)	jq (°)	jr (°)	js (°)	jt (°)	ju (°)	jv (°)	jw (°)	jx (°)	jy (°)	jz (°)	ka (°)	kb (°)	kc (°)	kd (°)	ke (°)	kf (°)	kg (°)	kh (°)	ki (°)	kj (°)	kk (°)	kl (°)	km (°)	kn (°)	ko (°)	kp (°)	kq (°)	kr (°)	ks (°)	kt (°)	ku (°)	kv (°)	kw (°)	kx (°)	ky (°)	kz (°)	la (°)	lb (°)	lc (°)	ld (°)	le (°)	lf (°)	lg (°)	lh (°)	li (°)	lj (°)	lk (°)	ll (°)	lm (°)	ln (°)	lo (°)	lp (°)	lq (°)	lr (°)	ls (°)	lt (°)	lu (°)	lv (°)	lw (°)	lx (°)	ly (°)	lz (°)	ma (°)	mb (°)	mc (°)	md (°)	me (°)	mf (°)	mg (°)	mh (°)	mi (°)	mj (°)	mk (°)	ml (°)	mm (°)	mn (°)	mo (°)	mp (°)	mq (°)	mr (°)	ms (°)	mt (°)	mu (°)	mv (°)	mw (°)	mx (°)	my (°)	mz (°)	na (°)	nb (°)	nc (°)	nd (°)	ne (°)	nf (°)	ng (°)	nh (°)	ni (°)	nj (°)	nk (°)	nl (°)	nm (°)	nn (°)	no (°)	np (°)	nq (°)	nr (°)	ns (°)	nt (°)	nu (°)	nv (°)	nw (°)	nx (°)	ny (°)	nz (°)	oa (°)	ob (°)	oc (°)	od (°)	oe (°)	of (°)	og (°)	oh (°)	oi (°)	oj (°)	ok (°)	ol (°)	om (°)	on (°)	oo (°)	op (°)	oq (°)	or (°)	os (°)	ot (°)	ou (°)	ov (°)	ow (°)	ox (°)	oy (°)	oz (°)	pa (°)	pb (°)	pc (°)	pd (°)	pe (°)	pf (°)	pg (°)	ph (°)	pi (°)	pj (°)	pk (°)	pl (°)	pm (°)	pn (°)	po (°)	pp (°)	pq (°)	pr (°)	ps (°)	pt (°)	pu (°)	pv (°)	pw (°)	px (°)	py (°)	pz (°)	qa (°)	qb (°)	qc (°)	qd (°)	qe (°)	qf (°)	qg (°)	qh (°)	qi (°)	qj (°)	qk (°)	ql (°)	qm (°)	qn (°)	qo (°)	qp (°)	qq (°)	qr (°)	qs (°)	qt (°)	qu (°)	qv (°)	qw (°)	qx (°)	qy (°)	qz (°)	ra (°)	rb (°)	rc (°)	rd (°)	re (°)	rf (°)	rg (°)	rh (°)	ri (°)	rj (°)	rk (°)	rl (°)	rm (°)	rn (°)	ro (°)	rp (°)	rq (°)	rr (°)	rs (°)	rt (°)	ru (°)	rv (°)	rw (°)	rx (°)	ry (°)	rz (°)	sa (°)	sb (°)	sc (°)	sd (°)	se (°)	sf (°)	sg (°)	sh (°)	si (°)	sj (°)	sk (°)	sl (°)	sm (°)	sn (°)	so (°)	sp (°)	sq (°)	sr (°)	ss (°)	st (°)	su (°)	sv (°)	sw (°)	sx (°)	sy (°)	sz (°)	ta (°)	tb (°)	tc (°)	td (°)	te (°)	tf (°)	tg (°)	th (°)	ti (°)	tj (°)	tk (°)	tl (°)	tm (°)	tn (°)	to (°)	tp (°)	tq (°)	tr (°)	ts (°)	tt (°)	tu (°)	tv (°)	tw (°)	tx (°)	ty (°)	tz (°)	ua (°)	ub (°)	uc (°)	ud (°)	ue (°)	uf (°)	ug (°)	uh (°)	ui (°)	uj (°)	uk (°)	ul (°)	um (°)	un (°)	uo (°)	up (°)	uq (°)	ur (°)	us (°)	ut (°)	uu (°)	uv (°)	uw (°)	ux (°)	uy (°)	uz (°)	va (°)	vb (°)	vc (°)	vd (°)	ve (°)	vf (°)	vg (°)	vh (°)	vi (°)	vj (°)	vk (°)	vl (°)	vm (°)	vn (°)	vo (°)	vp (°)	vq (°)	vr (°)	vs (°)	vt (°)	vu (°)	vv (°)	vw (°)	vx (°)	vy (°)	vz (°)	wa (°)	wb (°)	wc (°)	wd (°)	we (°)	wf (°)	wg (°)	wh (°)	wi (°)	wj (°)	wk (°)	wl (°)	wm (°)	wn (°)	wo (°)	wp (°)	wq (°)	wr (°)	ws (°)	wt (°)	wu (°)	wv (°)	ww (°)	wx (°)	wy (°)	wz (°)	xa (°)	xb (°)	xc (°)	xd (°)	xe (°)	xf (°)	xg (°)	xh (°)	xi (°)	xj (°)	xk (°)	xl (°)	xm (°)	xn (°)	xo (°)	xp (°)	xq (°)	xr (°)	xs (°)	xt (°)	xu (°)	xv (°)	xw (°)	xx (°)	xy (°)	xz (°)	ya (°)	yb (°)	yc (°)	yd (°)	ye (°)	yf (°)	yg (°)	yh (°)	yi (°)	yj (°)	yk (°)	yl (°)	ym (°)	yn (°)	yo (°)	yp (°)	yq (°)	yr (°)	ys (°)	yt (°)	yu (°)	yv (°)	yw (°)	yx (°)	yy (°)	yz (°)	za (°)	zb (°)	zc (°)	zd (°)	ze (°)	zf (°)	zg (°)	zh (°)	zi (°)	zj (°)	zk (°)	zl (°)	zm (°)	zn (°)	zo (°)	zp (°)	zq (°)	zr (°)	zs (°)	zt (°)	zu (°)	zv (°)	zw (°)	zx (°)	zy (°)	zz (°)
-------	-------	-------	-------	-------	-------	-------	-------	-------	-------	-------	-------	-------	-------	-------	-------	-------	-------	-------	-------	-------	-------	-------	-------	-------	-------	-------	-------	-------	-------	-------	-------	-------	-------	--------	--------	--------	--------	--------	--------	--------	--------	--------	--------	--------	--------	--------	--------	--------	--------	--------	--------	--------	--------	--------	--------	--------	--------	--------	--------	--------	--------	--------	--------	--------	--------	--------	--------	--------	--------	--------	--------	--------	--------	--------	--------	--------	--------	--------	--------	--------	--------	--------	--------	--------	--------	--------	--------	--------	--------	--------	--------	--------	--------	--------	--------	--------	--------	--------	--------	--------	--------	--------	--------	--------	--------	--------	--------	--------	--------	--------	--------	--------	--------	--------	--------	--------	--------	--------	--------	--------	--------	--------	--------	--------	--------	--------	--------	--------	--------	--------	--------	--------	--------	--------	--------	--------	--------	--------	--------	--------	--------	--------	--------	--------	--------	--------	--------	--------	--------	--------	--------	--------	--------	--------	--------	--------	--------	--------	--------	--------	--------	--------	--------	--------	--------	--------	--------	--------	--------	--------	--------	--------	--------	--------	--------	--------	--------	--------	--------	--------	--------	--------	--------	--------	--------	--------	--------	--------	--------	--------	--------	--------	--------	--------	--------	--------	--------	--------	--------	--------	--------	--------	--------	--------	--------	--------	--------	--------	--------	--------	--------	--------	--------	--------	--------	--------	--------	--------	--------	--------	--------	--------	--------	--------	--------	--------	--------	--------	--------	--------	--------	--------	--------	--------	--------	--------	--------	--------	--------	--------	--------	--------	--------	--------	--------	--------	--------	--------	--------	--------	--------	--------	--------	--------	--------	--------	--------	--------	--------	--------	--------	--------	--------	--------	--------	--------	--------	--------	--------	--------	--------	--------	--------	--------	--------	--------	--------	--------	--------	--------	--------	--------	--------	--------	--------	--------	--------	--------	--------	--------	--------	--------	--------	--------	--------	--------	--------	--------	--------	--------	--------	--------	--------	--------	--------	--------	--------	--------	--------	--------	--------	--------	--------	--------	--------	--------	--------	--------	--------	--------	--------	--------	--------	--------	--------	--------	--------	--------	--------	--------	--------	--------	--------	--------	--------	--------	--------	--------	--------	--------	--------	--------	--------	--------	--------	--------	--------	--------	--------	--------	--------	--------	--------	--------	--------	--------	--------	--------	--------	--------	--------	--------	--------	--------	--------	--------	--------	--------	--------	--------	--------	--------	--------	--------	--------	--------	--------	--------	--------	--------	--------	--------	--------	--------	--------	--------	--------	--------	--------	--------	--------	--------	--------	--------	--------	--------	--------	--------	--------	--------	--------	--------	--------	--------	--------	--------	--------	--------	--------	--------	--------	--------	--------	--------	--------	--------	--------	--------	--------	--------	--------	--------	--------	--------	--------	--------	--------	--------	--------	--------	--------	--------	--------	--------	--------	--------	--------	--------	--------	--------	--------	--------	--------	--------	--------	--------	--------	--------	--------	--------	--------	--------	--------	--------	--------	--------	--------	--------	--------	--------	--------	--------	--------	--------	--------	--------	--------	--------	--------	--------	--------	--------	--------	--------	--------	--------	--------	--------	--------	--------	--------	--------	--------	--------	--------	--------	--------	--------	--------	--------	--------	--------	--------	--------	--------	--------	--------	--------	--------	--------	--------	--------	--------	--------	--------	--------	--------	--------	--------	--------	--------	--------	--------	--------	--------	--------	--------	--------	--------	--------	--------	--------	--------	--------	--------	--------	--------	--------	--------	--------	--------	--------	--------	--------	--------	--------	--------	--------	--------	--------	--------	--------	--------	--------	--------	--------	--------	--------	--------	--------	--------	--------	--------	--------	--------	--------	--------	--------	--------	--------	--------	--------	--------	--------	--------	--------	--------	--------	--------	--------	--------	--------	--------	--------	--------	--------	--------	--------	--------	--------	--------	--------	--------	--------	--------	--------	--------	--------	--------	--------	--------	--------	--------	--------	--------	--------	--------	--------	--------	--------	--------	--------	--------	--------	--------	--------	--------	--------	--------	--------	--------	--------	--------	--------	--------	--------	--------	--------	--------	--------	--------	--------	--------	--------	--------	--------	--------	--------	--------	--------	--------	--------	--------	--------	--------	--------	--------	--------	--------	--------	--------	--------	--------	--------	--------	--------	--------	--------	--------	--------	--------	--------	--------	--------	--------	--------	--------	--------	--------	--------	--------	--------	--------	--------	--------	--------	--------	--------	--------	--------	--------	--------	--------	--------	--------	--------	--------	--------	--------	--------	--------	--------	--------	--------	--------	--------	--------	--------	--------	--------	--------	--------	--------	--------	--------	--------	--------	--------	--------	--------	--------	--------	--------	--------	--------	--------	--------	--------	--------

TX= 125 MM TO=297.5 K DEL 955= 52 @ MM
DEL ME 9 01 of 0'6, MEASURED P. ME=0 955 (MEASURED P.)

$x = 174$ mm $16 \pm 2.5^\circ$ $4 \times$ $[\Delta L]_{55} = 52.6$ mm
 $[\Delta L]_{75} = 9.85 \pm 0.6$ mm $[\Delta L]_{85} = 0$ mm $[\Delta L]_{95} = 344$ mm $[\Delta L]_{105} = 0$ mm

$x = 221$ mm $16 = 236$ g $16 \times 95 = 529$ mm

$\lambda = 0.1381583 \text{ m}$ $\nu = 2.17 \times 10^{15} \text{ s}^{-1}$ $E = 8.8 \times 10^{-18} \text{ J}$
 $\lambda = 0.55 \text{ nm}$ $\nu = 5.45 \times 10^{14} \text{ s}^{-1}$ $E = 3.3 \times 10^{-19} \text{ J}$

CUST ID	DATE		QUANTITY	PRICE		TOTAL PRICE	TAX	TOTAL AMOUNT
	DATE	TIME		PRICE	PRICE			
1001	2023-01-01	10:00	100	1.50	150.00	15.00	165.00	
1002	2023-01-02	11:30	200	2.00	400.00	20.00	420.00	
1003	2023-01-03	09:45	150	1.20	180.00	18.00	198.00	
1004	2023-01-04	14:20	300	2.50	750.00	30.00	780.00	
1005	2023-01-05	16:00	250	1.80	450.00	22.50	472.50	
1006	2023-01-06	12:15	180	1.00	180.00	18.00	198.00	
1007	2023-01-07	13:45	220	2.20	484.00	26.40	510.40	
1008	2023-01-08	10:30	160	1.10	176.00	17.60	193.60	
1009	2023-01-09	15:10	280	2.00	560.00	28.00	588.00	
1010	2023-01-10	11:00	190	1.30	247.00	23.00	270.00	
1011	2023-01-11	14:45	320	2.80	896.00	36.80	932.80	
1012	2023-01-12	09:20	210	1.60	336.00	25.20	361.20	
1013	2023-01-13	12:55	260	2.10	546.00	27.30	573.30	
1014	2023-01-14	10:10	170	1.05	178.50	17.85	196.35	
1015	2023-01-15	13:30	290	2.30	667.00	33.00	700.00	
1016	2023-01-16	11:45	180	1.25	225.00	22.50	247.50	
1017	2023-01-17	14:00	310	2.70	837.00	36.90	873.90	
1018	2023-01-18	09:50	200	1.55	310.00	23.00	333.00	
1019	2023-01-19	12:25	270	2.05	553.50	27.00	580.50	
1020	2023-01-20	10:40	160	1.15	184.00	17.60	201.60	
1021	2023-01-21	13:15	300	2.60	780.00	30.00	810.00	
1022	2023-01-22	11:20	190	1.40	266.00	23.20	289.20	
1023	2023-01-23	14:55	330	2.90	957.00	38.40	995.40	
1024	2023-01-24	09:35	220	1.70	374.00	26.60	400.60	
1025	2023-01-25	12:05	280	2.15	602.00	27.00	629.00	
1026	2023-01-26	10:50	170	1.08	183.60	17.40	201.00	
1027	2023-01-27	13:25	310	2.75	852.50	36.30	888.80	
1028	2023-01-28	11:10	180	1.28	230.40	22.40	252.80	
1029	2023-01-29	14:35	320	2.85	912.00	36.50	948.50	
1030	2023-01-30	09:40	210	1.65	346.50	25.50	372.00	
1031	2023-01-31	12:30	260	2.08	540.80	26.30	567.10	
1032	2023-02-01	10:15	160	1.12	179.20	17.28	196.48	
1033	2023-02-02	13:00	290	2.35	681.50	33.30	714.80	
1034	2023-02-03	11:40	180	1.22	219.60	22.20	241.80	
1035	2023-02-04	14:25	300	2.55	765.00	30.60	795.60	
1036	2023-02-05	09:55	200	1.58	316.00	23.60	339.60	
1037	2023-02-06	12:40	270	2.02	545.40	26.80	572.20	
1038	2023-02-07	10:25	160	1.05	168.00	16.80	184.80	
1039	2023-02-08	13:10	310	2.72	843.20	36.00	879.20	
1040	2023-02-09	11:05	190	1.38	262.20	23.20	285.40	
1041	2023-02-10	14:40	320	2.82	902.40	36.30	938.70	
1042	2023-02-11	09:30	220	1.72	378.40	26.40	404.80	
1043	2023-02-12	12:15	280	2.12	593.60	26.70	620.30	
1044	2023-02-13	10:00	170	1.02	173.40	16.60	190.00	
1045	2023-02-14	12:50	300	2.52	756.00	30.20	786.20	

[illegible]

Y (km)	QUEST PN		WUE		H	REQUIRED P		WUE	P/P10 P/P10	
	N	WUE	N	WUE		N	WUE			
0.00	0.0000	0.0000	0.0000	0.0000	0.0000	0.0000	0.0000	0.0000	0.0000	0.0000
0.05	0.124	0.277	0.124	0.577	0.0000	0.0000	0.0000	0.0000	0.0000	0.0000
0.10	0.146	0.283	0.146	0.583	0.0000	0.0000	0.0000	0.0000	0.0000	0.0000
0.15	0.167	0.286	0.167	0.586	0.0000	0.0000	0.0000	0.0000	0.0000	0.0000
0.20	0.187	0.288	0.187	0.588	0.0000	0.0000	0.0000	0.0000	0.0000	0.0000
0.25	0.207	0.290	0.207	0.590	0.0000	0.0000	0.0000	0.0000	0.0000	0.0000
0.30	0.227	0.292	0.227	0.592	0.0000	0.0000	0.0000	0.0000	0.0000	0.0000
0.35	0.247	0.294	0.247	0.594	0.0000	0.0000	0.0000	0.0000	0.0000	0.0000
0.40	0.267	0.296	0.267	0.596	0.0000	0.0000	0.0000	0.0000	0.0000	0.0000
0.45	0.287	0.298	0.287	0.598	0.0000	0.0000	0.0000	0.0000	0.0000	0.0000
0.50	0.307	0.300	0.307	0.600	0.0000	0.0000	0.0000	0.0000	0.0000	0.0000
0.55	0.327	0.302	0.327	0.602	0.0000	0.0000	0.0000	0.0000	0.0000	0.0000
0.60	0.347	0.304	0.347	0.604	0.0000	0.0000	0.0000	0.0000	0.0000	0.0000
0.65	0.367	0.306	0.367	0.606	0.0000	0.0000	0.0000	0.0000	0.0000	0.0000
0.70	0.387	0.308	0.387	0.608	0.0000	0.0000	0.0000	0.0000	0.0000	0.0000
0.75	0.407	0.310	0.407	0.610	0.0000	0.0000	0.0000	0.0000	0.0000	0.0000
0.80	0.427	0.312	0.427	0.612	0.0000	0.0000	0.0000	0.0000	0.0000	0.0000
0.85	0.447	0.314	0.447	0.614	0.0000	0.0000	0.0000	0.0000	0.0000	0.0000
0.90	0.467	0.316	0.467	0.616	0.0000	0.0000	0.0000	0.0000	0.0000	0.0000
0.95	0.487	0.318	0.487	0.618	0.0000	0.0000	0.0000	0.0000	0.0000	0.0000
1.00	0.507	0.320	0.507	0.620	0.0000	0.0000	0.0000	0.0000	0.0000	0.0000
1.05	0.527	0.322	0.527	0.622	0.0000	0.0000	0.0000	0.0000	0.0000	0.0000
1.10	0.547	0.324	0.547	0.624	0.0000	0.0000	0.0000	0.0000	0.0000	0.0000
1.15	0.567	0.326	0.567	0.626	0.0000	0.0000	0.0000	0.0000	0.0000	0.0000
1.20	0.587	0.328	0.587	0.628	0.0000	0.0000	0.0000	0.0000	0.0000	0.0000
1.25	0.607	0.330	0.607	0.630	0.0000	0.0000	0.0000	0.0000	0.0000	0.0000
1.30	0.627	0.332	0.627	0.632	0.0000	0.0000	0.0000	0.0000	0.0000	0.0000
1.35	0.647	0.334	0.647	0.634	0.0000	0.0000	0.0000	0.0000	0.0000	0.0000
1.40	0.667	0.336	0.667	0.636	0.0000	0.0000	0.0000	0.0000	0.0000	0.0000
1.45	0.687	0.338	0.687	0.638	0.0000	0.0000	0.0000	0.0000	0.0000	0.0000
1.50	0.707	0.340	0.707	0.640	0.0000	0.0000	0.0000	0.0000	0.0000	0.0000
1.55	0.727	0.342	0.727	0.642	0.0000	0.0000	0.0000	0.0000	0.0000	0.0000
1.60	0.747	0.344	0.747	0.644	0.0000	0.0000	0.0000	0.0000	0.0000	0.0000
1.65	0.767	0.346	0.767	0.646	0.0000	0.0000	0.0000	0.0000	0.0000	0.0000
1.70	0.787	0.348	0.787	0.648	0.0000	0.0000	0.0000	0.0000	0.0000	0.0000
1.75	0.807	0.350	0.807	0.650	0.0000	0.0000	0.0000	0.0000	0.0000	0.0000
1.80	0.827	0.352	0.827	0.652	0.0000	0.0000	0.0000	0.0000	0.0000	0.0000
1.85	0.847	0.354	0.847	0.654	0.0000	0.0000	0.0000	0.0000	0.0000	0.0000
1.90	0.867	0.356	0.867	0.656	0.0000	0.0000	0.0000	0.0000	0.0000	0.0000
1.95	0.887	0.358	0.887	0.658	0.0000	0.0000	0.0000	0.0000	0.0000	0.0000
2.00	0.907	0.360	0.907	0.660	0.0000	0.0000	0.0000	0.0000	0.0000	0.0000

[illegible]

4663 MH
 10-2967 K DEL 995-632 MH
 974106 (UNPLACED P) NE-0 313 (UNPLACED P)

X= 761 MM 10-296 8 K DEL 395= 65 2 MM
 DEL 77= 7310'6 MEASURED P. ME 30 (MEASURED P)

x= 861 mm
 DEL. №= 3 75016 MEASURED F.
 10=26.8 k DEL. №= 681 mm
 №= 902 MEASURED F.

$$\ln 2.69 = 0.98 \approx 1 \quad \ln 2.56 = 0.94$$
[illegible][illegible][illegible][illegible]

10/1/11 continued

N (CONTINUED) = 1.3									
N = 2729 PA									
REZ/PA 9 344176 (MEASURED P) TR-254 8 K DEL 955-180 0 PA									
RE-4 838 (MEASURED P)									
Y (MD)	N	DATE	MEASURED P	N	DATE	P/P10	P1/P10	P1/P10	P1/P10
0.00	0.0000	0.0000	0.0000	0.0000	0.0000	0.0000	0.0000	0.0000	0.0000
0.05	0.4514	0.5605	0.4514	0.5605	0.4514	0.5605	0.4514	0.5605	0.4514
0.10	0.4543	0.5722	0.4543	0.5722	0.4543	0.5722	0.4543	0.5722	0.4543
0.15	0.4609	0.5801	0.4609	0.5801	0.4609	0.5801	0.4609	0.5801	0.4609
0.20	0.4704	0.5916	0.4704	0.5916	0.4704	0.5916	0.4704	0.5916	0.4704
0.25	0.4842	0.6002	0.4842	0.6002	0.4842	0.6002	0.4842	0.6002	0.4842
0.30	0.4913	0.6166	0.4913	0.6166	0.4913	0.6166	0.4913	0.6166	0.4913
0.35	0.5003	0.6378	0.5003	0.6378	0.5003	0.6378	0.5003	0.6378	0.5003
0.40	0.5133	0.6429	0.5133	0.6429	0.5133	0.6429	0.5133	0.6429	0.5133
0.45	0.5278	0.6601	0.5278	0.6601	0.5278	0.6601	0.5278	0.6601	0.5278
0.50	0.5371	0.6711	0.5371	0.6711	0.5371	0.6711	0.5371	0.6711	0.5371
0.55	0.5508	0.6807	0.5508	0.6807	0.5508	0.6807	0.5508	0.6807	0.5508
0.60	0.5701	0.7100	0.5701	0.7100	0.5701	0.7100	0.5701	0.7100	0.5701
0.65	0.5811	0.7228	0.5811	0.7228	0.5811	0.7228	0.5811	0.7228	0.5811
0.70	0.5997	0.7444	0.5997	0.7444	0.5997	0.7444	0.5997	0.7444	0.5997
0.75	0.6042	0.7496	0.6042	0.7496	0.6042	0.7496	0.6042	0.7496	0.6042
0.80	0.6141	0.7619	0.6141	0.7619	0.6141	0.7619	0.6141	0.7619	0.6141
0.85	0.6238	0.7713	0.6238	0.7713	0.6238	0.7713	0.6238	0.7713	0.6238
0.90	0.6313	0.7808	0.6313	0.7808	0.6313	0.7808	0.6313	0.7808	0.6313
0.95	0.6352	0.7852	0.6352	0.7852	0.6352	0.7852	0.6352	0.7852	0.6352
1.00	0.6533	0.8059	0.6533	0.8059	0.6533	0.8059	0.6533	0.8059	0.6533
1.05	0.6661	0.8204	0.6661	0.8204	0.6661	0.8204	0.6661	0.8204	0.6661
1.10	0.6819	0.8303	0.6819	0.8303	0.6819	0.8303	0.6819	0.8303	0.6819
1.15	0.6938	0.8338	0.6938	0.8338	0.6938	0.8338	0.6938	0.8338	0.6938
1.20	0.7076	0.8578	0.7076	0.8578	0.7076	0.8578	0.7076	0.8578	0.7076
1.25	0.7192	0.8799	0.7192	0.8799	0.7192	0.8799	0.7192	0.8799	0.7192
1.30	0.7345	0.8958	0.7345	0.8958	0.7345	0.8958	0.7345	0.8958	0.7345
1.35	0.7468	0.9183	0.7468	0.9183	0.7468	0.9183	0.7468	0.9183	0.7468
1.40	0.7722	0.9321	0.7722	0.9321	0.7722	0.9321	0.7722	0.9321	0.7722
1.45	0.7912	0.9536	0.7912	0.9536	0.7912	0.9536	0.7912	0.9536	0.7912
1.50	0.8100	0.9800	0.8100	0.9800	0.8100	0.9800	0.8100	0.9800	0.8100
1.55	0.8228	1.0021	0.8228	1.0021	0.8228	1.0021	0.8228	1.0021	0.8228
1.60	0.8389	0.9989	0.8389	0.9989	0.8389	0.9989	0.8389	0.9989	0.8389
1.65	0.8571	0.9972	0.8571	0.9972	0.8571	0.9972	0.8571	0.9972	0.8571
1.70	0.8653	0.9961	0.8653	0.9961	0.8653	0.9961	0.8653	0.9961	0.8653
1.75	0.8734	0.9938	0.8734	0.9938	0.8734	0.9938	0.8734	0.9938	0.8734
1.80	0.8819	0.9914	0.8819	0.9914	0.8819	0.9914	0.8819	0.9914	0.8819
1.85	0.8917	0.9917	0.8917	0.9917	0.8917	0.9917	0.8917	0.9917	0.8917
1.90	0.9016	0.9916	0.9016	0.9916	0.9016	0.9916	0.9016	0.9916	0.9016
1.95	0.9096	0.9916	0.9096	0.9916	0.9096	0.9916	0.9096	0.9916	0.9096

[illegible]

11/1/2011 10:10:10

M (INDICATOR) = 1.4

A: 2752 M 10-291 1 K DEL 995-137 4 M
RE-NE 3 334416 (MEASURED P) RE-8 835 (MEASURED P)

V (NO)	M	CONST PM	MEASURED P	DATE	P (NO)	P (NO)
0.00	0.0000	0.0000	0.0000	0.0000	0.0000	0.0000
0.06	0.4267	0.5353	0.4267	0.5353	0.4267	0.5353
0.06	0.4410	0.5308	0.4410	0.5308	0.4410	0.5308
1.06	0.4429	0.5331	0.4429	0.5331	0.4429	0.5331
1.36	0.4559	0.5687	0.4559	0.5687	0.4559	0.5687
1.46	0.4615	0.5754	0.4615	0.5754	0.4615	0.5754
1.66	0.4711	0.5868	0.4711	0.5868	0.4711	0.5868
2.16	0.4934	0.6134	0.4934	0.6134	0.4934	0.6134
2.66	0.4991	0.6201	0.4991	0.6201	0.4991	0.6201
3.16	0.5120	0.6251	0.5120	0.6251	0.5120	0.6251
3.66	0.5197	0.6444	0.5197	0.6444	0.5197	0.6444
4.66	0.5381	0.6566	0.5381	0.6566	0.5381	0.6566
6.66	0.5541	0.6946	0.5541	0.6946	0.5541	0.6946
8.66	0.5693	0.7023	0.5693	0.7023	0.5693	0.7023
10.66	0.5824	0.7175	0.5824	0.7175	0.5824	0.7175
12.66	0.5929	0.7296	0.5929	0.7296	0.5929	0.7296
14.66	0.5984	0.7336	0.5984	0.7336	0.5984	0.7336
16.66	0.6098	0.7481	0.6098	0.7481	0.6098	0.7481
18.66	0.6108	0.7581	0.6108	0.7581	0.6108	0.7581
20.66	0.6150	0.7558	0.6150	0.7558	0.6150	0.7558
25.67	0.6303	0.7723	0.6303	0.7723	0.6303	0.7723
30.66	0.6440	0.7878	0.6440	0.7878	0.6440	0.7878
35.66	0.6582	0.7948	0.6582	0.7948	0.6582	0.7948
40.66	0.6657	0.8122	0.6657	0.8122	0.6657	0.8122
45.66	0.6751	0.8227	0.6751	0.8227	0.6751	0.8227
50.67	0.6832	0.8318	0.6832	0.8318	0.6832	0.8318
55.66	0.6985	0.8465	0.6985	0.8465	0.6985	0.8465
60.66	0.7042	0.8558	0.7042	0.8558	0.7042	0.8558
70.66	0.7269	0.8800	0.7269	0.8800	0.7269	0.8800
80.66	0.7516	0.9053	0.7516	0.9053	0.7516	0.9053
90.71	0.7679	0.9246	0.7679	0.9246	0.7679	0.9246
100.43	0.7943	0.9528	0.7943	0.9528	0.7943	0.9528
110.43	0.8126	0.9722	0.8126	0.9722	0.8126	0.9722
120.43	0.8211	0.9812	0.8211	0.9812	0.8211	0.9812
130.44	0.8257	0.9868	0.8257	0.9868	0.8257	0.9868
140.43	0.8400	1.0010	0.8400	1.0010	0.8400	1.0010
150.44	0.8590	1.0000	0.8590	1.0000	0.8590	1.0000
160.43	0.8410	1.0021	0.8410	1.0021	0.8410	1.0021
170.43	0.8350	1.0005	0.8350	1.0005	0.8350	1.0005
180.43	0.8312	0.9918	0.8312	0.9918	0.8312	0.9918
190.46	0.8254	0.9857	0.8254	0.9857	0.8254	0.9857

R (NOMINAL) = 1.4

 X=245 MM
 DELTA=9.5418" (MEASURED P)
 DEL 995=25.4 MM
 ME=1.08 (MEASURED P)

 X=250 MM
 DELTA=9.59418" (MEASURED P)
 DEL 995=25.1 MM
 ME=1.08 (MEASURED P)

R (NOMINAL) = 1.4

 X=250 MM
 DELTA=9.59418" (MEASURED P)
 DEL 995=25.1 MM
 ME=1.08 (MEASURED P)

R (NOMINAL) = 1.4

 X=245 MM
 DELTA=9.5418" (MEASURED P)
 DEL 995=25.4 MM
 ME=1.08 (MEASURED P)

R (NOMINAL) = 1.4

 X=228 MM
 DELTA=9.41818" (MEASURED P)
 DEL 995=27.8 MM
 ME=1.06 (MEASURED P)

V (MM)	CONST	FM	MEASURED P	N	U/L	P/P10	P1/P10
0.00	0.0000	0.0000	0.0000	0.0000	0.0000	0.0000	0.0000
0.05	0.7264	0.5966	0.7365	0.5966	0.7365	0.5966	0.7365
0.10	0.7413	0.6023	0.7519	0.6023	0.7519	0.6023	0.7519
0.15	0.7579	0.6217	0.7679	0.6217	0.7679	0.6217	0.7679
0.20	0.7806	0.6452	0.7906	0.6452	0.7906	0.6452	0.7906
0.25	0.8036	0.6678	0.8136	0.6678	0.8136	0.6678	0.8136
0.30	0.8268	0.6898	0.8368	0.6898	0.8368	0.6898	0.8368
0.35	0.8500	0.7118	0.8600	0.7118	0.8600	0.7118	0.8600
0.40	0.8734	0.7338	0.8834	0.7338	0.8834	0.7338	0.8834
0.45	0.8969	0.7558	0.9069	0.7558	0.9069	0.7558	0.9069
0.50	0.9204	0.7778	0.9304	0.7778	0.9304	0.7778	0.9304
0.55	0.9439	0.7998	0.9539	0.7998	0.9539	0.7998	0.9539
0.60	0.9674	0.8218	0.9774	0.8218	0.9774	0.8218	0.9774
0.65	0.9909	0.8438	1.0009	0.8438	1.0009	0.8438	1.0009
0.70	1.0144	0.8658	1.0244	0.8658	1.0244	0.8658	1.0244
0.75	1.0379	0.8878	1.0479	0.8878	1.0479	0.8878	1.0479
0.80	1.0614	0.9098	1.0714	0.9098	1.0714	0.9098	1.0714
0.85	1.0849	0.9318	1.0949	0.9318	1.0949	0.9318	1.0949
0.90	1.1084	0.9538	1.1184	0.9538	1.1184	0.9538	1.1184
0.95	1.1319	0.9758	1.1419	0.9758	1.1419	0.9758	1.1419
1.00	1.1554	0.9978	1.1654	0.9978	1.1654	0.9978	1.1654
1.05	1.1789	1.0198	1.1889	1.0198	1.1889	1.0198	1.1889
1.10	1.2024	1.0418	1.2124	1.0418	1.2124	1.0418	1.2124
1.15	1.2259	1.0638	1.2359	1.0638	1.2359	1.0638	1.2359
1.20	1.2494	1.0858	1.2594	1.0858	1.2594	1.0858	1.2594
1.25	1.2729	1.1078	1.2829	1.1078	1.2829	1.1078	1.2829
1.30	1.2964	1.1298	1.3064	1.1298	1.3064	1.1298	1.3064
1.35	1.3199	1.1518	1.3299	1.1518	1.3299	1.1518	1.3299
1.40	1.3434	1.1738	1.3534	1.1738	1.3534	1.1738	1.3534
1.45	1.3669	1.1958	1.3769	1.1958	1.3769	1.1958	1.3769
1.50	1.3904	1.2178	1.4004	1.2178	1.4004	1.2178	1.4004
1.55	1.4139	1.2398	1.4239	1.2398	1.4239	1.2398	1.4239
1.60	1.4374	1.2618	1.4474	1.2618	1.4474	1.2618	1.4474
1.65	1.4609	1.2838	1.4709	1.2838	1.4709	1.2838	1.4709
1.70	1.4844	1.3058	1.4944	1.3058	1.4944	1.3058	1.4944
1.75	1.5079	1.3278	1.5179	1.3278	1.5179	1.3278	1.5179
1.80	1.5314	1.3498	1.5414	1.3498	1.5414	1.3498	1.5414
1.85	1.5549	1.3718	1.5649	1.3718	1.5649	1.3718	1.5649
1.90	1.5784	1.3938	1.5884	1.3938	1.5884	1.3938	1.5884
1.95	1.6019	1.4158	1.6119	1.4158	1.6119	1.4158	1.6119
2.00	1.6254	1.4378	1.6354	1.4378	1.6354	1.4378	1.6354
2.05	1.6489	1.4598	1.6589	1.4598	1.6589	1.4598	1.6589
2.10	1.6724	1.4818	1.6824	1.4818	1.6824	1.4818	1.6824
2.15	1.6959	1.5038	1.7059	1.5038	1.7059	1.5038	1.7059
2.20	1.7194	1.5258	1.7294	1.5258	1.7294	1.5258	1.7294
2.25	1.7429	1.5478	1.7529	1.5478	1.7529	1.5478	1.7529
2.30	1.7664	1.5698	1.7764	1.5698	1.7764	1.5698	1.7764
2.35	1.7899	1.5918	1.7999	1.5918	1.7999	1.5918	1.7999
2.40	1.8134	1.6138	1.8234	1.6138	1.8234	1.6138	1.8234
2.45	1.8369	1.6358	1.8469	1.6358	1.8469	1.6358	1.8469
2.50	1.8604	1.6578	1.8704	1.6578	1.8704	1.6578	1.8704
2.55	1.8839	1.6798	1.8939	1.6798	1.8939	1.6798	1.8939
2.60	1.9074	1.7018	1.9174	1.7018	1.9174	1.7018	1.9174
2.65	1.9309	1.7238	1.9409	1.7238	1.9409	1.7238	1.9409
2.70	1.9544	1.7458	1.9644	1.7458	1.9644	1.7458	1.9644
2.75	1.9779	1.7678	1.9879	1.7678	1.9879	1.7678	1.9879
2.80	2.0014	1.7898	2.0114	1.7898	2.0114	1.7898	2.0114
2.85	2.0249	1.8118	2.0349	1.8118	2.0349	1.8118	2.0349
2.90	2.0484	1.8338	2.0584	1.8338	2.0584	1.8338	2.0584
2.95	2.0719	1.8558	2.0819	1.8558	2.0819	1.8558	2.0819
3.00	2.0954	1.8778	2.1054	1.8778	2.1054	1.8778	2.1054
3.05	2.1189	1.8998	2.1289	1.8998	2.1289	1.8998	2.1289
3.10	2.1424	1.9218	2.1524	1.9218	2.1524	1.9218	2.1524
3.15	2.1659	1.9438	2.1759	1.9438	2.1759	1.9438	2.1759
3.20	2.1894	1.9658	2.1994	1.9658	2.1994	1.9658	2.1994
3.25	2.2129	1.9878	2.2229	1.9878	2.2229	1.9878	2.2229
3.30	2.2364	2.0098	2.2464	2.0098	2.2464	2.0098	2.2464
3.35	2.2599	2.0318	2.2699	2.0318	2.2699	2.0318	2.2699
3.40	2.2834	2.0538	2.2934	2.0538	2.2934	2.0538	2.2934
3.45	2.3069	2.0758	2.3169	2.0758	2.3169	2.0758	2.3169
3.50	2.3304	2.0978	2.3404	2.0978	2.3404	2.0978	2.3404
3.55	2.3539	2.1198	2.3639	2.1198	2.3639	2.1198	2.3639
3.60	2.3774	2.1418	2.3874	2.1418	2.3874	2.1418	2.3874
3.65	2.4009	2.1638	2.4109	2.1638	2.4109	2.1638	2.4109
3.70	2.4244	2.1858	2.4344	2.1858	2.4344	2.1858	2.4344
3.75	2.4479	2.2078	2.4579	2.2078	2.4579	2.2078	2.4579
3.80	2.4714	2.2298	2.4814	2.2298	2.4814	2.2298	2.4814
3.85	2.4949	2.2518	2.5049	2.2518	2.5049	2.2518	2.5049
3.90	2.5184	2.2738	2.5284	2.2738	2.5284	2.2738	2.5284
3.95	2.5419	2.2958	2.5519	2.2958	2.5519	2.2958	2.5519
4.00	2.5654	2.3178	2.5754	2.3178	2.5754	2.3178	2.5754
4.05	2.5889	2.3398	2.5989	2.3398	2.5989	2.3398	2.5989
4.10	2.6124	2.3618	2.6224	2.3618	2.6224	2.3618	2.6224
4.15	2.6359	2.3838	2.6459	2.3838	2.6459	2.3838	2.6459
4.20	2.6594	2.4058	2.6694	2.4058	2.6694	2.4058	2.6694
4.25	2.6829	2.4278	2.6929	2.4278	2.6929	2.4278	2.6929
4.30	2.7064	2.4498	2.7164	2.4498	2.7164	2.4498	2.7164
4.35	2.7299	2.4718	2.7399	2.4718	2.7399	2.4718	2.7399
4.40	2.7534	2.4938	2.7634	2.4938	2.7634	2.4938	2.7634
4.45	2.7769	2.5158	2.7869	2.5158	2.7869	2.5158	2.7869
4.50	2.8004	2.5378	2.8104	2.5378	2.8104	2.5378	2.8104
4.55	2.8239	2.5598	2.8339	2.5598	2.8339	2.5598	2.8339
4.60	2.8474	2.5818	2.8574	2.5818	2.8574	2.5818	2.8574
4.65	2.8709	2.6038	2.8809	2.6038	2.8809	2.6038	2.8809
4.70	2.8944	2.6258	2.9044	2.6258	2.9044	2.6258	2.9044
4.75	2.9179	2.6478	2.9279	2.6478	2.9279	2.6478	2.9279
4.80	2.9414	2.6698	2.9514	2.6698	2.9514	2.6698	2.9514
4.85	2.9649	2.6918	2.9749	2.6918	2.9749	2.6918	2.9749
4.90	2.9884	2.7138	2.9984	2.7138	2.9984	2.7138	2.9984
4.95	3.0119	2.7358	3.0219	2.7358	3.0219	2.7358	3.0219
5.00	3.0354	2.7578	3.0454	2.7578	3.0454	2.7578	3.0454

V (MM)	CONST	FM	N	U/L	N	U/L	P/P10	P1/P10
0.00	0.0000	0.0000	0.0000	0.0000	0.0000	0.0000	0.0000	0.0000
0.05	0.7241	0.5817	0.7241	0.5817	0.7241	0.5817	0.7241	0.5817
0.10	0.7390	0.5976	0.7390	0.5976	0.7390	0.5976	0.7390	0.5976
0.15	0.7539	0.6135	0.7539	0.6135	0.7539	0.6135	0.7539	0.6135
0.20	0.7688	0.6294	0.7688	0.6294	0.7688	0.6294	0.7688	0.6294
0.25	0.7837	0.6453	0.7837	0.6453	0.7837	0.6453	0.7837	0.6453
0.30	0.7986	0.6612	0.7986	0.6612	0.7986	0.6612	0.7986	0.6612
0.35	0.8135	0.6771	0.8135	0.6771	0.8135	0.6771	0.8135	0.6771
0.40	0.8284	0.6930	0.8284	0.6930	0.8284	0.6930	0.8284	0.6930
0.45	0.8433	0.7089	0.8433	0.7089	0.8433	0.7089	0.8433	0.7089
0.50	0.8582	0.7248	0.8582	0.7248	0.8582	0.7248	0.8582	0.7248
0.55	0.8731	0.7407	0.8731	0.7407	0.8731	0.7407	0.8731	0.7407
0.60	0.8880	0.7566	0.8880	0.7566	0.8880	0.7566	0.8880	0.7566
0.65	0.9029	0.7725	0.9029	0.7725	0.9029	0.7725	0.9029	0.7725
0.70	0.9178	0.7884	0.9178	0.7884	0.9178	0.7884	0.9178	0.7884
0.75	0.9327	0.8043	0.9327	0.8043	0.9327	0.8043	0.9327	0.8043
0.80	0.9476	0.8202	0.9476	0.8202	0.9476	0.8202	0.9476	0.8202
0.85	0.9625	0.8361	0.9625	0.8361	0.9625	0.8361	0.9625	0.8361
0.90	0.9774	0.8520	0.9774	0.8520	0.9774	0.8520	0.9774	0.8520
0.95	0.9923	0.8679	0.9923	0.8679	0.9923	0.8679	0.9923	0.8679
1.00	1.0072	0.8838	1.0072	0.8838	1.0072	0.8838	1.0072	0.8838
1.05	1.0221	0.8997	1.0221	0.8997	1.0221	0.8997	1.0221	0.8997
1.10	1.0370	0.9156	1.0370	0.9156	1.0370	0.9156	1.0370	0.9156
1.15	1.0519	0.9315	1.0519	0.9315	1.0519	0.9315	1.0519	0.9315
1.20	1.0668	0.9474	1.0668	0.9474	1.0668	0.9474	1.0668	0.9474
1.25	1.0817	0.9633	1.0817	0.9633	1.0817	0.9633	1.0817	0.9633
1.30	1.0966	0.9792	1.0966	0.9792	1.0966	0.9792	1.0966	0.9792
1.35	1.1115	0.9951	1.1115	0.9951	1.1115	0.9951	1.1115	0.9951
1.40	1.1264	1.0110	1.1264	1.0110	1.1264	1.0110	1.1264	1.0110
1.45	1.1413	1.0269	1.1413	1.0269	1.1413	1.0269	1.1413	1.0269
1.50	1.1562	1.0428	1.1562	1.0428	1.1562	1.0428	1.1562	1.0428
1.55	1.1711	1.0587	1.1711	1.0587	1.1711	1.0587	1.1711	1.0587
1.60	1.1860	1.0746	1.1860	1.0746	1.1860	1.0746	1.1860	1.0746
1.65	1.2009	1.0905	1.2009	1.0905	1.2009	1.0905	1.2009	1.0905
1.70	1.2158	1.1064	1.2158	1.1064	1.2158	1.1064	1.2158	1.1064
1.75	1.2307	1.1223	1.2307	1.1223	1.2307	1.1223	1.2307	1.1223
1.80	1.2456	1.1382	1.2456	1.1382	1.2456	1.1382	1.2456	1.1382
1.85	1.2605	1.1541	1.2605	1.1541	1.2605	1.1541	1.2605	1.1541
1.90	1.2754	1.1700	1.2754	1.1700	1.2754	1.1700	1.2754	1.1700
1.95	1.2903	1.1859	1.2903	1.1859	1.2903	1.1859	1.2903	1.1859
2.00	1.3052	1.2018	1.3052	1.2018	1.3052	1.2018	1.3052	1.2018
2.05	1.3201	1.2177	1.3201	1.2177	1.3201	1.2177	1.3201	1.2177
2.10	1.3350	1.2336	1.3350	1.2336	1.3350	1.2336	1.3350	1.2336
2.15	1.3499	1.2495	1.3499	1.2495	1.3499	1.2495	1.3499	1.2495
2.20	1.3648	1.2654	1.3648	1.2654	1.3648	1.2654	1.3648	1.2654
2.25	1.3797	1.2813	1.3797	1.2813	1.3797	1.2813	1.3797	1.2813
2.30	1.3946	1.2972	1.3946	1.2972	1.3946	1.2972	1.3946	1.2972
2.35	1.4095	1.3131	1.4095	1.3131	1.4095	1.3131	1.4095	1.3131
2.40	1.4244	1.3290	1.4244	1.3290	1.4244	1.3290	1.4244	1.3290
2.45	1.4393	1.3449	1.4393	1.3449	1.4393	1.3449	1.4393	1.3449
2.50	1.4542	1.3608	1.4542	1.3608	1.4542	1.3608	1.4542	1.3608
2.55	1.4691	1.3767	1.4691	1.3767	1.4691	1.3767	1.4691	1.3767
2.60	1.4840	1.3926	1.4840	1.3926	1.4840	1.3926	1.4840	1.3926
2.65	1.4989	1.4085	1.4989	1.4085	1.4989	1.4085	1.4989	1.4085
2.70	1.5138	1.4244	1.5138	1.4244	1.5138	1.4244	1.5138	1.4244
2.75	1.5287	1.4403	1.5287	1.4403	1.5287	1.4403	1.5287	1.4403
2.80	1.5436	1.4562	1.5436	1.4562	1.5436	1.4562	1.5436	1.4562
2.85	1.5585	1.4721	1.5585	1.4721	1.5585	1.4721	1.5585	1.4721
2.90	1.5734	1.4880	1.5734	1.4880	1.5734	1.4880	1.5734	1.4880
2.95	1.5883	1.5039	1.5883	1.5039	1.5883	1.5039	1.5883	1.5039
3.00	1.6032	1.5198	1.6032	1.5198	1.6032	1.5198	1.6032	1.5198
3.05	1.6181	1.5357	1.6181	1.5357	1.6181	1.5357	1.6181	1.5357
3.10	1.6330	1.5516	1.6330	1.5516	1.6330	1.5516	1.6330	1.5516
3.15	1.6479	1.5675	1.6479	1.5675	1.6479	1.5675	1.6479	1.5675
3.20	1.6628	1.5834	1.6628	1.5834	1.6628	1.5834	1.6628	1.5834
3.25	1.6777	1.5993	1.6777	1.5993	1.6777	1.5993	1.6777	1.5993
3.30	1.6926	1.6152	1.6926	1.6152	1.6926	1.6152	1.6926	1.6152
3.35	1.7075	1.6311	1.7075	1.6311	1.7075	1.6311	1.7075	1.6311
3.40	1.7224	1.6470	1.7224	1.6470	1.7224	1.6470	1.7224	1.6470
3.45	1.7373	1.6629	1.7373	1.6629	1.7373	1.6629	1.7373	1.6629
3.50	1.7522	1.6788	1.7522	1.6788	1.7522	1.6788	1.7522	1.6788
3.55	1.7671	1.6947	1.7671	1.6947	1.7671	1.6947	1.7671	1.6947
3.60	1.7820	1.7106	1.7820	1.7106	1.7820	1.7106	1.7820	1.7106
3.65	1.7969	1.7265	1.7969	1.7265	1.7969	1.7265	1.7969	1.7265
3.70	1.8118	1.7424	1.8118	1.7424	1.8118	1.7424	1.8118	1.7424
3.75	1.8267	1.7583	1.8267	1.7583	1.8267	1.7583	1.8267	1.7583
3.80	1.8416	1.7742	1.8416	1.7742	1.8416	1.7742	1.8416	1.7742
3.85	1.8565	1.7901	1.8565	1.7901	1.8565	1.7901	1.8565	1.7901
3.90	1.8714	1.8060	1.8714	1.8060	1.8714	1.8060	1.8714	1.8060
3.95	1.8863	1.8219	1.8863	1.8219	1.8863	1.8219	1.8863	1.8219
4.00	1.9012	1.8378	1.9012	1.8378	1.9012	1.8378	1.9012	1.8378
4.05	1.9161	1.8537	1.9161	1.8537	1.9161	1.8537	1.9161	1.8537
4.10	1.9310	1.8696	1.9310	1.8696	1.9310	1.8696	1.9310	1.8696
4.15	1.9459	1.8855	1.9459	1.8855	1.9459	1.8855	1.9459	1.8855
4.20	1.9608	1.9014	1.9608	1.9014	1.9608	1.9014	1.9608	1.9014
4.25	1.9757	1.9173	1.9757	1.9173	1.9757	1.9173	1.9757	1.9173
4.30	1.9906	1.9332	1.9906	1.9332	1.9906	1.9332	1.9906	1.9332
4.35	2.0055	1.9491	2.0055	1.9491	2.0055	1.9491	2.0055	1.9491
4.40	2.0204	1.9650	2.0204	1.9650	2.0204	1.9650	2.0204	1.9650
4.45	2.0353	1.9809	2.0353	1.9809	2.0353	1.9809	2.0353	1.9809
4.50	2.0502	1.9968	2.0502	1.9968	2.0502	1.9968	2.0502	1.9968
4.55	2.0651	2.0127	2.0651	2.0127	2.0651	2.0127	2.0651	2.0127
4.60	2.0800	2.0286	2.0800	2.0286	2.0800	2.0286	2.0800	2.0286
4.65	2.0949	2.0445	2.0949	2.0445	2.0949	2.0445	2.0949	2.0445
4.70	2.1098	2.0604	2.1098	2.0604	2.1098	2.0604	2.1098	2.0604
4.75	2.1247	2.0763	2.1247	2.0763	2.1247	2.0763	2.1247	2.0763
4.80	2.1396	2.0922	2.1396	2.0922	2.1396	2.0922	2.1396	2.0922
4.85	2.1545	2.1081	2.1545	2.1081	2.1545	2.1081	2.1545	2.1081
4.90	2.1694	2.1240	2.1694	2.1240	2.1694	2.1240	2.1694	2.1240
4.95	2.1843	2.1399	2.1843	2.1399	2.1843	2.1399	2.1843	2.1399
5.00	2.1992	2.1558	2.1992	2.1558	2.1992	2.1558	2.1992	2.1558

[illegible]

Y (MM)	N	WUE	N	WUE	P/P10	P1/P10
1 (01)	1	0.00	1	0.00	0.00	0.00
2 (02)	1	0.00	1	0.00	0.00	0.00
3 (03)	1	0.00	1	0.00	0.00	0.00
4 (04)	1	0.00	1	0.00	0.00	0.00
5 (05)	1	0.00	1	0.00	0.00	0.00
6 (06)	1	0.00	1	0.00	0.00	0.00
7 (07)	1	0.00	1	0.00	0.00	0.00
8 (08)	1	0.00	1	0.00	0.00	0.00
9 (09)	1	0.00	1	0.00	0.00	0.00
10 (10)	1	0.00	1	0.00	0.00	0.00
11 (11)	1	0.00	1	0.00	0.00	0.00
12 (12)	1	0.00	1	0.00	0.00	0.00

5 6 - (continued)

Y (MM)	CONST PM	MEASURED P
	M	M
	UAE	UAE
	P/P10	P/P10

1. *Is the study a cohort study?*

P (MPa)	CONST PW		MEASURED P	
	M	U-VE	M	U-VE
0.1				
0.2				
0.3				
0.4				
0.5				
0.6				
0.7				
0.8				
0.9				
1.0				
1.1				
1.2				
1.3				
1.4				
1.5				
1.6				
1.7				
1.8				
1.9				
2.0				
2.1				
2.2				
2.3				
2.4				
2.5				
2.6				
2.7				
2.8				
2.9				
3.0				
3.1				
3.2				
3.3				
3.4				
3.5				
3.6				
3.7				
3.8				
3.9				
4.0				
4.1				
4.2				
4.3				
4.4				
4.5				
4.6				
4.7				
4.8				
4.9				
5.0				
5.1				
5.2				
5.3				
5.4				
5.5				
5.6				
5.7				
5.8				
5.9				
6.0				
6.1				
6.2				
6.3				
6.4				
6.5				
6.6				
6.7				
6.8				
6.9				
7.0				
7.1				
7.2				
7.3				
7.4				
7.5				
7.6				
7.7				
7.8				
7.9				
8.0				
8.1				
8.2				
8.3				
8.4				
8.5				
8.6				
8.7				
8.8				
8.9				
9.0				
9.1				
9.2				
9.3				
9.4				
9.5				
9.6				
9.7				
9.8				
9.9				
10.0				

1. *Journal of the American Medical Association*, 1997; 278: 1039-1044.

[illegible][illegible]

$$M(\text{Methyl}) = 15$$

$\lambda = 456 \text{ nm}$ $T = 291.8 \text{ K}$ $\Delta T = 102.3 \text{ mK}$
 $\Delta T / T = 3.54 \times 10^{-6}$ (MEASURED P) $\Delta T = 1.008$ (MEASURED P)

CONST	N	UVE	N	UVE	REPROD	P	P/PTO	P/PTO
0.00	0.000	0.000	0.000	0.000	0.000	0.000	0.000	0.000
0.05	0.505	0.654	0.505	0.654	0.505	0.504	0.507	0.508
0.09	0.849	0.735	0.849	0.735	0.849	0.736	0.740	0.742
1.10	1.555	1.640	1.555	1.640	1.555	1.640	1.580	1.580
1.15	1.555	1.658	1.555	1.658	1.555	1.658	1.580	1.580
1.49	1.654	1.743	1.654	1.743	1.654	1.743	1.580	1.580
1.71	1.705	1.815	1.705	1.815	1.705	1.815	1.580	1.580
2.15	2.658	2.729	2.658	2.729	2.658	2.729	2.580	2.580
2.70	2.701	2.814	2.701	2.814	2.701	2.814	2.580	2.580
3.19	3.032	3.032	3.032	3.032	3.032	3.032	2.580	2.580
2.69	3.026	3.194	3.026	3.194	3.026	3.194	2.580	2.580
4.49	3.164	3.507	3.164	3.507	3.164	3.507	2.580	2.580
6.70	3.190	2.861	3.190	2.861	3.190	2.861	2.580	2.580
10.70	3.166	1.998	3.166	1.998	3.166	1.998	2.580	2.580
10.70	2.061	1.356	2.061	1.356	2.061	1.356	2.580	2.580
12.19	2.159	0.299	2.159	0.299	2.159	0.299	2.580	2.580
14.14	2.418	1.572	2.418	1.572	2.418	1.572	2.580	2.580
16.16	2.485	0.642	2.485	0.642	2.485	0.642	2.580	2.580
18.18	2.721	0.000	2.721	0.000	2.721	0.000	2.580	2.580
20.19	2.780	0.000	2.780	0.000	2.780	0.000	2.580	2.580
22.20	2.780	0.000	2.780	0.000	2.780	0.000	2.580	2.580
24.21	2.780	0.000	2.780	0.000	2.780	0.000	2.580	2.580
26.22	2.780	0.000	2.780	0.000	2.780	0.000	2.580	2.580
28.23	2.780	0.000	2.780	0.000	2.780	0.000	2.580	2.580
30.24	2.780	0.000	2.780	0.000	2.780	0.000	2.580	2.580
32.25	2.780	0.000	2.780	0.000	2.780	0.000	2.580	2.580
34.26	2.780	0.000	2.780	0.000	2.780	0.000	2.580	2.580
36.27	2.780	0.000	2.780	0.000	2.780	0.000	2.580	2.580
38.28	2.780	0.000	2.780	0.000	2.780	0.000	2.580	2.580
40.29	2.780	0.000	2.780	0.000	2.780	0.000	2.580	2.580
42.30	2.780	0.000	2.780	0.000	2.780	0.000	2.580	2.580
44.31	2.780	0.000	2.780	0.000	2.780	0.000	2.580	2.580
46.32	2.780	0.000	2.780	0.000	2.780	0.000	2.580	2.580
48.33	2.780	0.000	2.780	0.000	2.780	0.000	2.580	2.580
50.34	2.780	0.000	2.780	0.000	2.780	0.000	2.580	2.580
52.35	2.780	0.000	2.780	0.000	2.780	0.000	2.580	2.580
54.36	2.780	0.000	2.780	0.000	2.780	0.000	2.580	2.580
56.37	2.780	0.000	2.780	0.000	2.780	0.000	2.580	2.580
58.38	2.780	0.000	2.780	0.000	2.780	0.000	2.580	2.580
60.39	2.780	0.000	2.780	0.000	2.780	0.000	2.580	2.580
62.40	2.780	0.000	2.780	0.000	2.780	0.000	2.580	2.580
64.41	2.780	0.000	2.780	0.000	2.780	0.000	2.580	2.580
66.42	2.780	0.000	2.780	0.000	2.780	0.000	2.580	2.580
68.43	2.780	0.000	2.780	0.000	2.780	0.000	2.580	2.580
70.44	2.780	0.000	2.780	0.000	2.780	0.000	2.580	2.580
72.45	2.780	0.000	2.780	0.000	2.780	0.000	2.580	2.580
74.46	2.780	0.000	2.780	0.000	2.780	0.000	2.580	2.580
76.47	2.780	0.000	2.780	0.000	2.780	0.000	2.580	2.580
78.48	2.780	0.000	2.780	0.000	2.780	0.000	2.580	2.580
80.49	2.780	0.000	2.780	0.000	2.780	0.000	2.580	2.580
82.50	2.780	0.000	2.780	0.000	2.780	0.000	2.580	2.580
84.51	2.780	0.000	2.780	0.000	2.780	0.000	2.580	2.580
86.52	2.780	0.000	2.780	0.000	2.780	0.000	2.580	2.580
88.53	2.780	0.000	2.780	0.000	2.780	0.000	2.580	2.580
90.54	2.780	0.000	2.780	0.000	2.780	0.000	2.580	2.580
92.55	2.780	0.000	2.780	0.000	2.780	0.000	2.580	2.580
94.56	2.780	0.000	2.780	0.000	2.780	0.000	2.580	2.580
96.57	2.780	0.000	2.780	0.000	2.780	0.000	2.580	2.580
98.58	2.780	0.000	2.780	0.000	2.780	0.000	2.580	2.580
100.59	2.780	0.000	2.780	0.000	2.780	0.000	2.580	2.580

$$H(\text{NORMAL}) = 1.5$$

```

X= 749 MH      10= 291 S K      DEL 995=118 ; MH
DE ME= } 53106 (MEASURED P)      ME=0 975 (MEASURED P)

```

[illegible] $\mu(\text{NOMINER}) = 1.5$

$\tau = 1043$ MHz $\tau = 291$ @ K DEL 995 = 129 @ MH

[illegible]

5 4 5

10-282 6 K DEL 995-139 5 MM

CONST	PVE		REGRESSED P		PVE		PVE		PVE	
	N	WVE	N	WVE	N	WVE	N	WVE	N	WVE
0.00	0.0000	0.0000	0.0000	0.0000	0.0000	0.0000	0.0000	0.0000	0.0000	0.0000
0.05	0.3544	0.4141	0.3544	0.4141	0.3544	0.4141	0.3544	0.4141	0.3544	0.4141
0.10	0.3666	0.4007	0.3666	0.4007	0.3666	0.4007	0.3666	0.4007	0.3666	0.4007
0.15	0.3788	0.3870	0.3788	0.3870	0.3788	0.3870	0.3788	0.3870	0.3788	0.3870
0.20	0.3910	0.3731	0.3910	0.3731	0.3910	0.3731	0.3910	0.3731	0.3910	0.3731
0.25	0.4032	0.3592	0.4032	0.3592	0.4032	0.3592	0.4032	0.3592	0.4032	0.3592
0.30	0.4154	0.3453	0.4154	0.3453	0.4154	0.3453	0.4154	0.3453	0.4154	0.3453
0.35	0.4276	0.3314	0.4276	0.3314	0.4276	0.3314	0.4276	0.3314	0.4276	0.3314
0.40	0.4398	0.3175	0.4398	0.3175	0.4398	0.3175	0.4398	0.3175	0.4398	0.3175
0.45	0.4520	0.3036	0.4520	0.3036	0.4520	0.3036	0.4520	0.3036	0.4520	0.3036
0.50	0.4642	0.2897	0.4642	0.2897	0.4642	0.2897	0.4642	0.2897	0.4642	0.2897
0.55	0.4764	0.2758	0.4764	0.2758	0.4764	0.2758	0.4764	0.2758	0.4764	0.2758
0.60	0.4886	0.2619	0.4886	0.2619	0.4886	0.2619	0.4886	0.2619	0.4886	0.2619
0.65	0.5008	0.2480	0.5008	0.2480	0.5008	0.2480	0.5008	0.2480	0.5008	0.2480
0.70	0.5130	0.2341	0.5130	0.2341	0.5130	0.2341	0.5130	0.2341	0.5130	0.2341
0.75	0.5252	0.2202	0.5252	0.2202	0.5252	0.2202	0.5252	0.2202	0.5252	0.2202
0.80	0.5374	0.2063	0.5374	0.2063	0.5374	0.2063	0.5374	0.2063	0.5374	0.2063
0.85	0.5496	0.1924	0.5496	0.1924	0.5496	0.1924	0.5496	0.1924	0.5496	0.1924
0.90	0.5618	0.1785	0.5618	0.1785	0.5618	0.1785	0.5618	0.1785	0.5618	0.1785
0.95	0.5740	0.1646	0.5740	0.1646	0.5740	0.1646	0.5740	0.1646	0.5740	0.1646
1.00	0.5862	0.1507	0.5862	0.1507	0.5862	0.1507	0.5862	0.1507	0.5862	0.1507

N. NUMBER = 1.5

 25 1250 MH
 DEL 995-157.6 MH
 MEAS 1.25016 S (MEASURED P)
 MEAS 875 (MEASURED P)

V (MH)	CONST	PIV	MEASURED P	PIV	P/PIV	P/PIV
0.00	0.0000	0.0000	0.0000	0.0000	0.0015	0.0015
0.66	0.3020	0.421	0.320	0.421	0.0015	0.0015
0.85	0.3526	0.476	0.356	0.476	0.0015	0.0015
1.06	0.4015	0.529	0.4015	0.529	0.0015	0.0015
1.26	0.4488	0.575	0.4488	0.575	0.0015	0.0015
1.46	0.4758	0.613	0.4758	0.613	0.0015	0.0015
1.66	0.4939	0.646	0.4939	0.646	0.0015	0.0015
1.86	0.5069	0.675	0.5069	0.675	0.0015	0.0015
2.06	0.5168	0.700	0.5168	0.700	0.0015	0.0015
2.26	0.5240	0.721	0.5240	0.721	0.0015	0.0015
2.46	0.5291	0.739	0.5291	0.739	0.0015	0.0015
2.66	0.5327	0.754	0.5327	0.754	0.0015	0.0015
2.86	0.5351	0.767	0.5351	0.767	0.0015	0.0015
3.06	0.5365	0.778	0.5365	0.778	0.0015	0.0015
3.26	0.5370	0.787	0.5370	0.787	0.0015	0.0015
3.46	0.5374	0.794	0.5374	0.794	0.0015	0.0015
3.66	0.5377	0.800	0.5377	0.800	0.0015	0.0015
3.86	0.5379	0.805	0.5379	0.805	0.0015	0.0015
4.06	0.5380	0.809	0.5380	0.809	0.0015	0.0015
4.26	0.5381	0.812	0.5381	0.812	0.0015	0.0015
4.46	0.5382	0.815	0.5382	0.815	0.0015	0.0015
4.66	0.5383	0.817	0.5383	0.817	0.0015	0.0015
4.86	0.5384	0.819	0.5384	0.819	0.0015	0.0015
5.06	0.5385	0.821	0.5385	0.821	0.0015	0.0015
5.26	0.5386	0.823	0.5386	0.823	0.0015	0.0015
5.46	0.5387	0.825	0.5387	0.825	0.0015	0.0015
5.66	0.5388	0.827	0.5388	0.827	0.0015	0.0015
5.86	0.5389	0.829	0.5389	0.829	0.0015	0.0015
6.06	0.5390	0.831	0.5390	0.831	0.0015	0.0015
6.26	0.5391	0.833	0.5391	0.833	0.0015	0.0015
6.46	0.5392	0.835	0.5392	0.835	0.0015	0.0015
6.66	0.5393	0.837	0.5393	0.837	0.0015	0.0015
6.86	0.5394	0.839	0.5394	0.839	0.0015	0.0015
7.06	0.5395	0.841	0.5395	0.841	0.0015	0.0015
7.26	0.5396	0.843	0.5396	0.843	0.0015	0.0015
7.46	0.5397	0.845	0.5397	0.845	0.0015	0.0015
7.66	0.5398	0.847	0.5398	0.847	0.0015	0.0015
7.86	0.5399	0.849	0.5399	0.849	0.0015	0.0015
8.06	0.5400	0.851	0.5400	0.851	0.0015	0.0015
8.26	0.5401	0.853	0.5401	0.853	0.0015	0.0015
8.46	0.5402	0.855	0.5402	0.855	0.0015	0.0015
8.66	0.5403	0.857	0.5403	0.857	0.0015	0.0015
8.86	0.5404	0.859	0.5404	0.859	0.0015	0.0015
9.06	0.5405	0.861	0.5405	0.861	0.0015	0.0015
9.26	0.5406	0.863	0.5406	0.863	0.0015	0.0015
9.46	0.5407	0.865	0.5407	0.865	0.0015	0.0015
9.66	0.5408	0.867	0.5408	0.867	0.0015	0.0015
9.86	0.5409	0.869	0.5409	0.869	0.0015	0.0015
10.06	0.5410	0.871	0.5410	0.871	0.0015	0.0015
10.26	0.5411	0.873	0.5411	0.873	0.0015	0.0015
10.46	0.5412	0.875	0.5412	0.875	0.0015	0.0015
10.66	0.5413	0.877	0.5413	0.877	0.0015	0.0015
10.86	0.5414	0.879	0.5414	0.879	0.0015	0.0015
11.06	0.5415	0.881	0.5415	0.881	0.0015	0.0015
11.26	0.5416	0.883	0.5416	0.883	0.0015	0.0015
11.46	0.5417	0.885	0.5417	0.885	0.0015	0.0015
11.66	0.5418	0.887	0.5418	0.887	0.0015	0.0015
11.86	0.5419	0.889	0.5419	0.889	0.0015	0.0015
12.06	0.5420	0.891	0.5420	0.891	0.0015	0.0015
12.26	0.5421	0.893	0.5421	0.893	0.0015	0.0015
12.46	0.5422	0.895	0.5422	0.895	0.0015	0.0015
12.66	0.5423	0.897	0.5423	0.897	0.0015	0.0015
12.86	0.5424	0.899	0.5424	0.899	0.0015	0.0015
13.06	0.5425	0.901	0.5425	0.901	0.0015	0.0015
13.26	0.5426	0.903	0.5426	0.903	0.0015	0.0015
13.46	0.5427	0.905	0.5427	0.905	0.0015	0.0015
13.66	0.5428	0.907	0.5428	0.907	0.0015	0.0015
13.86	0.5429	0.909	0.5429	0.909	0.0015	0.0015
14.06	0.5430	0.911	0.5430	0.911	0.0015	0.0015
14.26	0.5431	0.913	0.5431	0.913	0.0015	0.0015
14.46	0.5432	0.915	0.5432	0.915	0.0015	0.0015
14.66	0.5433	0.917	0.5433	0.917	0.0015	0.0015
14.86	0.5434	0.919	0.5434	0.919	0.0015	0.0015
15.06	0.5435	0.921	0.5435	0.921	0.0015	0.0015
15.26	0.5436	0.923	0.5436	0.923	0.0015	0.0015
15.46	0.5437	0.925	0.5437	0.925	0.0015	0.0015
15.66	0.5438	0.927	0.5438	0.927	0.0015	0.0015
15.86	0.5439	0.929	0.5439	0.929	0.0015	0.0015
16.06	0.5440	0.931	0.5440	0.931	0.0015	0.0015
16.26	0.5441	0.933	0.5441	0.933	0.0015	0.0015
16.46	0.5442	0.935	0.5442	0.935	0.0015	0.0015
16.66	0.5443	0.937	0.5443	0.937	0.0015	0.0015
16.86	0.5444	0.939	0.5444	0.939	0.0015	0.0015
17.06	0.5445	0.941	0.5445	0.941	0.0015	0.0015
17.26	0.5446	0.943	0.5446	0.943	0.0015	0.0015
17.46	0.5447	0.945	0.5447	0.945	0.0015	0.0015
17.66	0.5448	0.947	0.5448	0.947	0.0015	0.0015
17.86	0.5449	0.949	0.5449	0.949	0.0015	0.0015
18.06	0.5450	0.951	0.5450	0.951	0.0015	0.0015
18.26	0.5451	0.953	0.5451	0.953	0.0015	0.0015
18.46	0.5452	0.955	0.5452	0.955	0.0015	0.0015
18.66	0.5453	0.957	0.5453	0.957	0.0015	0.0015
18.86	0.5454	0.959	0.5454	0.959	0.0015	0.0015
19.06	0.5455	0.961	0.5455	0.961	0.0015	0.0015
19.26	0.5456	0.963	0.5456	0.963	0.0015	0.0015
19.46	0.5457	0.965	0.5457	0.965	0.0015	0.0015
19.66	0.5458	0.967	0.5458	0.967	0.0015	0.0015
19.86	0.5459	0.969	0.5459	0.969	0.0015	0.0015
20.06	0.5460	0.971	0.5460	0.971	0.0015	0.0015
20.26	0.5461	0.973	0.5461	0.973	0.0015	0.0015
20.46	0.5462	0.975	0.5462	0.975	0.0015	0.0015
20.66	0.5463	0.977	0.5463	0.977	0.0015	0.0015
20.86	0.5464	0.979	0.5464	0.979	0.0015	0.0015
21.06	0.5465	0.981	0.5465	0.981	0.0015	0.0015
21.26	0.5466	0.983	0.5466	0.983	0.0015	0.0015
21.46	0.5467	0.985	0.5467	0.985	0.0015	0.0015
21.66	0.5468	0.987	0.5468	0.987	0.0015	0.0015
21.86	0.5469	0.989	0.5469	0.989	0.0015	0.0015
22.06	0.5470	0.991	0.5470	0.991	0.0015	0.0015
22.26	0.5471	0.993	0.5471	0.993	0.0015	0.0015
22.46	0.5472	0.995	0.5472	0.995	0.0015	0.0015
22.66	0.5473	0.997	0.5473	0.997	0.0015	0.0015
22.86	0.5474	0.999	0.5474	0.999	0.0015	0.0015
23.06	0.5475	1.001	0.5475	1.001	0.0015	0.0015
23.26	0.5476	1.003	0.5476	1.003	0.0015	0.0015
23.46	0.5477	1.005	0.5477	1.005	0.0015	0.0015
23.66	0.5478	1.007	0.5478	1.007	0.0015	0.0015
23.86	0.5479	1.009	0.5479	1.009	0.0015	0.0015
24.06	0.5480	1.011	0.5480	1.011	0.0015	0.0015
24.26	0.5481	1.013	0.5481	1.013	0.0015	0.0015
24.46	0.5482	1.015	0.5482	1.015	0.0015	0.0015
24.66	0.5483	1.017	0.5483	1.017	0.0015	0.0015
24.86	0.5484	1.019	0.5484	1.019	0.0015	0.0015
25.06	0.5485	1.021	0.5485	1.021	0.0015	0.0015

N. NUMBER = 1.5

 25 2250 MH
 DEL 995-172.0 MH
 MEAS 1.25016 S (MEASURED P)
 MEAS 875 (MEASURED P)

V (MH)	CONST	PIV	MEASURED P	PIV	P/PIV	P/PIV
0.00	0.0000	0.0000	0.0000	0.0000	0.0015	0.0015
0.66	0.3931	0.467	0.3931	0.467	0.0015	0.0015
0.85	0.4405	0.512	0.4405	0.512	0.0015	0.0015
1.06	0.4751	0.557	0.4751	0.557	0.0015	0.0015
1.26	0.4973	0.593	0.4973	0.593	0.0015	0.0015
1.46	0.5168	0.621	0.5168	0.621	0.0015	0.0015
1.66	0.5339	0.646	0.5339	0.646	0.0015	0.0015
1.86	0.5488	0.668	0.5488	0.668	0.0015	0.0015
2.06	0.5616	0.687	0.5616	0.687	0.0015	0.0015
2.26	0.5724	0.704	0.5724	0.704	0.0015	0.0015
2.46	0.5813	0.718	0.5813	0.718	0.0015	0.0015
2.66	0.5885	0.730	0.5885	0.730	0.0015	0.0015
2.86	0.5941	0.740	0.5941	0.740	0.0015	0.0015
3.06	0.5982	0.749	0.5982	0.749	0.0015	0.0015
3.26	0.6018	0.757	0.6018	0.757	0.0015	0.0015
3.46	0.6049	0.764	0.6049	0.764	0.0015	0.0015
3.66	0.6075	0.770	0.6075	0.770	0.0015	0.0015
3.86	0.6097	0.776	0.6097	0.776	0.0015	0.0015
4.06	0.6115	0.781	0.6115	0.781	0.0015	0.0015
4.26	0.6130	0.786	0.6130	0.786	0.0015	0.0015
4.46	0.6143	0.790	0.6143	0.790	0.0015	0.0015
4.66	0.6155	0.794	0.6155	0.794	0.0015	0.0015
4.86	0.6166	0.798	0.6166	0.798	0.0015	0.0015
5.06	0.6176	0.802	0.6176	0.802	0.0015	0.0015
5.26	0.6185	0.806	0.6185	0.806	0.0015	0.0015
5.46	0.6193	0.810	0.6193	0.810	0.0015	0.0015
5.66	0.6201	0.814	0.6201	0.814	0.0015	0.0015
5.86	0.6208	0.818	0.6208	0.818	0.0015	0.0015
6.06	0.6215	0.822	0.6215	0.822	0.0015	0.0015
6.26	0.6222	0.826	0.6222	0.826	0.0015	0.0015
6.46	0.6229	0.830	0.6229	0.830	0.0015	0.0015
6.66	0.6236	0.834	0.6236	0.834	0.0015	0.0015
6.86	0.6243	0.838	0.6243	0.838	0.0015	0.0015
7.06	0.6250	0.842	0.6250	0.842	0.0015	0.0015
7.26	0.6257	0.846	0.6257	0.846	0.0015	0.0015
7.46	0.6264	0.850	0.6264	0.850	0.0015	0.0015
7.66	0.6271	0.854	0.6271	0.854	0.0015	0.0015
7.86	0.6278	0.858	0.6278	0.858	0.0015	0.0015
8.06	0.6285	0.862	0.6285	0.862	0.0015	0.0015
8.26	0.6292	0.866	0.6292	0.866	0.0015	0.0015
8.46	0.6299	0.870	0.6299	0.870	0.0015	0.0015
8.66	0.6306	0.874	0.6306	0.874	0.0015	0.0015
8.86	0.6313	0.878	0.6313	0.878	0.0015	0.0015
9.06	0.6320	0.882	0.6320	0.882	0.0015	0.0015
9.26	0.6327	0.886	0.6327	0.886	0.0015	0.0015
9.46	0.6334	0.890	0.6334	0.890	0.0015	0.0015
9.66	0.6341	0.894	0.6341	0.894	0.0015	0.0015
9.86	0.6348	0.898	0.6348	0.898	0.0015	0.0015
10.06	0.6355	0.902	0.6355	0.902	0.0015	0.0015
10.26	0.6362	0.906	0.6362	0.906	0.0015	0.0015
10.46	0.6369	0.910	0.6369	0.910	0.0015	0.0015
10.66	0.6376	0.914	0.6376	0.914	0.0015	0.0015
10.86	0.6383	0.918	0.6383	0.918	0.0015	0.0015
11.06	0.6390	0.922	0.6390	0.922	0.0015	0.0015
11.26	0.6397	0.926	0.6397	0.926	0.0015	0.0015
11.46	0.6404	0.930	0.6404	0.930	0.0015	0.0015
11.66	0.6411	0.934	0.6411	0.934	0.0015	0.0015
11.86	0.6418	0.938	0.6418	0.938	0.0015	0.0015
12.06	0.6425	0.942	0.6425	0.942	0.0015	0.0015
12.26	0.6432	0.946	0.6432	0.946	0.0015	0.0015
12.46	0.6439	0.950	0.6439	0.950	0.0015	0.0015
12.66	0.6446	0.954	0.6446	0.954	0.0015	0.0015
12.86	0.6453	0.958	0.6453	0.958	0.0015	0.0015
13.06	0.6460	0.962	0.6460	0.962	0.0015	0.0015
13.26	0.6467	0.966	0.6467	0.966	0.0015	0.0015
13.46	0.6474	0.970	0.6474	0.970	0.0015	0.0015
13.66	0.6481	0.974	0.6481	0.974	0.0015	0.0015
13.86	0.6488	0.978	0.6488	0.978	0.0015	0.0015
14.06	0.6495	0.982	0.6495	0.982	0.0015	0.0015
14.26	0.6502	0.986	0.6502	0.986	0.0015	0.0015
14.46	0.6509	0.990	0.6509	0.990	0.0015	0.0015
14.66	0.6516	0.994	0.6516	0.994	0.0015	0.0015
14.86	0.6523	0.998	0.6523	0.998	0.0015	0.0015
15.06	0.6530	1.002	0.6530	1.002	0.0015	0.0015
15.26	0.6537	1.006	0.6537	1.006	0.0015	0.0015
15.46	0.6544	1.010	0.6544	1.010	0.0015	0.0015
15.66	0.6551	1.014	0.6551	1.014	0.0015	0.0015
15.86	0.6558	1.018	0.6558	1.018	0.0015	0.0015
16.06	0.6565	1.022	0.6565	1.022	0.0015	0.0015
16.26	0.6572	1.026	0.6572	1.026	0.0015	0.0015
16.46	0.6579	1.030	0.6579	1.030	0.0015	0.0015
16.66	0.6586	1.034	0.6586	1.034	0.0015	0.0015
16.86	0.6593	1.038	0.6593	1.038	0.0015	0.0015
17.06	0.6600	1.042	0.6600	1.042	0.0015	0.0015
17.26	0.6607	1.046	0.6607	1.046	0.0015	0.0015
17.46	0.6614	1.050	0.6614	1.050	0.0015	0.0015
17.66	0.6621	1.054	0.6621	1.054	0.0015	0.0015
17.86	0.6628	1.058	0.6628	1.058	0.0015	0.0015
18.06	0.6635	1.062	0.6635	1.062	0.0015	0.0015
18.26	0.6642	1.066	0.6642	1.066	0.0015	0.0015
18.46	0.6649	1.070	0.6649	1.070	0.0015	0.0015
18.66	0.6656	1.074	0.6656	1.074	0.0015	0.0015
18.86	0.6663	1.078	0.6663	1.078	0.0015	0.0015
19.06	0.6670	1.082	0.6670	1.082	0.0015	0.0015
19.26	0.6677	1.086	0.6677	1.086	0.0015	0.0015
19.46	0.6684	1.090	0.6684	1.090	0.0015	0.0015
19.66	0.6691	1.094	0.6691	1.094	0.0015	0.0015
19.86	0.6698	1.098	0.6698	1.098	0.0015	0.0015
20.06	0.6705	1.102	0.6705	1.102	0.0015	0.0015
20.26	0.6712	1.106	0.6712	1.106	0.0015	0.0015
20.46	0.6719	1.110	0.6719	1.110	0.0015	0.0015
20.66	0.6726	1.114	0.6726	1.114	0.0015	0.0015
20.86	0.6733	1.118	0.6733	1.118	0.0015	0.0015
21.06	0.6740	1.122	0.6740	1.122	0.0015	0.0015
21.26	0.6747	1.126	0.6747	1.126	0.0015	0.0015
21.46	0.6754	1.130	0.6754	1.130	0.0015	0.0015
21.66	0.6761	1.134	0.6761	1.134	0.0015	0.0015
21.86	0.6768	1.138	0.6768	1.138	0.0015	0.0015
22.06	0.6775	1.142	0.6775	1.142	0.0015	0.0015
22.26	0.6782	1.146	0.6782	1.146	0.0015	0.0015
22.46	0.6789	1.150	0.6789	1.150	0.0015	0.0015
22.66	0.6796	1.154	0.6796	1.154	0.0015	0.0015
22.86	0.6803	1.158	0.6803	1.158	0.0015	0.0015
23.06	0.6810	1.162	0.6810	1.162	0.0015	0.0015
23.26	0.6817	1.166	0.6817	1.166	0.0015	0.0015
23.46	0.6824	1.170	0.6824	1.170	0.0015	0.0015
23.66	0.6831	1.174	0.6831	1.174	0.0015	0.0015
23.86	0.6838	1.178	0.6838	1.178	0.0015	0.0015
24.06	0.6845	1.182	0.6845	1.182	0.0015	0.0015
24.26	0.6852	1.186	0.6852	1.186	0.0015	0.0015
24.46	0.6859	1.190	0.6859	1.190	0.0015	0.0015
24.66	0.6866	1.194	0.6866	1.194	0.0015	0.0015
24.86	0.6873	1.198	0.6873	1.198	0.0015	0.0015
25.06	0.6880	1.202	0.6880	1.202	0.0015	0.0015
25.26	0.6887	1.206	0.6887	1.206	0.0015	0.0015
25.46	0.6894	1.210	0.6894	1.210	0.0015	0.0015
25.66	0.6901	1.214	0.6901	1.214	0.0015	0.0015
25.86	0.6908	1.218	0.6908	1.218	0.0015	0.0015
26.06	0.6915	1.222	0.6915	1.222	0.0015	0.0015
26.26	0.6922	1.226	0.6922	1.226	0.0015	0.0015
26.46	0.6929	1.230	0.6929	1.230	0.0015	0.0015
26.66	0.6936	1.234	0.6936	1.234	0.0015	0.0015
26.86	0.6943	1.238	0.6943	1.238	0.0015	0.0015
27.06	0.6950	1.242	0.6950	1.242	0.0015	0.0015
27.26	0.6957	1.246	0.6957	1.246	0.0015	0.0015
27.46	0.6964	1.250	0.6964	1.250	0.0015	0.0015
27.66	0.6971	1.254	0.6971	1.254	0.0015	0.0015
27.86	0.6978	1.258	0.6978	1.258	0.0015	0.0015
28.06	0.6985	1.262	0.6985	1.262	0.0015	0.0015
28.26	0.6992	1.266	0.6992	1.266	0.0015	0.0015
28.46	0.6999	1.270	0.6999	1.270	0.0015	0.0015
28.66	0.7006	1.274	0.7006	1.274	0.0015	0.0015
28.86	0.7013	1.278	0.7013	1.278	0.0015	0.0015
29.06	0.7020	1.282	0.7020	1.282	0.0015	0.0015
29.26	0.7027	1.286	0.7027	1.286	0.0015	0.0015
29.46	0.7034	1.290	0.7034	1.290	0.0015	0.0015
29.66	0.7041	1.294	0.7041	1.294	0.0015	0.0015
29.86	0.7048	1.298	0.7048	1.298	0.0015	0.0015
30.06	0.7055	1.302	0.7055	1.302	0.0015	0.0015
30.26	0.7062	1.306	0.7062	1.306	0.0015	0.0015
30.46	0.7069	1.310	0.7069	1.310	0.0015	0.0015
30.66	0.7076	1.314	0.7076	1.314	0.0015	0.0015
30.86	0.7083	1.318	0.7083	1.318	0.0015	0.0015
31.06	0.7090	1.322	0.7090	1.322	0.0015	0.0015
31.26	0.7097	1.326	0.7097	1.326	0.0015	0.0015
31.46	0.7104	1.330	0.7104	1.330	0.0015	0.0015
31.66	0.7111	1.334	0.7111	1.334	0.0015	0.0015
31.86	0.7118	1.338	0.7118	1.338	0.0015	0.0015
32.06	0.7125	1.342	0.7125	1.		

Table 1 (continued)

N (NORMAL)=1.5										N (NORMAL)=1.5										N (NORMAL)=1.5										N (NORMAL)=1.5									
X=124 MI DEL=6.54MI(6 (MEASURED) P)					X=148 MI DEL=6.54MI(6 (MEASURED) P)					X=173 MI DEL=6.54MI(6 (MEASURED) P)					X=205.4 K DEL=295.4 K (MEASURED) P)					X=257.2 K DEL=257.2 K (MEASURED) P)					X=297.2 K DEL=297.2 K (MEASURED) P)					X=324 MI DEL=6.54MI(6 (MEASURED) P)									
CONST		M		UAE		MEASURED P		P/P10		CONST		M		UAE		MEASURED P		P/P10		CONST		M		UAE		MEASURED P		P/P10		CONST		M		UAE		MEASURED P		P/P10	
V (MI)	N	V (MI)	N	V (MI)	N	V (MI)	N	V (MI)	N	V (MI)	N	V (MI)	N	V (MI)	N	V (MI)	N	V (MI)	N	V (MI)	N	V (MI)	N	V (MI)	N	V (MI)	N	V (MI)	N	V (MI)	N	V (MI)	N	V (MI)	N	V (MI)	N		
0.00	0.0000	0.0000	0.0000	0.0000	0.0000	0.0000	0.0000	0.0000	0.0000	0.00	0.0000	0.0000	0.0000	0.0000	0.0000	0.0000	0.0000	0.0000	0.0000	0.00	0.0000	0.0000	0.0000	0.0000	0.0000	0.0000	0.0000	0.0000	0.0000	0.0000	0.0000	0.0000	0.0000	0.0000	0.0000	0.0000	0.0000		
0.05	0.4421	0.3880	0.4421	0.3880	0.384	0.384	0.384	0.384	0.384	0.05	0.1794	0.1645	0.1794	0.1645	0.1719	0.1638	0.1719	0.1638	0.1719	0.05	0.1794	0.1645	0.1794	0.1645	0.1719	0.1638	0.1719	0.1638	0.1719	0.1638	0.1719	0.1638	0.1719	0.1638	0.1719	0.1638	0.1719	0.1638	
0.10	0.4883	0.4188	0.4883	0.4188	0.408	0.408	0.408	0.408	0.408	0.10	0.2341	0.2142	0.2341	0.2142	0.2319	0.2034	0.2319	0.2034	0.2319	0.10	0.2341	0.2142	0.2341	0.2142	0.2319	0.2034	0.2319	0.2034	0.2319	0.2034	0.2319	0.2034	0.2319	0.2034	0.2319	0.2034	0.2319	0.2034	
0.15	0.5288	0.4508	0.5288	0.4508	0.438	0.438	0.438	0.438	0.438	0.15	0.2802	0.2578	0.2802	0.2578	0.2802	0.2578	0.2802	0.2578	0.2802	0.15	0.2802	0.2578	0.2802	0.2578	0.2802	0.2578	0.2802	0.2578	0.2802	0.2578	0.2802	0.2578	0.2802	0.2578	0.2802	0.2578	0.2802	0.2578	
0.20	0.5648	0.4768	0.5648	0.4768	0.462	0.462	0.462	0.462	0.462	0.20	0.3139	0.2859	0.3139	0.2859	0.3139	0.2859	0.3139	0.2859	0.3139	0.20	0.3139	0.2859	0.3139	0.2859	0.3139	0.2859	0.3139	0.2859	0.3139	0.2859	0.3139	0.2859	0.3139	0.2859	0.3139	0.2859	0.3139	0.2859	
0.25	0.5968	0.5018	0.5968	0.5018	0.484	0.484	0.484	0.484	0.484	0.25	0.3348	0.3068	0.3348	0.3068	0.3348	0.3068	0.3348	0.3068	0.3348	0.25	0.3348	0.3068	0.3348	0.3068	0.3348	0.3068	0.3348	0.3068	0.3348	0.3068	0.3348	0.3068	0.3348	0.3068	0.3348	0.3068	0.3348	0.3068	
0.30	0.6248	0.5218	0.6248	0.5218	0.504	0.504	0.504	0.504	0.504	0.30	0.3548	0.3268	0.3548	0.3268	0.3548	0.3268	0.3548	0.3268	0.3548	0.30	0.3548	0.3268	0.3548	0.3268	0.3548	0.3268	0.3548	0.3268	0.3548	0.3268	0.3548	0.3268	0.3548	0.3268	0.3548	0.3268	0.3548	0.3268	
0.35	0.6488	0.5368	0.6488	0.5368	0.519	0.519	0.519	0.519	0.519	0.35	0.3748	0.3468	0.3748	0.3468	0.3748	0.3468	0.3748	0.3468	0.3748	0.35	0.3748	0.3468	0.3748	0.3468	0.3748	0.3468	0.3748	0.3468	0.3748	0.3468	0.3748	0.3468	0.3748	0.3468	0.3748	0.3468	0.3748	0.3468	
0.40	0.6688	0.5468	0.6688	0.5468	0.534	0.534	0.534	0.534	0.534	0.40	0.3948	0.3668	0.3948	0.3668	0.3948	0.3668	0.3948	0.3668	0.3948	0.40	0.3948	0.3668	0.3948	0.3668	0.3948	0.3668	0.3948	0.3668	0.3948	0.3668	0.3948	0.3668	0.3948	0.3668	0.3948	0.3668	0.3948	0.3668	
0.45	0.6888	0.5568	0.6888	0.5568	0.544	0.544	0.544	0.544	0.544	0.45	0.4148	0.3868	0.4148	0.3868	0.4148	0.3868	0.4148	0.3868	0.4148	0.45	0.4148	0.3868	0.4148	0.3868	0.4148	0.3868	0.4148	0.3868	0.4148	0.3868	0.4148	0.3868	0.4148	0.3868	0.4148	0.3868	0.4148	0.3868	
0.50	0.7088	0.5668	0.7088	0.5668	0.554	0.554	0.554	0.554	0.554	0.50	0.4348	0.4068	0.4348	0.4068	0.4348	0.4068	0.4348	0.4068	0.4348	0.50	0.4348	0.4068	0.4348	0.4068	0.4348	0.4068	0.4348	0.4068	0.4348	0.4068	0.4348	0.4068	0.4348	0.4068	0.4348	0.4068	0.4348	0.4068	
0.55	0.7288	0.5768	0.7288	0.5768	0.564	0.564	0.564	0.564	0.564	0.55	0.4548	0.4268	0.4548	0.4268	0.4548	0.4268	0.4548	0.4268	0.4548	0.55	0.4548	0.4268	0.4548	0.4268	0.4548	0.4268	0.4548	0.4268	0.4548	0.4268	0.4548	0.4268	0.4548	0.4268	0.4548	0.4268	0.4548	0.4268	
0.60	0.7488	0.5868	0.7488	0.5868	0.574	0.574	0.574	0.574	0.574	0.60	0.4748	0.4468	0.4748	0.4468	0.4748	0.4468	0.4748	0.4468	0.4748	0.60	0.4748	0.4468	0.4748	0.4468	0.4748	0.4468	0.4748	0.4468	0.4748	0.4468	0.4748	0.4468	0.4748	0.4468	0.4748	0.4468	0.4748	0.4468	
0.65	0.7688	0.5968	0.7688	0.5968	0.584	0.584	0.584	0.584	0.584	0.65	0.4948	0.4668	0.4948	0.4668	0.4948	0.4668	0.4948	0.4668	0.4948	0.65	0.4948	0.4668	0.4948	0.4668	0.4948	0.4668	0.4948	0.4668	0.4948	0.4668	0.4948	0.4668	0.4948	0.4668	0.4948	0.4668	0.4948	0.4668	
0.70	0.7888	0.6068	0.7888	0.6068	0.594	0.594	0.594	0.594	0.594	0.70	0.5148	0.4868	0.5148	0.4868	0.5148	0.4868	0.5148	0.4868	0.5148	0.70	0.5148	0.4868	0.5148	0.4868	0.5148	0.4868	0.5148	0.4868	0.5148	0.4868	0.5148	0.4868	0.5148	0.4868	0.5148	0.4868	0.5148	0.4868	
0.75	0.8088	0.6168	0.8088	0.6168	0.604	0.604	0.604	0.604	0.604	0.75	0.5348	0.5068	0.5348	0.5068	0.5348	0.5068	0.5348	0.5068	0.5348	0.75	0.5348	0.5068	0.5348	0.5068	0.5348	0.5068	0.5348	0.5068	0.5348	0.5068	0.5348	0.5068	0.5348	0.5068	0.5348	0.5068	0.5348	0.5068	
0.80	0.8288	0.6268	0.8288	0.6268	0.614	0.614	0.614	0.614	0.614	0.80	0.5548	0.5268	0.5548	0.5268	0.5548	0.5268	0.5548	0.5268	0.5548	0.80	0.5548	0.5268	0.5548	0.5268	0.5548	0.5268	0.5548	0.5268	0.5548	0.5268	0.5548	0.5268	0.5548	0.5268	0.5548	0.5268	0.5548	0.5268	
0.85	0.8488	0.6368	0.8488	0.6368	0.624	0.624	0.624	0.624	0.624	0.85	0.5748	0.5468	0.5748	0.5468	0.5748	0.5468	0.5748	0.5468	0.5748	0.85	0.5748	0.5468	0.5748	0.5468	0.5748	0.5468	0.5748	0.5468	0.5748	0.5468	0.5748	0.5468	0.5748	0.5468	0.5748	0.5468	0.5748	0.5468	
0.90	0.8688	0.6468	0.8688	0.6468	0.634	0.634	0.634	0.634	0.634	0.90	0.5948	0.5668	0.5948	0.5668	0.5948	0.5668	0.5948	0.5668	0.5948	0.90	0.5948	0.5668	0.5948	0.5668	0.5948	0.5668	0.5948	0.5668	0.5948	0.5668	0.5948	0.5668	0.5948	0.5668	0.5948	0.5668	0.5948	0.5668	
0.95	0.8888	0.6568	0.8888	0.6568	0.644	0.644	0.644	0.644	0.644	0.95	0.6148	0.5868	0.6148	0.5868	0.6148	0.5868	0.6148	0.5868	0.6148	0.95	0.6148	0.5868	0.6148	0.5868	0.6148	0.5868	0.6148	0.5868	0.6148	0.5868	0.6148	0.5868	0.6148	0.5868	0.6148	0.5868	0.6148	0.5868	
1.00	0.9088	0.6668	0.9088	0.6668	0.654	0.654	0.654	0.654	0.654	1.00	0.6348	0.6068	0.6348	0.6068	0.6348	0.6068	0.6348	0.6068	0.6348	1.00	0.6348	0.6068	0.6348	0.6068	0.6348	0.6068	0.6348	0.6068	0.6348	0.6068	0.6348	0.6068	0.6348	0.6068	0.6348	0.6068	0.6348	0.6068	
1.05	0.9288	0.6768	0.9288	0.6768	0.664	0.664	0.664	0.664	0.664	1.05	0.6548	0.6268	0.6548	0.6268	0.6548	0.6268	0.6548	0.6268	0.6548	1.05	0.6548	0.6268	0.6548	0.6268	0.6548	0.6268	0.6548	0.6268	0.6548	0.6268	0.6548	0.6268	0.6548	0.6268	0.6548	0.6268	0.6548	0.6268	
1.10	0.9488	0.6868	0.9488	0.6868	0.674	0.674	0.674	0.674	0.674	1.10	0.6748	0.6468	0.6748	0.6468	0.6748	0.6468	0.6748	0.6468	0.6748	1.10	0.6748	0.6468	0.6748	0.6468	0.6748	0.6468	0.6748	0.6468	0.6748	0.6468	0.6748	0.6468	0.6748	0.6468	0.6748	0.6468	0.6748	0.6468	
1.15	0.9688	0.6968	0.9688	0.6968	0.684	0.684	0.684	0.684	0.684	1.15	0.6948	0.6668	0.6948	0.6668	0.6948	0.6668	0.6948	0.6668	0.6948	1.15	0.6948	0.6668	0.6948	0.6668	0.6948	0.6668	0.6948	0.6668	0.6948	0.6668	0.6948	0.6668	0.6948	0.6668	0.6948	0.6668	0.6948	0.6668	
1.20	0.9888	0.7068	0.9888	0.7068	0.694	0.694	0.694	0.694	0.694	1.20	0.7148	0.6868	0.7148	0.6868	0.7148	0.6868	0.7148	0.6868	0.7148	1.20	0.7148	0.6868	0.7148	0.6868	0.7148	0.6868	0.7148	0.6868	0.7148	0.6868	0.7148	0.6868	0.7148	0.6868	0.7148	0.6868	0.7148	0.6868	
1.25	1.0088	0.7168	1.0088	0.7168	0.704	0.704	0.704	0.704	0.704	1.25	0.7348	0.7068	0.7348	0.7068	0.7348	0.7068	0.7348	0.7068	0.7348	1.25	0.7348	0.7068	0.7348	0.7068	0.7348	0.7068	0.7348	0.7068	0.7348	0.7068	0.7348	0.7068	0.7348	0.7068	0.7348	0.7068	0.7348	0.7068	
1.30	1.0288	0.7268	1.0288	0.7268	0.714	0.714	0.714	0.714	0.714	1.30	0.7548	0.7268	0.7548	0.7268	0.7548	0.7268	0.7548	0.7268	0.7548	1.30	0.7548	0.7268	0.7548	0.7268	0.7548	0.7268	0.7548	0.7268	0.7548	0.7268	0.7548	0.7268	0.7548	0.7268	0.7548	0.7268	0.7548	0.7268	
1.35	1.0488	0.7368	1.0488	0.7368	0.724	0.724	0.724	0.724	0.724	1.35	0.7748	0.7468	0.7748	0.7468	0.7748	0.7468	0.7748	0.7468	0.7748	1.35	0.7748	0.7468	0.7748	0															

Table 2 (continued)

[illegible]

N (NUMBER) = 1.5												
Δ	1236 W	10-25.4 k	DEL 995-11.6 W	Δ	1776 W	10-27.3 k	DEL 995-15.1 W	Δ	2205 W	10-28.2 k	DEL 995-17.7 W	
RES/6	6.26x10 ⁶ (MEASURED P)	RES/6	6.26x10 ⁶ (MEASURED P)	RES/6	6.88x10 ⁶ (MEASURED P)	RES/6	6.88x10 ⁶ (MEASURED P)	RES/6	5.53x10 ⁶ (MEASURED P)	RES/6	5.53x10 ⁶ (MEASURED P)	
	Y (W)	N	UVE	P	Y (W)	N	UVE	P	Y (W)	N	UVE	P
1	0.00	0.0000	0.0000	0.0000	0.00	0.0000	0.0000	0.0000	0.00	0.0000	0.0000	0.0000
2	0.66	0.3505	0.4388	0.3605	0.66	0.4015	0.4944	0.4015	0.66	0.3507	0.3683	0.3507
3	0.86	0.3642	0.4374	0.3642	0.86	0.4086	0.4987	0.4086	0.86	0.4028	0.4123	0.4028
4	1.06	0.3717	0.4438	0.3717	1.06	0.4229	0.5197	0.4229	1.06	0.4286	0.5126	0.4286
5	1.27	0.3851	0.4593	0.3851	1.27	0.4297	0.5195	0.4297	1.27	0.4284	0.5203	0.4284
6	1.47	0.3941	0.4584	0.3941	1.46	0.4756	0.5148	0.4756	1.56	0.4344	0.5321	0.4344
7	1.70	0.3931	0.4637	0.3931	1.66	0.4461	0.5403	0.4461	1.66	0.4385	0.5547	0.4385
8	2.17	0.3957	0.4763	0.3957	2.17	0.4572	0.5601	0.4572	2.17	0.4498	0.5706	0.4498
9	2.70	0.4246	0.5049	0.4246	2.67	0.4636	0.5654	0.4636	2.67	0.4601	0.5932	0.4601
10	3.20	0.4313	0.5126	0.4313	3.17	0.4699	0.5753	0.4699	3.16	0.4729	0.5986	0.4729
11	3.85	0.4384	0.5116	0.4384	3.66	0.4744	0.5985	0.4744	3.65	0.4758	0.6015	0.4758
12	4.67	0.4341	0.5169	0.4341	4.67	0.4836	0.5913	0.4836	4.66	0.4898	0.6185	0.4898
13	6.70	0.4709	0.4576	0.4709	6.66	0.5014	0.6143	0.5014	6.70	0.5077	0.6416	0.5077
14	8.71	0.4654	0.5315	0.4654	8.67	0.5127	0.6262	0.5127	8.70	0.5107	0.6541	0.5107
15	10.76	0.4738	0.5288	0.4738	10.70	0.5127	0.6302	0.5127	10.66	0.5208	0.6651	0.5208
16	12.71	0.4678	0.5159	0.4678	12.67	0.5337	0.6494	0.5337	12.70	0.5351	0.6785	0.5351
17	14.71	0.4678	0.5671	0.4678	14.66	0.5337	0.6494	0.5337	14.67	0.5445	0.6859	0.5445
18	16.66	0.4637	0.5671	0.4637	16.71	0.5449	0.6523	0.5449	16.67	0.5475	0.6885	0.5475
19	20.66	0.5077	0.5976	0.5077	19.71	0.5493	0.6505	0.5493	19.70	0.5486	0.6908	0.5486
20	25.63	0.5106	0.6259	0.5106	25.67	0.5493	0.6675	0.5493	25.67	0.5493	0.6675	0.5493
21	30.63	0.5462	0.6423	0.5462	30.67	0.5747	0.6581	0.5747	30.67	0.5747	0.6581	0.5747
22	35.66	0.5727	0.6716	0.5727	35.70	0.5918	0.7157	0.5918	35.67	0.5918	0.7157	0.5918
23	40.65	0.5916	0.6921	0.5916	40.70	0.6041	0.7293	0.6041	40.66	0.5917	0.7447	0.5917
24	45.67	0.6111	0.7136	0.6111	45.66	0.6227	0.7581	0.6227	45.66	0.6111	0.7632	0.6111
25	50.67	0.6338	0.7379	0.6338	50.70	0.6367	0.7668	0.6367	50.71	0.6248	0.7762	0.6248
26	55.66	0.6481	0.7666	0.6481	55.70	0.6496	0.7803	0.6496	55.71	0.6373	0.7936	0.6373
27	60.66	0.6727	0.7945	0.6727	60.70	0						

Table 2 (continued)

[illegible]

$\mu(\text{NOMINAL}) = 1.5$ [illegible]

[illegible]

N (UNIT) = 1.5										N (UNIT) = 1.5										N (UNIT) = 1.5										N (UNIT) = 1.5									
X = 600 MM DEPTH = 9.76418'6 (MEASURED P)					10-255.0 K DEL. 995-111.0 MM HE-# 319 (REQUIRED P)					X = 600 MM DEPTH = 9.76418'6 (MEASURED P)					10-255.0 K DEL. 995-111.0 MM HE-# 319 (REQUIRED P)					X = 600 MM DEPTH = 9.76418'6 (MEASURED P)					10-255.0 K DEL. 995-111.0 MM HE-# 319 (REQUIRED P)														
CONST. P/N		REQUIRED P		P/N		CONST. P/N		REQUIRED P		P/N		CONST. P/N		REQUIRED P		P/N		CONST. P/N		REQUIRED P		P/N		CONST. P/N		REQUIRED P		P/N											
Y (MM)	U (FE)	M	U (FE)	M	U (FE)	Y (MM)	U (FE)	M	U (FE)	M	U (FE)	Y (MM)	U (FE)	M	U (FE)	M	U (FE)	Y (MM)	U (FE)	M	U (FE)	M	U (FE)	Y (MM)	U (FE)	M	U (FE)	M	U (FE)										
0.00	0.0000	0.0000	0.0000	0.0000	0.0000	0.00	0.0000	0.0000	0.0000	0.0000	0.0000	0.00	0.0000	0.0000	0.0000	0.0000	0.0000	0.00	0.0000	0.0000	0.0000	0.0000	0.0000	0.00	0.0000	0.0000	0.0000	0.0000	0.0000										
0.03	0.2827	0.2299	0.2827	0.2299	0.2827	0.03	0.2827	0.2299	0.2827	0.2299	0.2827	0.03	0.2827	0.2299	0.2827	0.2299	0.2827	0.03	0.2827	0.2299	0.2827	0.2299	0.2827	0.03	0.2827	0.2299	0.2827	0.2299	0.2827										
0.06	0.5654	0.4598	0.5654	0.4598	0.5654	0.06	0.5654	0.4598	0.5654	0.4598	0.5654	0.06	0.5654	0.4598	0.5654	0.4598	0.5654	0.06	0.5654	0.4598	0.5654	0.4598	0.5654	0.06	0.5654	0.4598	0.5654	0.4598	0.5654										
0.09	0.8481	0.6897	0.8481	0.6897	0.8481	0.09	0.8481	0.6897	0.8481	0.6897	0.8481	0.09	0.8481	0.6897	0.8481	0.6897	0.8481	0.09	0.8481	0.6897	0.8481	0.6897	0.8481	0.09	0.8481	0.6897	0.8481	0.6897	0.8481										
0.12	1.1308	0.9214	1.1308	0.9214	1.1308	0.12	1.1308	0.9214	1.1308	0.9214	1.1308	0.12	1.1308	0.9214	1.1308	0.9214	1.1308	0.12	1.1308	0.9214	1.1308	0.9214	1.1308	0.12	1.1308	0.9214	1.1308	0.9214	1.1308										
0.15	1.4135	1.1541	1.4135	1.1541	1.4135	0.15	1.4135	1.1541	1.4135	1.1541	1.4135	0.15	1.4135	1.1541	1.4135	1.1541	1.4135	0.15	1.4135	1.1541	1.4135	1.1541	1.4135	0.15	1.4135	1.1541	1.4135	1.1541	1.4135										
0.18	1.6962	1.3868	1.6962	1.3868	1.6962	0.18	1.6962	1.3868	1.6962	1.3868	1.6962	0.18	1.6962	1.3868	1.6962	1.3868	1.6962	0.18	1.6962	1.3868	1.6962	1.3868	1.6962	0.18	1.6962	1.3868	1.6962	1.3868	1.6962										
0.21	1.9789	1.6195	1.9789	1.6195	1.9789	0.21	1.9789	1.6195	1.9789	1.6195	1.9789	0.21	1.9789	1.6195	1.9789	1.6195	1.9789	0.21	1.9789	1.6195	1.9789	1.6195	1.9789	0.21	1.9789	1.6195	1.9789	1.6195	1.9789										
0.24	2.2616	1.8522	2.2616	1.8522	2.2616	0.24	2.2616	1.8522	2.2616	1.8522	2.2616	0.24	2.2616	1.8522	2.2616	1.8522	2.2616	0.24	2.2616	1.8522	2.2616	1.8522	2.2616	0.24	2.2616	1.8522	2.2616	1.8522	2.2616										
0.27	2.5443	2.0849	2.5443	2.0849	2.5443	0.27	2.5443	2.0849	2.5443	2.0849	2.5443	0.27	2.5443	2.0849	2.5443	2.0849	2.5443	0.27	2.5443	2.0849	2.5443	2.0849	2.5443	0.27	2.5443	2.0849	2.5443	2.0849	2.5443										
0.30	2.8270	2.3176	2.8270	2.3176	2.8270	0.30	2.8270	2.3176	2.8270	2.3176	2.8270	0.30	2.8270	2.3176	2.8270	2.3176	2.8270	0.30	2.8270	2.3176	2.8270	2.3176	2.8270	0.30	2.8270	2.3176	2.8270	2.3176	2.8270										
0.33	3.1097	2.5503	3.1097	2.5503	3.1097	0.33	3.1097	2.5503	3.1097	2.5503	3.1097	0.33	3.1097	2.5503	3.1097	2.5503	3.1097	0.33	3.1097	2.5503	3.1097	2.5503	3.1097	0.33	3.1097	2.5503	3.1097	2.5503	3.1097										
0.36	3.3924	2.7830	3.3924	2.7830	3.3924	0.36	3.3924	2.7830	3.3924	2.7830	3.3924	0.36	3.3924	2.7830	3.3924	2.7830	3.3924	0.36	3.3924	2.7830	3.3924	2.7830	3.3924	0.36	3.3924	2.7830	3.3924	2.7830	3.3924										
0.39	3.6751	3.0157	3.6751	3.0157	3.6751	0.39	3.6751	3.0157	3.6751	3.0157	3.6751	0.39	3.6751	3.0157	3.6751	3.0157	3.6751	0.39	3.6751	3.0157	3.6751	3.0157	3.6751	0.39	3.6751	3.0157	3.6751	3.0157	3.6751										
0.42	3.9578	3.2484	3.9578	3.2484	3.9578	0.42	3.9578	3.2484	3.9578	3.2484	3.9578	0.42	3.9578	3.2484	3.9578	3.2484	3.9578	0.42	3.9578	3.2484	3.9578	3.2484	3.9578	0.42	3.9578	3.2484	3.9578	3.2484	3.9578										
0.45	4.2405	3.4811	4.2405	3.4811	4.2405	0.45	4.2405	3.4811	4.2405	3.4811	4.2405	0.45	4.2405	3.4811	4.2405	3.4811	4.2405	0.45	4.2405	3.4811	4.2405	3.4811	4.2405	0.45	4.2405	3.4811	4.2405	3.4811	4.2405										
0.48	4.5232	3.7138	4.5232	3.7138	4.5232	0.48	4.5232	3.7138	4.5232	3.7138	4.5232	0.48	4.5232	3.7138	4.5232	3.7138	4.5232	0.48	4.5232	3.7138	4.5232	3.7138	4.5232	0.48	4.5232	3.7138	4.5232	3.7138	4.5232										
0.51	4.8059	3.9465	4.8059	3.9465	4.8059	0.51	4.8059	3.9465	4.8059	3.9465	4.8059	0.51	4.8059	3.9465	4.8059	3.9465	4.8059	0.51	4.8059	3.9465	4.8059	3.9465	4.8059	0.51	4.8059	3.9465	4.8059	3.9465	4.8059										
0.54	5.0886	4.1792	5.0886	4.1792	5.0886	0.54	5.0886	4.1792	5.0886	4.1792	5.0886	0.54	5.0886	4.1792	5.0886	4.1792	5.0886	0.54	5.0886	4.1792	5.0886	4.1792	5.0886	0.54	5.0886	4.1792	5.0886	4.1792	5.0886										
0.57	5.3713	4.4119	5.3713	4.4119	5.3713	0.57	5.3713	4.4119	5.3713	4.4119	5.3713	0.57	5.3713	4.4119	5.3713	4.4119	5.3713	0.57	5.3713	4.4119	5.3713	4.4119	5.3713	0.57	5.3713	4.4119	5.3713	4.4119	5.3713										
0.60	5.6540	4.6446	5.6540	4.6446	5.6540	0.60	5.6540	4.6446	5.6540	4.6446	5.6540	0.60	5.6540	4.6446	5.6540	4.6446	5.6540	0.60	5.6540	4.6446	5.6540	4.6446	5.6540	0.60	5.6540	4.6446	5.6540	4.6446	5.6540										
0.63	5.9367	4.8773	5.9367	4.8773	5.9367	0.63	5.9367	4.8773	5.9367	4.8773	5.9367	0.63	5.9367	4.8773	5.9367	4.8773	5.9367	0.63	5.9367	4.8773	5.9367	4.8773	5.9367	0.63	5.9367	4.8773	5.9367	4.8773	5.9367										
0.66	6.2194	5.1100	6.2194	5.1100	6.2194	0.66	6.2194	5.1100	6.2194	5.1100	6.2194	0.66	6.2194	5.1100	6.2194	5.1100	6.2194	0.66	6.2194	5.1100	6.2194	5.1100	6.2194	0.66	6.2194	5.1100	6.2194	5.1100	6.2194										
0.69	6.5021	5.3427	6.5021	5.3427	6.5021	0.69	6.5021	5.3427	6.5021	5.3427	6.5021	0.69	6.5021	5.3427	6.5021	5.3427	6.5021	0.69	6.5021	5.3427	6.5021	5.3427	6.5021	0.69	6.5021	5.3427	6.5021	5.3427	6.5021										
0.72	6.7848	5.5754	6.7848	5.5754	6.7848	0.72	6.7848	5.5754	6.7848	5.5754	6.7848	0.72	6.7848	5.5754	6.7848	5.5754	6.7848	0.72	6.7848	5.5754	6.7848	5.5754	6.7848	0.72	6.7848	5.5754	6.7848	5.5754	6.7848										
0.75	7.0675	5.8081	7.0675	5.8081	7.0675	0.75	7.0675	5.8081	7.0675	5.8081	7.0675	0.75	7.0675	5.8081	7.0675	5.8081	7.0675	0.75	7.0675	5.8081	7.0675	5.8081	7.0675	0.75	7.0675	5.8081	7.0675	5.8081	7.0675										
0.78	7.3502	6.0408	7.3502	6.0408	7.3502	0.78	7.3502	6.0408	7.3502	6.0408	7.3502	0.78	7.3502	6.0408	7.3502	6.0408	7.3502	0.78	7.3502	6.0408	7.3502	6.0408	7.3502	0.78	7.3502	6.0408	7.3502	6.0408	7.3502										
0.81	7.6329	6.2735	7.6329	6.2735	7.6329	0.81	7.6329	6.2735	7.6329	6.2735	7.6329	0.81	7.6329	6.2735	7.6329	6.2735	7.6329	0.81	7.6329	6.2735	7.6329	6.2735	7.6329	0.81	7.6329	6.2735	7.6329	6.2735	7.6329										
0.84	7.9156	6.5062	7.9156	6.5062	7.9156	0.84	7.9156	6.5062	7.9156	6.5062	7.9156	0.84	7.9156	6.5062	7.9156	6.5062	7.9156	0.84	7.9156	6.5062	7.9156	6.5062	7.9156	0.84	7.9156	6.5062	7.9156	6.5062	7.9156										
0.87	8.1983	6.7389	8.1983	6.7389	8.1983	0.87	8.1983	6.7389	8.1983	6.7389	8.1983	0.87	8.1983	6.7389	8.1983	6.7389	8.1983	0.87	8.1983	6.7389	8.1983	6.7389	8.1983	0.87	8.1983	6.7389	8.1983	6.7389	8.1983										
0.90	8.4810	6.9716	8.4810	6.9716	8.4810	0.90	8.4810	6.9716	8.4810	6.9716	8.4810	0.90	8.4810	6.9716	8.4810	6.9716	8.4810	0.90	8.4810	6.9716	8.4810	6.9716	8.4810	0.90	8.4810	6.9716	8.4810	6.9716	8.4810										
0.93	8.7637	7.2043	8.7637	7.2043	8.7637	0.93	8.7637	7.2043	8.7637	7.2043	8.7637	0.93	8.7637	7.2043	8.7637	7.2043	8.7637	0.93	8.7637	7.2043	8.7637	7.2043	8.7637	0.93	8.7637	7.2043	8.7637	7.2043	8.7637										
0.96	9.0464	7.4370	9.0464	7.4370	9.0464	0.96	9.0464	7.4370	9.0464	7.4370	9.0464	0.96	9.0464	7.4370	9.0464	7.4370	9.0464	0.96	9.0464	7.4370	9.0464	7.4370	9.0464	0.96	9.0464	7.4370	9.0464	7.4370	9.0464										
0.99	9.3291	7.6697	9.3291	7.6697	9.3291	0.99	9.3291	7.6697	9.3291	7.6697	9.3291	0.99	9.3291	7.6697	9.3291	7.6697	9.3291	0.99	9.3291	7.6697	9.3291	7.6697	9.3291	0.99	9.3291	7.6697	9.3291	7.6697	9.3291										
1.02	9.6118	7.9024	9.6118	7.9024	9.6118	1.02	9.6118	7.9024	9.6118	7.9024	9.6118	1.02	9.6118	7.9024	9.6118	7.9024	9.6118	1.02	9.6118	7.9024	9.6118	7.9024	9.6118	1.02	9.6118	7.9024	9.6118	7.9024	9.6118										
1.05	9.8945	8.1351	9.8945	8.1351	9.8945	1.05	9.8945	8.1351	9.8945	8.1351	9.8945	1.05	9.8945	8.1351	9.8945	8.1351	9.8945	1.05	9.8945	8.1351	9.8945	8.1351	9.8945	1.05	9.8945	8.1351	9.8945	8.1351	9.8945										
1.08	10.1772	8																																					

Table 3
SUMMARY OF BOUNDARY-LAYER PARAMETERS

$$M_0 = 1.270 \quad Re/m = 3.66 \times 10^6$$

CONSTANT PM										MEASURED P										CALCULATED P											
X	DEL 95	RE/M	ME	DEL*	THETA	H	HEBR	HI	DELE	CFP	CF	RE/M	ME	DEL*	THETA	H	HEBR	HI	CF	DEL95	DEL95	THETA	H	HEBR	HI	DEL95	DEL95	THETA	H	HEBR	
MM	MM	MM	MM	MM	MM	MM	MM	MM	MM	MM	MM	MM	MM	MM	MM	MM	MM	MM	MM	MM	MM	MM	MM	MM	MM	MM	MM	MM	MM	MM	MM
-675.0	35.7	3.66	1.291	6.573	3.156	2.082	1.312	9.228	5.66	2.127	2.169	3.66	1.291	6.573	3.156	2.082	1.312	9.228	2.169							6.573	3.156	2.082	1.312		
-481.0	38.3	3.67	1.270	7.404	3.568	2.080	1.329	8.678	6.35	1.992	2.041	3.67	1.270	7.404	3.568	2.080	1.329	8.678	2.041							7.404	3.568	2.080	1.329		
-479.0	38.3	3.64	1.267	7.286	3.587	2.078	1.338	8.844	6.25	1.998	2.053	3.64	1.267	7.286	3.587	2.078	1.338	8.844	2.053							7.286	3.587	2.078	1.338		
-285.0	40.0	3.67	1.261	7.788	3.739	2.061	1.323	8.635	6.68	2.065	2.111	3.67	1.261	7.788	3.739	2.061	1.323	8.635	2.111							7.788	3.739	2.061	1.323		
-187.0	40.7	3.67	1.269	7.841	3.812	2.057	1.313	8.628	6.82	2.069	2.136	3.67	1.269	7.841	3.812	2.057	1.313	8.628	2.136							7.841	3.812	2.057	1.313		
-162.0	41.4	3.66	1.270	7.955	3.863	2.059	1.313	8.657	6.91	2.066	2.110	3.66	1.270	7.955	3.863	2.059	1.313	8.657	2.110							7.955	3.863	2.059	1.313		
-138.0	40.1	3.67	1.265	8.010	3.888	2.060	1.318	8.254	6.95	2.064	2.069	3.67	1.265	8.010	3.888	2.060	1.318	8.255	2.069							7.997	3.914	2.043	1.309		
-115.0	41.3	3.61	1.258	8.327	4.040	2.061	1.327	8.162	7.20	1.996	2.038	3.61	1.258	8.325	4.044	2.059	1.325	8.154	2.024							8.399	3.949	2.127	1.295		
-89.0	42.8	3.60	1.215	8.979	4.370	2.053	1.366	7.739	7.70	1.739	1.886	3.61	1.249	9.021	4.369	2.053	1.367	7.697	1.781							9.222	4.011	2.302	1.347		
-66.0	44.8	3.59	1.178	9.877	4.768	2.075	1.408	7.337	8.31	1.536	1.682	3.60	1.184	9.891	4.763	2.076	1.410	7.329	1.598							9.972	4.610	2.163	1.374		
-41.0	45.3	3.60	1.141	11.224	5.259	2.118	1.476	6.438	9.11	1.344	1.366	3.60	1.151	11.244	5.304	2.120	1.478	6.421	1.359							11.307	5.174	2.185	1.432		
-15.0	48.9	3.58	1.100	12.918	5.944	2.172	1.554	6.055	10.06	1.106	1.168	3.58	1.100	12.989	5.944	2.172	1.554	6.055	1.168							13.033	5.438	2.397	1.511		
6.0	50.9	3.56	1.070	14.394	6.382	2.241	1.638	5.734	10.67	0.898	0.897	3.52	1.019	14.390	6.372	2.258	1.648	5.738	0.930							14.398	6.372	2.258	1.648		
34.0	52.5	3.54	1.033	15.889	6.792	2.339	1.747	5.398	11.16	0.688	0.715	3.51	0.995	16.094	6.745	2.368	1.793	5.398	0.737							16.094	6.745	2.368	1.793		
57.0	53.4	3.54	1.018	16.879	7.194	2.376	1.792	5.141	11.58	0.633	0.644	3.51	0.987	16.989	7.078	2.400	1.819	5.144	0.661							16.989	7.078	2.400	1.819		
106.0	53.8	3.51	0.994	17.921	7.551	2.373	1.815	4.751	12.22	0.678	0.704	3.50	0.981	17.948	7.549	2.378	1.821	4.750	0.772							17.948	7.549	2.378	1.821		
204.0	56.0	3.49	0.974	17.862	7.907	2.259	1.739	4.823	12.87	0.940	0.962	3.49	0.974	17.862	7.907	2.259	1.739	4.823	0.962							17.862	7.907	2.259	1.739		
302.0	57.4	3.50	0.963	17.638	8.123	2.171	1.675	4.895	13.30	1.068	1.138	3.50	0.963	17.638	8.123	2.171	1.675	4.895	1.138							17.638	8.123	2.171	1.675		
500.0	63.0	3.49	0.955	17.042	8.431	2.021	1.555	5.451	14.13	1.315	1.376	3.49	0.955	17.042	8.431	2.021	1.555	5.451	1.376							17.042	8.431	2.021	1.555		
789.0	67.9	3.47	0.937	16.754	8.828	1.898	1.465	5.793	15.09	1.568	1.598	3.47	0.937	16.754	8.828	1.898	1.465	5.793	1.590							16.754	8.828	1.898	1.465		
1085.0	78.4	3.47	0.923	16.649	9.213	1.887	1.398	6.702	16.02	1.753	1.774	3.47	0.923	16.649	9.213	1.887	1.398	6.702	1.774							16.649	9.213	1.887	1.398		
1321.0	85.0	3.44	0.914	17.085	9.640	1.764	1.368	7.053	16.90	1.943	1.835	3.44	0.914	17.085	9.640	1.764	1.368	7.053	1.835							17.085	9.640	1.764	1.368		
1811.0	95.2	3.41	0.899	17.172	10.151	1.692	1.317	7.686	18.04	2.036	2.045	3.41	0.899	17.172	10.151	1.692	1.317	7.687	2.045							17.172	10.151	1.692	1.317		
2300.0	103.8	3.37	0.880	17.593	10.664	1.650	1.294	8.004	19.09	2.119	2.112	3.37	0.880	17.593	10.664	1.650	1.294	8.004	2.112							17.593	10.664	1.650	1.294		
2789.0	115.0	3.35	0.869	18.523	11.421	1.622	1.278	8.447	20.56	2.087	2.105	3.35	0.869	18.523	11.421	1.622	1.278	8.447	2.105							18.523	11.421	1.622	1.278		

Table 3 (continued)

$$N_0 = 1.272 \quad Re/m = 10.2 \times 10^6$$

CONSTANT PM										MEASURED P										CALCULATED P											
X	DEL	95	RE	ME	DEL*	THETA	H	HRR	HI	DELE	CF	CF	RE	ME	DEL*	THETA	H	HRR	HI	CF	DEL	THETA	H	HRR	HI	CF	DEL	THETA	H	HRR	
MM	MM	MM	MM	MM	MM	MM	MM	MM	MM	MM	MM	MM	MM	MM	MM	MM	MM	MM	MM	MM	MM	MM	MM	MM	MM	MM	MM	MM	MM	MM	MM
-68.0	33.4	18.14	1.308	5.744	2.810	2.044	1.275	9.044	5.09	1.851	1.818	18.14	1.308	5.744	2.810	2.044	1.275	9.044	1.818	5.744	2.810	2.044	1.275	9.044	1.818	5.744	2.810	2.044	1.275	9.044	1.818
-511.0	34.6	18.18	1.282	6.095	2.995	2.035	1.284	9.518	5.40	1.814	1.766	18.18	1.282	6.095	2.995	2.035	1.284	9.518	1.766	6.095	2.995	2.035	1.284	9.518	1.766	6.095	2.995	2.035	1.284	9.518	1.766
-411.0	35.6	18.19	1.267	6.384	3.144	2.030	1.294	9.292	5.66	1.800	1.733	18.19	1.267	6.384	3.144	2.030	1.294	9.292	1.733	6.384	3.144	2.030	1.294	9.292	1.733	6.384	3.144	2.030	1.294	9.292	1.733
-314.0	36.3	18.17	1.266	6.546	3.239	2.021	1.288	9.186	5.83	1.795	1.771	18.17	1.266	6.546	3.239	2.021	1.288	9.186	1.771	6.546	3.239	2.021	1.288	9.186	1.771	6.546	3.239	2.021	1.288	9.186	1.771
-215.0	36.4	18.21	1.272	6.639	3.293	2.016	1.279	9.038	5.95	1.832	1.796	18.21	1.272	6.639	3.293	2.016	1.279	9.038	1.796	6.639	3.293	2.016	1.279	9.038	1.796	6.639	3.293	2.016	1.279	9.038	1.796
-168.0	36.1	18.21	1.272	6.686	3.316	2.017	1.279	8.871	5.99	1.808	1.783	18.21	1.272	6.686	3.316	2.017	1.279	8.871	1.783	6.686	3.316	2.017	1.279	8.871	1.783	6.686	3.316	2.017	1.279	8.871	1.783
-143.0	37.5	18.22	1.268	6.743	3.358	2.008	1.277	8.758	6.07	1.793	1.747	18.22	1.273	6.762	3.365	2.010	1.279	8.758	1.744	6.788	3.342	2.029	1.271	8.758	1.744	6.788	3.342	2.029	1.271	8.758	1.744
-119.0	37.4	18.09	1.245	6.963	3.475	2.003	1.295	8.758	6.24	1.731	1.694	18.10	1.254	6.962	3.482	2.005	1.296	8.758	1.688	6.992	3.475	2.012	1.281	8.758	1.688	6.992	3.475	2.012	1.281	8.758	1.688
-94.0	38.7	18.13	1.222	7.289	3.650	1.997	1.315	8.685	6.52	1.586	1.551	18.16	1.249	7.357	3.670	2.004	1.320	8.540	1.534	7.345	3.712	1.979	1.294	8.540	1.534	7.345	3.712	1.979	1.294	8.540	1.534
-69.0	39.6	18.14	1.176	8.153	4.059	2.009	1.367	7.747	7.15	1.376	1.310	18.20	1.219	8.159	4.081	2.009	1.366	7.694	1.286	8.175	4.161	1.965	1.319	8.175	4.161	8.175	4.161	1.965	1.319	8.175	4.161
-47.0	42.5	18.21	1.136	9.182	4.494	2.043	1.429	7.413	7.80	1.101	1.047	18.27	1.181	9.156	4.515	2.028	1.414	7.385	1.024	9.250	4.287	2.150	1.389	9.250	4.287	9.250	4.287	2.150	1.389	9.250	4.287
-22.0	44.8	18.14	1.088	11.149	5.200	2.144	1.552	6.471	8.83	0.814	0.737	18.17	1.082	11.127	5.205	2.138	1.545	6.469	0.731	11.288	4.781	2.344	1.538	11.288	4.781	11.288	4.781	2.344	1.538	11.288	4.781
4.0	47.3	18.04	1.025	13.398	5.867	2.284	1.712	5.778	9.74	0.496	0.441	18.02	1.014	13.399	5.869	2.283	1.712	5.776	0.445	13.399	5.869	2.283	1.712	13.399	5.869	13.399	5.869	2.283	1.712	13.399	5.869
29.0	49.4	18.00	1.001	15.176	6.440	2.356	1.795	5.314	10.30	0.391	0.302	9.94	0.908	15.249	6.420	2.375	1.814	5.319	0.308	15.249	6.420	2.375	1.814	15.249	6.420	15.249	6.420	2.375	1.814	15.249	6.420
51.0	50.6	9.92	0.979	16.136	6.646	2.428	1.875	5.186	10.77	0.410	0.396	9.87	0.964	16.171	6.640	2.435	1.885	5.185	0.401	16.171	6.640	2.435	1.885	16.171	6.640	16.171	6.640	2.435	1.885	16.171	6.640
74.0	50.9	9.91	0.971	16.457	6.863	2.396	1.856	5.015	11.11	0.407	0.456	9.88	0.963	16.468	6.870	2.396	1.858	5.013	0.460	16.468	6.870	2.396	1.858	16.468	6.870	16.468	6.870	2.396	1.858	16.468	6.870
125.0	52.0	9.81	0.955	16.804	7.252	2.317	1.885	4.853	11.73	0.641	0.565	9.81	0.955	16.803	7.251	2.317	1.885	4.854	0.565	16.803	7.251	2.317	1.885	16.803	7.251	16.803	7.251	2.317	1.885	16.803	7.251
174.0	52.6	9.86	0.944	16.963	7.458	2.274	1.779	4.778	12.07	0.655	0.674	9.86	0.944	16.963	7.458	2.274	1.779	4.778	0.674	16.963	7.458	2.274	1.779	16.963	7.458	16.963	7.458	2.274	1.779	16.963	7.458
221.0	52.9	9.80	0.938	16.748	7.566	2.214	1.733	4.778	12.31	0.809	0.748	9.80	0.938	16.748	7.566	2.214	1.733	4.778	0.748	16.748	7.566	2.214	1.733	16.748	7.566	16.748	7.566	2.214	1.733	16.748	7.566
272.0	53.0	9.82	0.934	16.473	7.654	2.152	1.694	5.033	12.53	0.878	0.820	9.82	0.934	16.473	7.654	2.152	1.694	5.033	0.820	16.473	7.654	2.152	1.694	16.473	7.654	16.473	7.654	2.152	1.694	16.473	7.654
321.0	53.4	9.80	0.931	16.309	7.738	2.108	1.649	5.062	12.74	0.961	0.874	9.80	0.931	16.309	7.738	2.108	1.649	5.062	0.874	16.309	7.738	2.108	1.649	16.309	7.738	16.309	7.738	2.108	1.649	16.309	7.738
368.0	53.6	9.81	0.928	16.094	7.805	2.062	1.612	5.062	12.93	1.015	0.932	9.81	0.928	16.094	7.805	2.062	1.612	5.062	0.932	16.094	7.805	2.062	1.612	16.094	7.805	16.094	7.805	2.062	1.612	16.094	7.805
466.0	57.2	9.79	0.922	15.792	7.910	1.996	1.561	5.235	13.23	1.111	1.041	9.79	0.922	15.792	7.910	1.996	1.561	5.235	1.041	15.792	7.910	1.996	1.561	15.792	7.910	15.792	7.910	1.996	1.561	15.792	7.910
563.0	60.6	9.78	0.919	15.632	8.040	1.944	1.519	5.593	13.57	1.209	1.092	9.78	0.919	15.632	8.040	1.944	1.519	5.593	1.092	15.632	8.040	1.944	1.519	15.632	8.040	15.632	8.040	1.944	1.519	15.632	8.040
663.0	63.2	9.74	0.913	15.345	8.149	1.883	1.471	5.873	13.82	1.287	1.262	9.74	0.913	15.344	8.149	1.883	1.471	5.873	1.262	15.344	8.149	1.883	1.471	15.344	8.149	15.344	8.149	1.883	1.471	15.344	8.149
761.0	65.2	9.73	0.907	15.264	8.253	1.850	1.447	6.051	14.16	1.303	1.310	9.73	0.907	15.264	8.253	1.850	1.447	6.051	1.310	15.264	8.253	1.850	1.447	15.264	8.253	15.264	8.253	1.850	1.447	15.264	8.253
861.0	68.1	9.73	0.902	15.487	8.485	1.825	1.430	6.201	14.63	1.330	1.280	9.73	0.902	15.487	8.485	1.825	1.430	6.201	1.280	15.487	8.485	1.825	1.430	15.487	8.485	15.487	8.485	1.825	1.430	15.487	8.485
967.0	69.6	9.66	0.895	15.354	8.554	1.795	1.409	6.342	14.82	1.396	1.334	9.66	0.895	15.354	8.554	1.795	1.409	6.342	1.334	15.354	8.554	1.795	1.409	15.354	8.554	15.354	8.554	1.795	1.409	15.354	8.554
1065.0	72.1	9.69	0.891	15.283	8.625	1.772	1.392	6.588	15.04	1.445	1.350	9.69	0.891	15.283	8.625	1.772	1.392	6.588	1.350	15.283	8.625	1.772	1.392	15.283	8.625	15.283	8.625	1.772	1.392	15.283	8.625
1099.0	73.9	9.67	0.893	15.329	8.731	1.756	1.377	6.708	15.29	1.519	1.444	9.67	0.893	15.329	8.731	1.756	1.377	6.708	1.444	15.329	8.731	1.756	1.377	15.329	8.731	15.329	8.731	1.756	1.377	15.329	8.731
1197.0	75.9	9.74	0.892	15.010	8.714	1.722	1.349	6.907	15.47	1.567	1.544	9.74	0.892	15.010	8.714	1.722	1.349	6.907	1.544	15.010	8.714	1.722	1.349	15.010	8.714	15.010	8.714	1.722	1.349	15.010	8.714
1294.0	77.8	9.75	0.887	15.072	8.819	1.709	1.341	7.113	15.63	1.644	1.606	9.75	0.887	15.072	8.819	1.709	1.341	7.113	1.606	15.072	8.819	1.709	1.341	15.072	8.819	15.072	8.819	1.709	1.341	15.072	8.819
1538.0	84.6	9.60	0.875	15.466	9.182	1.678	1.322	7.535	16.30	1.732	1.577	9.60	0.875	15.466	9.182	1.678	1.322	7.535	1.577	15.466	9.182	1.678	1.322	15.466	9.182	15.466	9.182	1.678	1.322	15.466	9.182
1585.0	85.3	9.47	0.873	15.437	9.244	1.670	1.317	7.558	16.43	1.680	1.582	9.47	0.873	15.437																	

Table 3 (continued)

$$M_0 = 1.373 \quad Re/m = 3.67 \times 10^6$$

CONSTANT PM										MEASURED P										CALCULATED P									
X	DEL	95	RE/M	ME	DEL*	THETA	H	HBR	HI	DEL	CF	DEL*	THETA	H	HBR	HI	CF	DEL	THETA	H	HBR	DEL	THETA	H	HBR	DEL	THETA	H	HBR
MM	MM	MM	X10-6	MM	MM	MM	MM	MM	MM	X10-6	X10-3	MM	MM	MM	MM	MM	X10-3	MM	MM	MM	MM	MM	MM	MM	MM	MM	MM	MM	MM
-712.0	34.1	3.64	1.413	6.516	2.927	2.227	1.386	9.425	5.26	2.891	2.198	3.64	1.413	6.516	2.927	2.227	1.386	9.425	5.26	2.891	2.198	6.516	2.927	2.227	1.386	9.425	5.26	2.891	2.198
-710.0	34.1	3.64	1.414	6.595	2.961	2.227	1.385	9.289	5.32	2.893	2.189	3.64	1.414	6.594	2.961	2.227	1.385	9.290	5.29	2.893	2.189	6.594	2.961	2.227	1.385	9.290	5.29	2.893	2.189
-708.0	34.7	3.64	1.385	7.542	3.482	2.217	1.316	9.168	6.89	2.819	2.892	3.64	1.385	7.542	3.482	2.217	1.316	9.168	6.89	2.819	2.892	7.542	3.482	2.217	1.316	9.168	6.89	2.819	2.892
-722.0	39.4	3.67	1.377	8.108	3.661	2.213	1.329	8.598	6.53	1.894	1.978	3.67	1.377	8.108	3.661	2.213	1.329	8.598	6.53	1.894	1.978	8.108	3.661	2.213	1.329	8.598	6.53	1.894	1.978
-191.0	39.4	3.67	1.373	8.179	3.699	2.211	1.332	8.441	6.59	1.965	1.966	3.67	1.373	8.179	3.699	2.211	1.332	8.441	6.59	1.966	1.966	8.179	3.699	2.211	1.332	8.441	6.59	1.966	1.966
-171.0	39.2	3.68	1.378	8.345	3.767	2.215	1.338	8.191	6.78	1.891	1.939	3.68	1.378	8.345	3.767	2.215	1.338	8.191	6.78	1.891	1.939	8.345	3.767	2.215	1.338	8.191	6.78	1.891	1.939
-148.0	40.4	3.65	1.358	8.647	3.913	2.218	1.352	8.114	6.93	1.819	1.879	3.65	1.358	8.647	3.913	2.218	1.352	8.114	6.93	1.819	1.879	8.647	3.913	2.218	1.352	8.114	6.93	1.819	1.879
-121.0	39.9	3.61	1.279	9.479	4.277	2.216	1.423	7.112	7.45	1.448	1.581	3.61	1.279	9.479	4.277	2.216	1.423	7.113	7.11	1.448	1.581	9.479	4.277	2.216	1.423	7.113	7.11	1.448	1.581
-101.0	41.5	3.64	1.232	18.935	4.828	2.269	1.587	6.341	8.24	1.149	1.191	3.64	1.232	18.935	4.828	2.269	1.587	6.341	8.24	1.191	1.191	18.935	4.828	2.269	1.587	6.341	8.24	1.191	1.191
-76.0	44.3	3.65	1.194	12.798	5.461	2.342	1.688	5.769	9.17	0.899	0.954	3.65	1.194	12.798	5.461	2.342	1.688	5.778	9.54	0.954	0.954	12.798	5.461	2.342	1.688	5.778	9.54	0.954	0.954
-58.0	49.1	3.65	1.155	15.154	6.144	2.467	1.736	5.525	18.18	0.718	0.669	3.65	1.155	15.154	6.144	2.467	1.736	5.525	18.18	0.669	0.669	15.154	6.144	2.467	1.736	5.525	18.18	0.669	0.669
-27.0	53.4	3.62	1.129	17.855	6.814	2.628	1.885	5.216	18.98	0.682	0.555	3.62	1.129	17.855	6.814	2.628	1.885	5.216	18.98	0.555	0.555	17.855	6.814	2.628	1.885	5.216	18.98	0.555	0.555
-1.0	54.6	3.63	1.183	28.482	7.382	2.764	2.027	4.632	11.78	0.478	0.418	3.63	1.183	28.482	7.382	2.764	2.027	4.632	11.78	0.418	0.418	28.482	7.382	2.764	2.027	4.632	11.78	0.418	0.418
22.0	57.4	3.67	1.065	22.618	7.834	2.887	2.147	4.448	12.28	0.384	0.312	3.67	1.065	22.618	7.834	2.887	2.147	4.448	12.28	0.312	0.312	22.618	7.834	2.887	2.147	4.448	12.28	0.312	0.312
71.0	61.8	3.65	1.055	25.587	8.417	3.048	2.384	4.287	13.82	0.344	0.283	3.65	1.055	25.587	8.417	3.048	2.384	4.287	13.82	0.283	0.283	25.587	8.417	3.048	2.384	4.287	13.82	0.283	0.283
128.0	63.4	3.63	1.033	26.934	8.839	3.047	2.335	4.126	13.98	0.311	0.251	3.63	1.033	26.934	8.839	3.047	2.335	4.126	13.98	0.251	0.251	26.934	8.839	3.047	2.335	4.126	13.98	0.251	0.251
189.0	65.1	3.64	1.023	27.187	9.233	2.936	2.255	4.115	14.22	0.414	0.373	3.64	1.023	27.187	9.233	2.936	2.255	4.115	14.22	0.373	0.373	27.187	9.233	2.936	2.255	4.115	14.22	0.373	0.373
267.0	65.5	3.63	1.003	26.296	9.721	2.785	2.085	4.013	15.11	0.548	0.519	3.63	1.003	26.296	9.721	2.785	2.085	4.013	15.11	0.519	0.519	26.296	9.721	2.785	2.085	4.013	15.11	0.519	0.519
463.0	71.8	3.59	0.972	25.073	18.682	2.385	1.838	4.528	16.96	0.794	0.843	3.59	0.972	25.073	18.682	2.385	1.838	4.521	16.96	0.843	0.843	25.073	18.682	2.385	1.838	4.521	16.96	0.843	0.843
756.0	82.6	3.56	0.946	21.288	11.266	2.659	1.688	5.273	18.71	1.168	1.198	3.56	0.946	21.288	11.266	2.659	1.688	5.273	18.71	1.198	1.198	21.288	11.266	2.659	1.688	5.273	18.71	1.198	1.198
1852.0	92.7	3.54	0.916	22.329	11.848	1.886	1.471	5.943	28.22	1.444	1.462	3.54	0.916	22.329	11.848	1.886	1.471	5.943	28.22	1.462	1.462	22.329	11.848	1.886	1.471	5.943	28.22	1.462	1.462
1284.0	101.4	3.58	0.985	21.752	12.137	1.792	1.399	6.562	21.88	1.784	1.788	3.58	0.985	21.752	12.137	1.792	1.399	6.562	21.88	1.784	1.788	21.752	12.137	1.792	1.399	6.562	21.88	1.784	1.788
1776.0	117.6	3.43	0.878	21.788	12.916	1.686	1.327	7.419	22.88	1.998	1.975	3.43	0.878	21.788	12.916	1.686	1.327	7.419	22.88	1.975	1.975	21.788	12.916	1.686	1.327	7.419	22.88	1.975	1.975
2267.0	129.2	3.39	0.861	22.111	13.583	1.628	1.288	7.884	24.32	2.131	2.119	3.39	0.861	22.111	13.583	1.628	1.288	7.884	24.32	2.131	2.119	22.111	13.583	1.628	1.288	7.884	24.32	2.131	2.119
2752.0	137.4	3.33	0.839	22.253	14.088	1.589	1.278	8.225	25.26	2.185	2.189	3.33	0.839	22.253	14.088	1.589	1.278	8.225	25.26	2.185	2.189	22.253	14.088	1.589	1.278	8.225	25.26	2.185	2.189

Table 3 (continued)

$$M_0 = 1.386 \quad R_e/m = 10.0 \times 10^6$$

CONSTANT PM										MEASURED P										CALCULATED P									
X	DEL 955	RE/M	ME	DEL*	THEIR	H	HEPR	HI	DELE	OP	OF	RE/M	ME	DEL*	THEIR	H	HEPR	HI	OF	DELEPR	THEIRPR	H	HEPR						
MM	MM	X10-6	MM	MM	MM	X10+3	X10+3	MM	MM	X10+3	X10+3	X10-6	MM	MM	MM	MM	MM	MM	X10+3	MM	MM	MM	MM						
-729.0	32.4	9.92	1.420	5.660	2.594	2.190	1.273	18.348	4.68	1.891	1.787	9.92	1.420	5.660	2.594	2.190	1.273	18.348	1.787	5.660	2.594	2.190	1.273						
-635.0	33.0	9.97	1.425	5.819	2.633	2.193	1.271	18.244	4.81	1.894	1.797	9.97	1.425	5.819	2.633	2.193	1.271	18.245	1.797	5.819	2.633	2.193	1.271						
-537.0	34.2	9.96	1.417	6.086	2.779	2.190	1.276	18.115	5.03	1.837	1.757	9.96	1.417	6.086	2.779	2.190	1.276	18.115	1.757	6.086	2.779	2.190	1.276						
-439.0	34.4	9.95	1.414	6.292	2.873	2.190	1.279	9.784	5.20	1.823	1.729	9.95	1.414	6.292	2.873	2.190	1.279	9.784	1.729	6.292	2.873	2.190	1.279						
-343.0	35.4	9.96	1.408	6.466	2.970	2.177	1.275	9.743	5.37	1.816	1.776	9.96	1.408	6.466	2.970	2.177	1.275	9.743	1.776	6.466	2.970	2.177	1.275						
-292.0	35.1	9.99	1.406	6.680	3.028	2.180	1.279	9.413	5.47	1.818	1.746	9.99	1.406	6.680	3.028	2.180	1.279	9.413	1.746	6.680	3.028	2.180	1.279						
-245.0	36.6	10.00	1.396	6.742	3.109	2.169	1.280	9.604	5.62	1.779	1.766	10.00	1.396	6.742	3.109	2.169	1.280	9.604	1.766	6.742	3.109	2.169	1.280						
-208.0	37.0	10.03	1.386	6.900	3.150	2.158	1.282	9.586	5.73	1.750	1.733	10.03	1.386	6.900	3.150	2.158	1.282	9.586	1.733	6.900	3.150	2.158	1.282						
-192.0	37.5	10.03	1.381	7.003	3.238	2.162	1.290	9.417	5.83	1.695	1.682	10.04	1.384	7.003	3.243	2.164	1.291	9.398	1.681	6.954	3.244	2.098	1.284						
-171.0	38.6	10.02	1.373	7.029	3.266	2.152	1.293	9.655	5.87	1.738	1.679	10.04	1.387	7.058	3.274	2.156	1.295	9.624	1.673	7.059	3.274	2.156	1.288						
-144.0	37.1	10.02	1.341	7.211	3.379	2.134	1.314	8.946	6.04	1.614	1.549	10.06	1.375	7.287	3.403	2.141	1.319	8.762	1.533	7.251	3.447	2.103	1.307						
-128.0	38.3	9.96	1.307	7.471	3.526	2.119	1.337	8.177	6.25	1.490	1.488	10.01	1.355	7.633	3.590	2.138	1.353	8.001	1.466	7.547	3.729	2.024	1.321						
-95.0	38.7	10.14	1.258	8.758	4.004	2.145	1.406	7.332	7.12	1.127	1.153	10.22	1.335	8.965	4.156	2.157	1.420	7.154	1.124	8.988	4.400	2.002	1.384						
-73.0	40.6	10.21	1.210	10.115	4.579	2.209	1.497	6.558	7.83	0.880	0.917	10.29	1.279	10.246	4.627	2.215	1.507	6.561	0.892	10.133	4.861	2.005	1.461						
-48.0	44.2	10.20	1.157	12.610	5.440	2.318	1.627	5.887	9.09	0.683	0.683	10.27	1.213	12.694	5.468	2.321	1.636	5.762	0.665	12.687	5.565	2.200	1.575						
-24.0	48.6	10.23	1.107	15.648	6.131	2.352	1.856	5.375	9.94	0.322	0.299	10.25	1.123	15.640	6.137	2.348	1.853	5.371	0.296	15.761	5.725	2.753	1.819						
1.0	51.1	10.20	1.061	18.261	6.748	2.706	1.997	4.867	10.79	0.206	0.321	10.10	1.029	18.374	6.721	2.734	2.021	4.869	0.333	18.374	6.721	2.734	2.021						
50.0	56.3	10.01	1.039	22.020	7.703	2.962	2.256	4.346	11.94	0.104	0.224	9.95	1.015	22.066	7.697	2.971	2.264	4.344	0.228	22.066	7.697	2.971	2.264						
99.0	59.1	9.97	1.012	24.694	8.161	3.015	2.330	4.227	12.53	0.236	0.241	9.92	0.995	24.687	8.160	3.016	2.333	4.227	0.244	24.687	8.160	3.016	2.333						
148.0	60.5	9.94	0.995	25.126	8.572	2.931	2.281	4.127	13.17	0.257	0.264	9.92	0.988	25.124	8.572	2.931	2.281	4.127	0.266	25.124	8.572	2.931	2.281						
197.0	61.0	9.92	0.994	24.856	8.858	2.886	2.188	4.000	13.66	0.218	0.311	9.92	0.994	24.855	8.858	2.886	2.189	4.000	0.311	24.855	8.858	2.886	2.189						
246.0	61.3	9.93	0.973	24.280	9.097	2.669	2.065	4.063	14.15	0.400	0.378	9.92	0.973	24.279	9.097	2.669	2.065	4.070	0.378	24.279	9.097	2.669	2.065						
295.0	61.7	9.89	0.963	23.927	9.348	2.560	2.003	4.041	14.63	0.501	0.518	9.89	0.963	23.927	9.348	2.560	2.003	4.041	0.518	23.927	9.348	2.560	2.003						
342.0	63.5	9.89	0.956	23.492	9.499	2.473	1.936	4.212	14.96	0.533	0.588	9.89	0.956	23.492	9.499	2.473	1.936	4.212	0.588	23.492	9.499	2.473	1.936						
444.0	66.2	9.84	0.942	22.838	9.867	2.315	1.815	4.394	15.78	0.690	0.684	9.84	0.942	22.838	9.867	2.315	1.815	4.394	0.684	22.838	9.867	2.315	1.815						
539.0	70.2	9.88	0.931	21.976	10.065	2.183	1.713	4.791	16.37	0.819	0.821	9.88	0.931	21.976	10.065	2.183	1.713	4.791	0.821	21.976	10.065	2.183	1.713						
637.0	74.0	9.76	0.921	21.442	10.373	2.077	1.631	5.091	17.03	0.940	0.920	9.76	0.921	21.442	10.373	2.077	1.631	5.091	0.920	21.442	10.373	2.077	1.631						
755.0	76.7	9.74	0.912	20.997	10.583	1.999	1.571	5.384	17.53	1.107	1.011	9.74	0.912	20.997	10.583	1.999	1.571	5.384	1.011	20.997	10.583	1.999	1.571						
833.0	80.6	9.77	0.903	20.469	10.614	1.928	1.518	5.665	17.91	1.185	1.108	9.77	0.903	20.469	10.614	1.928	1.518	5.665	1.108	20.469	10.614	1.928	1.518						
931.0	86.1	9.57	0.895	20.146	10.729	1.878	1.400	6.147	18.26	1.247	1.185	9.57	0.895	20.145	10.729	1.878	1.400	6.147	1.185	20.145	10.729	1.878	1.400						
1027.0	89.5	9.82	0.890	20.118	10.978	1.833	1.445	6.320	18.85	1.262	1.210	9.82	0.890	20.118	10.977	1.833	1.445	6.320	1.210	20.118	10.977	1.833	1.445						
1755.0	107.1	9.24	0.856	19.400	11.073	1.634	1.297	7.386	21.28	1.067	1.794	9.24	0.856	19.400	11.073	1.634	1.297	7.386	1.794	19.400	11.073	1.634	1.297						
2244.0	113.9	9.10	0.832	18.588	11.804	1.575	1.262	8.075	21.28	1.900	1.948	9.10	0.832	18.588	11.804	1.575	1.262	8.075	1.948	18.588	11.804	1.575	1.262						
2733.0	116.3	8.92	0.800	17.901	11.670	1.534	1.241	8.432	21.22	2.023	1.935	8.92	0.800	17.901	11.670	1.534	1.241	8.432	1.935	17.901	11.670	1.534	1.241						
2933.0	118.1	8.80	0.799	17.693	11.617	1.523	1.237	8.643	21.17	2.001	1.941	8.80	0.799	17.693	11.617	1.523	1.237	8.643	1.941	17.693	11.617	1.523	1.237						

Table 3 (continued)

$$M_0 = 1.522 \quad Re/m = 3.51 \times 10^6$$

CONSTANT PA										MEASURED P										CALCULATED P									
X	DEL 95	RE/M	ME	DEL*	THEIR	H	HEAR	HI	DELE	CFP	CF	RE/M	ME	DEL*	THEIR	H	HEAR	HI	CF	DELOR	THEIROR	H	HEOR						
MM	MM	X10-6	MM	MM	MM	MM	MM	MM	MM	X10-3	X10-3	X10-6	MM	MM	MM	MM	MM	MM	X10-3	MM	MM	MM	MM						
-717.0	33.9	3.49	1.538	6.771	2.808	2.392	1.383	9.585	5.89	2.118	2.195	3.49	1.538	6.771	2.808	2.392	1.383	9.585	2.195	6.771	2.808	2.392	1.383						
-523.0	34.5	3.48	1.542	7.144	2.904	2.394	1.388	9.167	5.38	2.088	2.171	3.48	1.542	7.144	2.904	2.394	1.388	9.167	2.171	7.144	2.904	2.394	1.388						
-327.0	37.4	3.51	1.522	7.647	3.211	2.382	1.311	9.267	5.76	1.959	2.867	3.51	1.522	7.647	3.211	2.382	1.311	9.267	2.867	7.647	3.211	2.382	1.311						
-278.6	37.4	3.53	1.524	7.893	3.365	2.388	1.313	8.927	5.93	1.954	2.856	3.53	1.524	7.893	3.365	2.388	1.313	8.927	2.856	7.893	3.365	2.388	1.313						
-255.0	37.7	3.51	1.522	7.997	3.357	2.382	1.311	8.948	6.02	1.959	2.862	3.51	1.522	7.997	3.357	2.382	1.311	8.949	2.862	8.169	3.214	2.542	1.385						
-229.0	38.4	3.59	1.491	8.207	3.482	2.357	1.325	8.678	6.28	1.828	1.938	3.59	1.498	8.246	3.493	2.351	1.328	8.633	1.927	8.289	3.465	2.387	1.382						
-206.0	37.8	3.58	1.447	8.318	3.578	2.338	1.356	8.259	6.33	1.646	1.735	3.52	1.466	8.465	3.685	2.348	1.371	8.137	1.728	8.633	3.454	2.388	1.342						
-188.0	37.6	3.59	1.333	9.337	3.975	2.349	1.497	7.189	6.82	1.885	1.878	3.54	1.448	9.786	4.089	2.373	1.527	6.821	1.838	9.558	4.282	2.241	1.583						
-155.0	41.2	3.57	1.273	11.722	4.683	2.546	1.781	6.483	7.77	0.372	0.452	3.61	1.383	11.978	4.782	2.547	1.721	6.215	0.436	11.514	5.278	2.181	1.663						
-131.0	45.5	3.62	1.252	15.946	5.597	2.831	1.939	5.298	9.85	0.349	0.346	3.67	1.382	16.186	5.768	2.818	1.968	5.889	0.331	16.834	5.988	2.678	1.917						
-108.0	58.9	3.65	1.227	18.946	6.127	1.876	2.133	5.232	9.72	0.088	0.088	3.67	1.282	18.714	6.284	1.816	2.111	5.188	0.088	18.786	6.099	1.888	2.114						
-83.0	56.1	3.65	1.286	21.357	6.347	1.688	2.625	5.159	9.99	0.088	0.088	3.66	1.225	21.285	6.376	1.652	2.613	5.146	0.088	21.288	6.032	1.619	2.561						
-57.0	68.8	3.65	1.183	28.232	6.668	1.242	3.896	4.887	18.48	0.088	0.088	3.65	1.193	28.256	6.665	1.240	3.188	4.883	0.088	28.289	6.759	1.186	2.945						
-34.0	67.4	3.65	1.174	32.189	7.837	1.453	3.361	5.815	11.83	0.088	0.088	3.65	1.162	31.537	7.382	1.284	3.138	4.871	0.088	31.528	6.485	1.922	3.228						
13.0	73.9	3.67	1.153	39.569	7.869	5.829	3.762	4.363	12.12	0.088	0.088	3.64	1.185	39.269	8.019	4.897	3.627	4.318	0.088	39.269	8.819	4.897	3.627						
64.0	79.2	3.66	1.134	44.142	8.137	5.425	4.111	4.389	12.54	0.088	0.088	3.62	1.078	44.188	8.128	5.431	4.879	4.322	0.088	44.188	8.128	5.431	4.879						
115.0	88.7	3.62	1.118	46.125	8.448	5.468	4.168	4.893	12.97	0.088	0.088	3.59	1.072	46.188	8.439	5.463	4.145	4.188	0.088	46.188	8.439	5.463	4.145						
162.0	84.2	3.63	1.104	46.857	9.148	5.839	3.855	4.173	13.93	0.088	0.088	3.61	1.071	46.838	9.134	5.848	3.841	4.178	0.088	46.838	9.134	5.848	3.841						
211.0	87.8	3.63	1.091	45.818	9.987	4.624	3.543	4.259	14.98	0.088	0.088	3.68	1.048	45.788	9.988	4.625	3.528	4.244	0.088	45.788	9.988	4.625	3.528						
268.0	98.8	3.62	1.078	44.958	11.128	4.843	3.892	4.122	16.61	0.088	0.088	3.68	1.044	44.949	11.115	4.844	3.883	4.125	0.088	44.949	11.115	4.844	3.883						
456.0	182.3	3.56	1.029	42.859	13.397	3.199	2.464	4.437	28.28	0.288	0.289	3.54	1.088	42.856	13.388	3.199	2.463	4.437	0.213	42.856	13.388	3.199	2.463						
749.0	118.3	3.53	0.975	38.177	15.832	2.411	1.866	5.861	25.38	0.638	0.665	3.53	0.975	38.177	15.832	2.411	1.866	5.861	0.665	38.177	15.832	2.411	1.866						
1043.0	129.0	3.48	0.931	35.255	17.887	2.873	1.619	5.512	28.28	0.954	0.956	3.48	0.931	35.254	17.887	2.873	1.619	5.512	0.986	35.254	17.887	2.873	1.619						
1279.0	139.5	3.46	0.913	33.425	17.386	1.923	1.585	6.181	29.49	1.346	1.341	3.45	0.913	33.425	17.386	1.923	1.585	6.181	1.341	33.425	17.386	1.923	1.585						
1769.0	157.6	3.35	0.875	32.437	18.581	1.753	1.388	6.785	32.21	1.659	1.684	3.35	0.875	32.437	18.588	1.753	1.388	6.785	1.684	32.437	18.588	1.753	1.388						
2258.0	172.9	3.32	0.851	31.496	18.962	1.661	1.244	7.457	33.61	1.845	1.882	3.32	0.851	31.496	18.962	1.661	1.244	7.457	1.882	31.496	18.962	1.661	1.244						
2745.0	181.9	3.25	0.827	31.597	19.647	1.688	1.294	7.658	35.18	1.958	1.944	3.25	0.827	31.597	19.647	1.688	1.294	7.658	1.944	31.597	19.647	1.688	1.294						
2945.0	186.5	3.23	0.822	31.773	19.963	1.592	1.283	7.751	35.74	1.961	2.083	3.23	0.822	31.773	19.963	1.592	1.283	7.751	2.083	31.773	19.963	1.592	1.283						

Table 3 (continued)

$$M_0 = 1.531 \quad Re/m = 6.47 \times 10^6$$

CONSTANT PM										MEASURED P										CALCULATED P										
X	DEL	RE/M	DEL*	THETA	H	HRR	HI	DEL*	CF	DEL*	RE/M	DEL*	THETA	H	HRR	HI	CF	DEL*	RE/M	DEL*	THETA	H	HRR	HI	DEL*	RE/M	DEL*	THETA	H	HRR
MM	MM	X10-6	MM	MM	MM	MM	MM	MM	X10-3	MM	MM	MM	MM	MM	MM	MM	X10-3	MM	MM	MM	MM	MM	MM	MM	MM	MM	MM	MM	MM	MM
-316.0	33.4	6.45	1.544	6.492	2.746	2.364	1.278	9.799	1.944	6.492	6.45	1.544	2.746	2.364	1.278	9.799	1.959	6.492	6.45	1.544	2.746	2.364	1.278	9.799	1.959	6.492	2.746	2.364	1.278	
-320.0	34.7	6.45	1.532	6.938	2.941	2.359	1.286	9.439	1.885	6.938	6.45	1.532	2.941	2.359	1.286	9.439	1.885	6.938	6.45	1.532	2.941	2.359	1.286	9.439	1.885	6.938	2.941	2.359	1.286	
-371.0	36.5	6.47	1.531	7.128	3.023	2.358	1.286	9.716	1.888	7.128	6.47	1.531	3.023	2.358	1.286	9.716	1.888	7.128	6.47	1.531	3.023	2.358	1.286	9.716	1.888	7.128	3.023	2.358	1.286	
-399.0	36.6	6.49	1.594	7.349	3.156	2.329	1.256	9.268	1.812	7.349	6.51	1.522	3.188	2.319	1.304	9.141	1.865	7.379	6.51	1.522	3.188	2.319	1.304	9.141	1.865	7.379	3.240	2.277	1.276	
-439.0	37.0	6.45	1.461	7.457	3.266	2.283	1.317	9.044	1.687	7.457	6.50	1.527	3.393	2.319	1.346	8.985	1.673	7.879	6.50	1.527	3.393	2.319	1.346	8.985	1.673	7.879	3.381	2.331	1.259	
-471.0	37.5	6.39	1.323	8.237	3.663	2.249	1.439	7.989	1.048	8.237	6.51	1.495	3.981	2.290	1.491	7.323	1.002	9.464	6.51	1.495	3.981	2.290	1.491	7.323	1.002	9.464	3.339	2.834	1.488	
-488.0	36.7	6.50	1.244	18.313	4.122	2.582	1.684	6.482	0.332	18.313	6.54	1.288	4.148	2.585	1.682	6.342	0.326	18.464	6.54	1.288	4.148	2.585	1.682	6.342	0.326	18.464	4.056	2.588	1.669	
-494.0	41.9	6.66	1.239	14.015	5.080	2.883	1.918	5.577	0.819	14.015	6.68	1.259	5.016	2.883	1.918	5.551	0.808	14.089	6.68	1.259	5.016	2.883	1.918	5.551	0.808	14.089	4.989	2.824	1.889	
-481.0	46.9	6.66	1.287	17.434	5.592	3.118	2.189	5.269	0.808	17.434	6.68	1.294	5.682	3.116	2.186	5.255	0.808	17.469	6.68	1.294	5.682	3.116	2.186	5.255	0.808	17.469	5.613	3.118	2.181	
-76.0	52.1	6.69	1.186	21.686	5.951	3.631	2.614	5.124	9.32	21.686	6.70	1.204	5.960	3.627	2.621	5.114	8.888	21.557	6.70	1.204	5.960	3.627	2.621	5.114	8.888	21.557	6.138	3.517	2.557	
-52.0	68.6	6.72	1.164	27.952	6.744	4.144	3.048	4.841	18.45	27.952	6.73	1.182	6.865	4.036	2.978	4.792	18.088	27.756	6.73	1.182	6.865	4.036	2.978	4.792	18.088	27.756	6.913	4.015	2.847	
-27.0	67.4	6.67	1.152	33.348	7.341	4.543	3.388	4.639	11.26	33.348	6.66	1.141	7.689	4.381	3.176	4.567	10.888	33.258	6.66	1.141	7.689	4.381	3.176	4.567	10.888	33.258	6.121	5.432	3.435	
22.0	72.9	6.66	1.134	40.028	7.276	5.611	4.259	4.488	11.41	40.028	6.58	1.062	8.318	5.252	3.893	4.273	10.888	40.044	6.58	1.062	8.318	5.252	3.893	4.273	10.888	40.044	7.689	5.288	3.893	
71.0	77.9	6.64	1.118	44.882	7.452	6.023	4.618	4.431	11.70	44.882	6.57	1.057	8.643	5.191	3.965	4.122	10.888	43.643	6.57	1.057	8.643	5.191	3.965	4.122	10.888	43.643	8.318	5.252	3.965	
128.0	82.1	6.64	1.102	46.649	8.083	5.771	4.448	4.386	12.52	46.649	6.59	1.062	8.882	5.191	3.959	4.137	10.888	45.698	6.59	1.062	8.882	5.191	3.959	4.137	10.888	45.698	8.882	5.191	3.959	
167.0	86.2	6.62	1.088	47.442	8.576	5.532	4.282	4.528	13.12	47.442	6.59	1.051	9.277	5.015	3.946	4.277	10.888	46.522	6.59	1.051	9.277	5.015	3.946	4.277	10.888	46.522	9.277	5.015	3.946	
218.0	90.0	6.63	1.074	46.767	18.346	4.528	3.486	4.179	15.29	46.767	6.59	1.042	18.342	4.521	3.476	4.182	10.888	46.755	6.59	1.042	18.342	4.521	3.476	4.182	10.888	46.755	18.342	4.521	3.476	
267.0	92.0	6.62	1.059	45.628	11.012	4.144	3.281	4.211	16.33	45.628	6.58	1.038	11.018	4.144	3.195	4.212	10.888	45.623	6.58	1.038	11.018	4.144	3.195	4.212	10.888	45.623	11.018	4.144	3.195	
463.0	101.4	6.55	1.088	42.753	13.788	3.181	2.488	4.254	28.94	42.753	6.55	1.065	13.788	3.181	2.488	4.254	28.211	42.752	6.55	1.065	13.788	3.181	2.488	4.254	28.211	42.752	13.788	3.181	2.488	
756.0	113.4	6.46	0.953	37.272	16.038	2.325	1.814	4.749	25.68	37.272	6.46	0.953	16.038	2.325	1.814	4.749	25.68	37.272	6.46	0.953	16.038	2.325	1.814	4.749	25.68	37.272	16.038	2.325	1.814	
1058.0	127.4	6.38	0.911	33.889	16.846	2.012	1.933	5.551	27.92	33.889	6.38	0.911	16.846	2.012	1.933	5.551	27.92	33.889	6.38	0.911	16.846	2.012	1.933	5.551	27.92	33.889	16.846	2.012	1.933	
1286.0	136.9	6.26	0.889	32.294	17.322	1.864	1.473	6.039	29.31	32.294	6.26	0.889	17.322	1.864	1.473	6.039	29.31	32.294	6.26	0.889	17.322	1.864	1.473	6.039	29.31	32.294	17.322	1.864	1.473	
1776.0	153.1	6.08	0.856	31.245	18.312	1.786	1.388	6.654	32.06	31.245	6.08	0.856	18.312	1.786	1.388	6.654	32.06	31.245	6.08	0.856	18.312	1.786	1.388	6.654	32.06	31.245	18.312	1.786	1.388	
2285.0	167.9	5.93	0.823	30.472	18.789	1.629	1.315	7.346	33.07	30.472	5.93	0.823	18.789	1.629	1.315	7.346	33.07	30.472	5.93	0.823	18.789	1.629	1.315	7.346	33.07	30.472	18.789	1.629	1.315	
2752.0	175.4	5.77	0.796	29.015	18.454	1.572	1.283	7.932	33.23	29.015	5.77	0.796	18.454	1.572	1.283	7.932	33.23	29.015	5.77	0.796	18.454	1.572	1.283	7.932	33.23	29.015	18.454	1.572	1.283	
2938.0	181.5	5.69	0.788	28.965	18.661	1.552	1.278	8.174	33.70	28.965	5.69	0.788	18.661	1.552	1.278	8.174	33.70	28.965	5.69	0.788	18.661	1.552	1.278	8.174	33.70	28.965	18.661	1.552	1.278	

Table 3 (concluded)

$$M_0 = 1.538 \quad Re/m = 9.96 \times 10^6$$

CONSTANT PM												MEASURED P				CALCULATED P								
X	DEL	995	RE/M	ME	DEL*	THEIR	H	HERR	HI	DELE	OFF	CF	RE/M	ME	DEL*	THEIR	H	HERR	HI	CF	DELE	THEIR	H	HERR
MM	MM	MM	X10-6	MM	MM	MM	MM	MM	MM	MM	X10-3	X10-3	MM	MM	MM	MM	MM	MM	MM	X10-3	MM	MM	MM	MM
-756.0	38.6	9.92	1.536	5.782	2.437	2.340	1.269	18.215	1.845	4.42	1.867	1.845	9.92	1.536	5.782	2.437	2.340	1.269	18.215	1.845	5.782	2.437	2.340	1.269
-658.0	32.3	9.92	1.544	5.961	2.534	2.353	1.278	18.386	1.777	4.60	1.874	1.777	9.92	1.544	5.961	2.534	2.353	1.278	18.386	1.777	5.961	2.534	2.353	1.278
-562.0	32.3	9.90	1.548	6.285	2.633	2.357	1.269	9.912	1.736	4.75	1.851	1.736	9.90	1.548	6.285	2.633	2.357	1.269	9.912	1.736	6.285	2.633	2.357	1.269
-465.0	33.3	9.91	1.554	6.278	2.664	2.354	1.261	18.146	1.836	4.85	1.924	1.836	9.91	1.554	6.278	2.664	2.354	1.261	18.146	1.836	6.278	2.664	2.354	1.261
-378.0	33.9	9.88	1.542	6.526	2.774	2.353	1.272	9.878	1.755	5.03	1.796	1.755	9.88	1.542	6.526	2.774	2.353	1.272	9.878	1.755	6.526	2.774	2.353	1.272
-319.0	34.8	9.95	1.542	6.730	2.857	2.355	1.274	9.823	1.716	5.18	1.789	1.716	9.95	1.542	6.730	2.857	2.355	1.274	9.823	1.716	6.730	2.857	2.355	1.274
-268.0	35.5	9.96	1.538	6.895	2.932	2.352	1.275	9.757	1.688	5.31	1.778	1.688	9.96	1.538	6.895	2.932	2.352	1.275	9.757	1.688	6.895	2.932	2.352	1.275
-245.0	36.0	9.98	1.525	6.922	2.972	2.329	1.276	9.783	1.785	5.38	1.757	1.785	10.00	1.541	6.933	2.978	2.334	1.278	9.786	1.788	6.958	2.955	2.352	1.274
-219.0	37.1	9.92	1.456	7.192	3.176	2.264	1.307	9.416	1.494	5.69	1.548	1.494	9.99	1.512	7.299	3.196	2.284	1.318	9.324	1.476	7.289	3.205	2.275	1.291
-196.0	35.9	9.87	1.392	7.312	3.318	2.284	1.346	8.617	1.319	5.86	1.286	1.319	10.03	1.522	7.757	3.439	2.256	1.383	8.104	1.278	7.627	3.556	2.145	1.357
-169.0	36.1	9.81	1.288	7.886	3.549	2.222	1.454	7.947	1.066	6.13	0.777	0.866	9.94	1.420	8.277	3.669	2.256	1.486	7.594	0.833	8.159	3.839	2.123	1.449
-147.0	36.9	10.00	1.235	9.939	4.121	2.412	1.666	6.543	0.935	6.95	0.231	0.286	10.23	1.443	10.897	4.540	2.400	1.683	5.728	0.278	10.782	4.706	2.291	1.661
-122.0	38.7	10.42	1.218	13.884	4.878	2.851	1.978	5.896	0.795	6.95	0.000	0.000	10.48	1.272	13.904	4.969	2.833	1.979	5.651	0.000	11.831	5.047	2.740	1.949
-96.0	38.8	10.54	1.186	17.768	5.525	3.216	2.291	5.979	0.890	6.95	0.000	0.000	10.63	1.239	17.747	5.591	3.188	2.287	5.922	0.000	17.678	5.728	3.091	2.263
-73.0	38.3	10.33	1.171	21.917	6.161	3.557	2.576	5.985	0.938	6.98	0.000	0.000	10.37	1.198	21.749	6.241	3.485	2.551	5.857	0.000	21.736	6.277	3.463	2.519
-74.0	64.5	10.28	1.140	29.623	6.545	4.526	3.386	5.329	0.880	6.96	0.000	0.000	10.30	1.155	29.284	6.795	4.338	3.217	5.207	0.000	29.275	6.637	4.411	3.210
25.0	69.6	10.28	1.121	35.965	7.056	5.097	3.873	4.767	0.883	6.98	0.000	0.000	10.17	1.061	35.172	7.593	4.327	3.474	4.539	0.000	35.172	7.595	4.637	3.474
125.0	78.0	10.23	1.090	42.351	8.372	5.859	3.896	4.258	0.880	6.96	0.000	0.000	10.15	1.047	42.338	8.378	5.858	3.879	4.261	0.000	42.338	8.378	5.858	3.879
223.0	81.8	10.17	1.063	41.932	10.464	4.007	3.884	3.810	0.880	6.96	0.000	0.000	10.18	1.031	41.933	10.462	4.000	3.878	3.811	0.000	41.933	10.462	4.008	3.878
278.0	84.5	10.19	1.050	41.284	10.081	3.822	2.951	4.001	0.880	6.96	0.000	0.000	10.14	1.028	41.284	10.080	3.823	2.948	4.001	0.000	41.284	10.080	3.823	2.948
293.0	85.3	10.16	1.044	40.763	11.231	3.638	2.881	3.966	0.880	6.96	0.000	0.000	10.11	1.024	40.762	11.230	3.638	2.798	3.966	0.000	40.762	11.230	3.638	2.798
321.0	87.8	10.16	1.035	40.989	11.365	3.687	2.794	4.119	0.880	6.96	0.000	0.000	10.13	1.019	40.980	11.364	3.687	2.792	4.119	0.000	40.980	11.364	3.687	2.792
415.0	92.4	10.08	1.012	39.794	12.412	3.266	2.498	4.238	0.880	6.96	0.193	0.175	10.05	1.003	39.794	12.413	3.266	2.491	4.238	0.176	39.794	12.413	3.266	2.491
514.0	95.5	10.13	0.988	37.921	13.172	2.879	2.245	4.371	0.880	6.96	0.245	0.233	10.12	0.986	37.920	13.172	2.879	2.245	4.371	0.233	37.920	13.172	2.879	2.245
612.0	99.1	9.97	0.969	36.716	14.142	2.596	2.028	4.411	0.880	6.96	0.376	0.401	9.97	0.969	36.716	14.142	2.596	2.028	4.411	0.401	36.716	14.142	2.596	2.028
710.0	103.7	9.93	0.953	34.866	14.531	2.396	1.874	4.731	0.880	6.96	0.618	0.490	9.93	0.953	34.866	14.531	2.396	1.874	4.731	0.490	34.866	14.531	2.396	1.874
888.0	107.5	9.94	0.937	33.757	14.995	2.251	1.766	4.918	0.880	6.96	0.661	0.641	9.94	0.937	33.757	14.995	2.251	1.766	4.918	0.641	33.757	14.995	2.251	1.766
986.0	111.0	9.76	0.919	32.698	15.282	2.140	1.686	5.124	0.880	6.96	0.703	0.719	9.76	0.919	32.697	15.282	2.140	1.686	5.124	0.719	32.697	15.282	2.140	1.686
1084.0	114.6	9.70	0.906	31.437	15.398	2.042	1.613	5.401	0.880	6.96	0.865	0.866	9.70	0.906	31.437	15.398	2.042	1.613	5.401	0.866	31.437	15.398	2.042	1.613
1146.0	120.9	9.48	0.892	30.923	16.077	1.923	1.522	5.597	0.880	6.96	1.047	1.102	9.48	0.892	30.923	16.077	1.923	1.522	5.597	1.102	30.923	16.077	1.923	1.522
1248.0	123.4	9.39	0.885	29.533	15.867	1.861	1.474	5.916	0.880	6.96	1.241	1.218	9.39	0.885	29.533	15.867	1.861	1.474	5.916	1.218	29.533	15.867	1.861	1.474
154.0	134.4	9.39	0.859	29.489	16.837	1.751	1.384	6.231	0.880	6.96	1.461	1.384	9.39	0.859	29.489	16.837	1.751	1.384	6.231	1.384	29.489	16.837	1.751	1.384
1925.0	146.1	9.26	0.836	29.044	17.372	1.672	1.344	6.738	0.880	6.96	1.614	1.449	9.26	0.836	29.044	17.372	1.672	1.344	6.738	1.449	29.044	17.372	1.672	1.344
2317.0	154.6	9.13	0.817	28.010	17.478	1.683	1.297	7.246	0.880	6.96	1.783	1.621	9.13	0.817	28.010	17.478	1.683	1.297	7.246	1.621	28.010	17.478	1.683	1.297
2788.0	162.8	8.62	0.792	26.789	17.214	1.556	1.271	7.981	0.880	6.96	1.984	1.824	8.62	0.792	26.789	17.214	1.556	1.271	7.981	1.824	26.789	17.214	1.556	1.271
2984.0	161.4	8.30	0.781	25.523	16.653	1.533	1.257	8.159	0.880	6.96	1.944	1.776	8.30	0.781	25.523	16.653	1.533	1.257	8.159	1.776	25.523	16.653	1.533	1.257

LIST OF SYMBOLS

(Bracketed symbols represent computer headings)

A,B		'law of the wall' constants in equation (28)
C_f	(CF)	local skin friction coefficient obtained from East's prediction of the law of the wall; see equation (6)
C_{fp}	(CFP)	local skin friction coefficient based on Patel's Preston tube calibration as formulated by Head and Vasanta Ram; see section 3.3
C_p		pressure coefficient based on local conditions
d		probe diameter
D		constant in equation (6)
E_f		equilibrium factor in equation (36)
E_p		equilibrium factor in equation (37)
F		compressibility factor in equation (6)
G		Clauser shape parameter in equation (32)
h		distance of probe centre line above wall
H	(H)	boundary layer shape parameter in equations (9) and (13)
\bar{H}	(HBAR)	boundary layer shape parameter in equations (10), (14) and (20)
H_l	(HI)	boundary layer shape parameter $\frac{\delta_{0.995} - \delta^*}{\theta}$
J,K		normalised 'law of the wake' constants in equation (41)
l		effective turbulent run ahead of normal part of shock wave
M	(M)	Mach number
	(ME)	Mach number at edge of boundary layer
p	(P)	static pressure
	(PI)	equivalent inviscid static pressure
p_{t0}	(PTO)	tunnel total pressure
p_{t1}		local total pressure
Re	(RE)	unit Reynolds number; see equation (3)
T		temperature in Kelvins
	(TO)	total temperature in Kelvins
U		horizontal component of velocity
	(UE)	horizontal component of velocity at edge of boundary layer
ΔU		wake component of velocity profile
U_τ		friction velocity

LIST OF SYMBOLS (concluded)

U_{τ}^i		equivalent incompressible friction velocity; see equation (26)
V		vertical component of velocity
X		streamwise position relative to the normal part of the main shock wave
y	(Y)	equivalent height above wall; see equations (1) and (2)
y^*		non-dimensionalised y with respect to wall parameters in equation (6)
Z		distance perpendicular to flow but parallel to surface
δ		boundary layer thickness
$\delta_{0.995}$	(DEL995)	boundary layer thickness at $U/U_{\delta} = 0.995$
$\delta_{0.999}$		boundary layer thickness at $U/U_{\delta} = 0.999$
δ_E	(DELE)	boundary layer energy thickness; see equation (15)
$\bar{\delta}$	(DELBAR)	boundary layer thickness parameters; see equation (7)
δ^*	(DEL*)	boundary layer displacement thickness; see equations (11) and (18)
θ	(THETA)	boundary layer momentum thickness; see equations (12) and (13)
$\bar{\theta}$	(THETABAR)	boundary layer thickness parameter; see equation (8)
κ		mixing length constant in equation (27)
κ_s		surface curvature
μ		viscosity of fluid
ν		kinematic viscosity of fluid
Π		pressure gradient parameter for equilibrium flows; see equation (9)
ρ		density

Subscripts

i	equivalent inviscid flow quantities
I	inner static pressure probe
m	measured quantities
N	normalised quantities
O	free-stream conditions before start of interaction
P	intermediate equivalent inviscid flow quantities
U	outer static pressure probe
w	wall conditions
A, B, C	regions in Fig 28a&b
s	edge of boundary layer conditions

Superscript

i	equivalent incompressible flow quantities
-----	---

AD-A132 033

A STUDY OF NORMAL SHOCK-WAVE TURBULENT BOUNDARY-LAYER
INTERACTIONS AT MAC=0.10 ROYAL AIRCRAFT ESTABLISHMENT
FARNBOROUGH (ENGLAND) W G SAWYER ET AL. OCT 82
RAE-TR-82099 DRIC-BR-88360

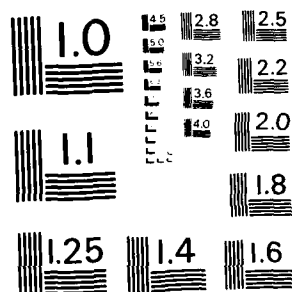
2/2

UNCLASSIFIED

F/G 20/4

NL

END
DATE
FILED
9 83
DTIC



MICROCOPY RESOLUTION TEST CHART
NATIONAL BUREAU OF STANDARDS - 1963 - A

REFERENCES

<u>No.</u>	<u>Author</u>	<u>Title, etc</u>
1	J.B. Abbiss L.F. East C.R. Nash P. Parker E.R. Pyke W.G. Sawyer	A study of the interaction of a normal shock wave and a turbulent boundary layer using a laser anemometer. RAE Technical Report 75141 (1976)
2	W.G. Sawyer L.F. East C.R. Nash	A preliminary study of normal shock-wave turbulent boundary-layer interactions. RAE Technical Memorandum Aero 1714 (1977)
3	L.F. East	The application of a laser anemometer to the investigation of shock-wave boundary-layer interactions. AGARD CPP 193 (1976); Also RAE Technical Memorandum Aero 1666 (1976)
4	J.B. Abbiss H.S. Dhadwal P.R. Sharpe M.P. Wright	Laser anemometry studies of a separated turbulent boundary layer in supersonic flow using a ten-nanosecond data acquisition system. 9th International Congress in Instrumentation in Aerospace Simulation Facilities (1981)
5	J. Seddon	The flow produced by interaction of a turbulent boundary layer with a normal shock wave of strength sufficient to cause separation. ARC R&M 3502 (1967)
6	R.J. Vidal C.E. Whittliff P.A. Catlin B.H. Sheen	Reynolds number effects on the shock wave turbulent boundary layer interaction at transonic speeds. AIAA Paper 73-661 (1973)
7	J.W. Kooi	Experiment on transonic shock-wave boundary-layer interaction. AGARD CPP 168 (1975)
8	J. Delery	Recherches sur l'interaction onde de choc-couche limite turbulente. Onera TP 1976-135 (1976)
9	C.F. Lo F.L. Heltsley M.C. Alstatt	A study of laser velocimeter measurements in a viscous transonic flow. AIAA Paper 76-333 (1976)
10	H. Sobieczky E. Stanewsky	The design of transonic aerofoils under consideration of shock wave boundary layer interaction. ICAS Paper 76-14 (1976)
11	K.P. Burdges	Experimental measurements of shock wave boundary layer interaction on a supercritical airfoil. AIAA Paper 79-1499 (1979)

REFERENCES (continued)

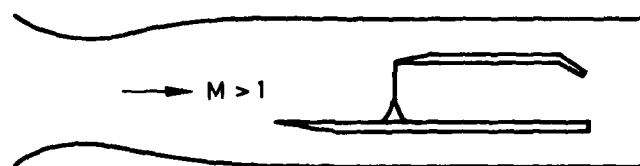
<u>No.</u>	<u>Author</u>	<u>Title, etc</u>
12	G.E. Gadd	Interactions between normal shock waves and turbulent boundary layers. ARC R&M 3262 (1961)
13	G.G. Mateer A. Brosch J.R. Viegas	A normal shock wave turbulent boundary layer interaction at transonic speeds. AIAA Paper 76-161 (1976)
14	E.P. Sutton	The development of slotted working-section liners for transonic operation of the RAE Bedford 3ft wind tunnel. ARC R&M 3085 (1955)
15	L.F. East	A representation of second-order boundary layer effects in the momentum integral equation and in viscous-inviscid interactions. RAE Technical Report 81002 (1981)
16	L.F. East	A prediction of the law of the wall in compressible three-dimensional turbulent boundary layers. RAE Technical Report 72178 (1972)
17	D.E. Coles	The turbulent boundary layer in a compressible fluid. Project Rand Report R-403-PR (1962)
18	Editors: D.E. Coles E.A. Hirst	Proceedings, Computation of turbulent boundary-layers. Vol.II. AFOSR-IFP Stanford Conference (1968)
19	D.F. Myring	The effects of normal pressure gradients on the boundary layer momentum integral equation. RAE Technical Report 68214 (1968)
20	P.H. Cook M.A. McDonald M.C.P. Firmin	Aerofoil RAE 2822 - pressure distributions and boundary layer and wake measurements. AGARD AR-138, Paper A6; Also RAE Technical Memorandum Aero 1725 (1979)
21	V.C. Patel	Calibration of the Preston tube and limitations on its use in pressure gradients. J. Fluid Mechanics, Vol.23, 1, pp.185-208 (1965)
22	M.R. Head V. Vasanta Ram	Improved presentation of Preston tube calibration. India Indian Inst. Tech., Kampur, Department of Aero Engineering, AE-10/1970. Also Aeronaut. Q. XXII, Vol.3 (1971)
23	F.W. Fenter C.J. Stalmach	The measurement of local turbulent skin friction at supersonic speeds by means of surface impact-pressure probes. J. Aero/Sp Sci. Vol.25, 12, pp.793-794 (1958)

REFERENCES (concluded)

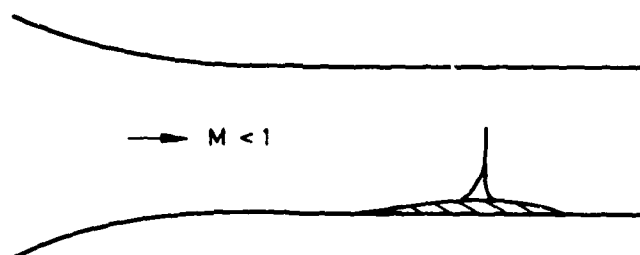
<u>No.</u>	<u>Author</u>	<u>Title, etc</u>
24	J.E. Green D.J. Weeks J.W.F. Brooman	Prediction of turbulent boundary layers and wakes in compressible flow by a lag-entrainment method. ARC R&M 3791 (1973)
25	K.G. Winter L. Gaudet	Turbulent boundary-layer studies at high Reynolds number at Mach numbers between 0.2 and 2.8. ARC R&M 3712 (1970)
26	E.R. van Driest	Turbulent boundary layer in compressible fluids. J. Aeronautical Sci., Vol.18, 3, pp.145-160 & 216 (1951)
27	L.F. East P.D. Smith P.J. Merryman	Prediction of the development of separated turbulent boundary layers by the lag-entrainment method. RAE Technical Report 77046 (1977)
28	L.F. East W.G. Sawyer C.R. Nash	An investigation of the structure of equilibrium turbulent boundary layers. RAE Technical Report 79040 (1979)
29	T.D. Reed T.C. Pope J.M. Cooksey	Calibration of transonic and supersonic wind tunnels. NASA Contractor Report 2920 (1977)

Reports quoted are not necessarily available to members of the public or commercial organisations.

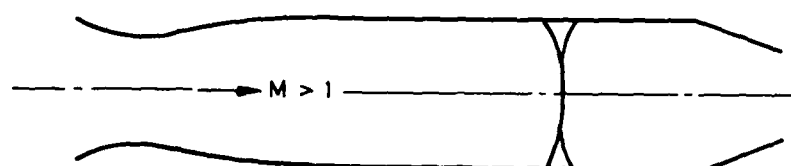
Fig 1a-c



a) Flat plate with shock-wave generator and downstream choking flap



b) Transonic bump



c) Conical shock in circular section

Fig 1a-c Three techniques for producing a normal shock-wave boundary-layer interaction

Fig 2

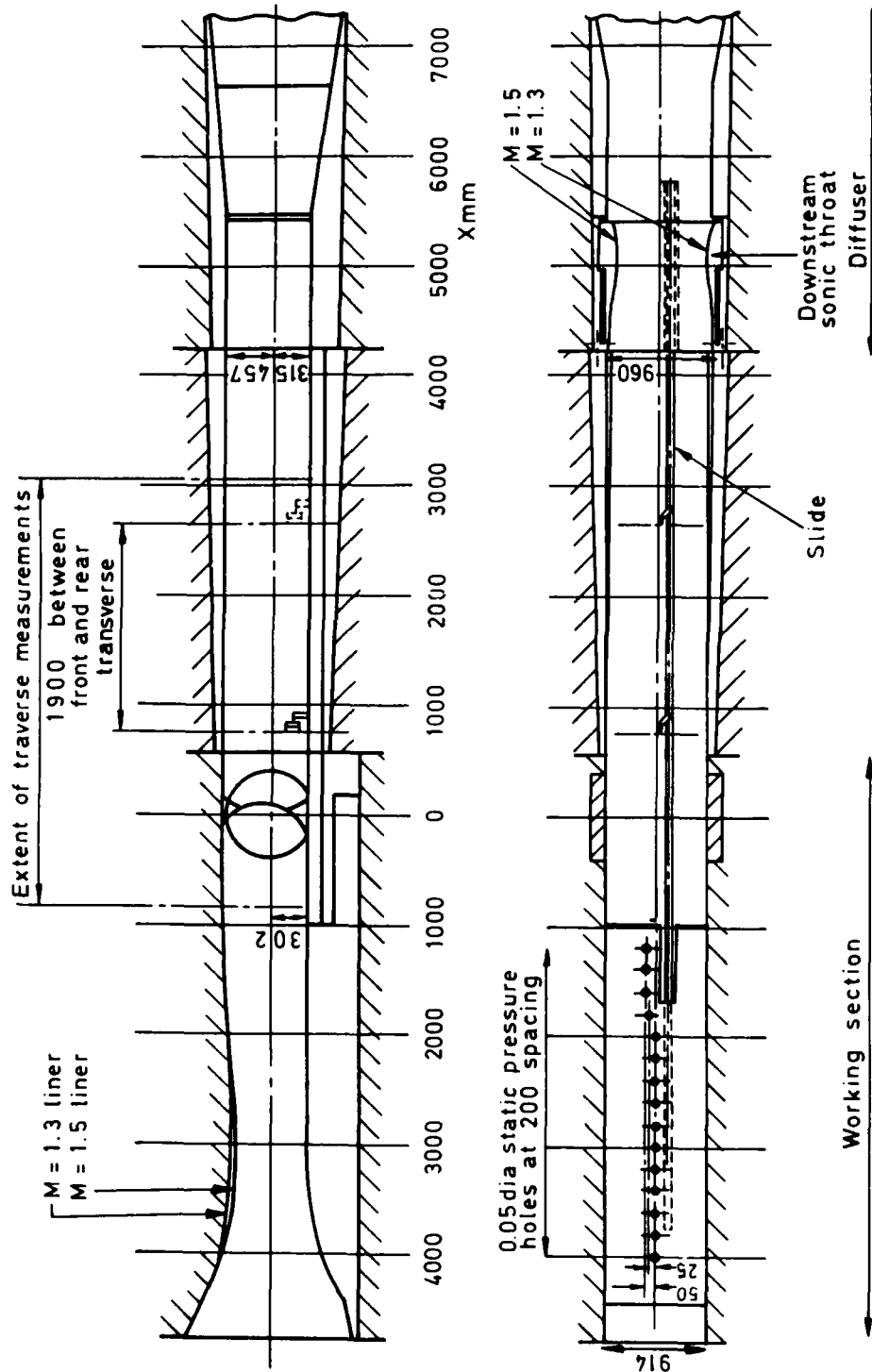


Fig 2 Experimental arrangement in the 3 ft x 3 ft wind tunnel

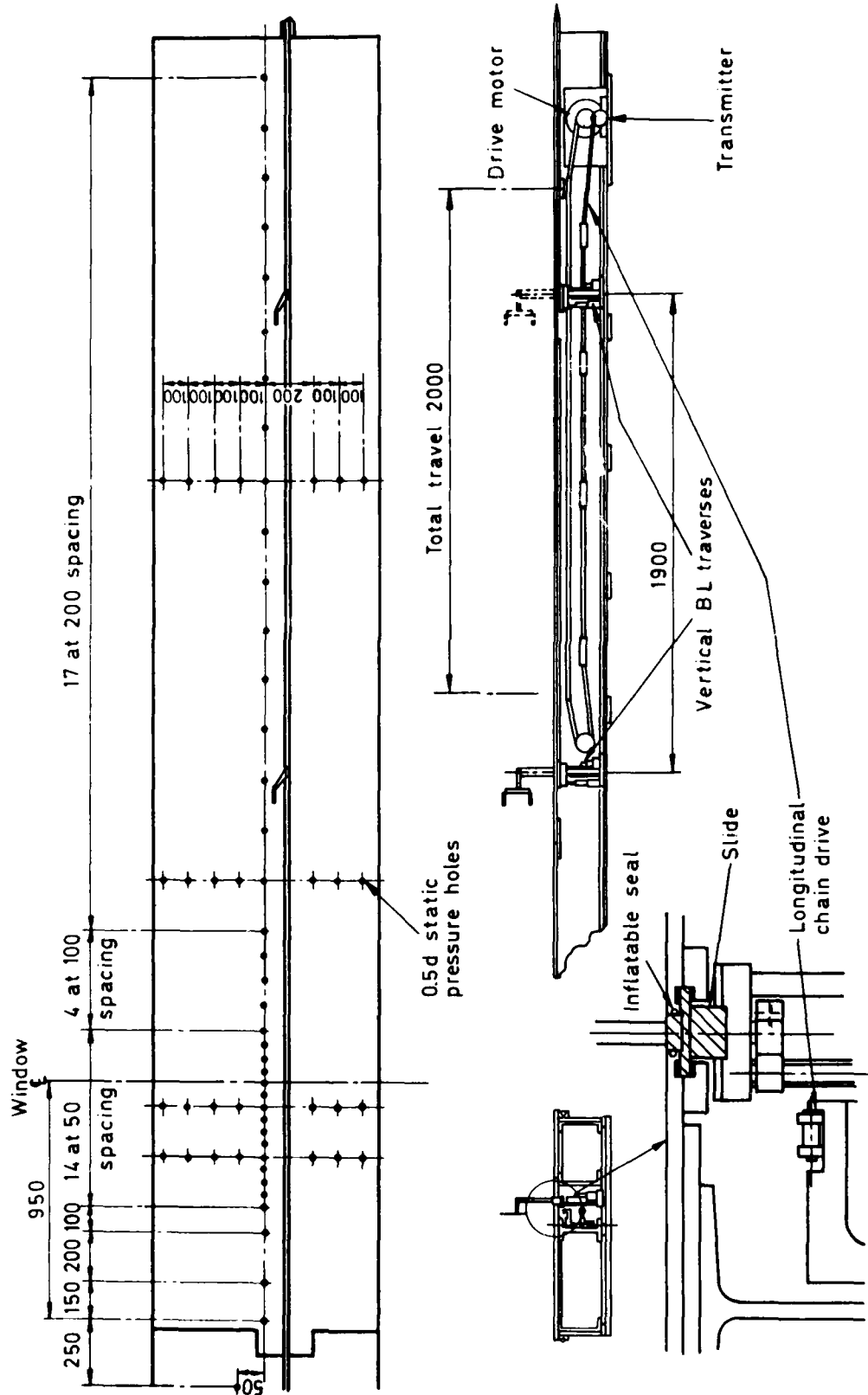


Fig 3 False floor and horizontal traverse mechanism

Fig 3

Fig 4

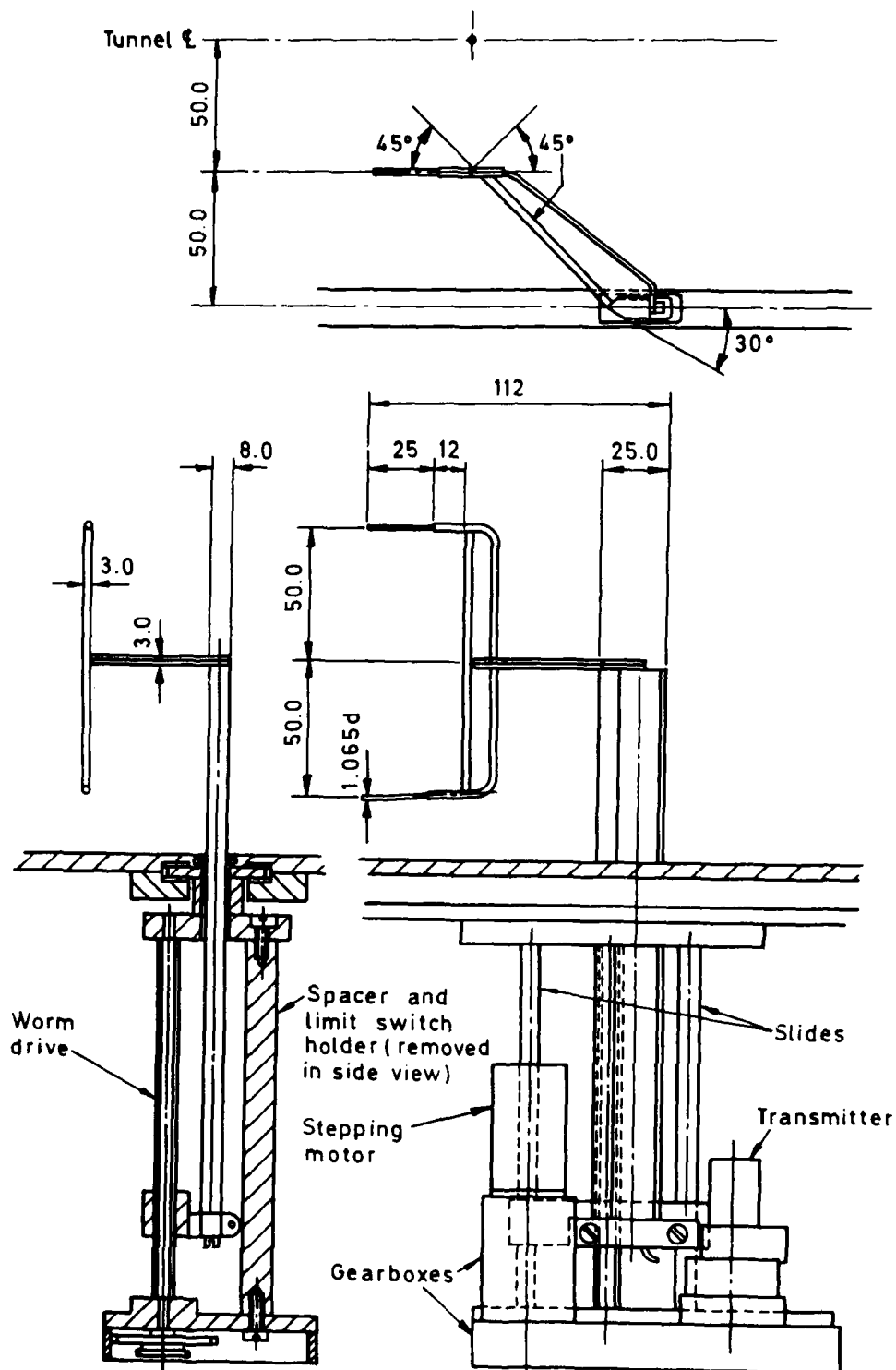


Fig 4 Pitot traverse mechanism and twin pitot probe

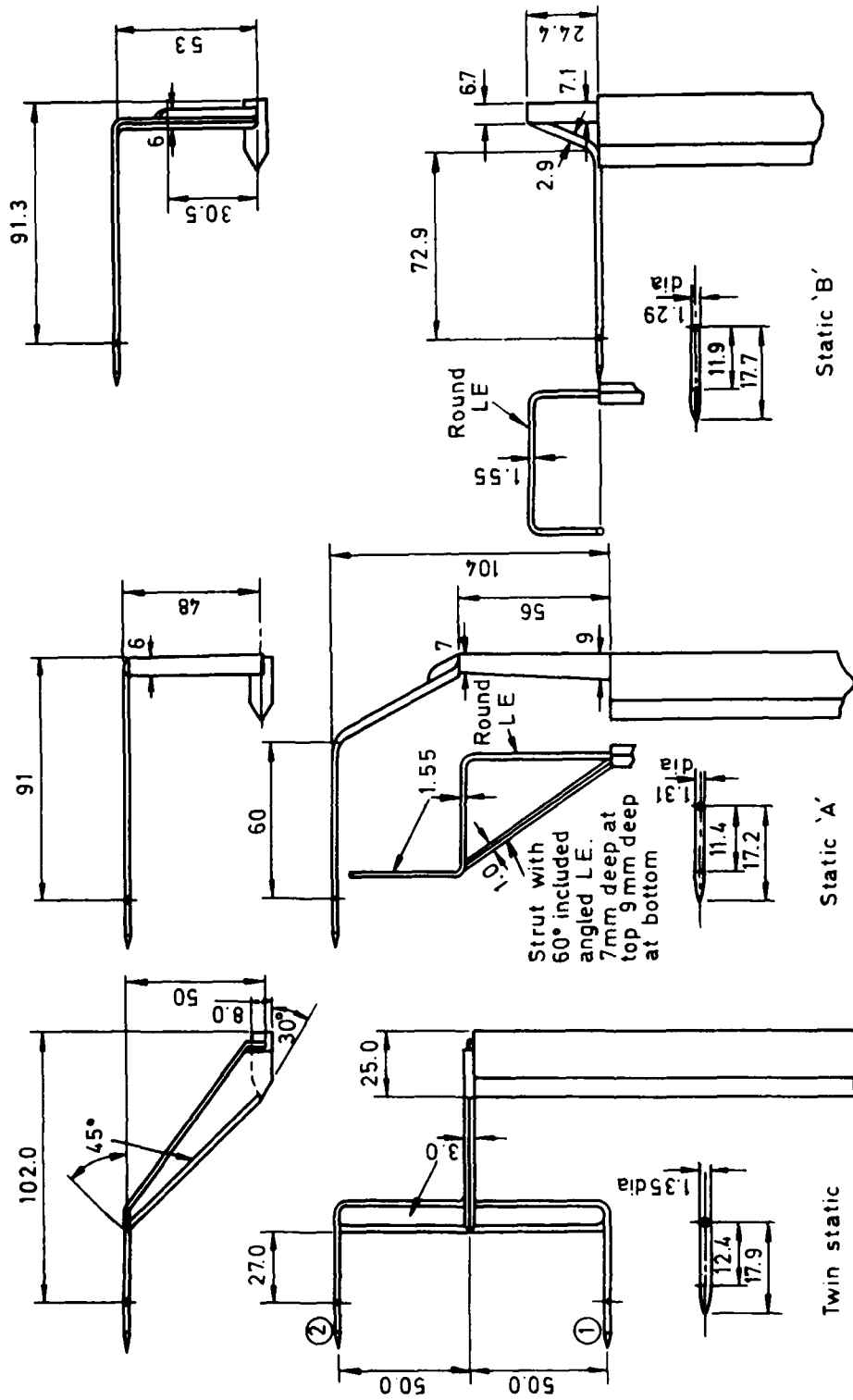


Fig 5 Details of static probes

Fig 6a

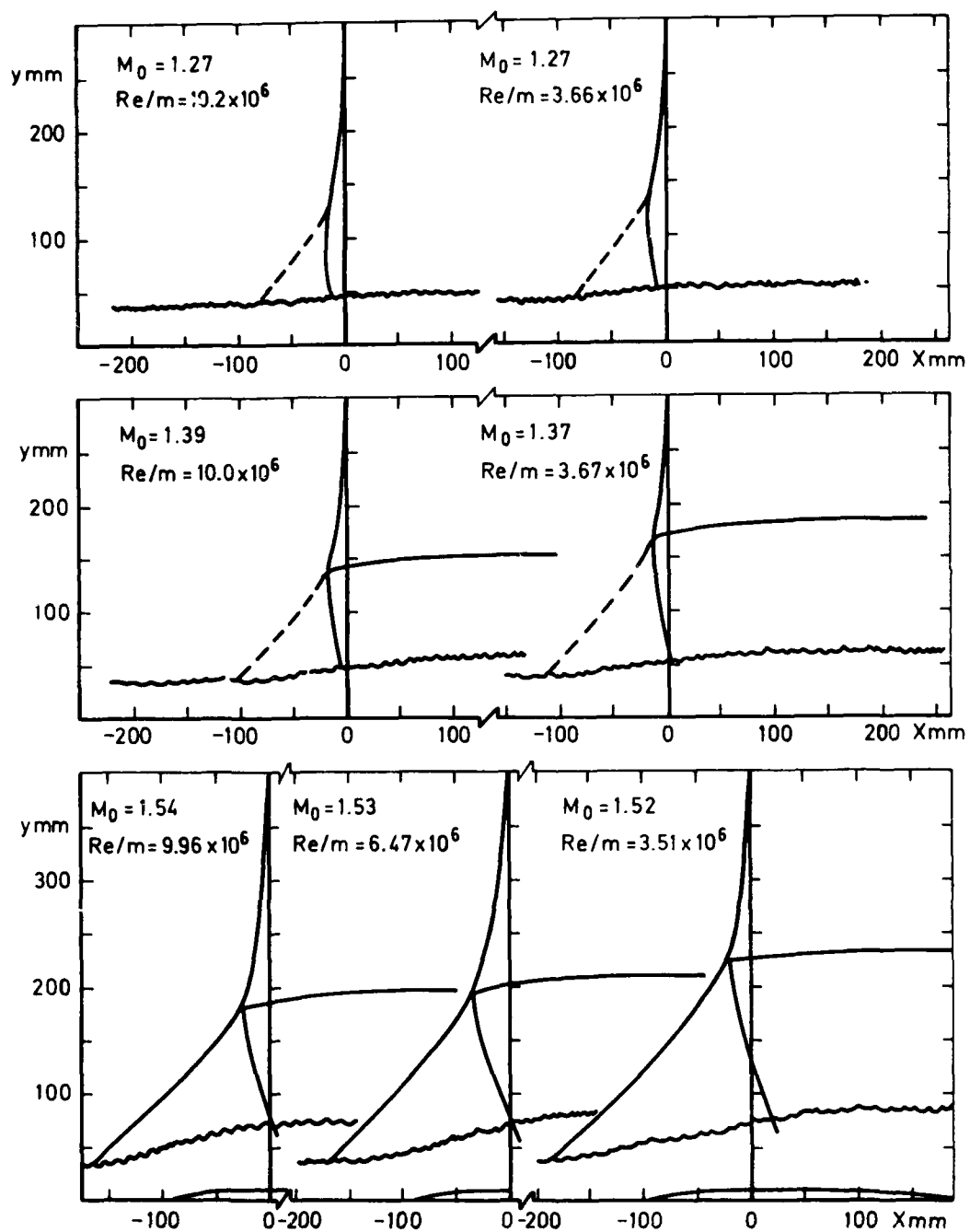
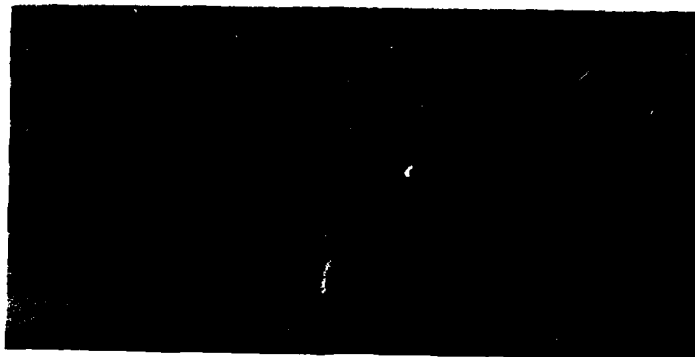


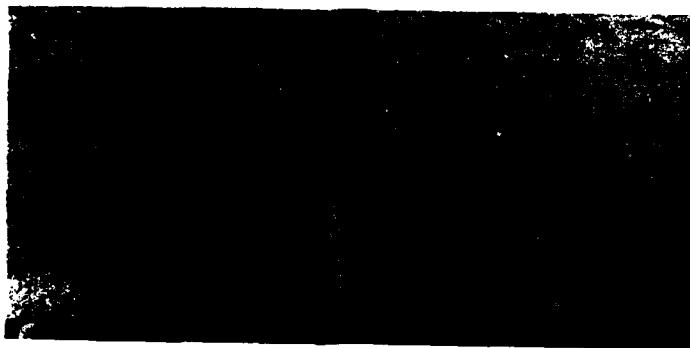
Fig 6a Normal shock-wave boundary-layer interactions

Fig 6b

$M_0 = 1.27$
 $Re/m = 10.2 \times 10^6$



$M_0 = 1.39$
 $Re/m = 10.0 \times 10^6$



$M_0 = 1.54$
 $Re/m = 9.96 \times 10^6$

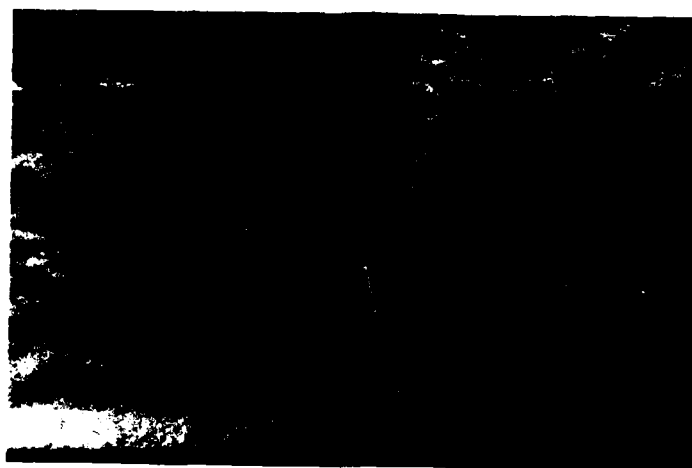


Fig 6b Schlieren photographs of normal shockwave boundary-layer interaction

Fig 7



$M = 1.5$



$M = 1.4$



$M = 1.3$

Fig 7 Oil flow under interaction regions



Fig 8 Oil flow under interaction region at $M = 1.5$

Fig 9

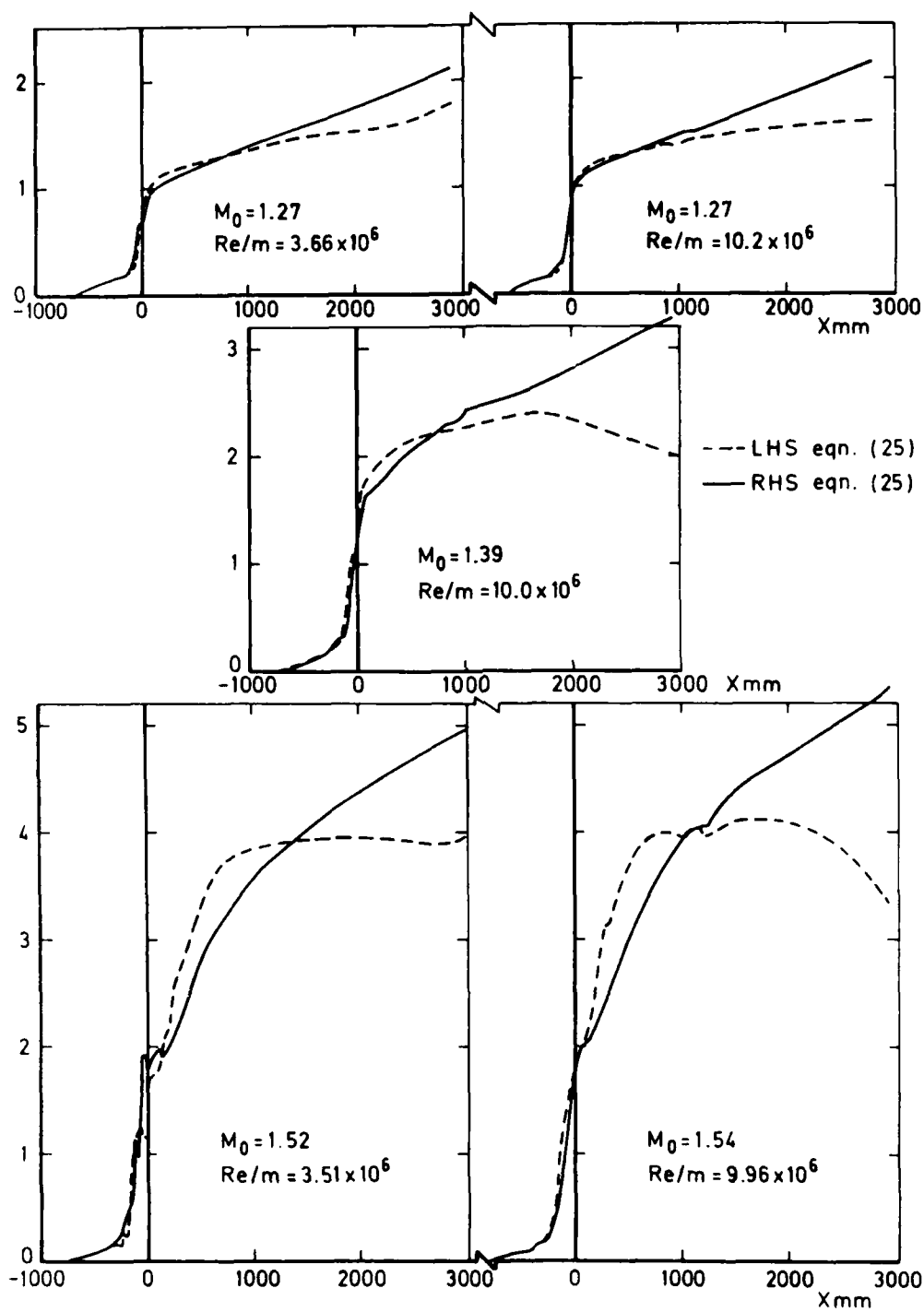


Fig 9 Momentum balance based on measured p + calculated p_i for $X < 0$

Fig 10a

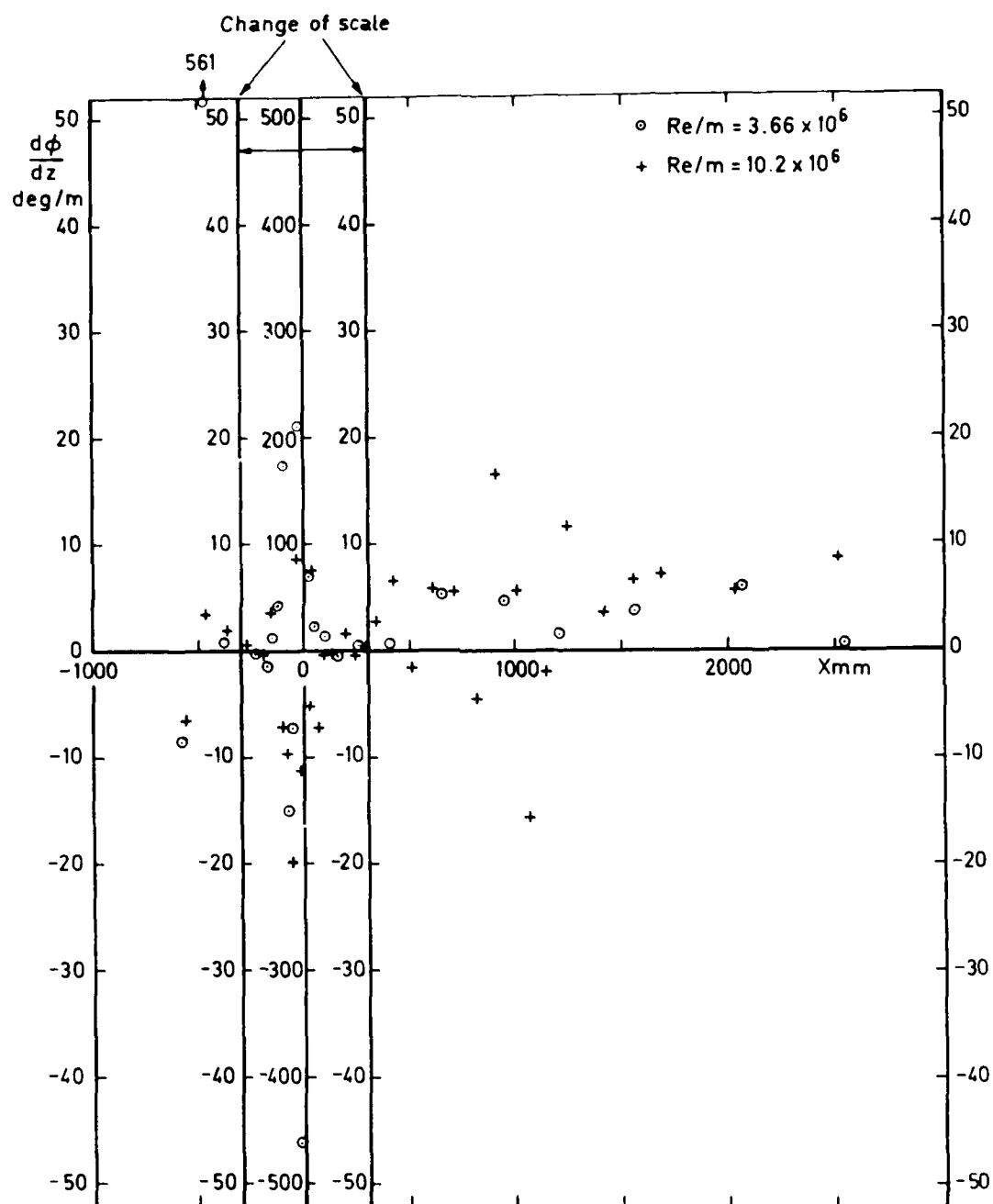


Fig 10a Flow divergence needed to balance momentum integral equation, $M = 1.3$

Fig 10b

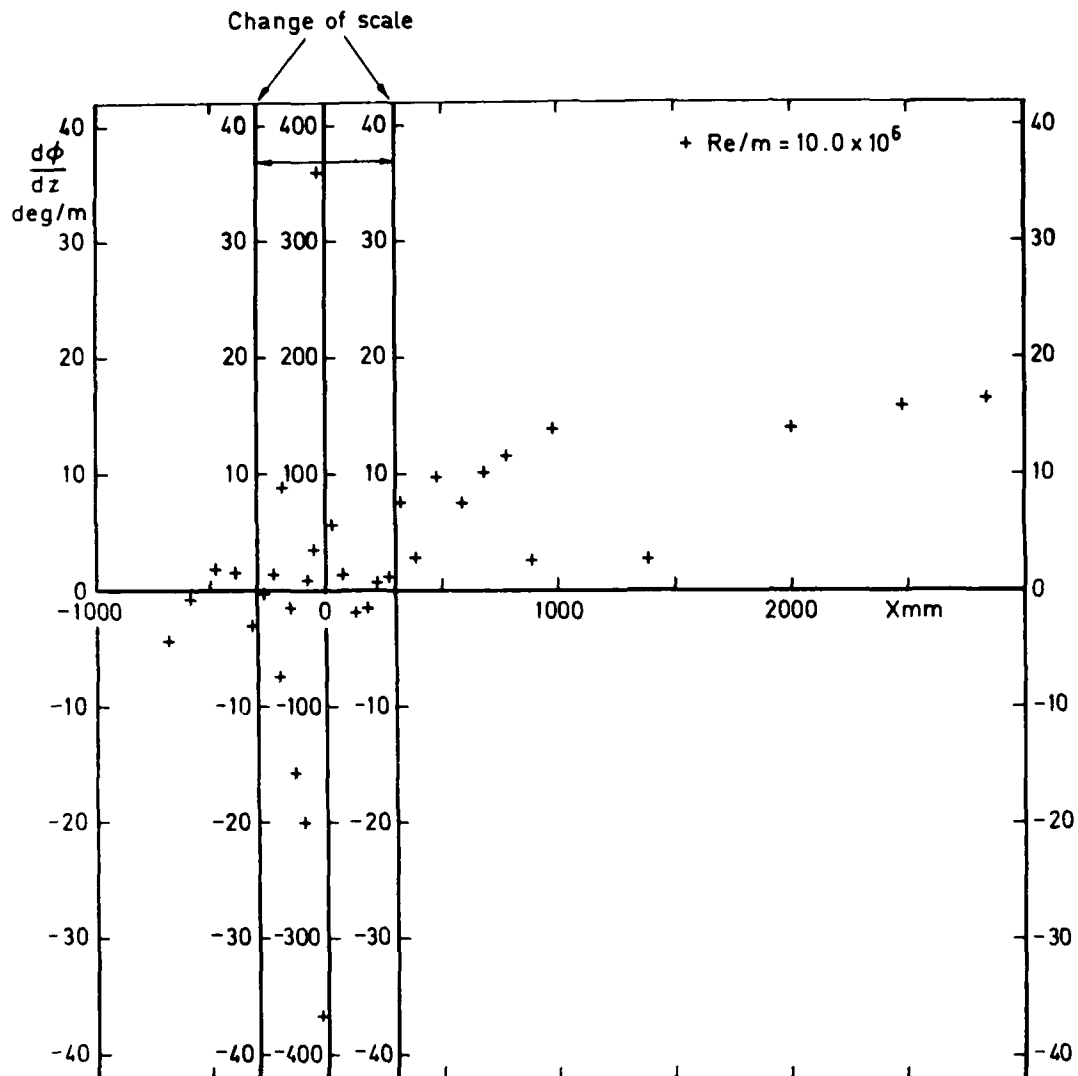


Fig 10b Flow divergence needed to balance momentum integral equation, $M = 1.4$

Fig 10c

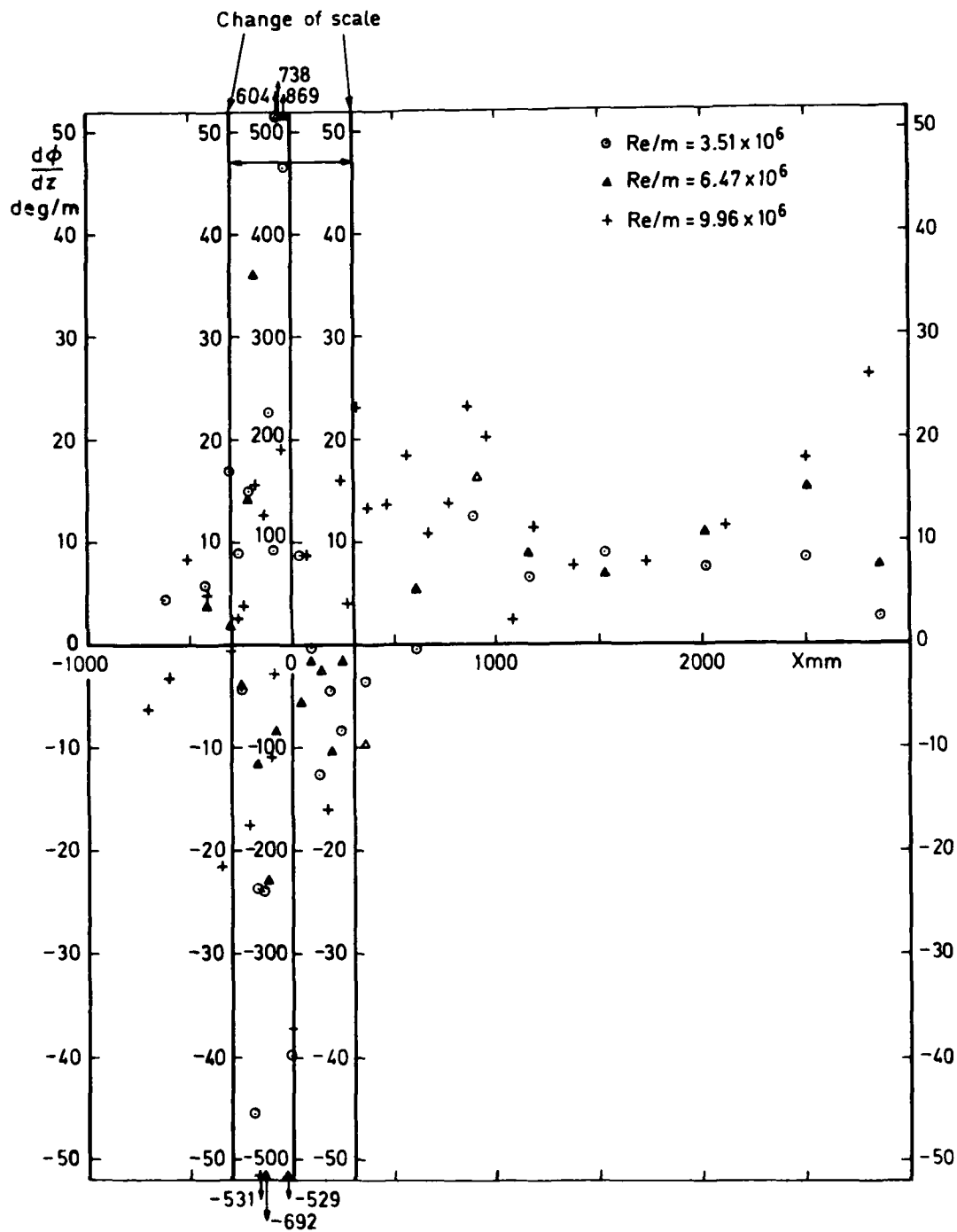
Fig 10c Flow divergence needed to balance momentum integral equation, $M = 1.5$

Fig 11

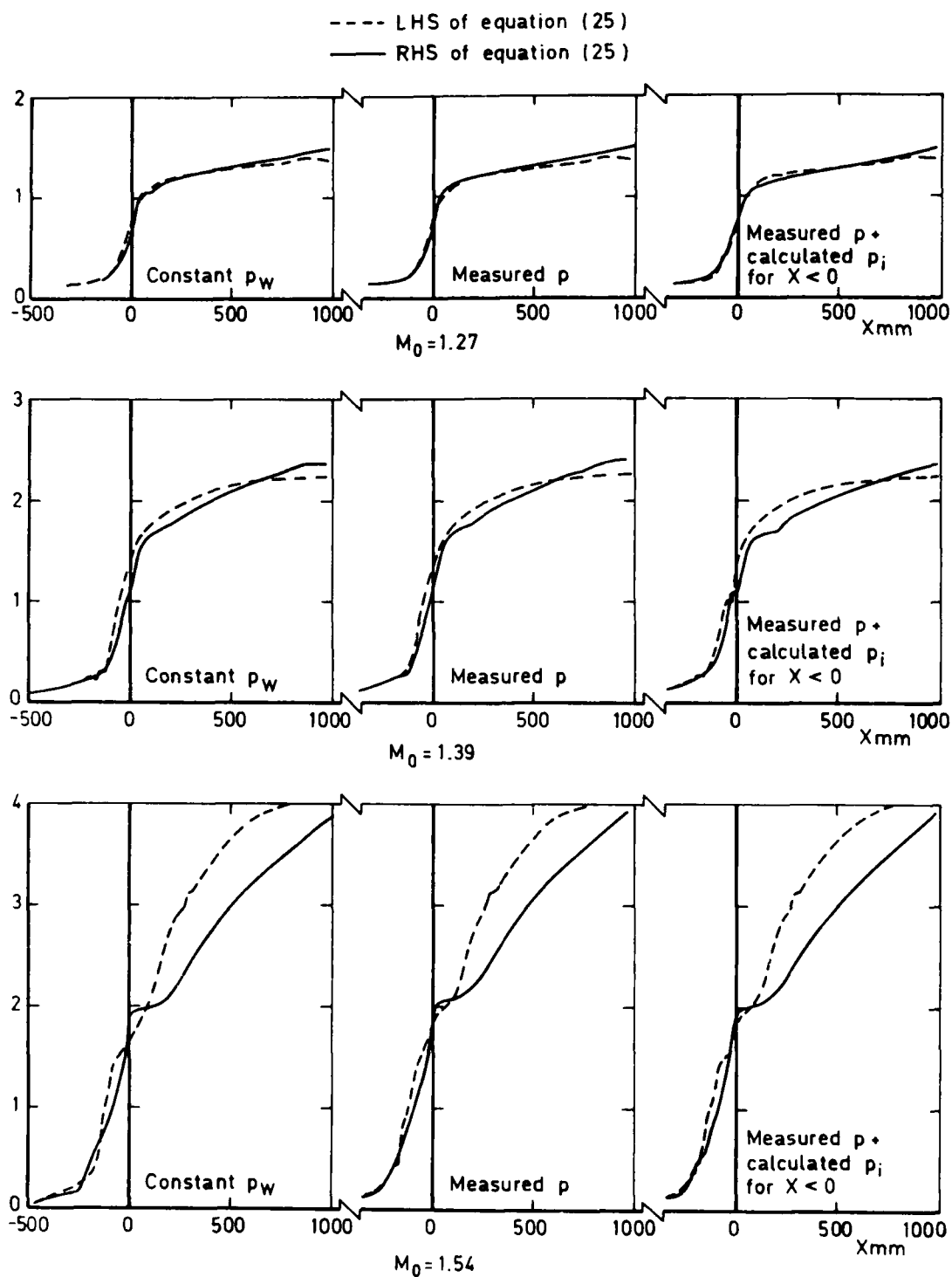


Fig 11 Comparison of momentum balance calculations at $Re/m = 10 \times 10^6$

Fig 12

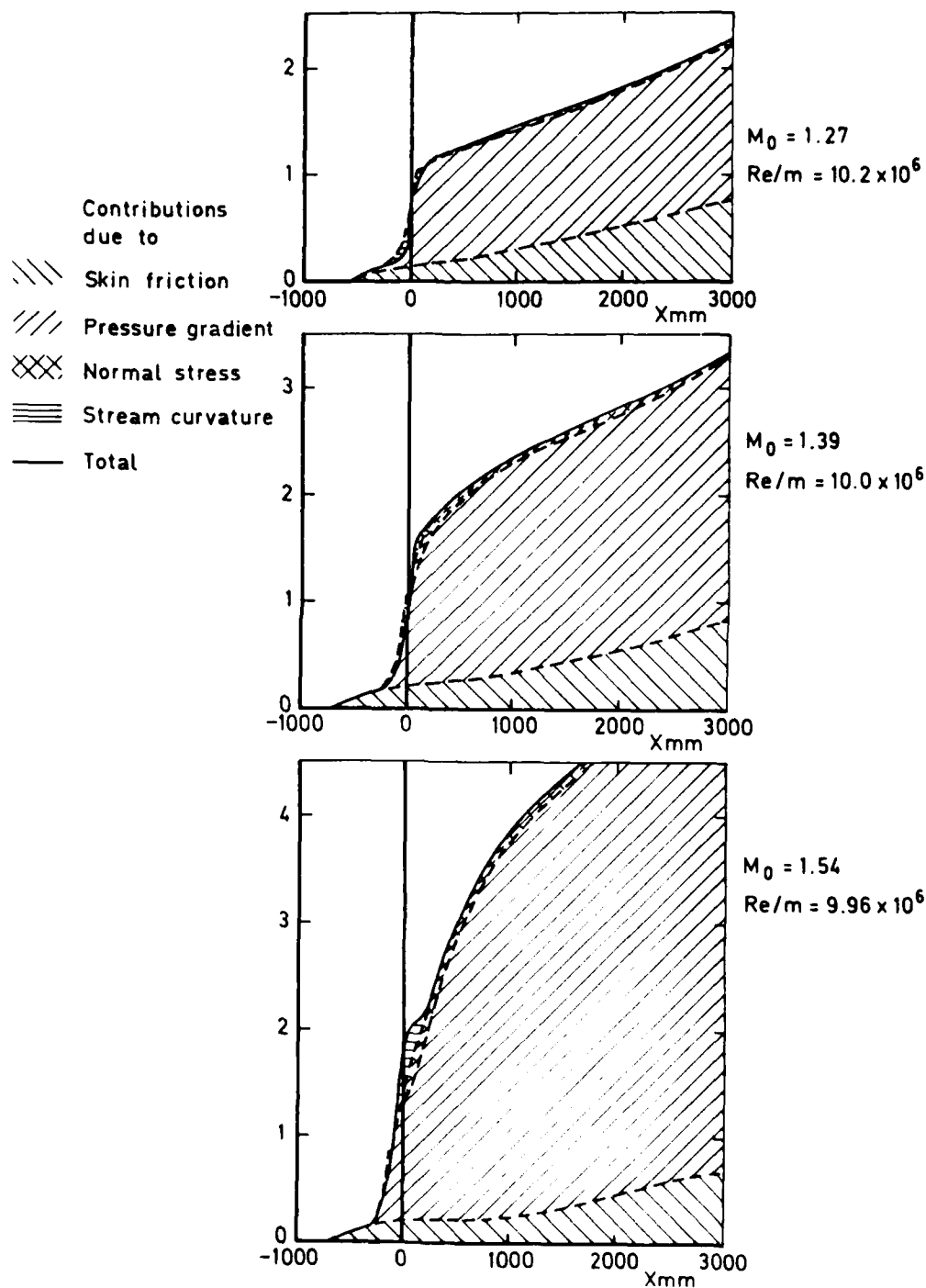


Fig 12 Composition of right hand side of momentum integral equation (measured p + calculated p_i)

Fig 13a

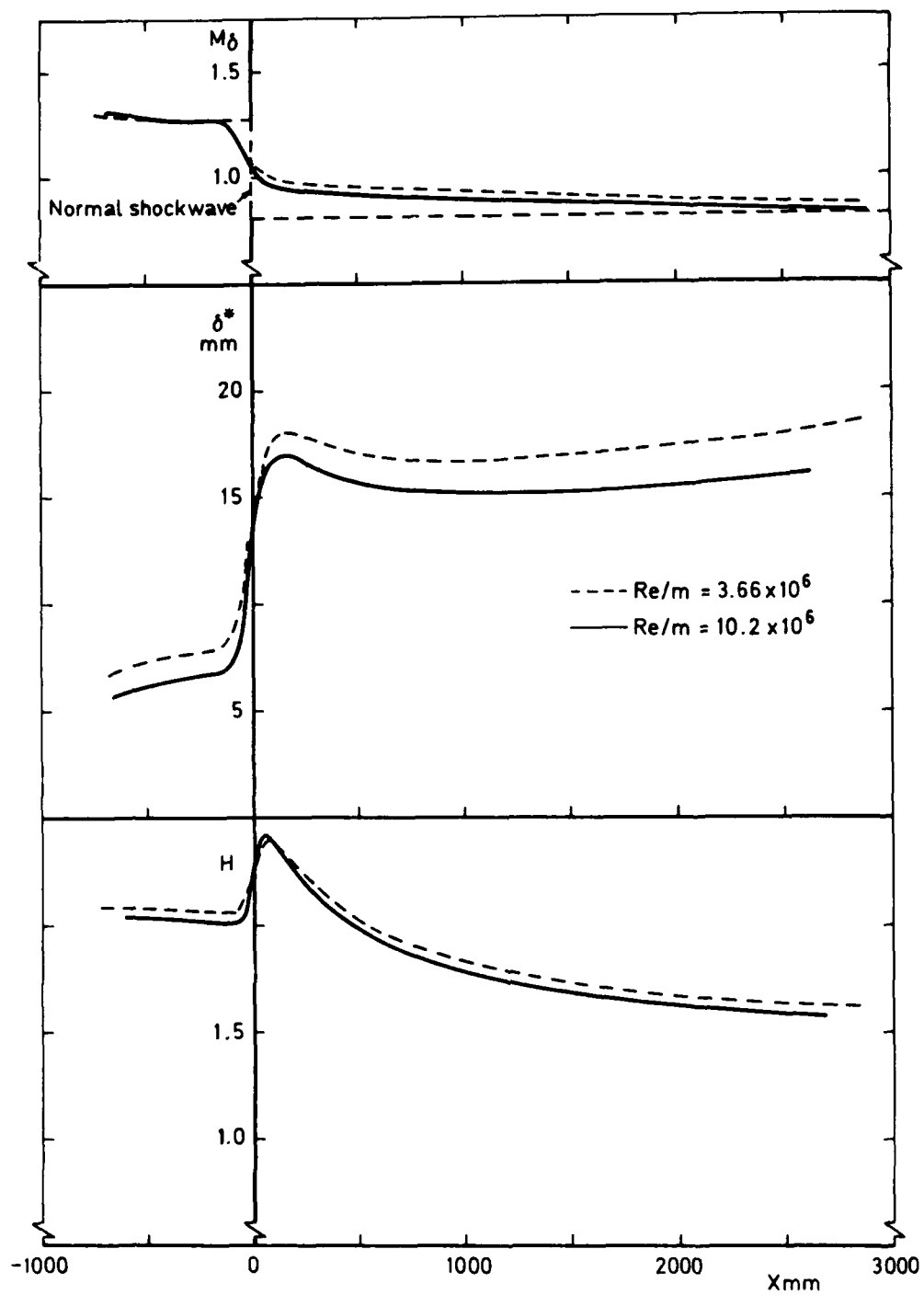


Fig 13a Boundary layer development ($p = p_w$) $M = 1.3$

Fig 13a (concl'd)

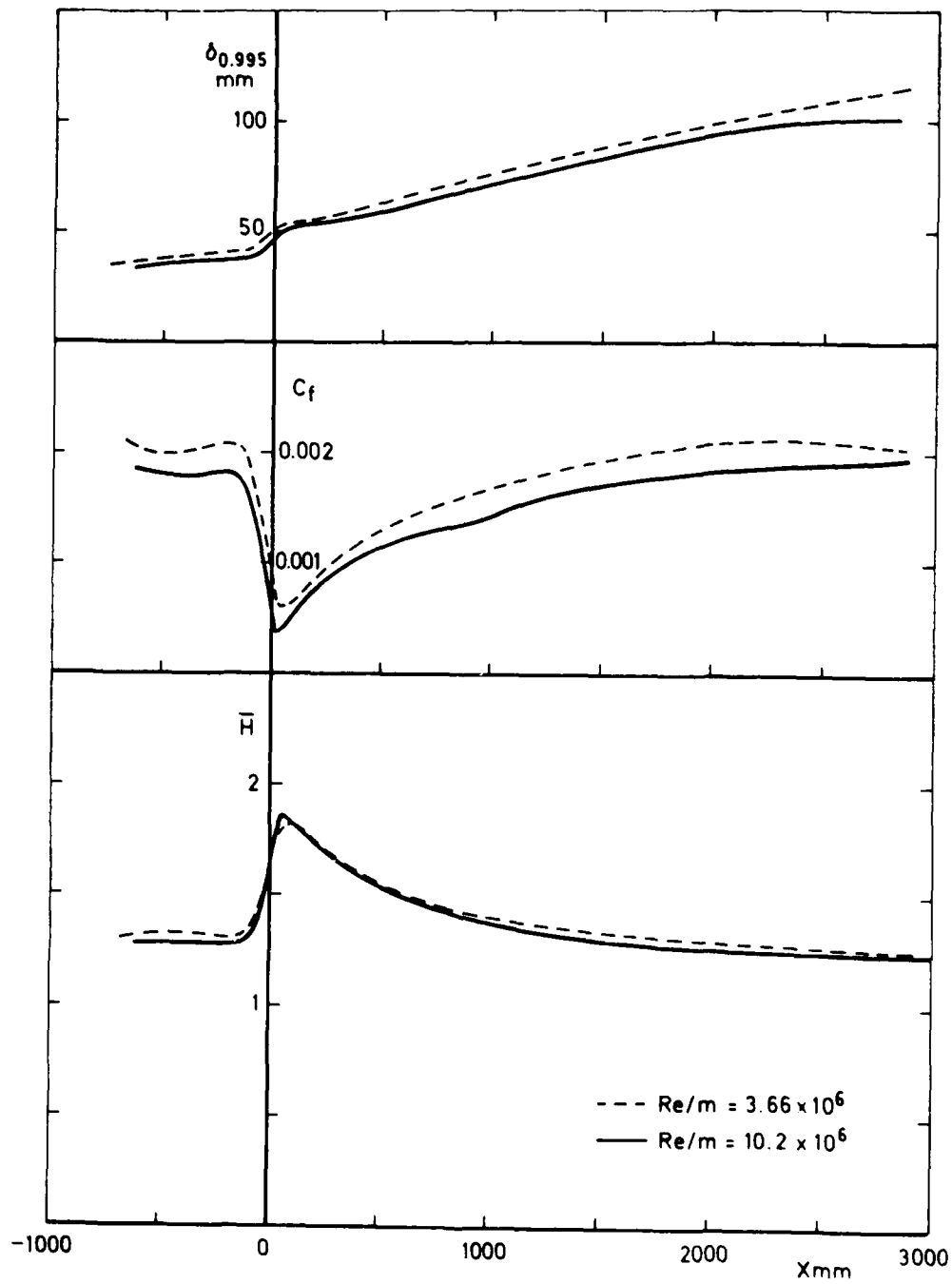


Fig 13a (concl'd) Boundary layer development ($p = p_w$) $M = 1.3$

Fig 13b

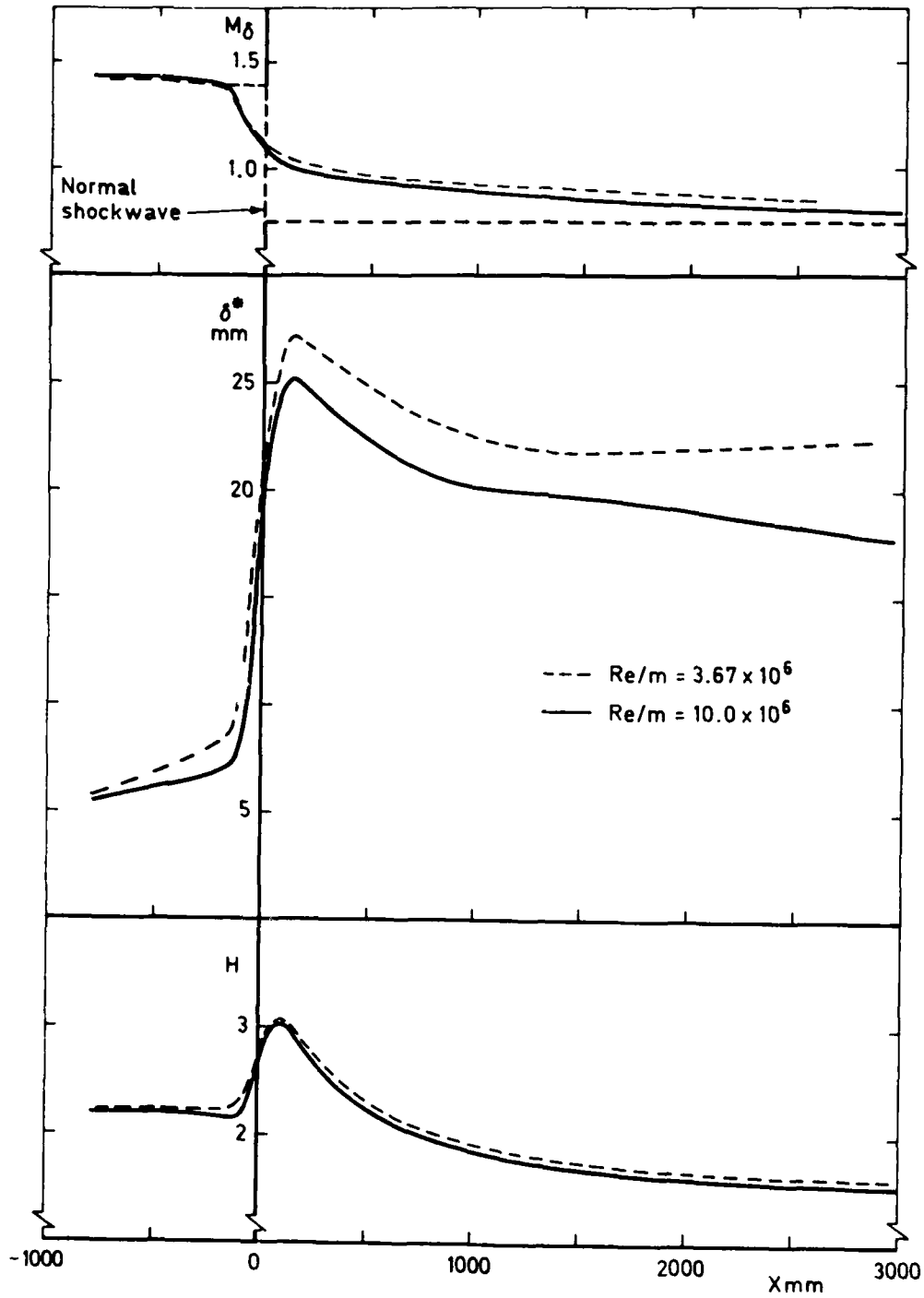


Fig 13b Boundary layer development ($p = p_w$) $M = 1.4$

Fig 13b (concl'd)

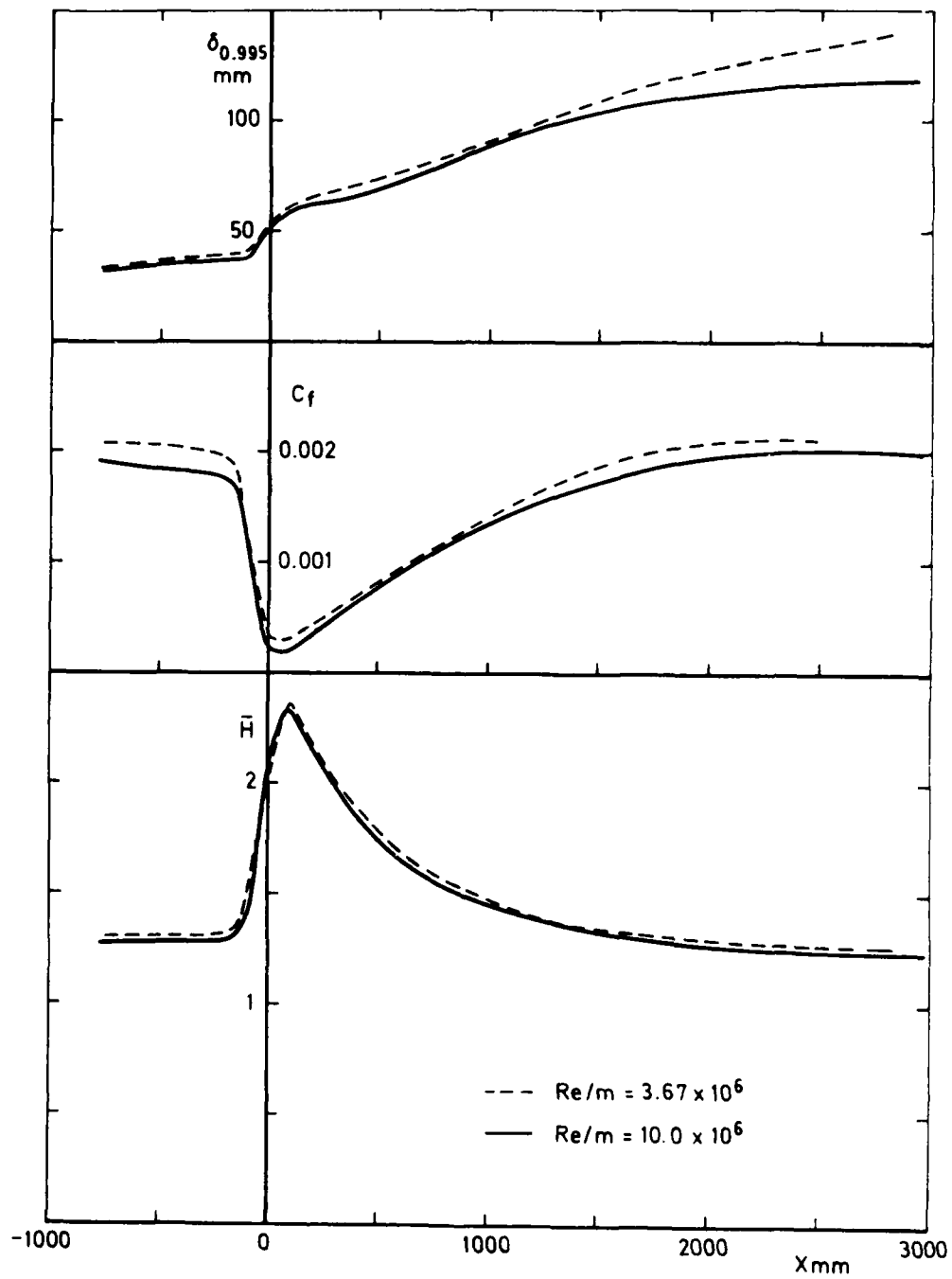


Fig 13b (concl'd) Boundary layer development ($p = p_w$) $M = 1.4$

Fig 13c

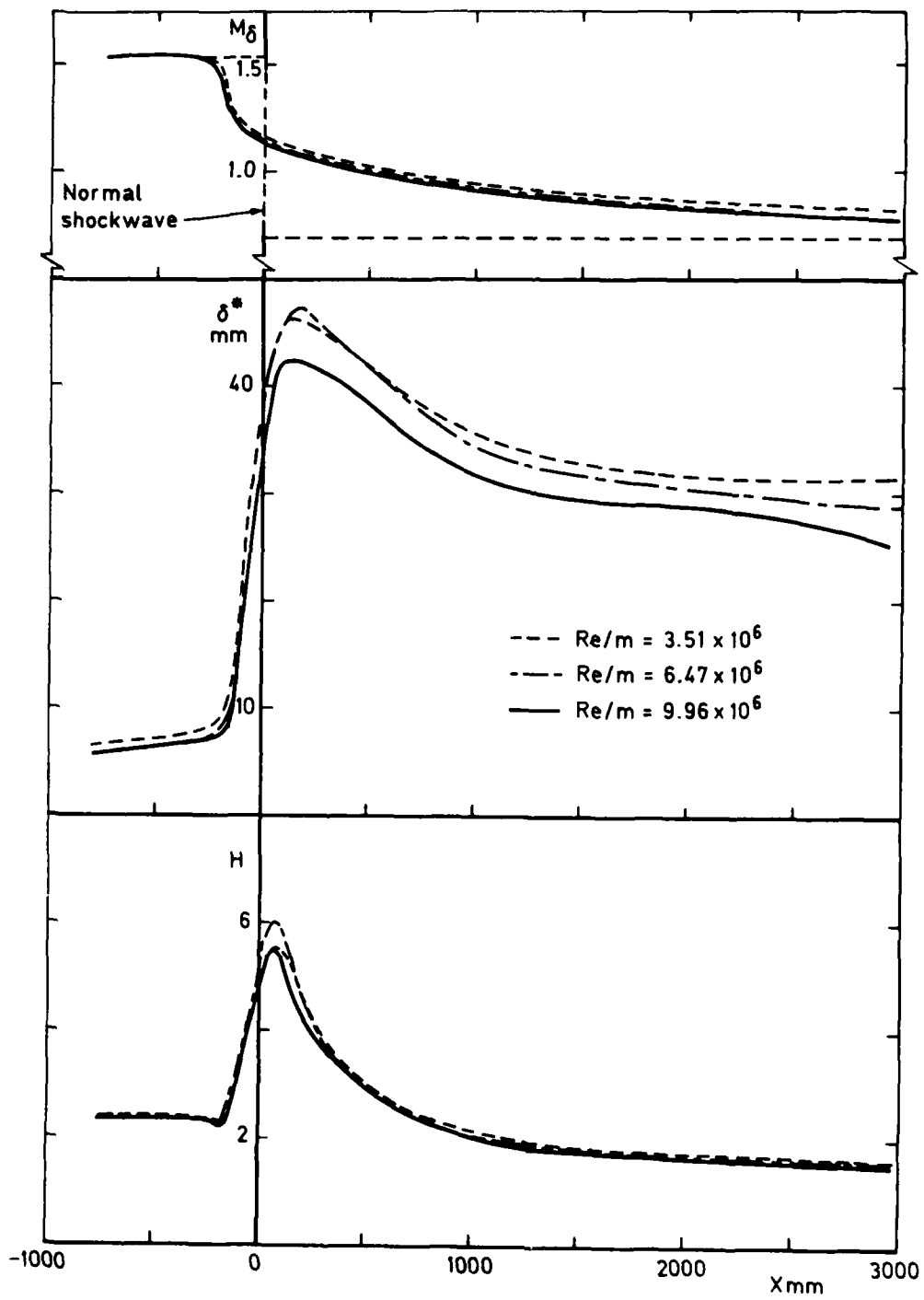


Fig 13c Boundary layer development ($p = p_w$) $M = 1.5$

Fig 13c (concl'd)

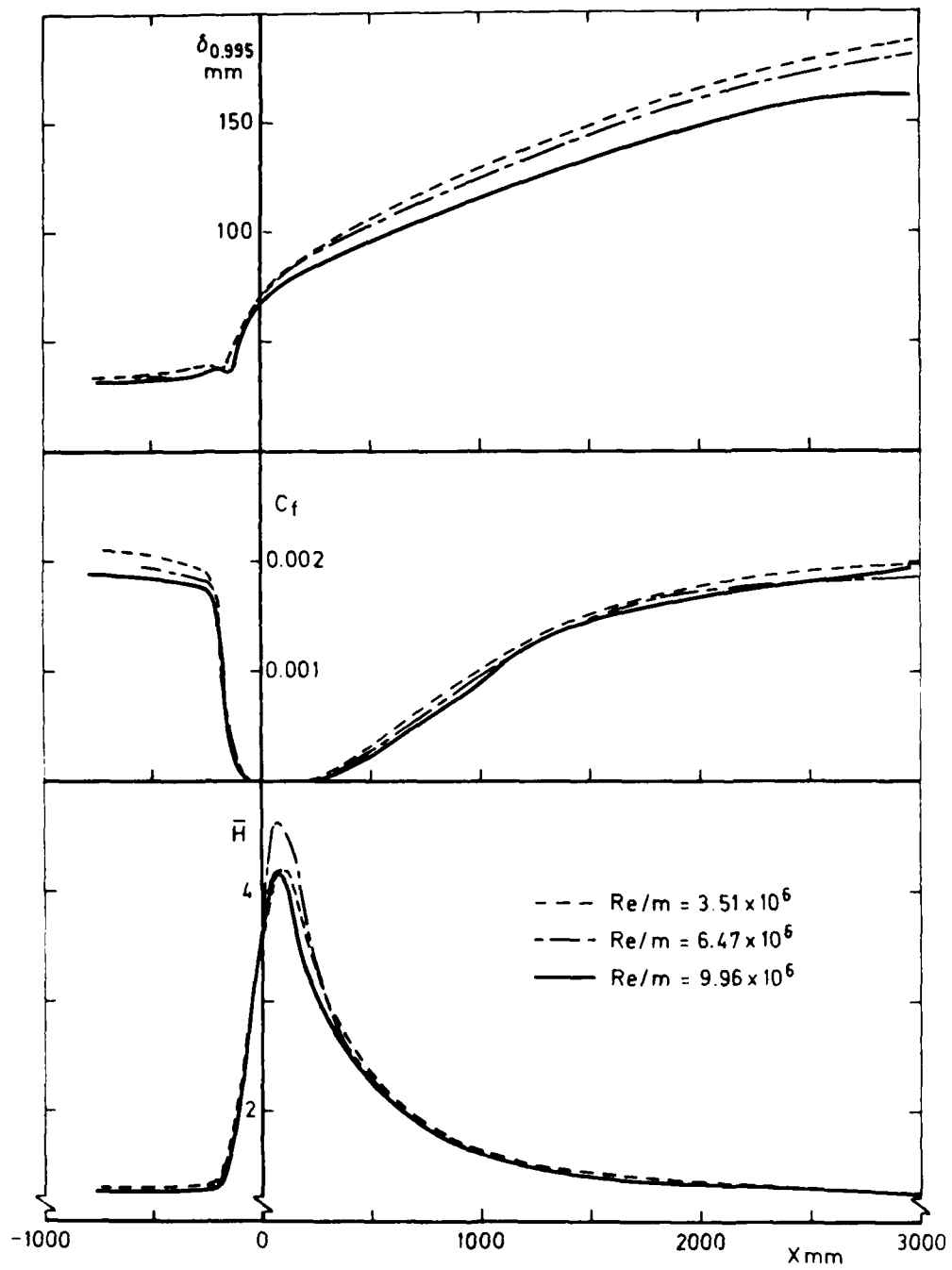


Fig 13c (concl'd) Boundary layer development ($p = p_w$) $M = 1.5$

Fig 14a

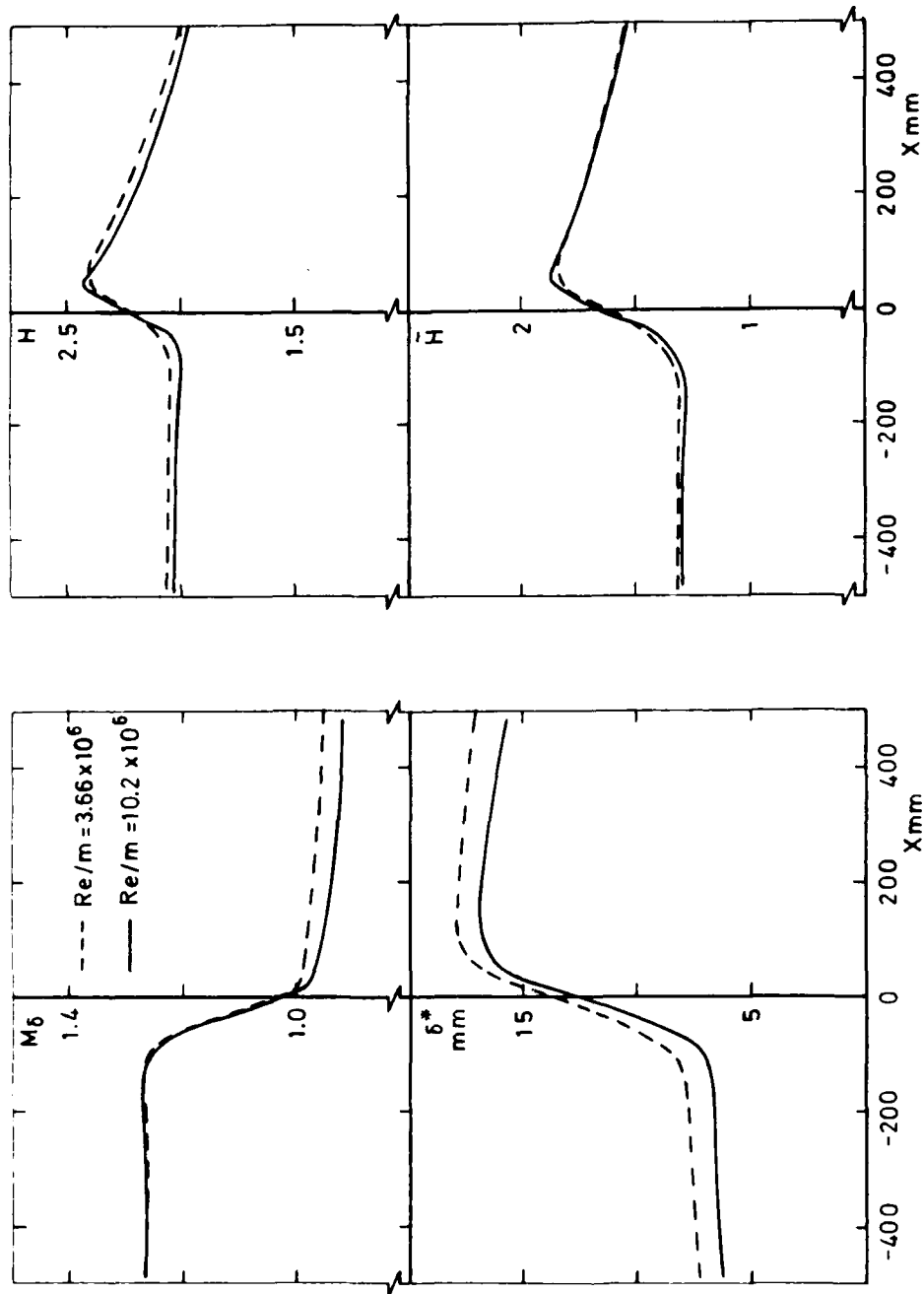


Fig 14a Boundary layer development (measured p) $M = 1.3$

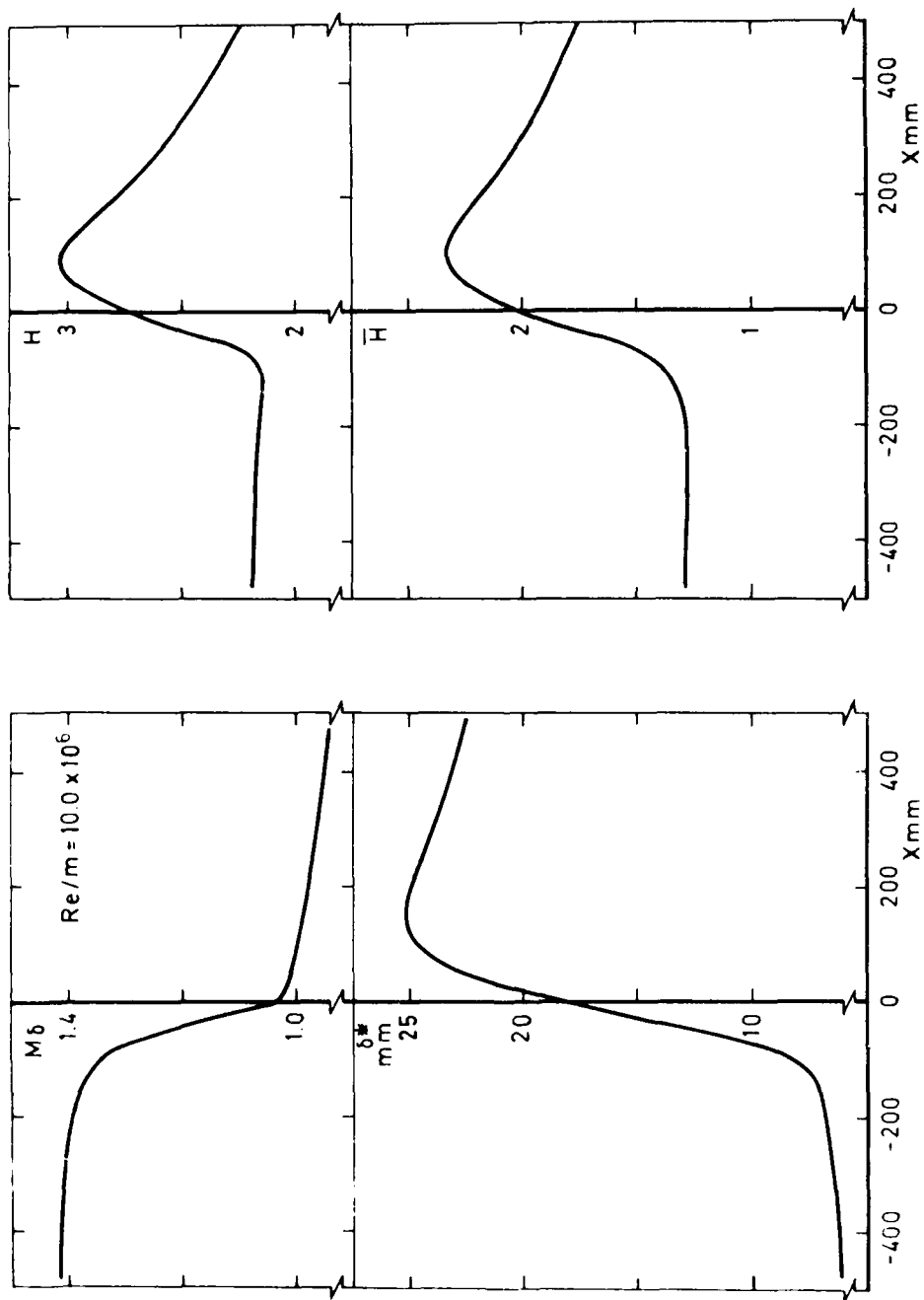


Fig 14b Boundary layer development (measured p) $M = 1.4$

Fig 14b

Fig 14c

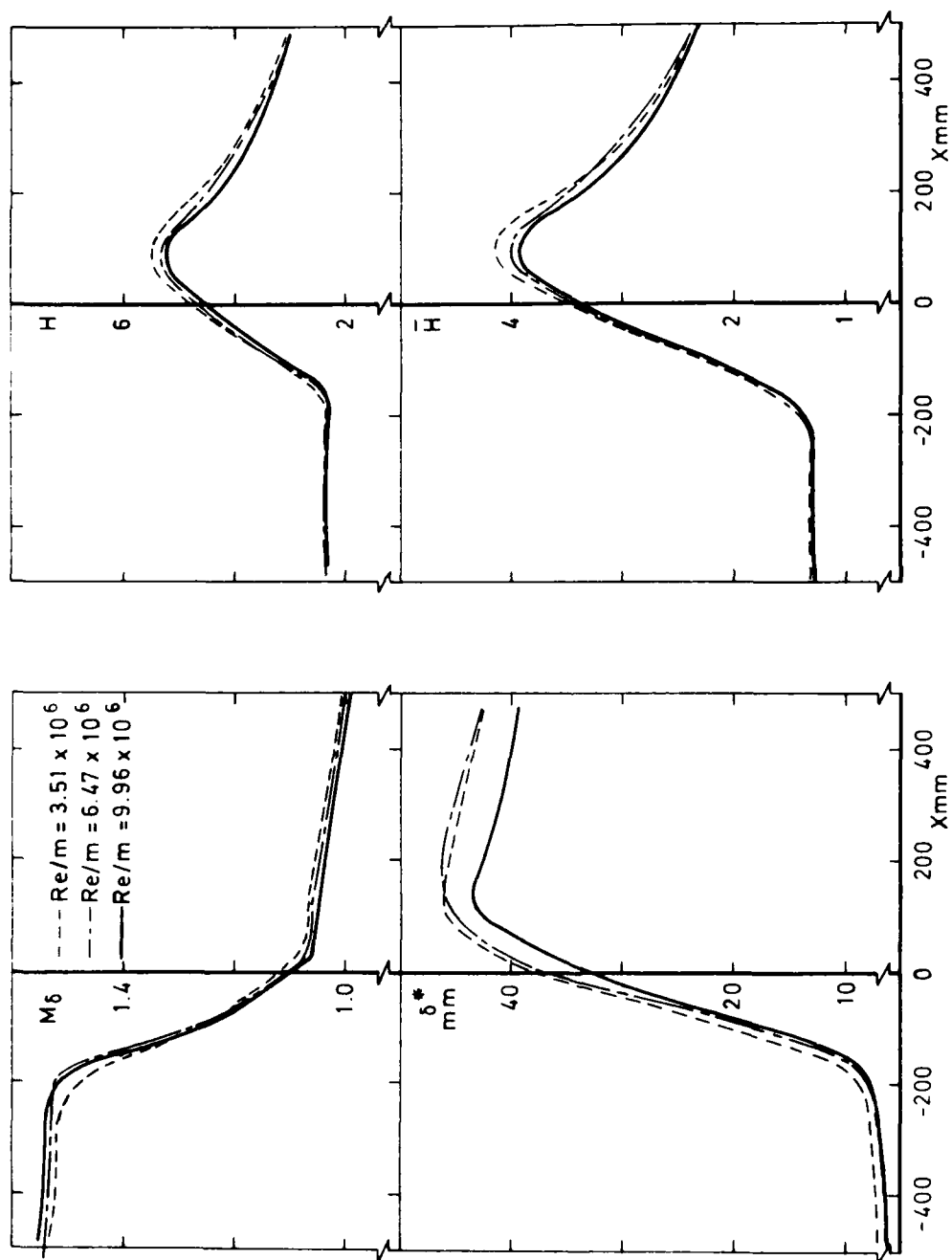


Fig 14c Boundary layer development (measured p) $M = 1.5$

Fig 15a

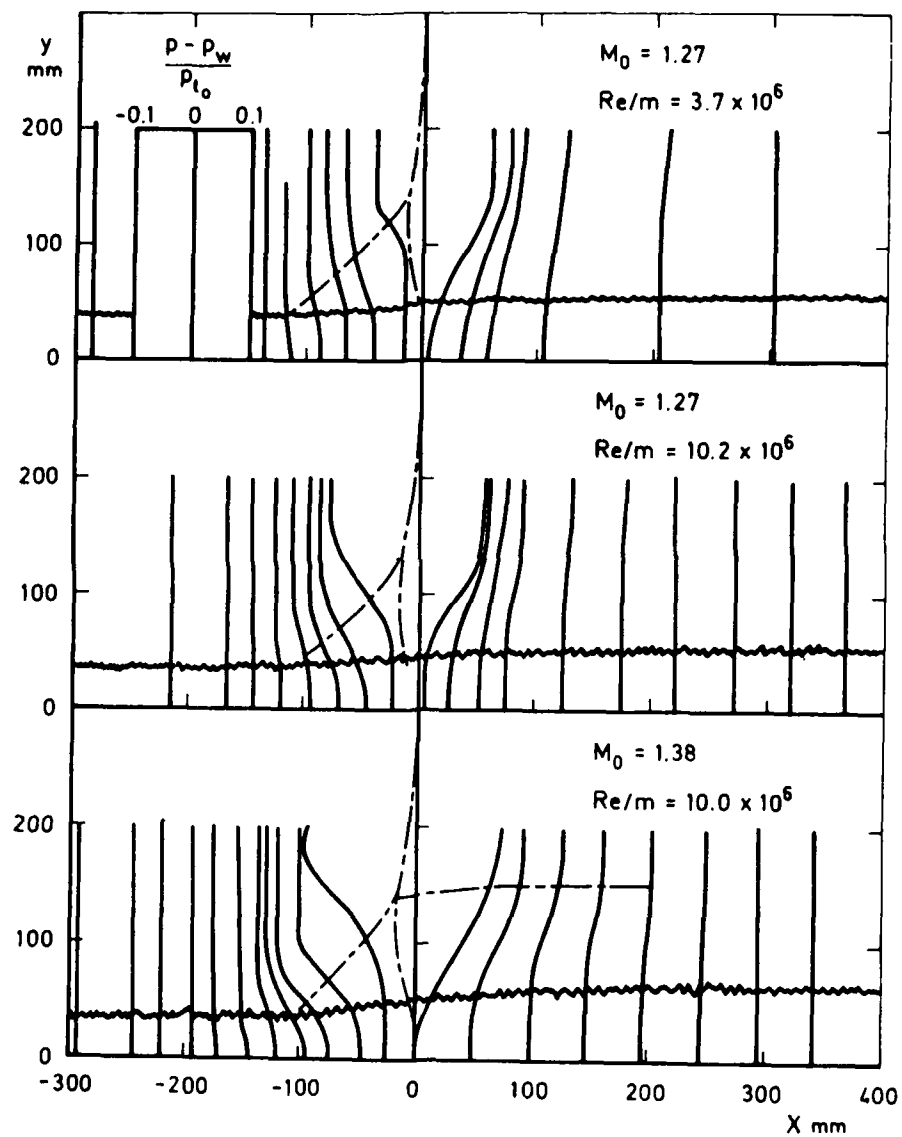


Fig 15a Measured static pressures

Fig 15b

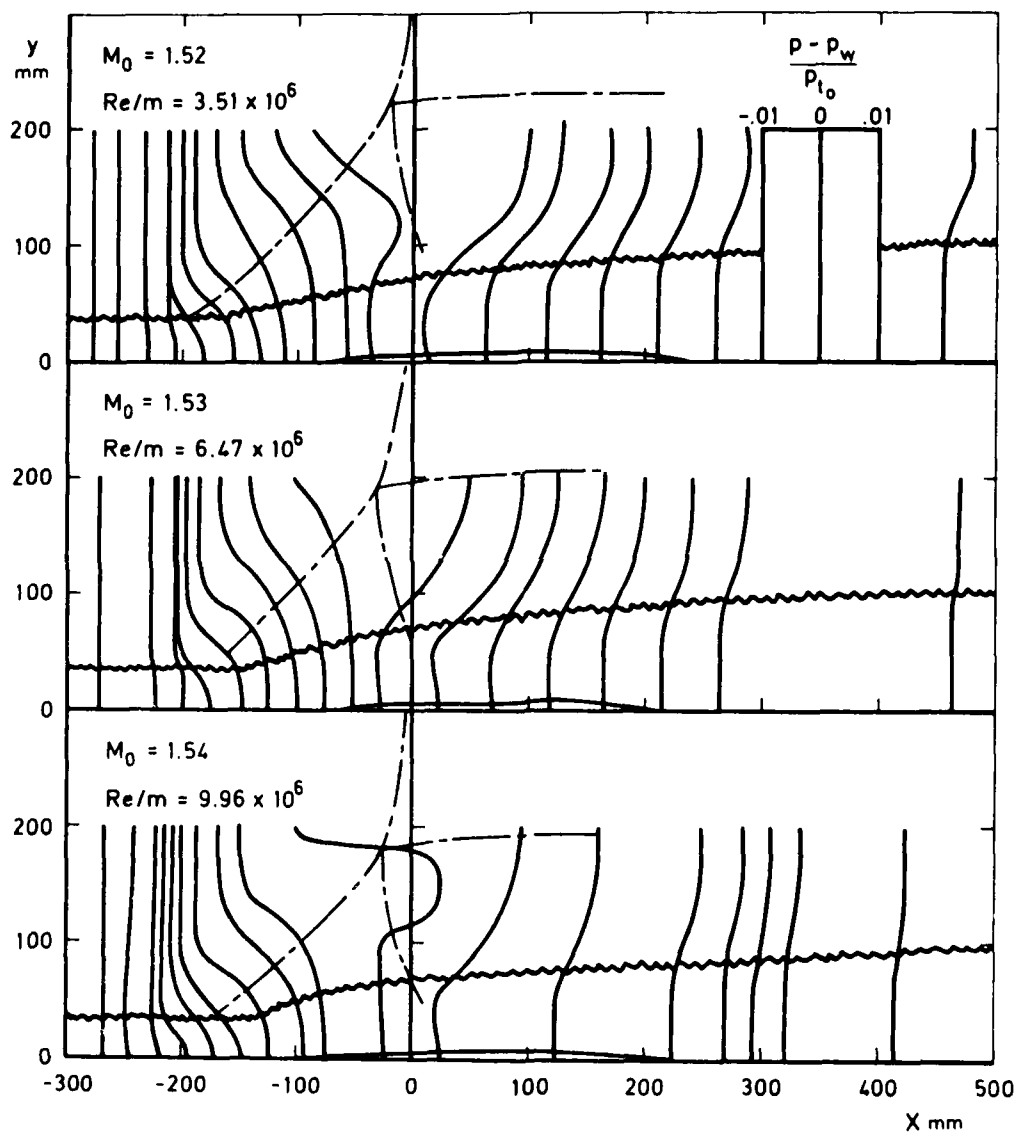


Fig 15b Measured static pressures

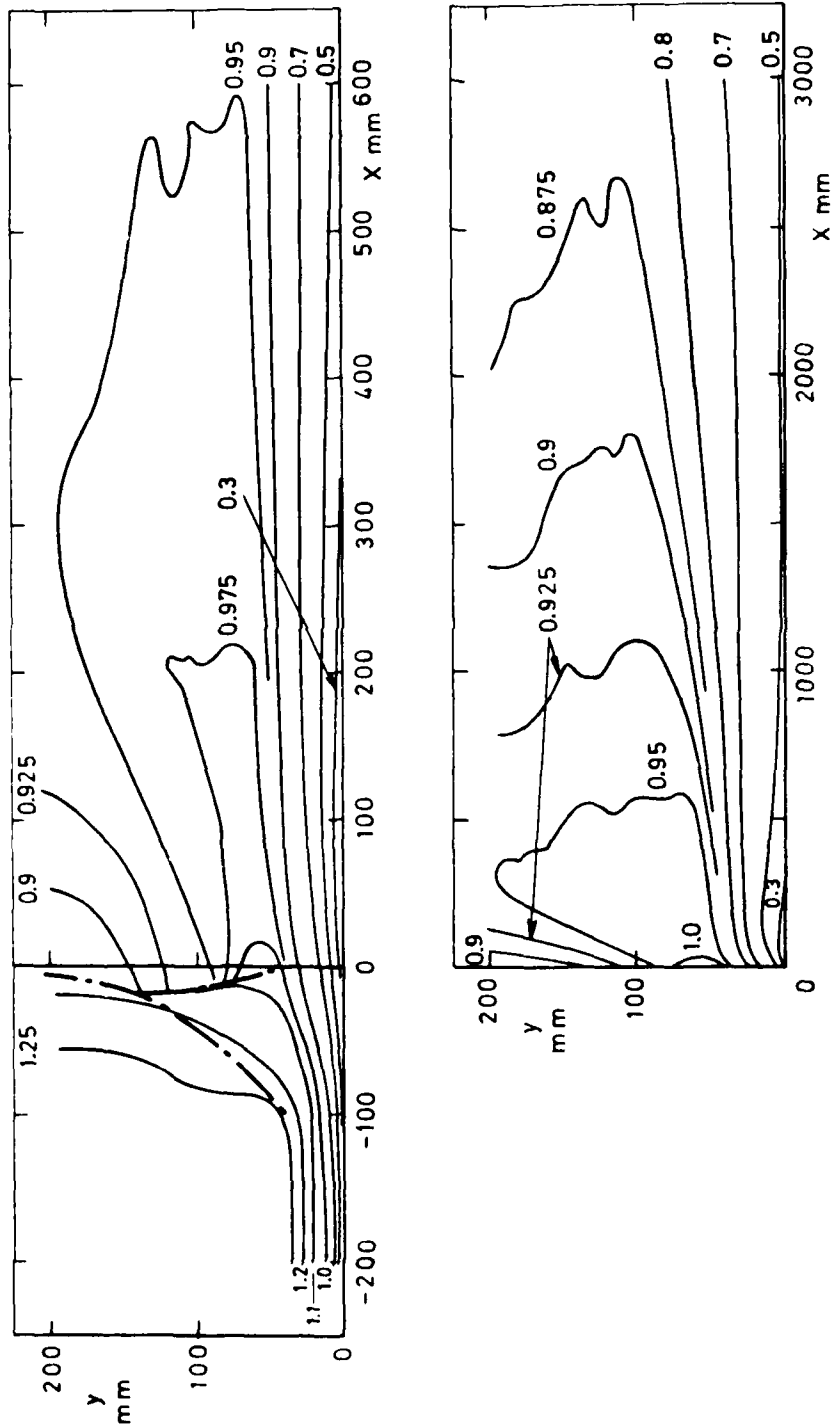


Fig 16a Mach number distribution, $M_0 = 1.27$, $Re/m = 3.66 \times 10^6$

Fig 16b

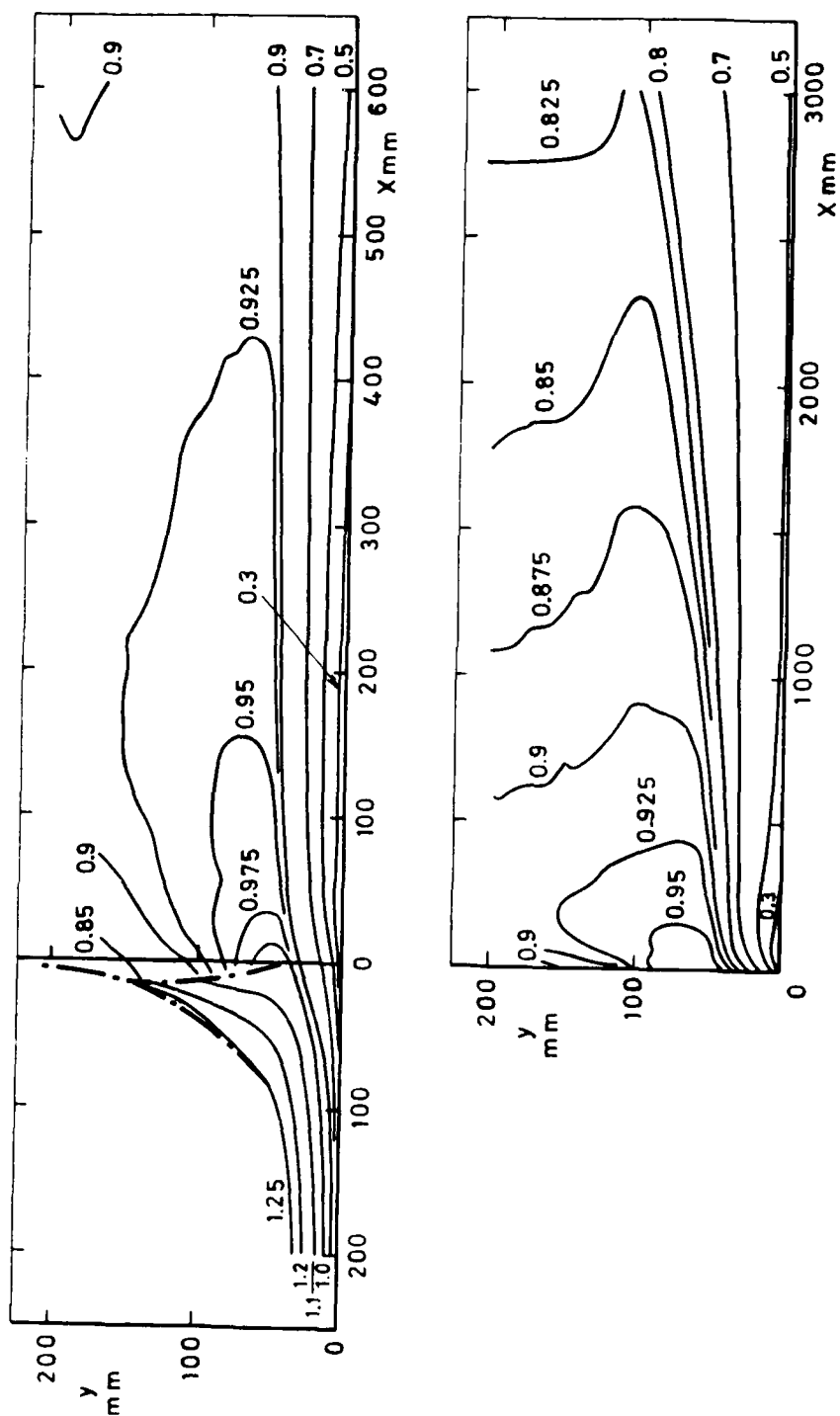


Fig 16b Mach number distribution, $M_0 = 1.27$, $Re/m = 10.2 \times 10^6$

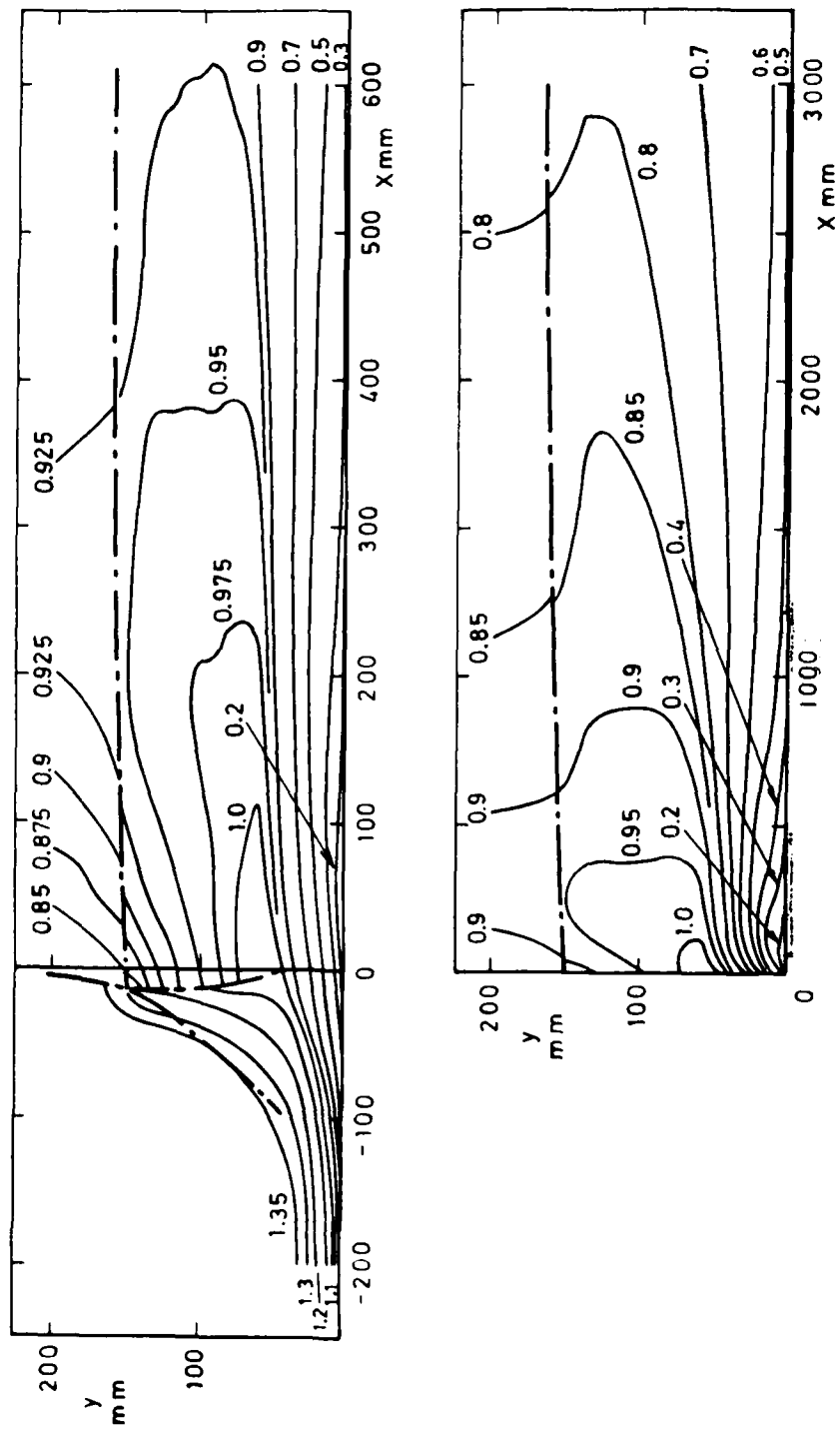


Fig 16c Mach number distribution, $M_0 = 1.39$, $Re/m = 10.0 \times 10^6$

Fig 16d

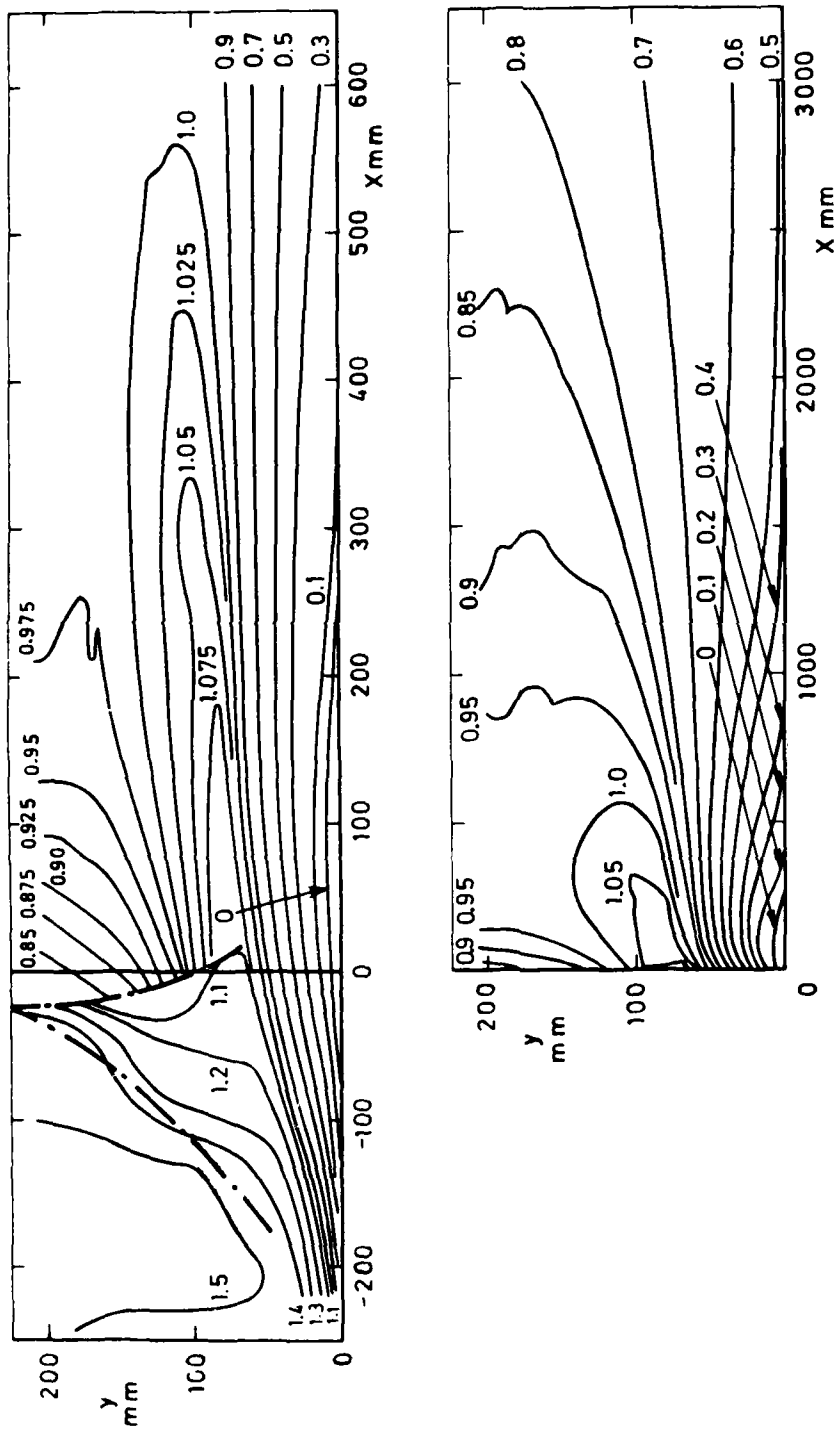


Fig 16d Mach number distribution, $M_0 = 1.52$, $Re/m = 3.51 \times 10^6$

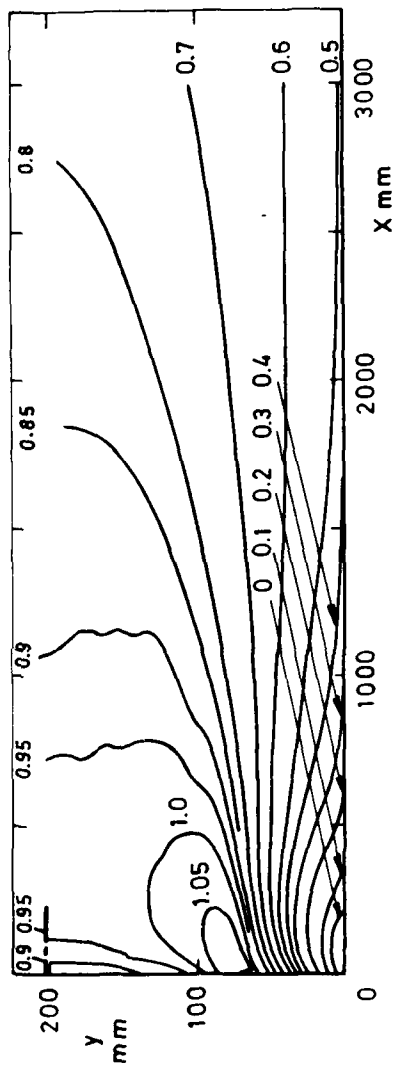
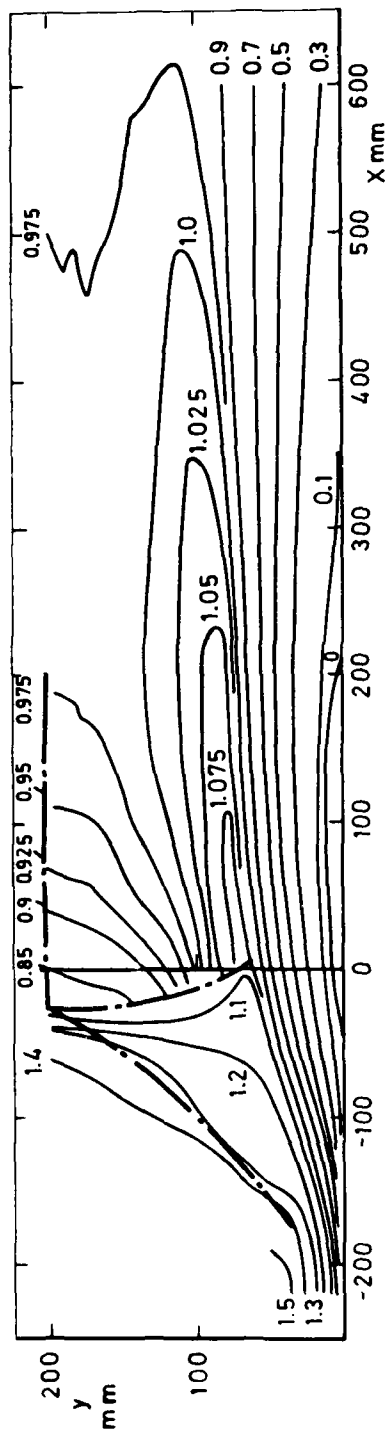


Fig 16e Mach number distribution, $M_0 = 1.53$, $Re/m = 6.47 \times 10^6$

Fig 16a

Fig 16f

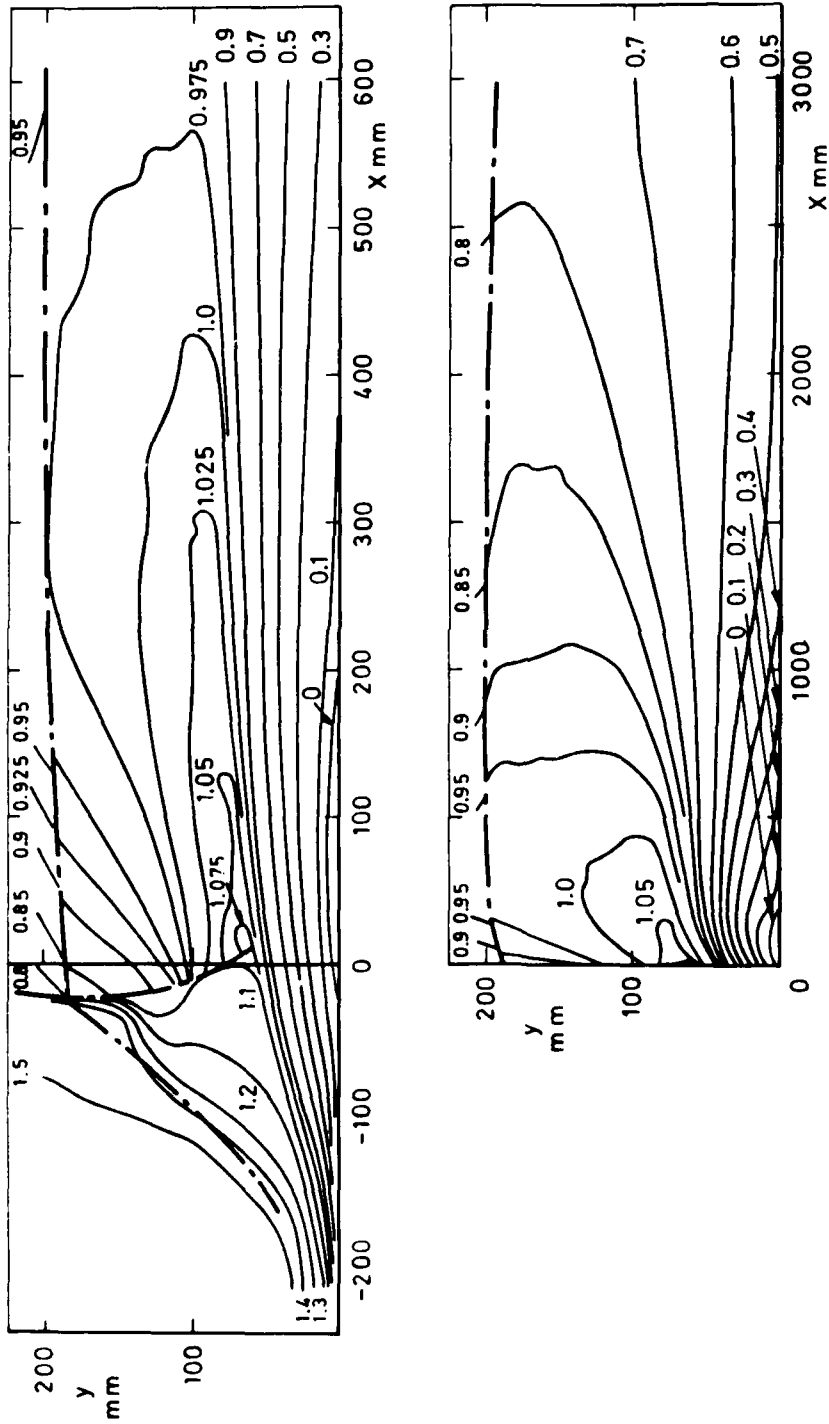


Fig 16f Mach number distribution, $M_0 = 1.54$, $Re/m = 9.95 \times 10^6$

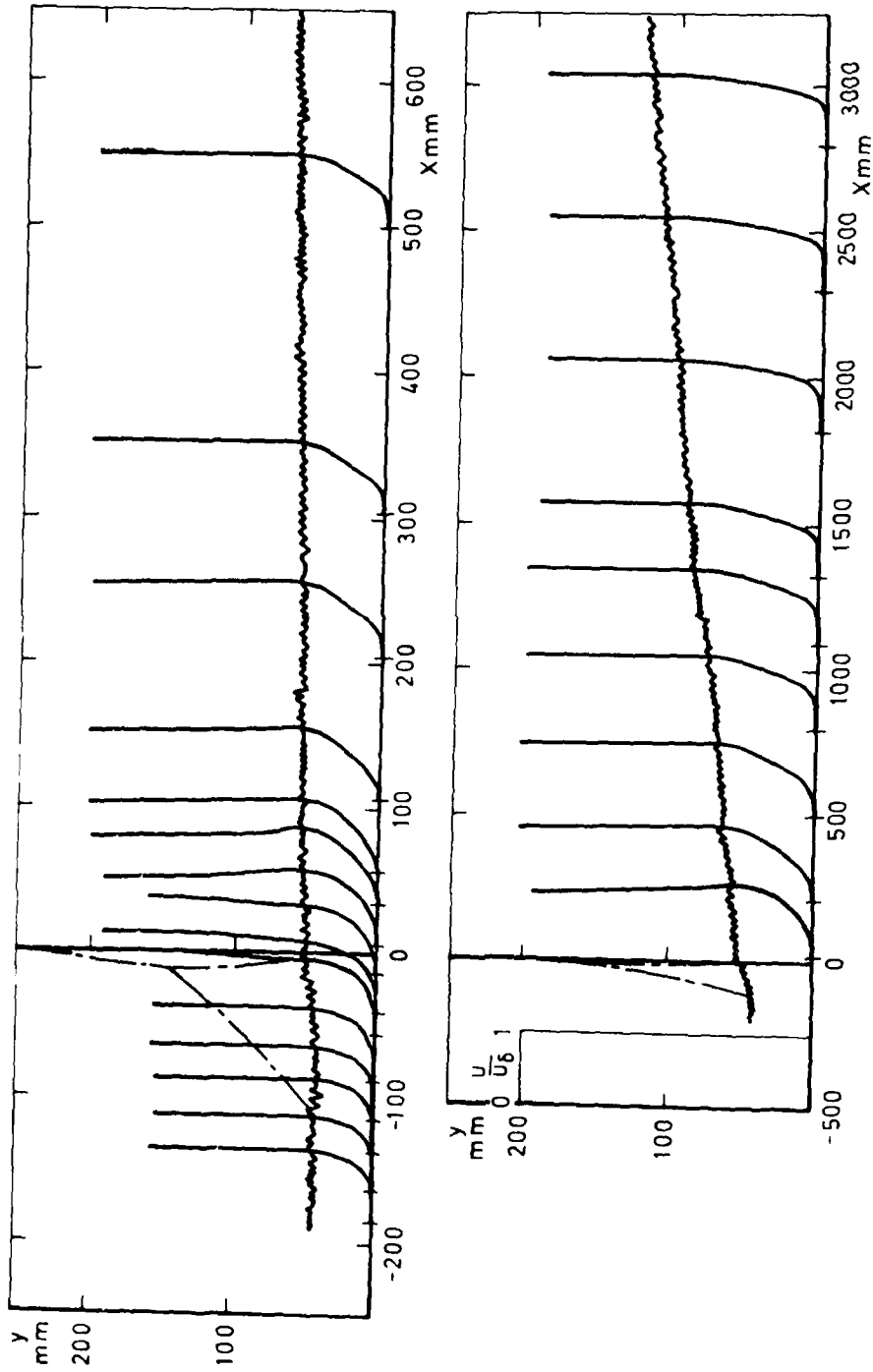


Fig 17a Velocity profiles, $M_0 = 1.27$, $Re/m = 3.66 \times 10^6$

Fig 17a

Fig 17b

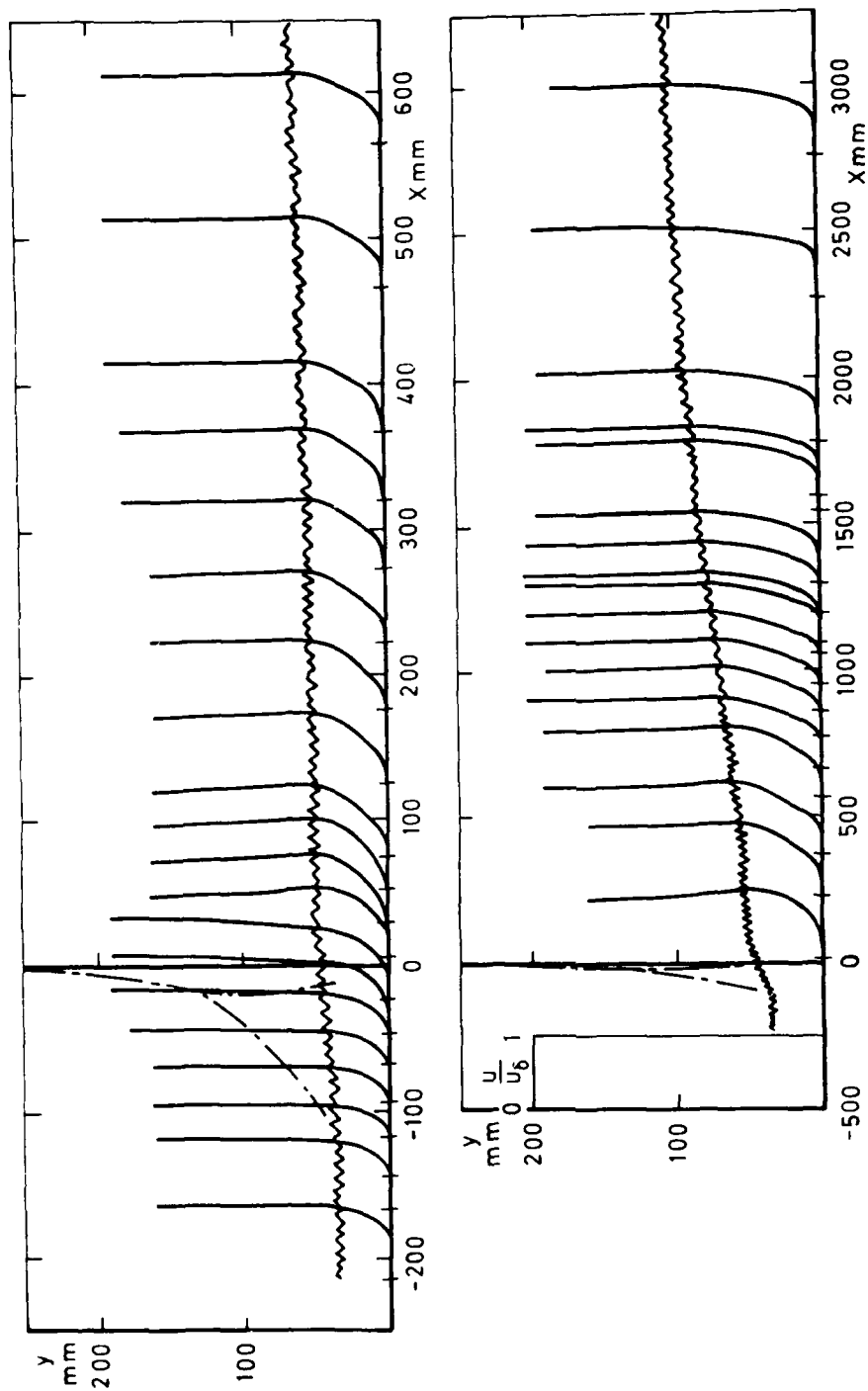


Fig 17b Velocity profiles, $M_0 = 1.27$, $Re/m = 10.2 \times 10^6$

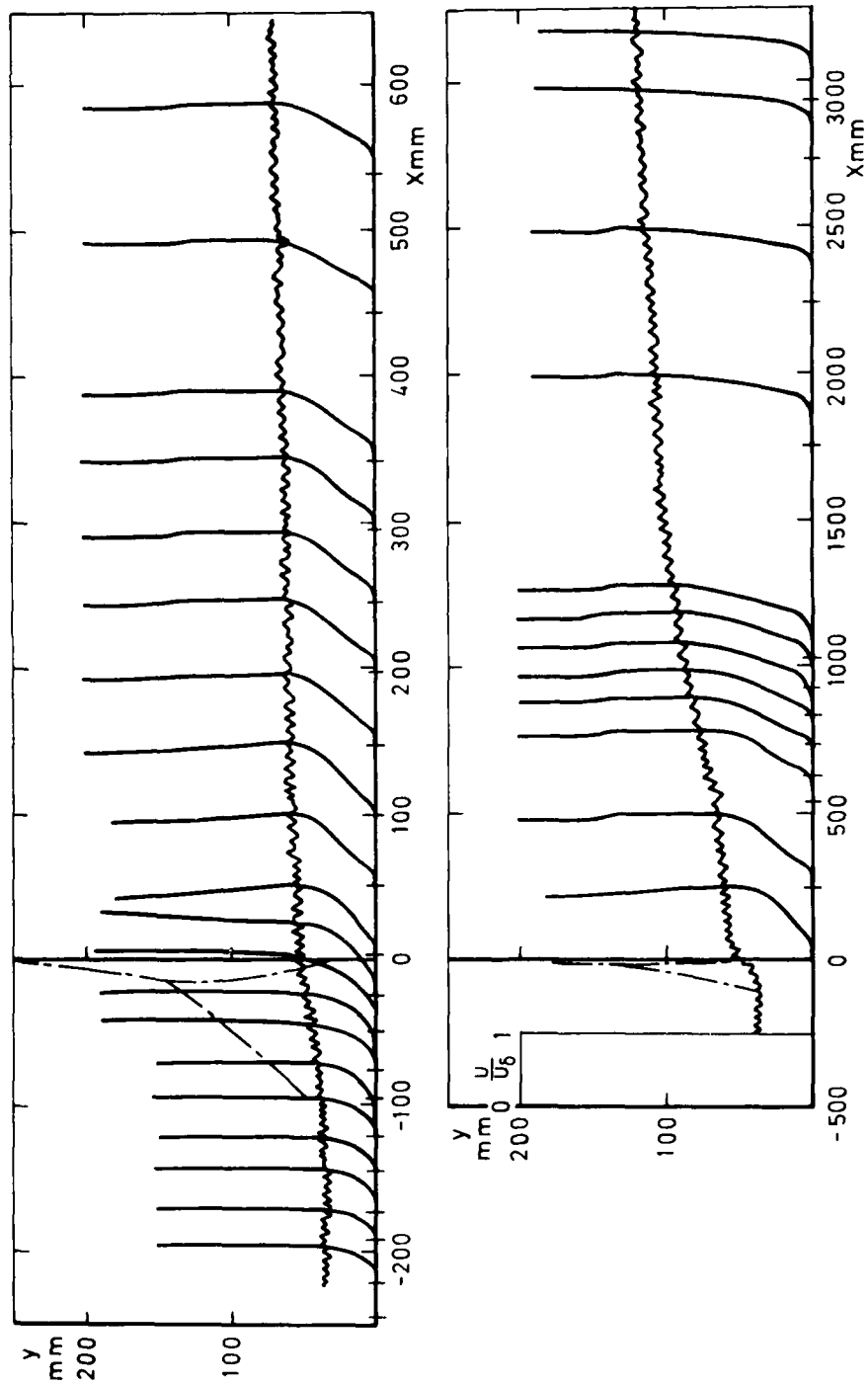


Fig 17c Velocity profiles, $M_0 = 1.39$, $Re/m = 10.0 \times 10^6$

Fig 17d

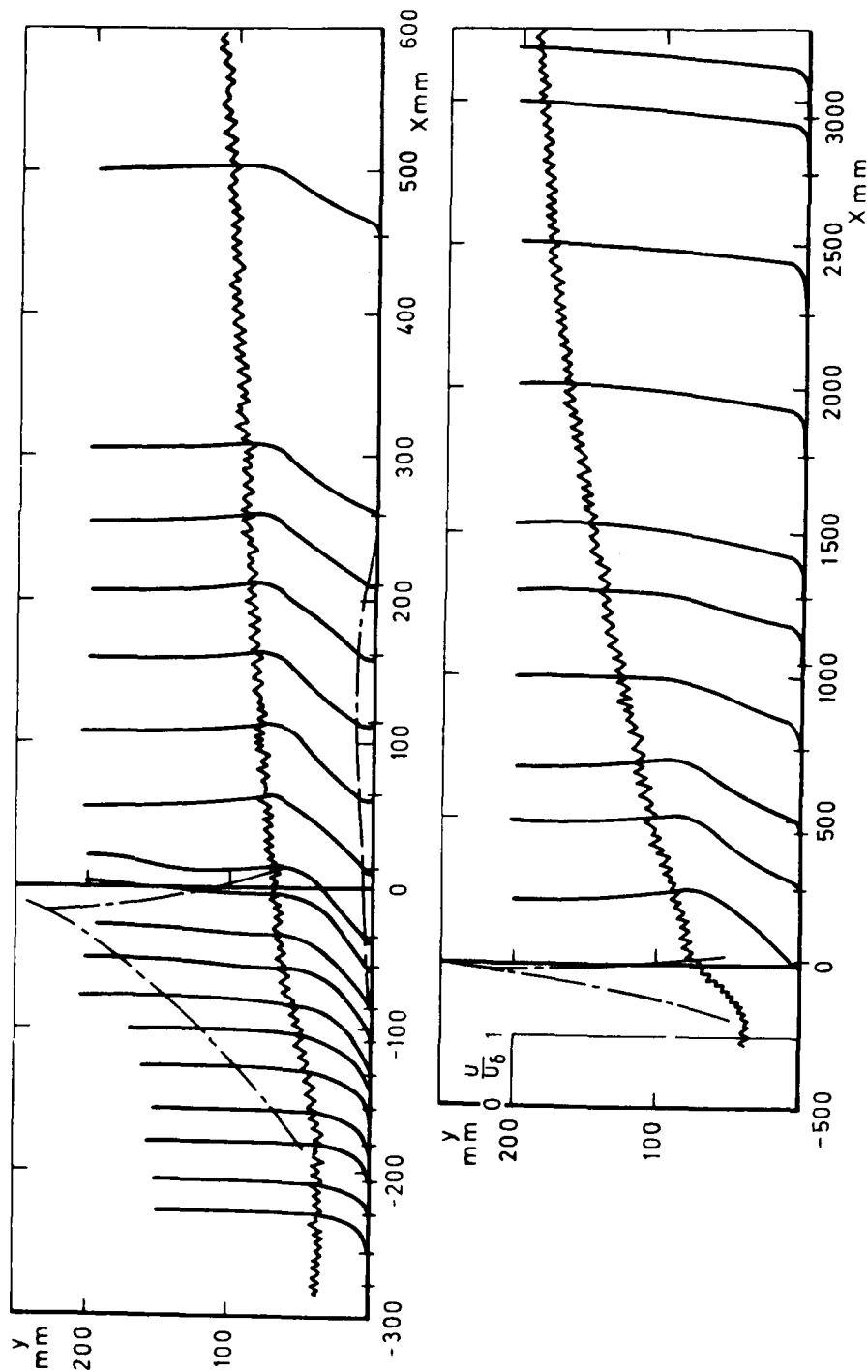


Fig 17d Velocity profiles, $M_0 = 1.52$, $Re/m = 3.51 \times 10^6$

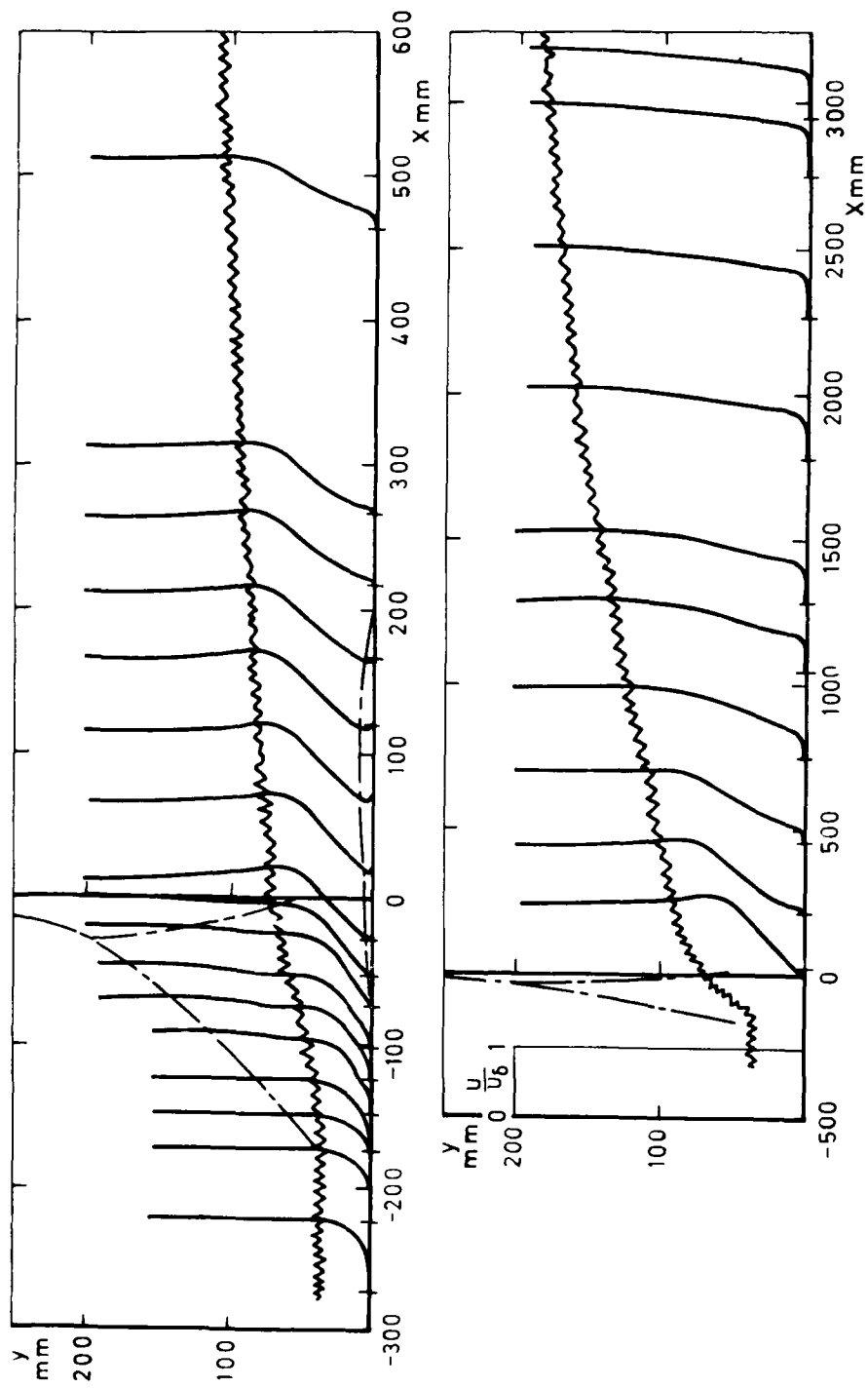


Fig 17e Velocity profiles, $M_0 = 1.53$, $Re/m = 6.47 \times 10^6$

Fig 17f

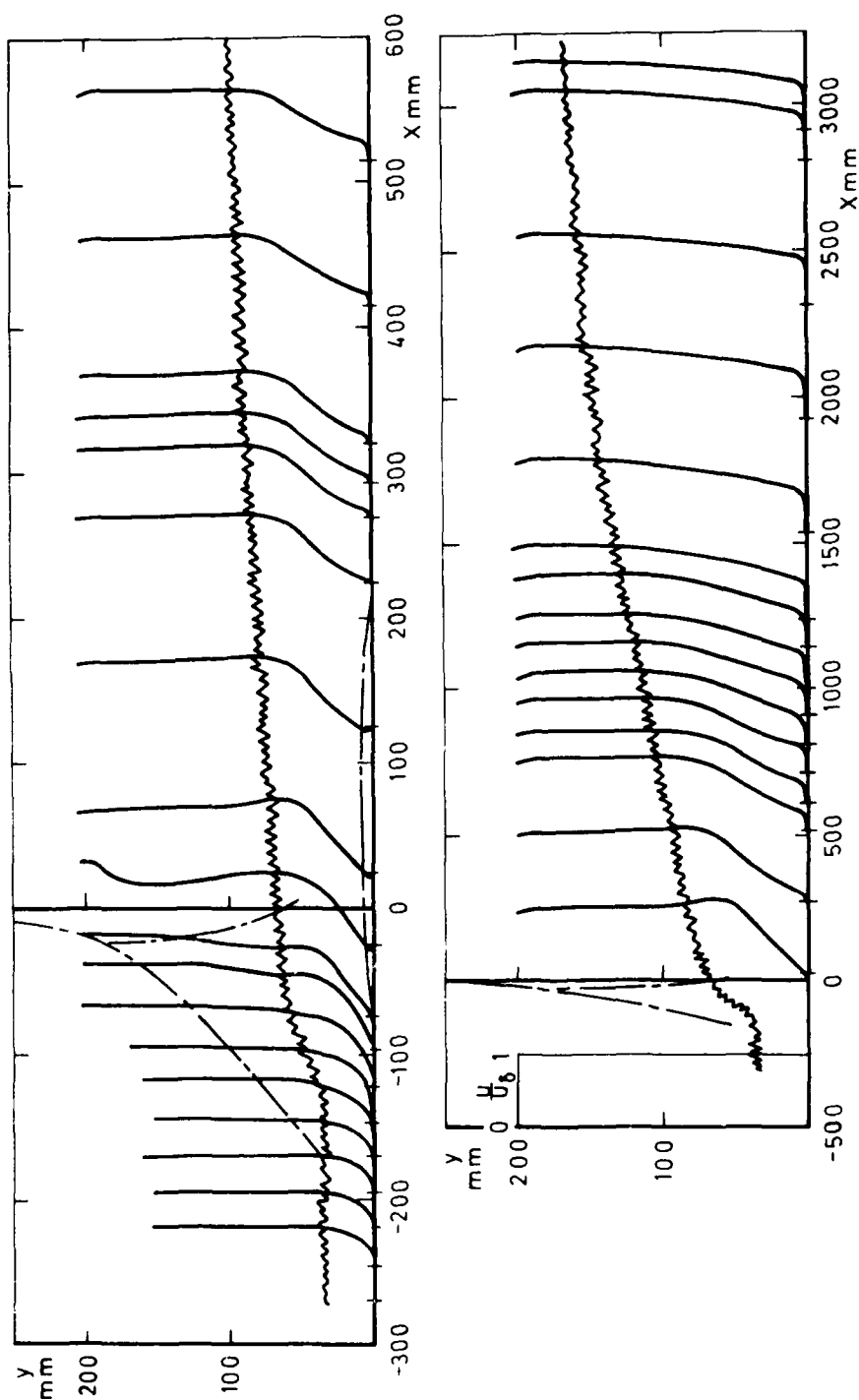


Fig 17f Velocity profiles, $M_0 = 1.54$, $Re/m = 9.96 \times 10^6$

Fig 18

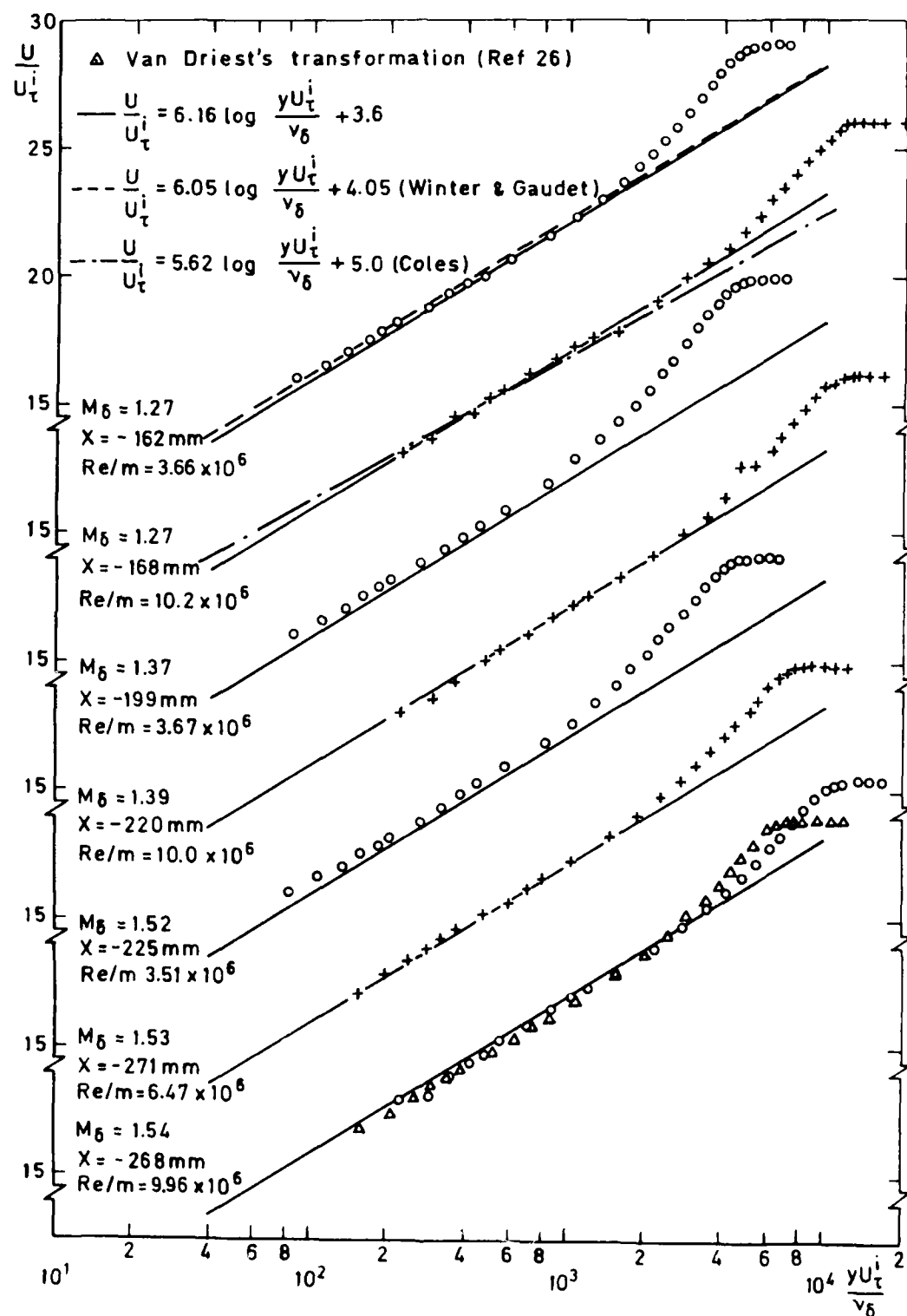


Fig 18 Logarithmic velocity profiles ahead of interaction (region A) (see Fig 22)

Fig 19

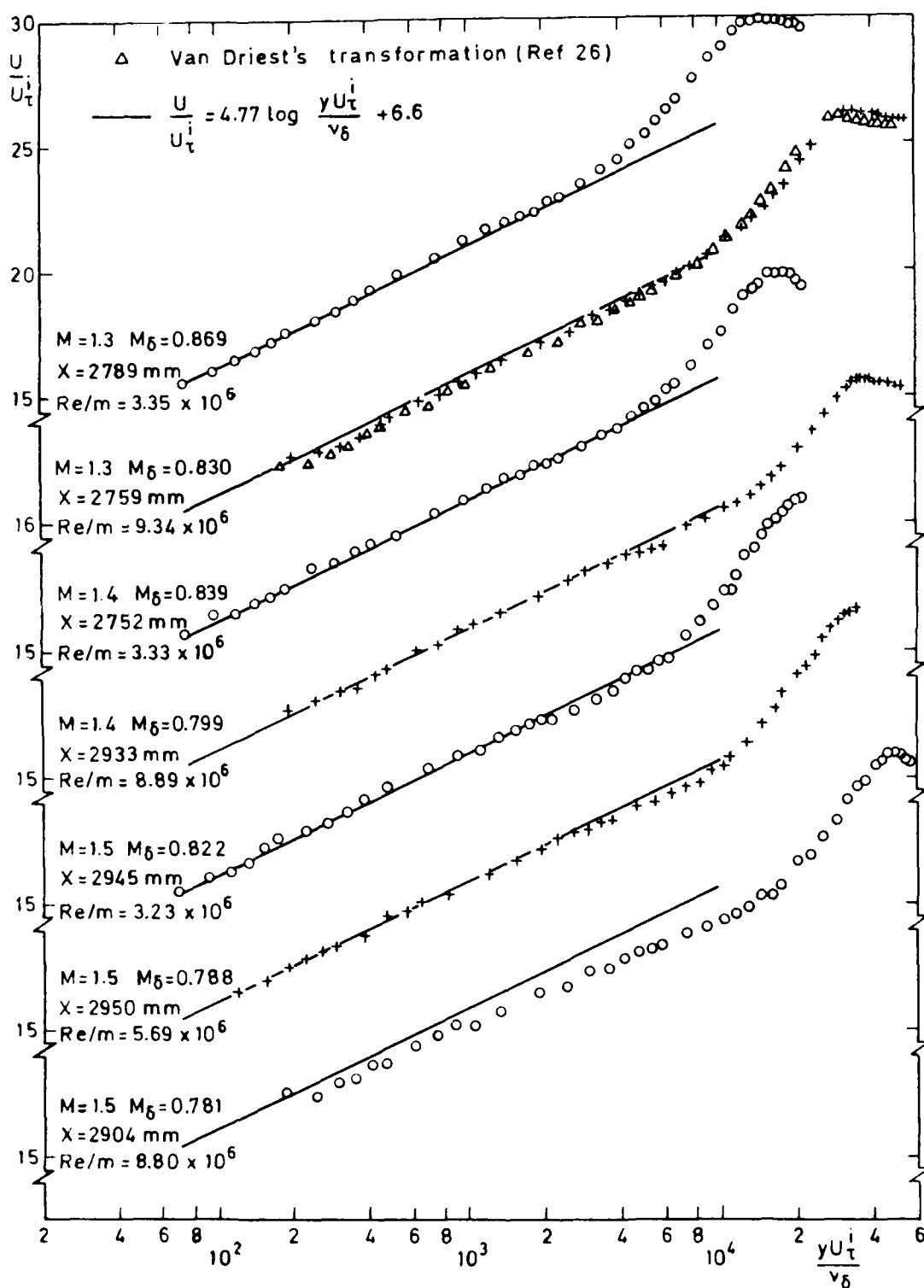


Fig 19 Logarithmic velocity profiles approx 3 m downstream of normal shock-wave (region D) (see Fig 22)

Fig 20

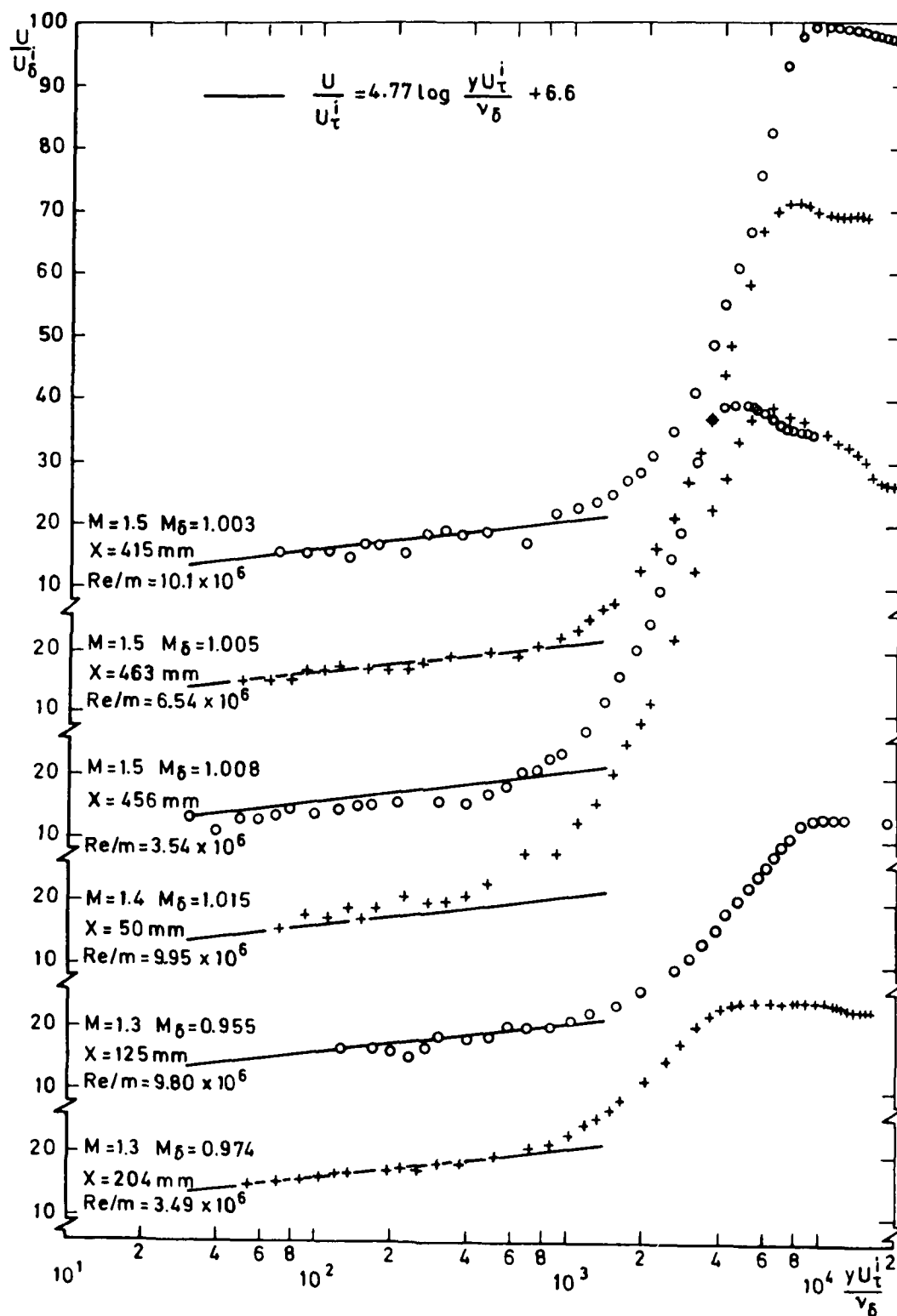


Fig 20 Logarithmic velocity profiles just downstream of normal shock-wave (region C) (see Fig 22)

Fig 21

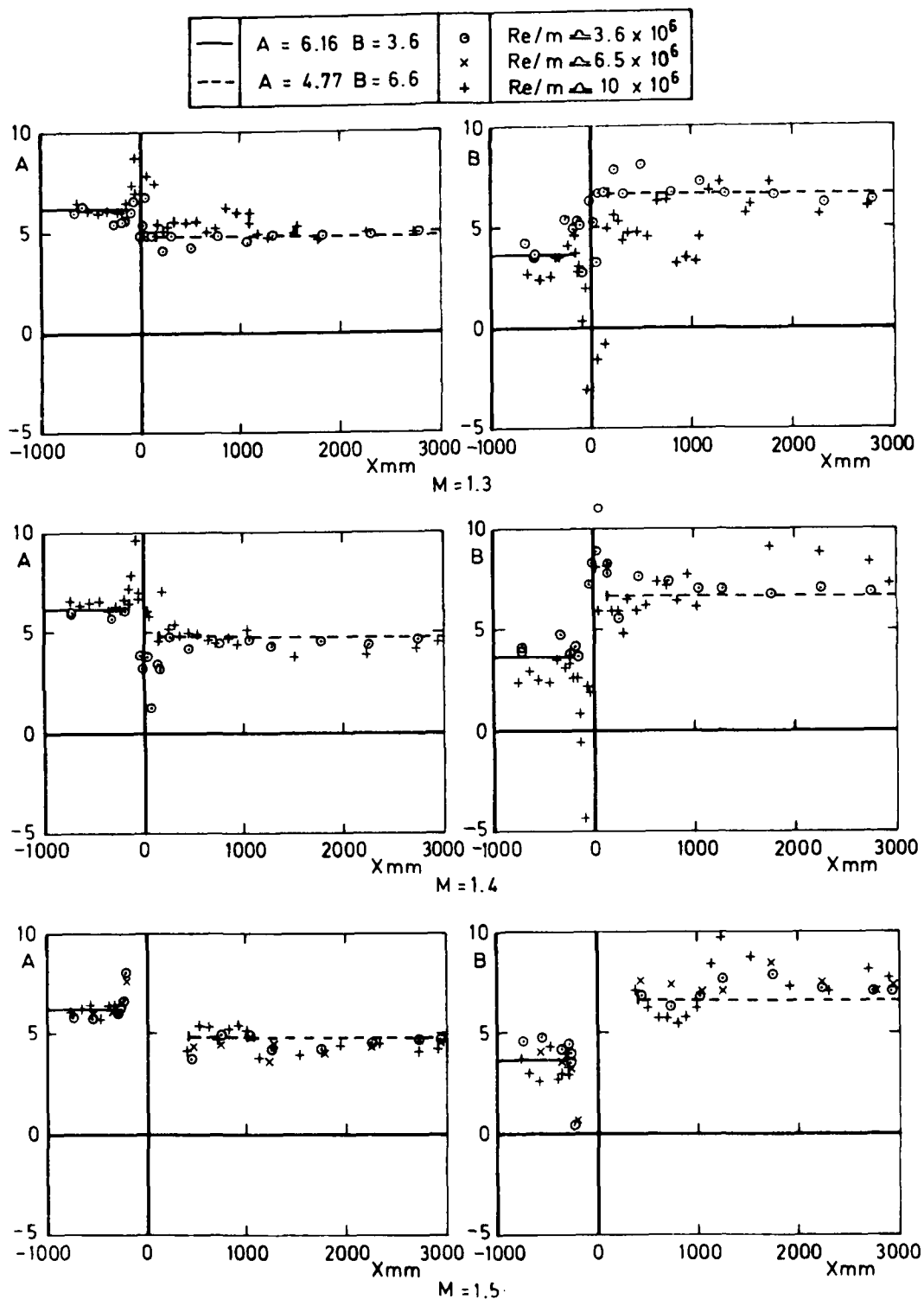


Fig 21 Variation of the constants A and B in the law of the wall
 $(U/U_T^i = A \log y U_T^i / \nu_\delta + B)$

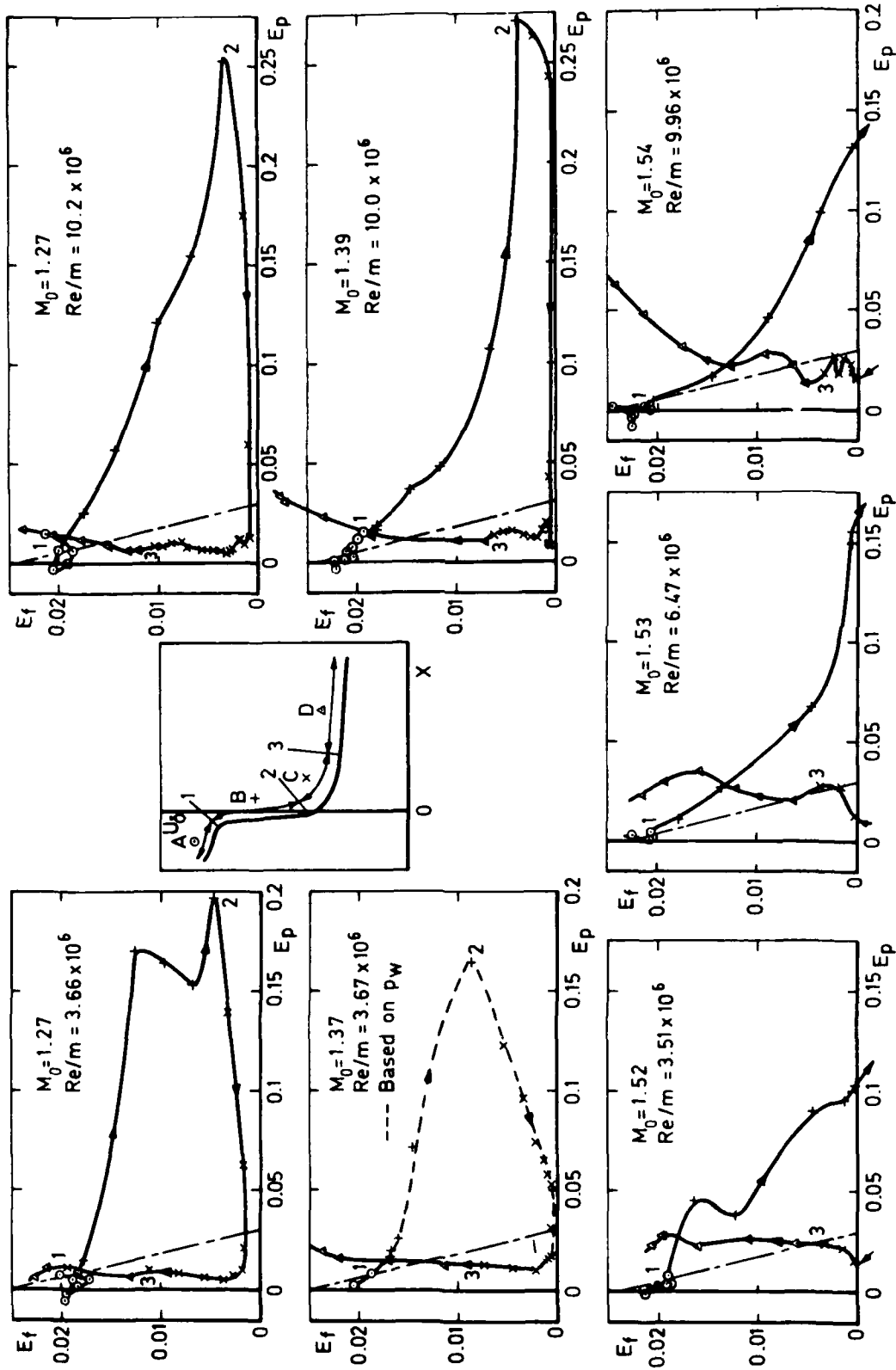


Fig 22 Equilibrium parameters

Fig 23a&b

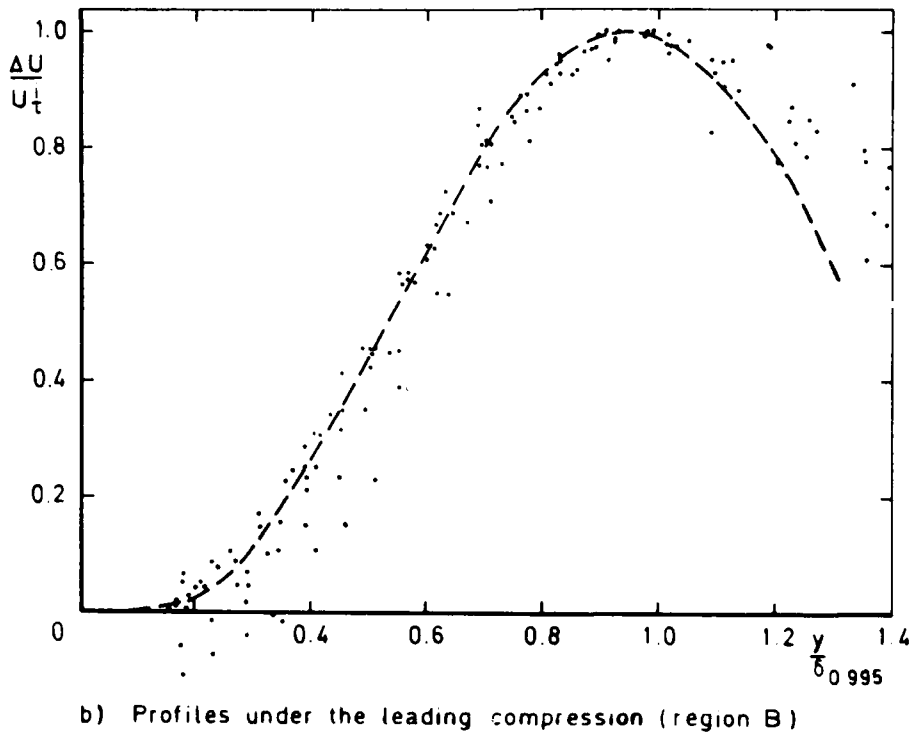
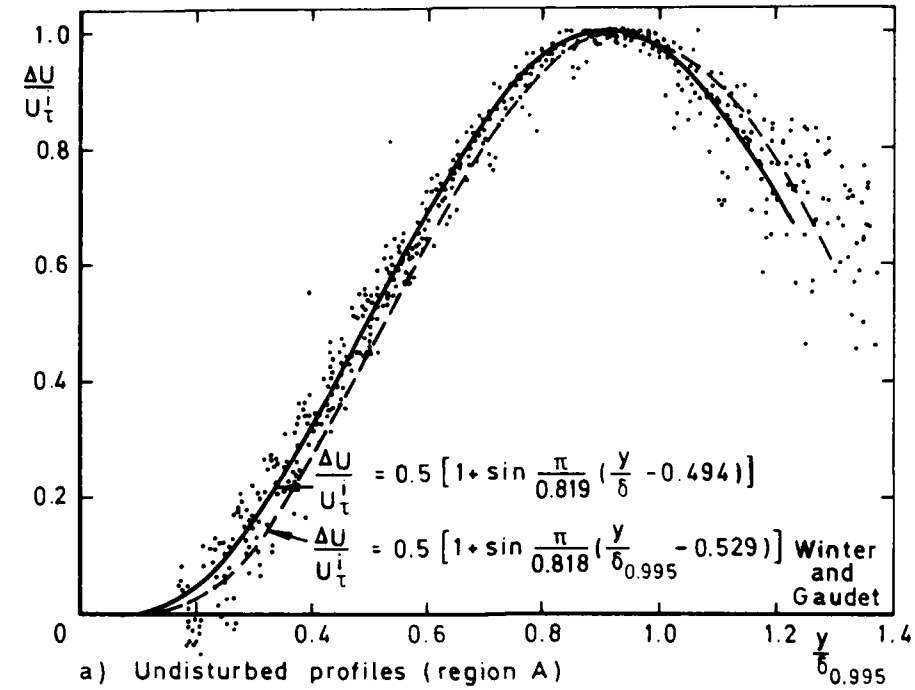
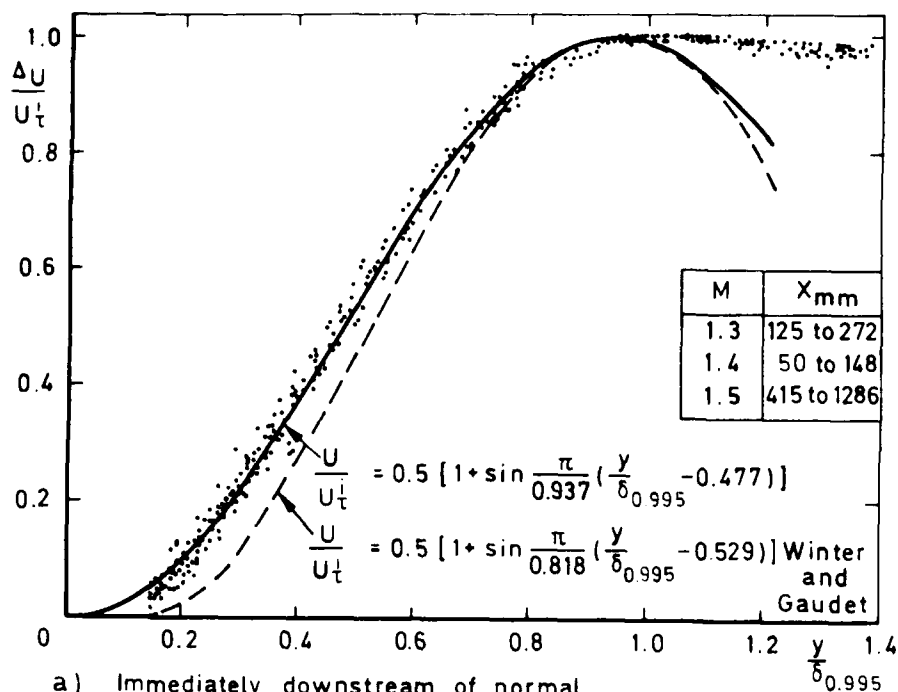
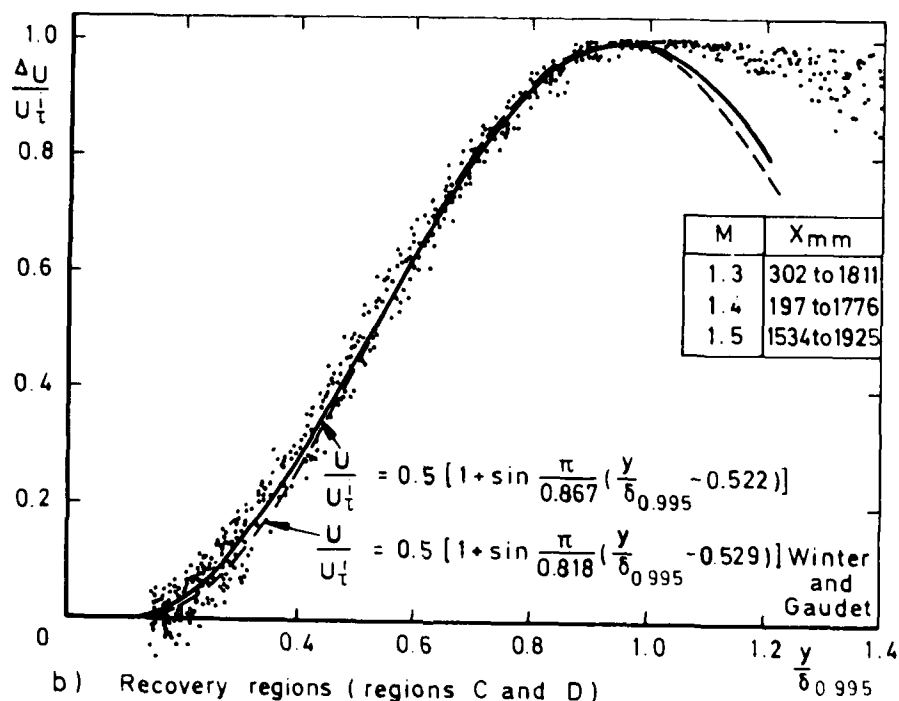


Fig 23a&b Wake components of velocity profiles ahead of shock-wave

Fig 24a&b



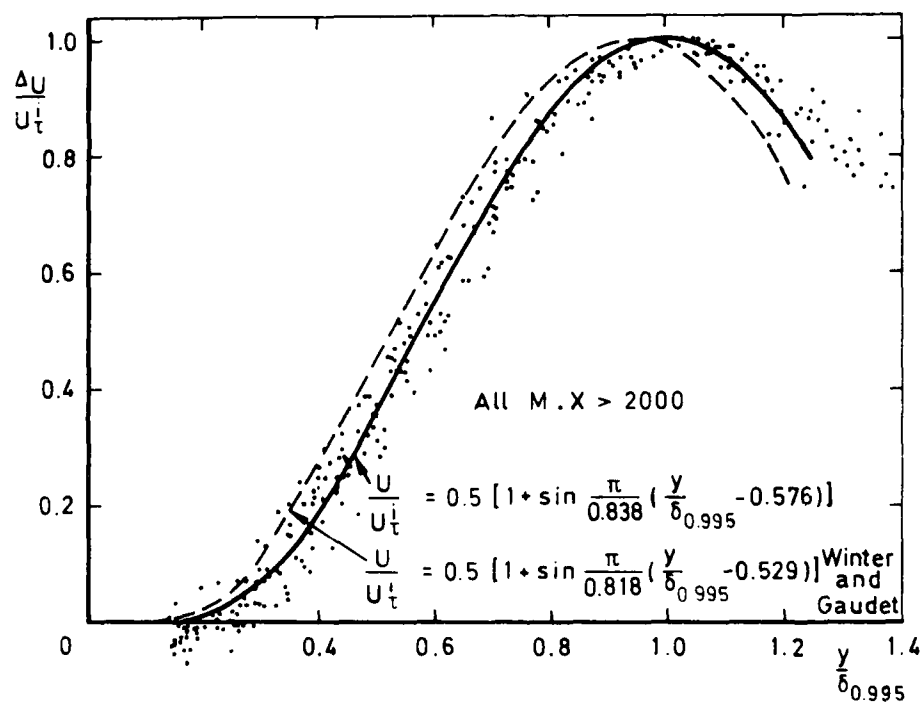
a) Immediately downstream of normal shock-wave (region C)



b) Recovery regions (regions C and D)

Fig 24a&b Wake components of velocity profiles downstream of shock-wave

Fig 24c



c) $X > 2000\text{mm}$ (region D)

Fig 24c Wake components of velocity profiles downstream of shock-wave

Fig 25a&b

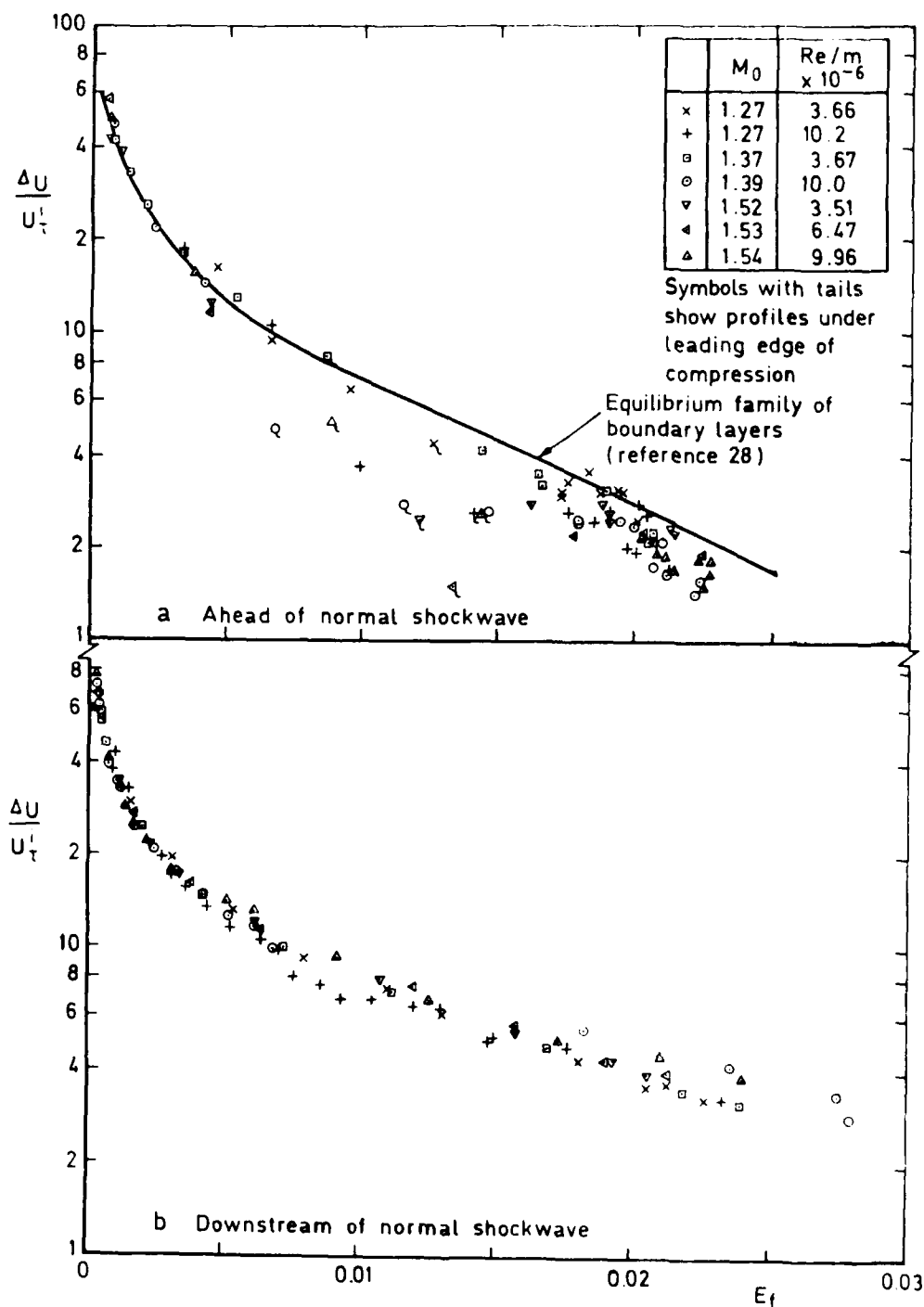
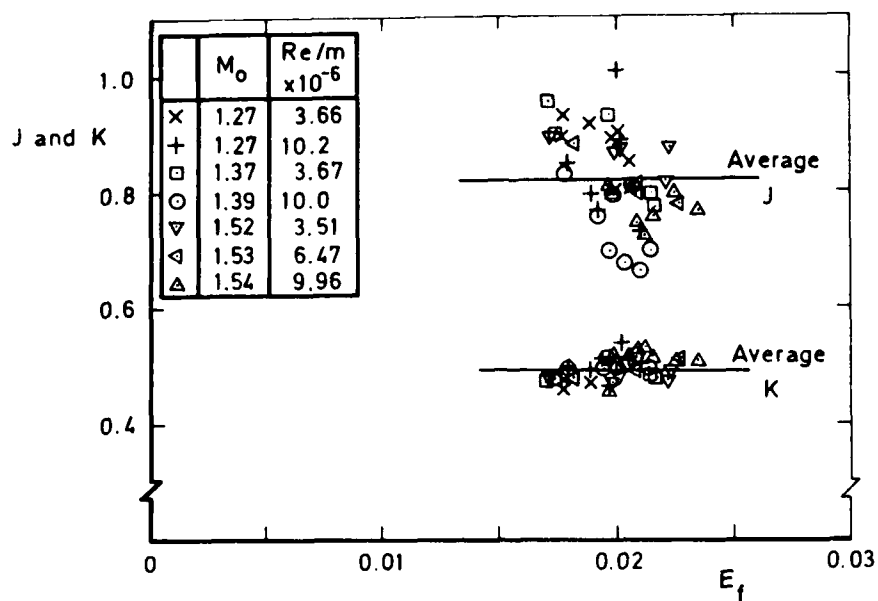
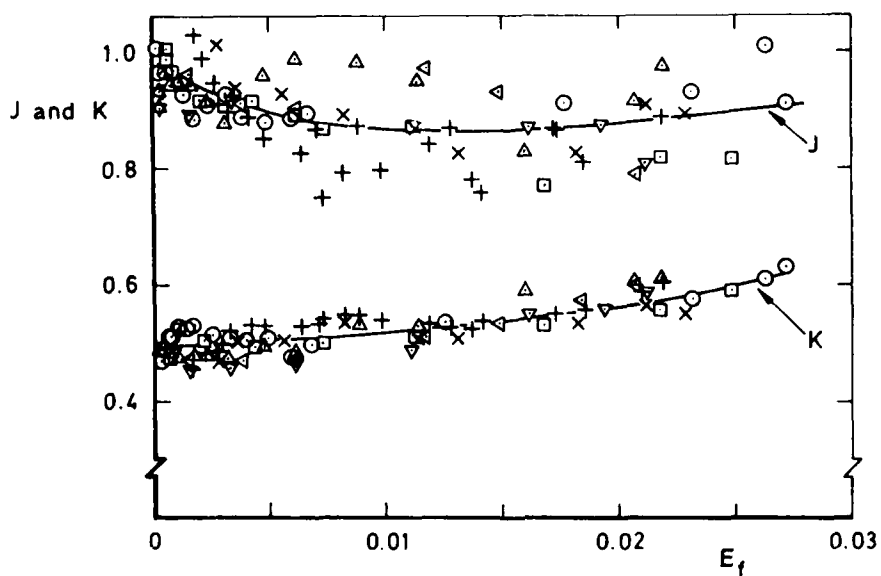


Fig 25a&b Maximum values of wake component

Fig 26a&b



(a) Ahead of interaction



(b) Downstream of normal shockwave

Fig 26a&b Constants J and K in $(\Delta U/U_r^i)_N = 0.5(1 + \sin \pi/(y/\delta_{0.995} - K))$

Fig 27a&b

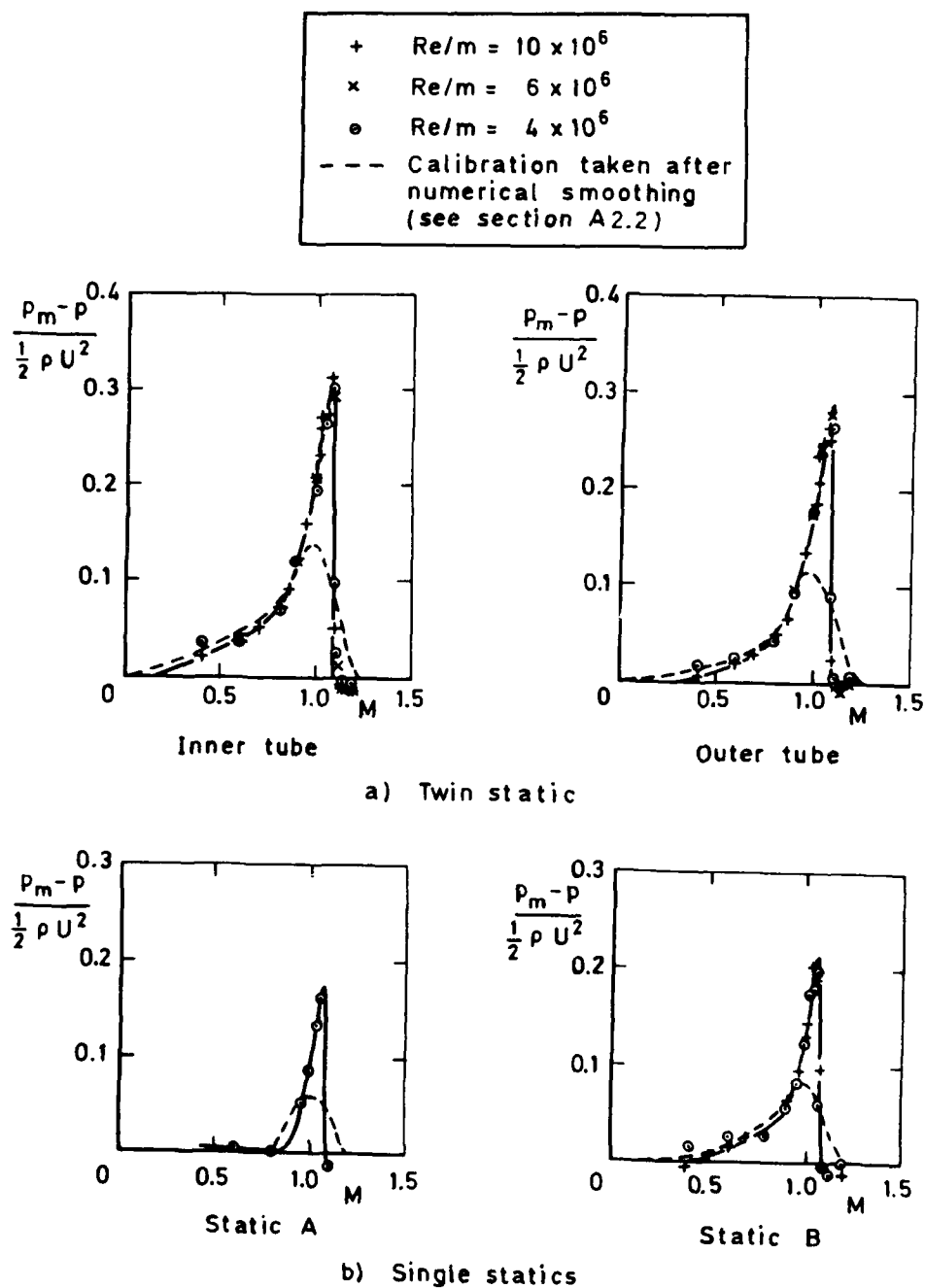
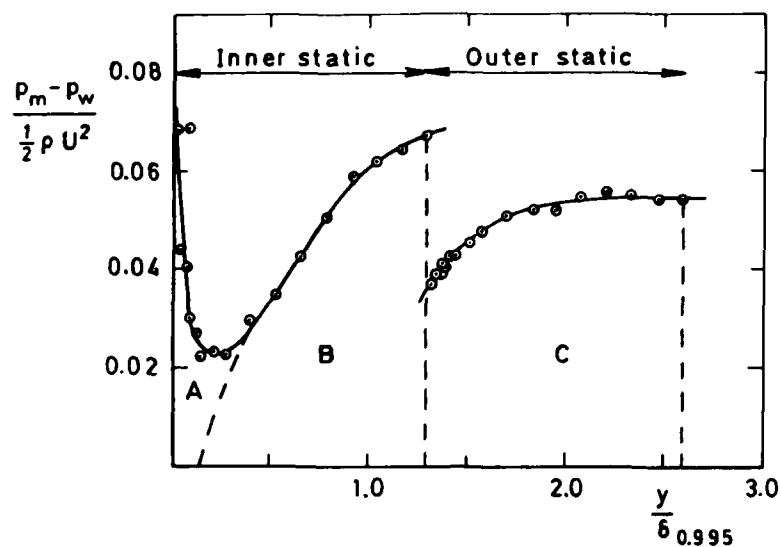
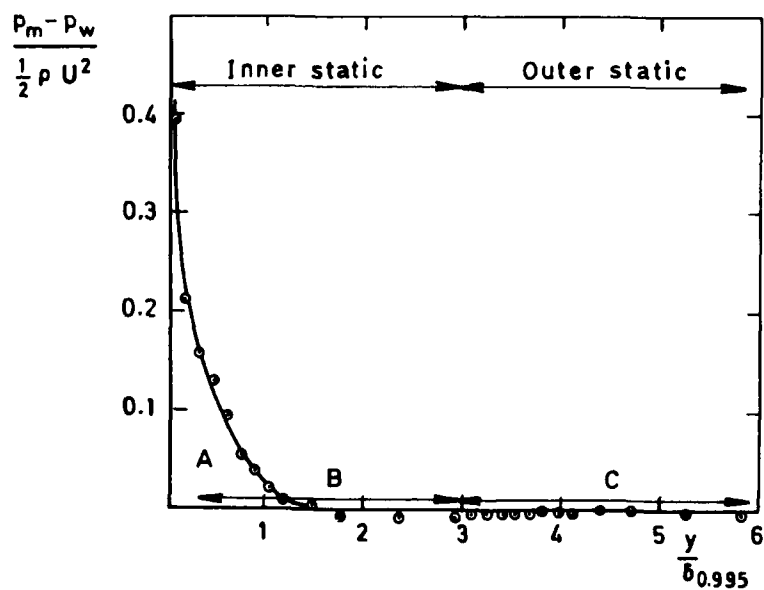


Fig 27a&b Free stream calibration of static probes

Fig 28a&b



a) Behind shockwave
X = 1296 mm $M_\delta = 0.887$



b) Ahead of shockwave
X = -523 mm $M_\delta = 1.284$

Fig 28a&b Typical static pressure measurement errors

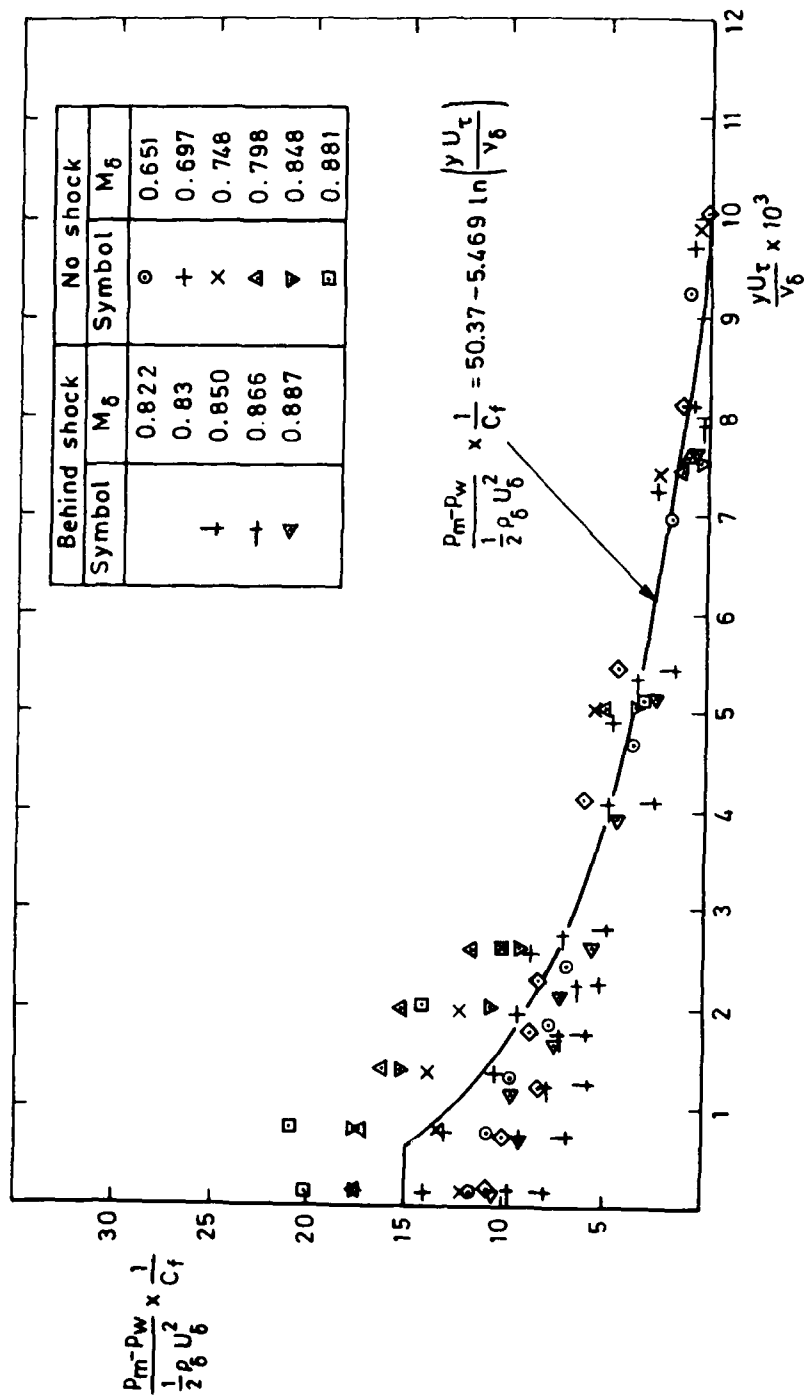


Fig 29 Wall/static interference errors, $M_u \leq 1.098$

Fig 30

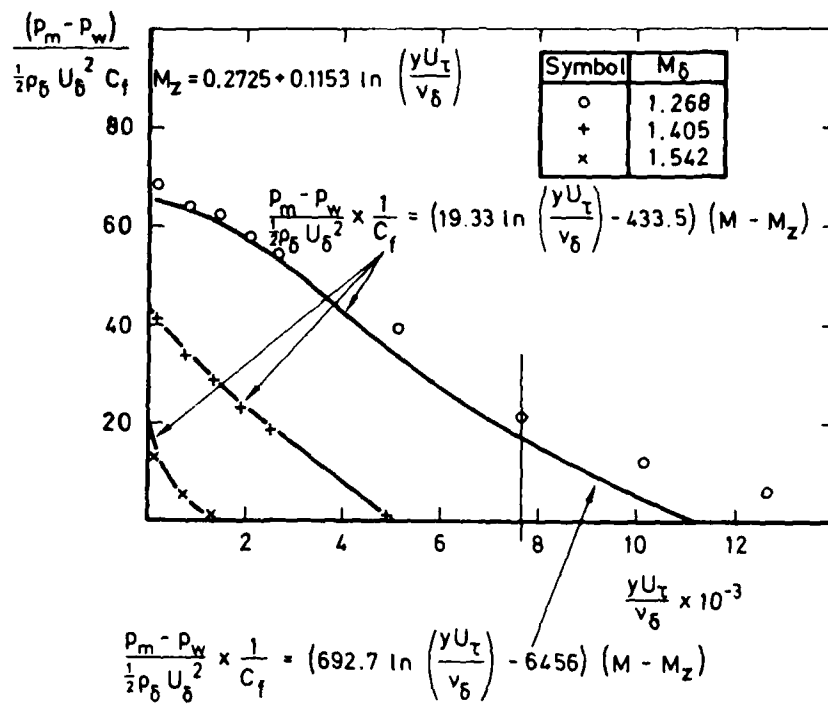


Fig 30 Wall/static interference errors, $M_u \geq 1.098$

Fig 31

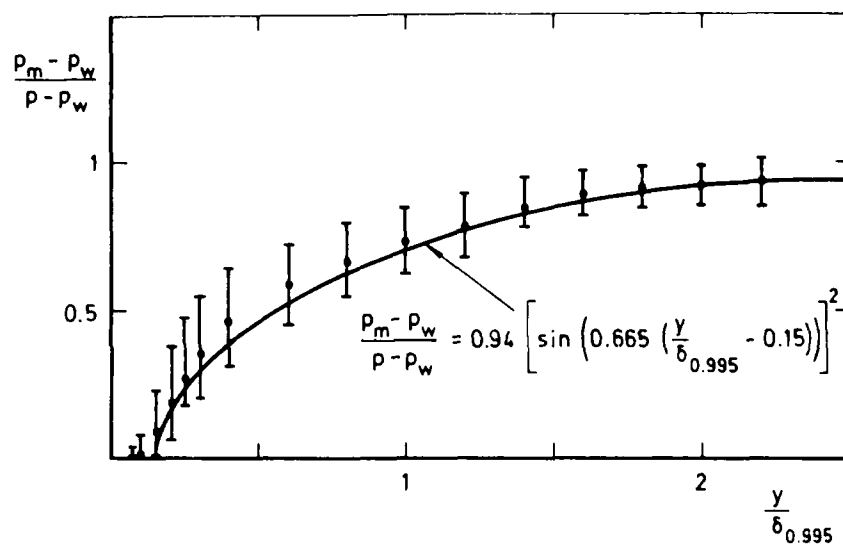


Fig 31 Modification to smoothed free stream static pressure calibration caused by probe position

Fig 32a&b

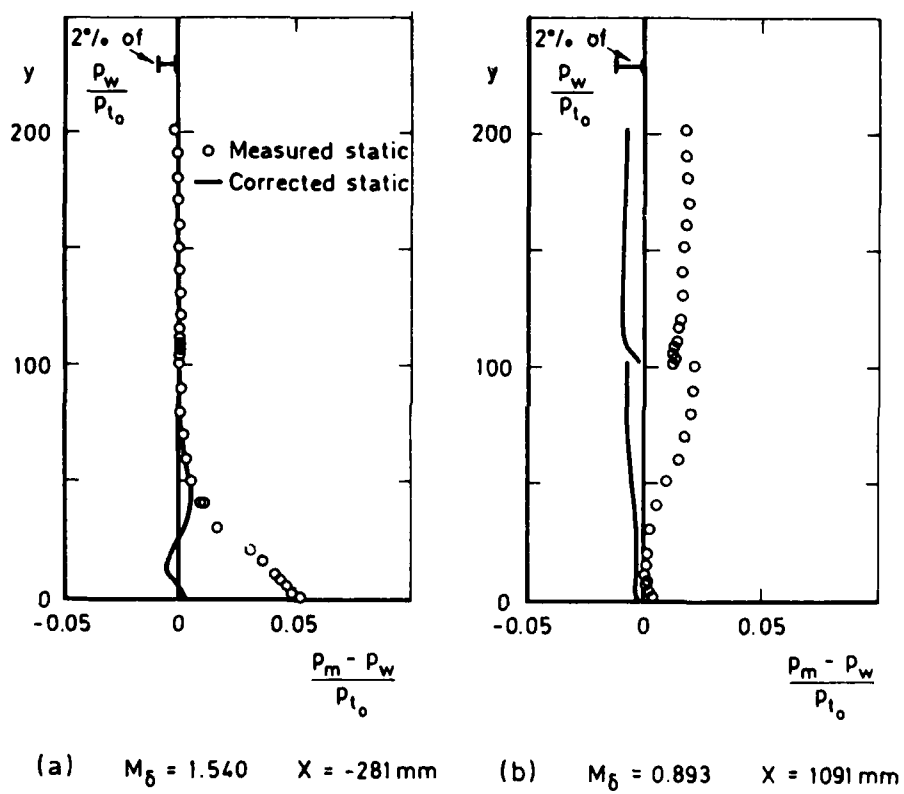
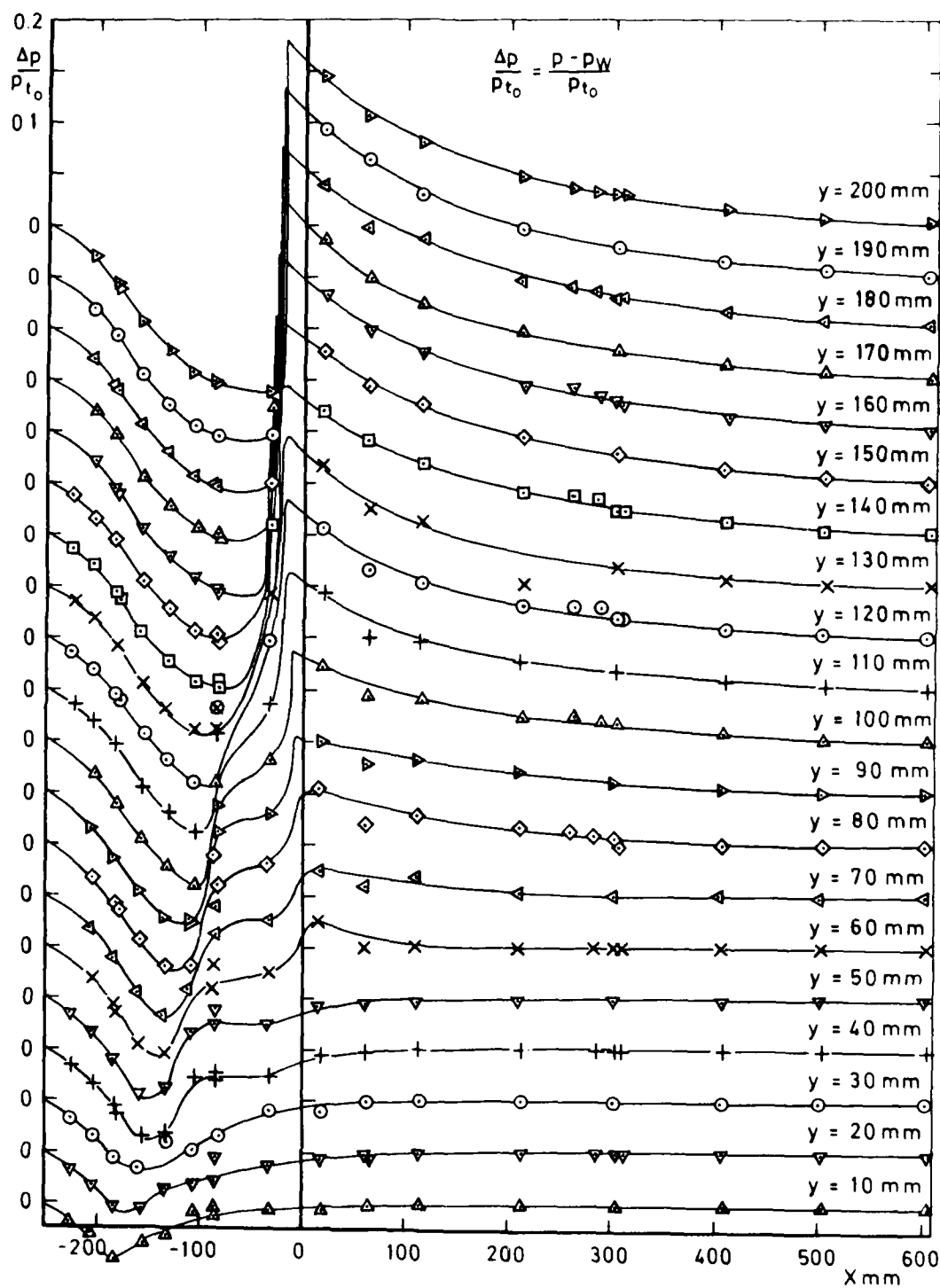


Fig 32a&b Typical corrected static pressures

Fig 33

Fig 33 Smoothed static pressure distribution, $M = 1.5$, $Re = 10 \times 10^6/\text{mm}$

REPORT DOCUMENTATION PAGE

Overall security classification of this page

UNLIMITED

As far as possible this page should contain only unclassified information. If it is necessary to enter classified information, the box above must be marked to indicate the classification, e.g. Restricted, Confidential or Secret.

1. DRIC Reference (to be added by DRIC)	2. Originator's Reference RAE TR 82099	3. Agency Reference N/A	4. Report Security Classification/Marking UNLIMITED		
5. DRIC Code for Originator 7673000W		6. Originator (Corporate Author) Name and Location Royal Aircraft Establishment, Farnborough, Hants, UK			
5a. Sponsoring Agency's Code N/A		6a. Sponsoring Agency (Contract Authority) Name and Location N/A			
7. Title A study of normal shock-wave turbulent boundary-layer interactions at Mach numbers of 1.3, 1.4 and 1.5					
7a. (For Translations) Title in Foreign Language					
7b. (For Conference Papers) Title, Place and Date of Conference					
8. Author 1. Surname, Initials Sawyer, W.G.	9a. Author 2 Long, Carol J.	9b. Authors 3, 4 -		10. Date October 1982	Pages 153
				Refs. 29	
11. Contract Number N/A	12. Period N/A	13. Project -		14. Other Reference Nos. Aero 3532	
15. Distribution statement (a) Controlled by - RAL Aerodynamics (b) Special limitations (if any) -					
16. Descriptors (Keywords) (Descriptors marked * are selected from TEST) Shock waves*. Turbulent boundary layers*. Boundary layer separation*.					
17. Abstract <p>This Report presents the results of a study of seven flows involving the interaction between a normal shock wave and a two-dimensional turbulent boundary layer. The measurements were made at free-stream Mach numbers of 1.3, 1.4 and 1.5 and at Reynolds numbers based on an effective streamwise run of 10×10^6 to 30×10^6. The results were obtained from comprehensive traverses with both pitot and static probes.</p> <p>Standard boundary-layer integral parameters based on wall and measured static pressures are presented, together with velocity profiles and the Mach number distribution over the interaction region.</p> <p>An investigation has been made of the 'law of the wall' and the 'law of the wake' under the influence of strong normal pressure gradients.</p>					

END

DATE
FILMED

9 - 83

DTI